Multi-task Bayesian Compressive Sensing for microwave imaging exploiting the minimum-norm current formulation

L. Poli, G. Oliveri, F. Viani, A. Massa

Abstract

In this report, an innovative three-step contrast-source probabilistic technique is proposed for the reconstruction of image 2D-sparse dielectric profiles. Within the formulation of the inverse scattering problem, such an approach combines (i) a SVD-based step to retrieve the minimum-norm currents, (ii) a probabilistic reformulation of the inverse scattering problem in terms of the real and imaginary parts of the sparse contrast currents (iii) a multi-task BCS strategy for properly correlating the unknown variables (real and imaginary parts of contrast source coefficients). An enhanced version of the multi-task implementation that takes into account the correlations real and imaginary parts of contrast source coefficients related to different views is also investigated through a wide set of numerical experiments.

Contents

1 Legend

- ST-BCS is the single-task Bayesian Compressive Sampling-based technique.
- MV-MT-BCS is the multi-task Bayesian Compressive Sampling-based technique that exploits the correlation between the views.
- MT-BCS-Jmn is the multi-task Bayesian Compressive Sampling-based technique that exploits the correlation between the real and imaginary parts of the source.
- MV-MT-BCS-Jmn is the multi-task Bayesian Compressive Sampling-based technique that exploits the correlation between the real and imaginary parts of the source, and between the views.

2 Calibration

2.1 TEST CASE: Square Cylinder $L = 0.16\lambda$

Goal: show the performances of BCS when dealing with a sparse scatterer

- Number of Views: V
- Number of Measurements: M
- Number of Cells for the Inversion: N
- Number of Cells for the Direct solver: D
- Side of the investigation domain: L

Test Case Description

Direct solver:

- Square domain divided in $\sqrt{D} \times \sqrt{D}$ cells
- Domain side: $L = 3\lambda$
- $D = 1296$ (discretization for the direct solver: $< \lambda/10$)

Investigation domain:

- Square domain divided in $\sqrt{N} \times \sqrt{N}$ cells
- $L = 3\lambda$
- $2ka = 2 \times \frac{2\pi}{\lambda} \times \frac{L\sqrt{2}}{2} = 6\pi\sqrt{2} = 26.65$
- $\#DOF = \frac{(2ka)^2}{2} = \frac{(2\times\frac{2\pi}{\lambda}\times\frac{L\sqrt{2}}{2})^2}{2} = 4\pi^2\left(\frac{L}{\lambda}\right)^2 = 4\pi^2 \times 9 \approx 355.3$
- N scelto in modo da essere vicino a $\#DOF$: $N = 324$ (18×18)

Measurement domain:

- Measurement points taken on a circle of radius $\rho = 3\lambda$
- Full-aspect measurements
- $M \approx 2ka \rightarrow M = 27$

Sources:

- Plane waves
- $V \approx 2ka \rightarrow V = 27$
- Amplitude: $A = 1$
- Frequency: 300 MHz ($\lambda = 1$)

Object:

- Square cylinder of side $\frac{\lambda}{6} = 0.1667$
- $\varepsilon_r = 2.0$
- $\sigma = 0$ [S/m]

BCS parameters:

- Gamma prior on noise variance parameter: $a \in \left\{1 \times 10^{0},\, 2 \times 10^{0},\, 5 \times 10^{0},\; 1 \times 10^{+1},\, 2 \times 10^{+1},\, 5 \times 10^{+1}, 1 \times 10^{+2},\, 2 \times 10^{+2},\, 5 \times 10^{+2}, 1 \times 10^{+3},\, 2 \times 10^{+3},\, 5 \times 10^{+3},\, 1 \times 10^{+4}\right\}$
- Gamma prior on noise variance parameter: $b \in \left\{1 \times 10^{+0},\, 5 \times 10^{-1},\, 2 \times 10^{-1}\,, 1 \times 10^{-1},\, 5 \times 10^{-2},\, 2 \times 10^{-2}\; 1 \times 10^{-2}, 5 \times 10^{-3},\, 2 \times 10^{-3},\, 1 \times 10^{-3}, 5 \times 10^{-4},\, 2 \times 10^{-4},\, 1 \times 10^{-4}\right\}$
- Convergenze parameter: $\tau = 1.0 \times 10^{-8}$

RESULTS: Calibration

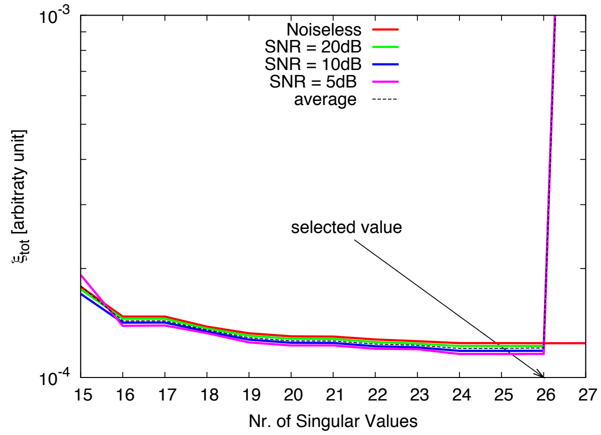

(a)

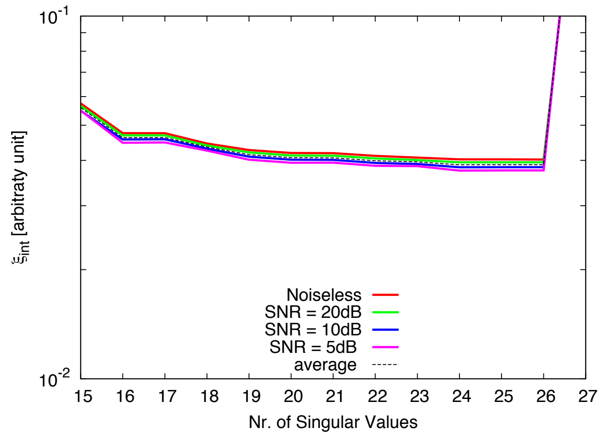

(b)

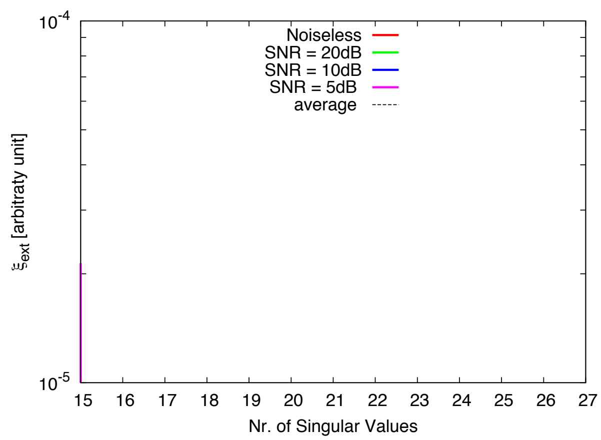

(c)

Figure 31. Behaviour of error figures as a function of the initial estimate of the noise n_0, for different SNR values: (a) total error ξ_{tot}, (b) internal error ξ_{int}, (c) external error ξ_{ext}.

Obervations:

The error function ξ_{tot} (averaged considering different SNR values: Noiseless, $SNR = 20dB$, $SNR = 10dB$ and $SNR = 5dB$) depending on the parameters (a, b) has a global minimum in ($a = 5 \times 10^0$, $b = 2 \times 10^{-2}$)

indipendently from the number of Singular Values selected. However, the depth of the global minimum depends on the number of Singular Values, Fig. 1 shows the values of the global minimum of the averaged error function ξ_{tot} with respect to the number of Singular Values. We have the deepest global minimum for 26 singular values.

RESULTS: Calibration - Nr. of Singular Values: $\rho = 26$

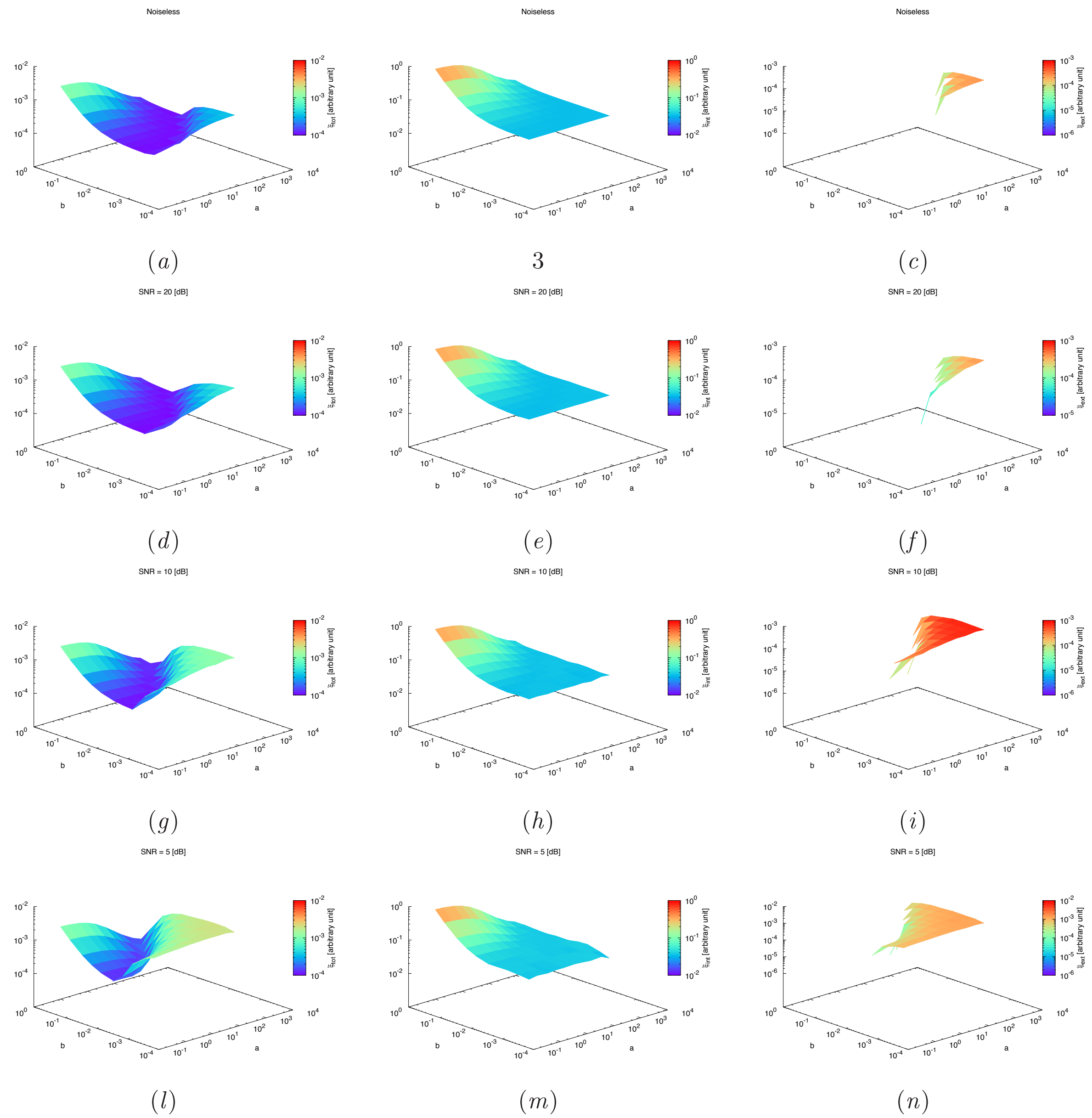

Figure 32. Behaviour of error figures as a function of the initial estimate of the Gamma prior on the noise variance parameters a and b, for different SNR values: (a), (d), (g) and (l) total error ξ_{tot}, (b), (e), (h) and (m) internal error ξ_{int}, (c), (f), (i) and (n) external error ξ_{ext}, for (a), (b) and (c) Noiseless case, (d), (e) and (f) $SNR = 20dB$, (g), (h) and (i) $SNR = 10dB$ and (l), (m) and (n) $SNR = 5dB$.

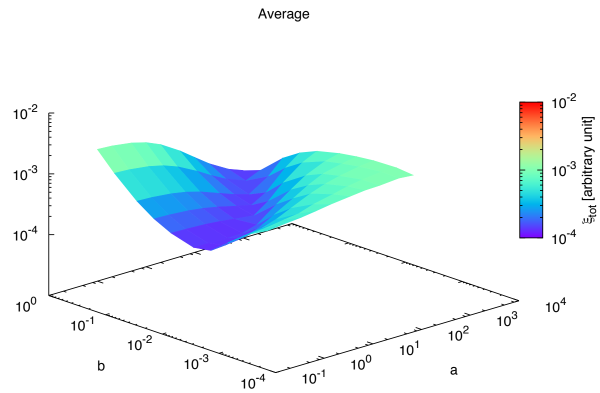

(a)

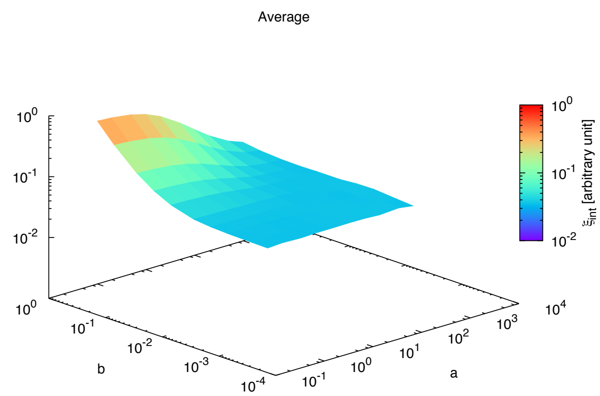

(b)

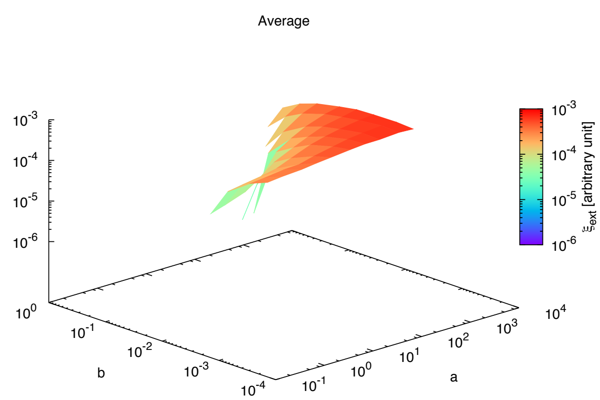

(c)

Figure 33. Averaged behaviour of error figures as a function of the initial estimate of the Gamma prior on the noise variance parameters a and b: (a) total error ξ_{tot}, (b) internal error ξ_{int}, (c) external error ξ_{ext}.

3 Basic Tests - Tests Dominio $L = 3.00\lambda$

3.1 TEST CASE: Two Square Cylinders $L = 0.16\lambda$

Goal: show the performances of BCS when dealing with a sparse scatterer

- Number of Views: V
- Number of Measurements: M
- Number of Cells for the Inversion: N
- Number of Cells for the Direct solver: D
- Side of the investigation domain: L

Test Case Description

Direct solver:

- Square domain divided in $\sqrt{D} \times \sqrt{D}$ cells
- Domain side: $L = 3\lambda$
- $D = 1296$ (discretization for the direct solver: $< \lambda/10$)

Investigation domain:

- Square domain divided in $\sqrt{N} \times \sqrt{N}$ cells
- $L = 3\lambda$
- $2ka = 2 \times \frac{2\pi}{\lambda} \times \frac{L\sqrt{2}}{2} = 6\pi\sqrt{2} = 26.65$
- $\#DOF = \frac{(2ka)^2}{2} = \frac{(2\times\frac{2\pi}{\lambda}\times\frac{L\sqrt{2}}{2})^2}{2} = 4\pi^2\left(\frac{L}{\lambda}\right)^2 = 4\pi^2 \times 9 \approx 355.3$
- N scelto in modo da essere vicino a $\#DOF$: $N = 324$ (18×18)

Measurement domain:

- Measurement points taken on a circle of radius $\rho = 3\lambda$
- Full-aspect measurements
- $M \approx 2ka \rightarrow M = 27$

Sources:

- Plane waves
- $V \approx 2ka \rightarrow V = 27$
- Amplitude: $A = 15.$
- Frequency: 300 MHz ($\lambda = 1$)

Object:

- Two square cylinders of side $\frac{\lambda}{6} = 0.1667$
- $\varepsilon_r \in \{1.5, 2.0, 2.5, 3.0, 3.5, 4.0, 4.5, 5.0\}$ (one square), $\varepsilon_r = 1.6$ (one square)
- $\sigma = 0$ [S/m]

MV-MT-BCS-Jmn parameters:

- Gamma prior on noise variance parameter: $a = 5 \times 10^0$
- Gamma prior on noise variance parameter: $b = 2 \times 10^{-2}$
- Convergenze parameter: $\tau = 1.0 \times 10^{-8}$

RESULTS: Two Square Cylinders $L = 0.16\lambda$

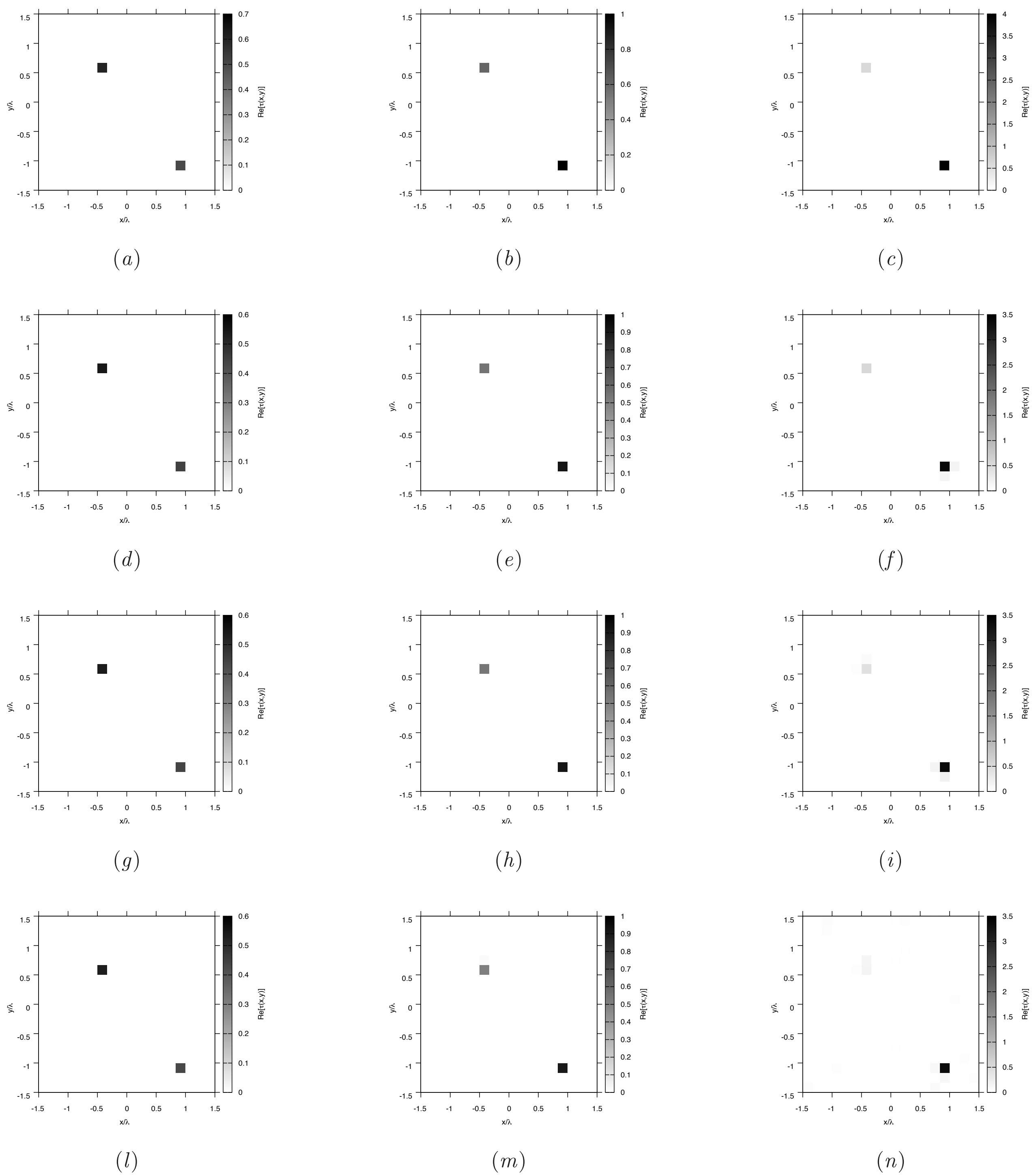

Figure 34. Actual object $(a)(b)(c)$ and MV-MT-BCS-Jmn reconstructed object with $\varepsilon_r = 1.5$ $(d)(g)(l)$, $\varepsilon_r = 2.0$ $(e)(h)(m)$, and $\varepsilon_r = 5.0$ $(f)(i)(n)$, for Noiseless case $(d)(e)(f)$, $SNR = 10$ [dB] $(g)(h)(i)$ and $SNR = 5$ [dB] $(l)(m)(n)$.

RESULTS: Two Square Cylinders $L = 0.16\lambda$ - Error Figures - Comparison ST-BCS/MT-BCS

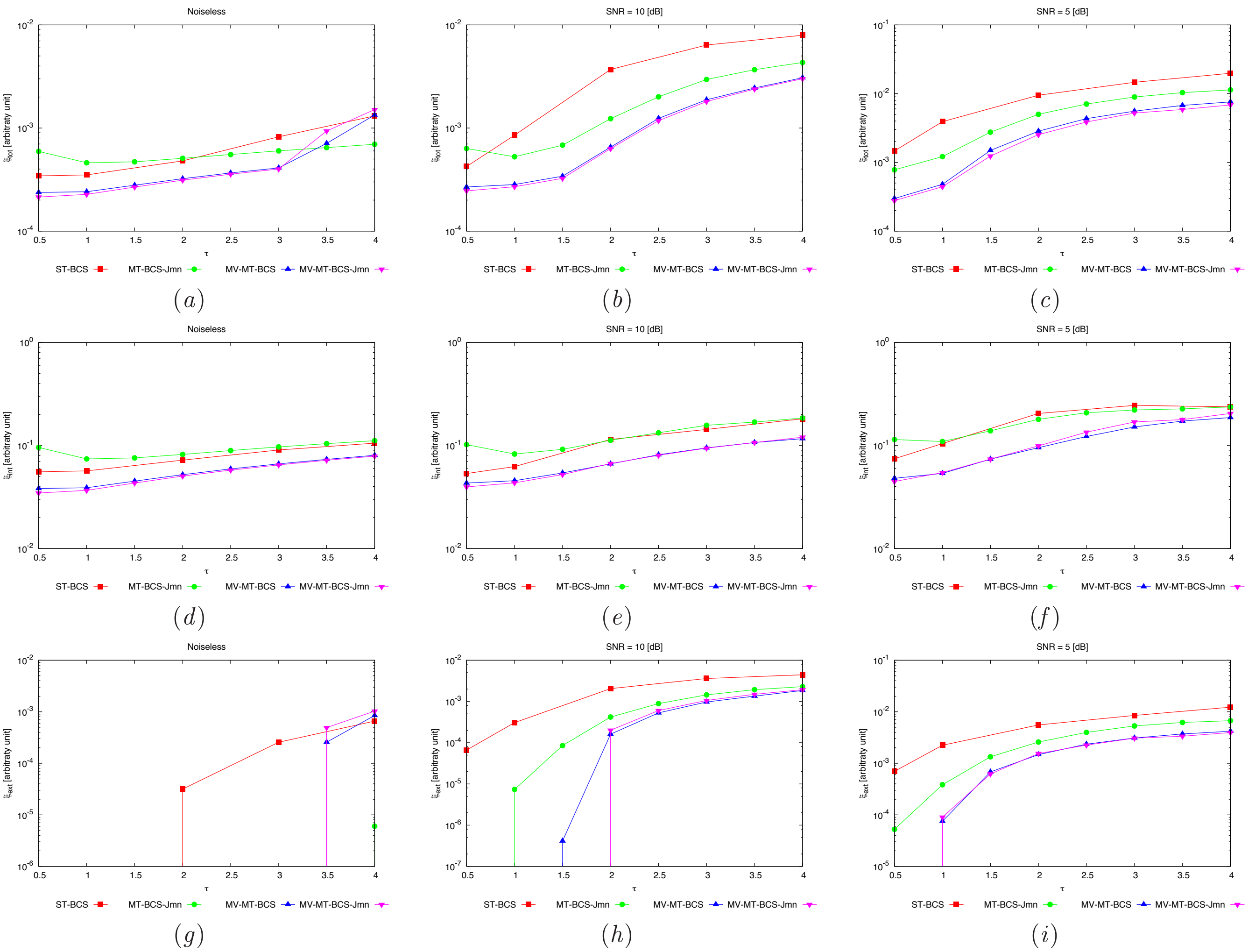

Figure 35. Behaviour of total error ξ_{tot} $(a)(b)(c)$, internal error ξ_{int} $(d)(e)(f)$ and external error ξ_{ext} $(g)(h)(i)$ for Noiseless case $(a)(d)(g)$, $SNR = 10$ [dB] $(b)(e)(h)$ and $SNR = 5$ [dB] $(c)(f)(i)$.

3.2 TEST CASE: Three Square Cylinders $L = 0.16\lambda$

Goal: show the performances of BCS when dealing with a sparse scatterer

- Number of Views: V
- Number of Measurements: M
- Number of Cells for the Inversion: N
- Number of Cells for the Direct solver: D
- Side of the investigation domain: L

Test Case Description

Direct solver:

- Square domain divided in $\sqrt{D} \times \sqrt{D}$ cells
- Domain side: $L = 3\lambda$
- $D = 1296$ (discretization for the direct solver: $< \lambda/10$)

Investigation domain:

- Square domain divided in $\sqrt{N} \times \sqrt{N}$ cells
- $L = 3\lambda$
- $2ka = 2 \times \frac{2\pi}{\lambda} \times \frac{L\sqrt{2}}{2} = 6\pi\sqrt{2} = 26.65$
- $\#DOF = \frac{(2ka)^2}{2} = \frac{(2\times\frac{2\pi}{\lambda}\times\frac{L\sqrt{2}}{2})^2}{2} = 4\pi^2\left(\frac{L}{\lambda}\right)^2 = 4\pi^2 \times 9 \approx 355.3$
- N scelto in modo da essere vicino a $\#DOF$: $N = 324$ (18×18)

Measurement domain:

- Measurement points taken on a circle of radius $\rho = 3\lambda$
- Full-aspect measurements
- $M \approx 2ka \rightarrow M = 27$

Sources:

- Plane waves
- $V \approx 2ka \rightarrow V = 27$
- Amplitude: $A = 1$
- Frequency: 300 MHz ($\lambda = 1$)

Object:

- Three square cylinders of side $\frac{\lambda}{6} = 0.1667$
- $\varepsilon_r \in \{1.5, 2.0, 2.5, 3.0, 3.5, 4.0, 4.5, 5.0\}$ (two square), $\varepsilon_r = 1.6$ (one square)
- $\sigma = 0$ [S/m]

MV-MT-BCS-Jmn parameters:

- Gamma prior on noise variance parameter: $a = 5 \times 10^0$
- Gamma prior on noise variance parameter: $b = 2 \times 10^{-2}$
- Convergenze parameter: $\tau = 1.0 \times 10^{-8}$

RESULTS: Three Square Cylinders $L = 0.16\lambda$

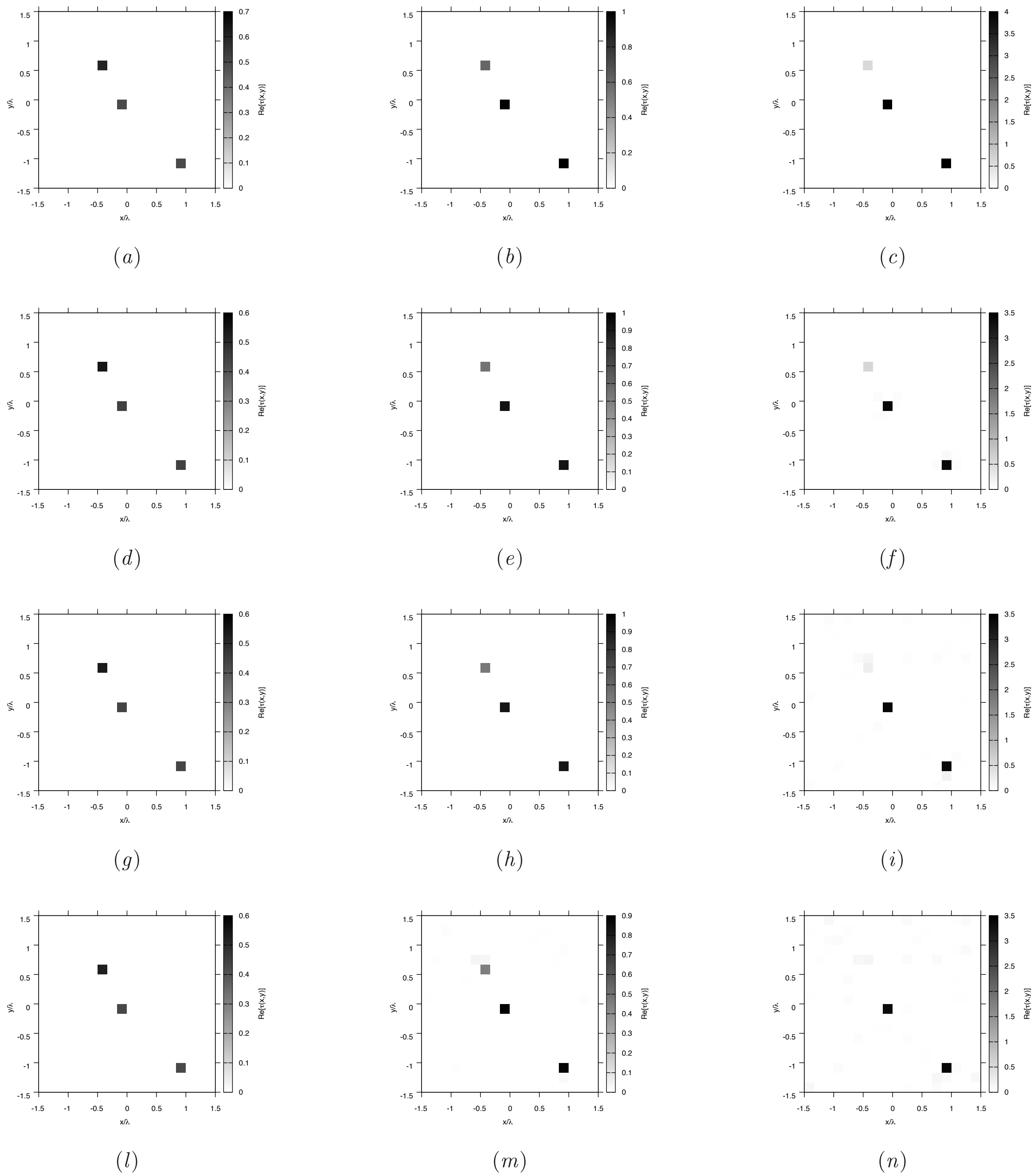

Figure 36. Actual object $(a)(b)(c)$ and MV-MT-BCS-Jmn reconstructed object with $\varepsilon_r = 1.5$ $(d)(g)(l)$, $\varepsilon_r = 2.0$ $(e)(h)(m)$, and $\varepsilon_r = 5.0$ $(f)(i)(n)$, for Noiseless case $(d)(e)(f)$, $SNR = 10$ [dB] $(g)(h)(i)$ and $SNR = 5$ [dB] $(l)(m)(n)$.

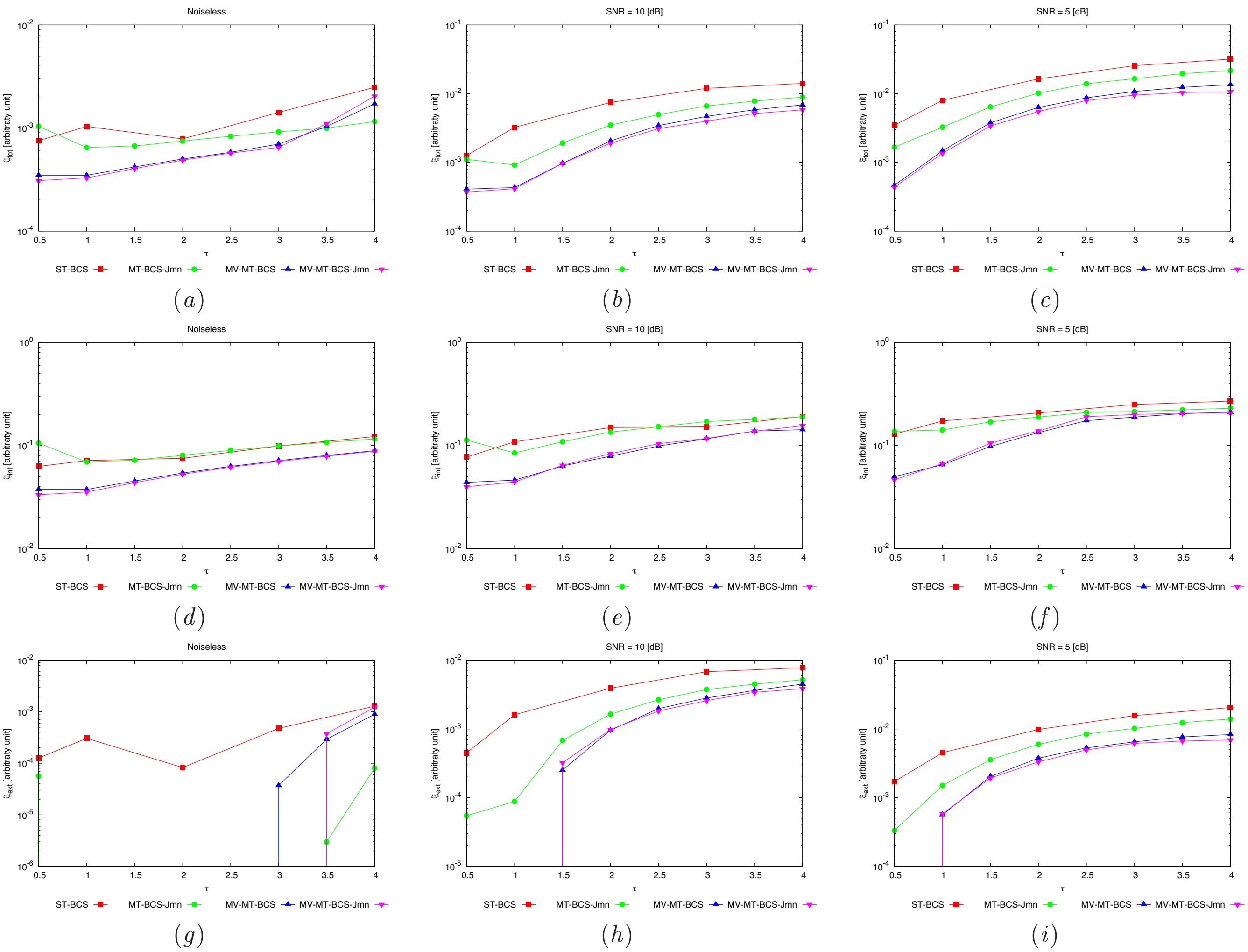

Figure 37. Behaviour of total error ξ_{tot} $(a)(b)(c)$, internal error ξ_{int} $(d)(e)(f)$ and external error ξ_{ext} $(g)(h)(i)$ for Noiseless case $(a)(d)(g)$, $SNR = 10$ [dB] $(b)(e)(h)$ and $SNR = 5$ [dB] $(c)(f)(i)$.

3.3 TEST CASE: Four Square Cylinders $L = 0.16\lambda$

Goal: show the performances of BCS when dealing with a sparse scatterer

- Number of Views: V
- Number of Measurements: M
- Number of Cells for the Inversion: N
- Number of Cells for the Direct solver: D
- Side of the investigation domain: L

Test Case Description

Direct solver:

- Square domain divided in $\sqrt{D} \times \sqrt{D}$ cells
- Domain side: $L = 3\lambda$
- $D = 1296$ (discretization for the direct solver: $< \lambda/10$)

Investigation domain:

- Square domain divided in $\sqrt{N} \times \sqrt{N}$ cells
- $L = 3\lambda$
- $2ka = 2 \times \frac{2\pi}{\lambda} \times \frac{L\sqrt{2}}{2} = 6\pi\sqrt{2} = 26.65$
- $\#DOF = \frac{(2ka)^2}{2} = \frac{(2\times\frac{2\pi}{\lambda}\times\frac{L\sqrt{2}}{2})^2}{2} = 4\pi^2 \left(\frac{L}{\lambda}\right)^2 = 4\pi^2 \times 9 \approx 355.3$
- N scelto in modo da essere vicino a $\#DOF$: $N = 324$ (18×18)

Measurement domain:

- Measurement points taken on a circle of radius $\rho = 3\lambda$
- Full-aspect measurements
- $M \approx 2ka \rightarrow M = 27$

Sources:

- Plane waves
- $V \approx 2ka \rightarrow V = 27$
- Amplitude: $A = 1$
- Frequency: 300 MHz ($\lambda = 1$)

Object:

- Four square cylinders of side $\frac{\lambda}{6} = 0.1667$
- $\varepsilon_r \in \{1.5, 2.0, 2.5, 3.0, 3.5, 4.0, 4.5, 5.0\}$ (two square), $\varepsilon_r = 1.6$ (two square)
- $\sigma = 0$ [S/m]

MV-MT-BCS-Jmn parameters:

- Gamma prior on noise variance parameter: $a = 5 \times 10^0$
- Gamma prior on noise variance parameter: $b = 2 \times 10^{-2}$
- Convergenze parameter: $\tau = 1.0 \times 10^{-8}$

RESULTS: Four Square Cylinders $L = 0.16\lambda$

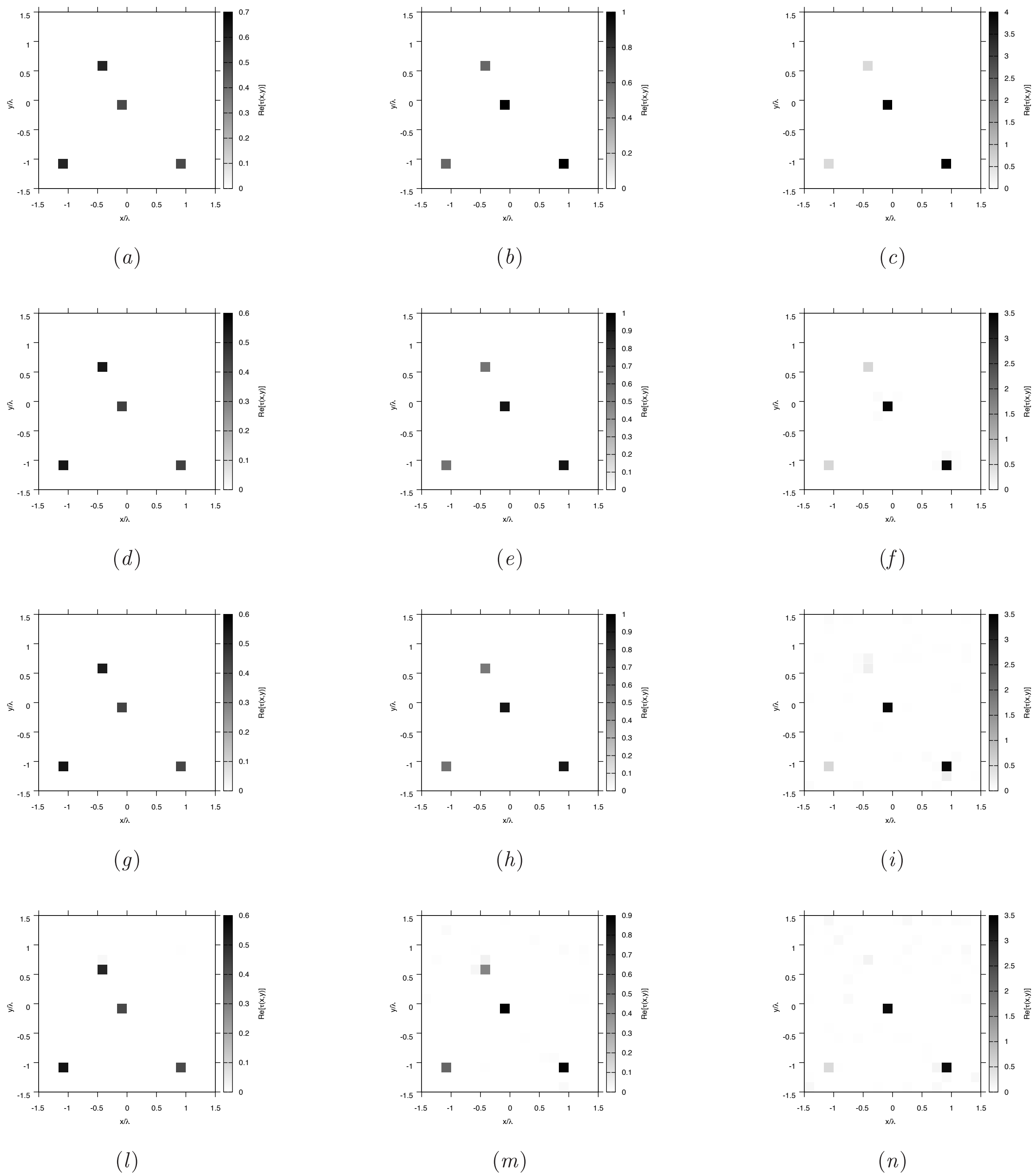

Figure 38. Actual object $(a)(b)(c)$ and MV-MT-BCS-Jmn reconstructed object with $\varepsilon_r = 1.5$ $(d)(g)(l)$, $\varepsilon_r = 2.0$ $(e)(h)(m)$, and $\varepsilon_r = 5.0$ $(f)(i)(n)$, for Noiseless case $(d)(e)(f)$, $SNR = 10$ [dB] $(g)(h)(i)$ and $SNR = 5$ [dB] $(l)(m)(n)$.

RESULTS: Four Square Cylinders $L = 0.16\lambda$ - Error Figures - Comparison ST-BCS/MT-BCS

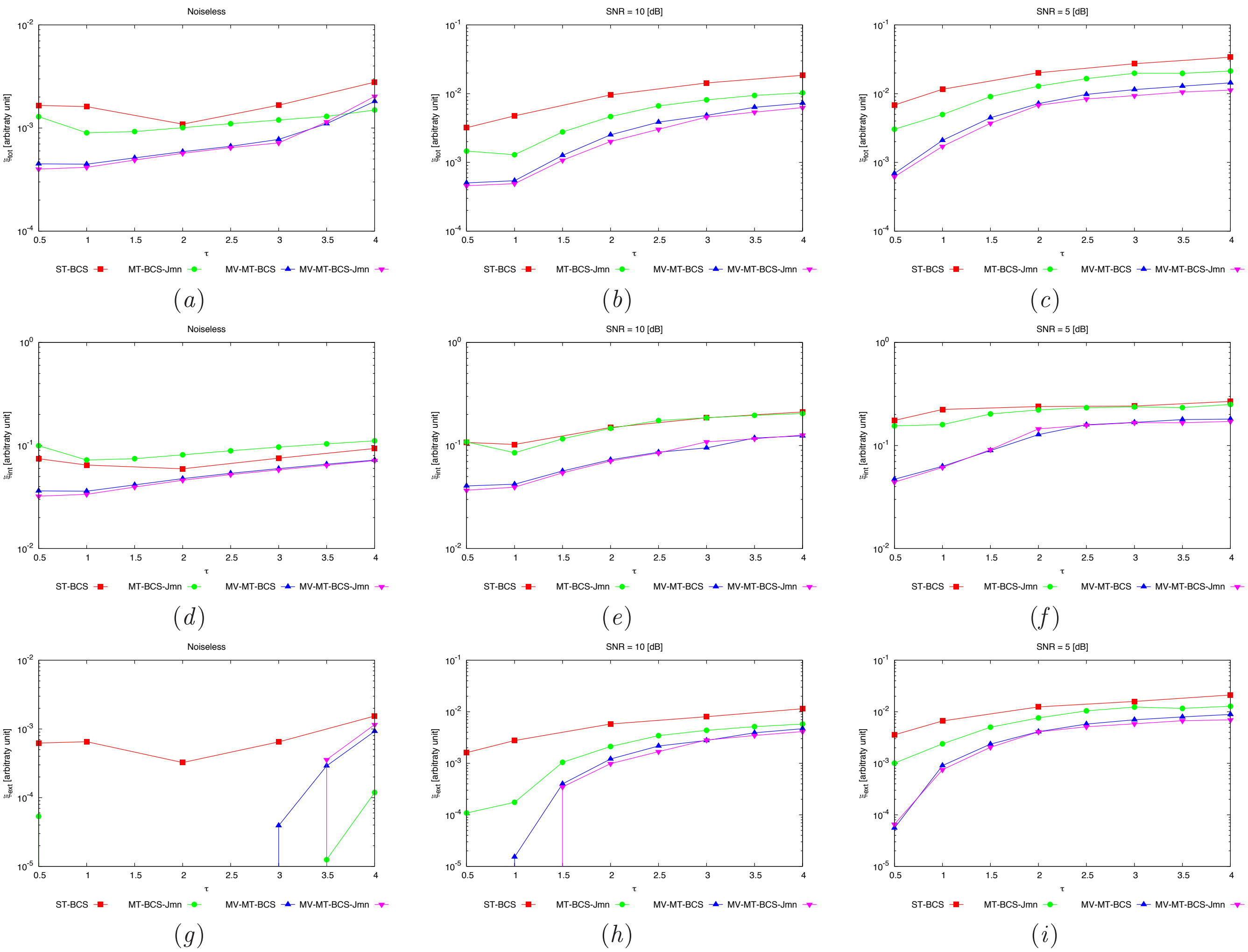

Figure 39. Behaviour of total error ξ_{tot} $(a)(b)(c)$, internal error ξ_{int} $(d)(e)(f)$ and external error ξ_{ext} $(g)(h)(i)$ for Noiseless case $(a)(d)(g)$, $SNR = 10$ [dB] $(b)(e)(h)$ and $SNR = 5$ [dB] $(c)(f)(i)$.

3.4 TEST CASE: Cross-Shaped Cylinder

Goal: show the performances of BCS when dealing with a sparse scatterer

- Number of Views: V
- Number of Measurements: M
- Number of Cells for the Inversion: N
- Number of Cells for the Direct solver: D
- Side of the investigation domain: L

Test Case Description

Direct solver:

- Square domain divided in $\sqrt{D} \times \sqrt{D}$ cells
- Domain side: $L = 3\lambda$
- $D = 1296$ (discretization for the direct solver: $< \lambda/10$)

Investigation domain:

- Square domain divided in $\sqrt{N} \times \sqrt{N}$ cells
- $L = 3\lambda$
- $2ka = 2 \times \frac{2\pi}{\lambda} \times \frac{L\sqrt{2}}{2} = 6\pi\sqrt{2} = 26.65$
- $\#DOF = \frac{(2ka)^2}{2} = \frac{(2\times\frac{2\pi}{\lambda}\times\frac{L\sqrt{2}}{2})^2}{2} = 4\pi^2\left(\frac{L}{\lambda}\right)^2 = 4\pi^2 \times 9 \approx 355.3$
- N scelto in modo da essere vicino a $\#DOF$: $N = 324$ (18×18)

Measurement domain:

- Measurement points taken on a circle of radius $\rho = 3\lambda$
- Full-aspect measurements
- $M \approx 2ka \rightarrow M = 27$

Sources:

- Plane waves
- $V \approx 2ka \rightarrow V = 27$
- Amplitude: $A = 1$
- Frequency: 300 MHz ($\lambda = 1$)

Object:

- Cross-shaped cylinder
- $\varepsilon_r \in \{1.5, 2.0, 2.5, 3.0, 3.5, 4.0, 4.5, 5.0\}$
- $\sigma = 0$ [S/m]

MV-MT-BCS-Jmn parameters:

- Gamma prior on noise variance parameter: $a = 5 \times 10^0$
- Gamma prior on noise variance parameter: $b = 2 \times 10^{-2}$
- Convergenze parameter: $\tau = 1.0 \times 10^{-8}$

RESULTS: Cross-Shaped Cylinder

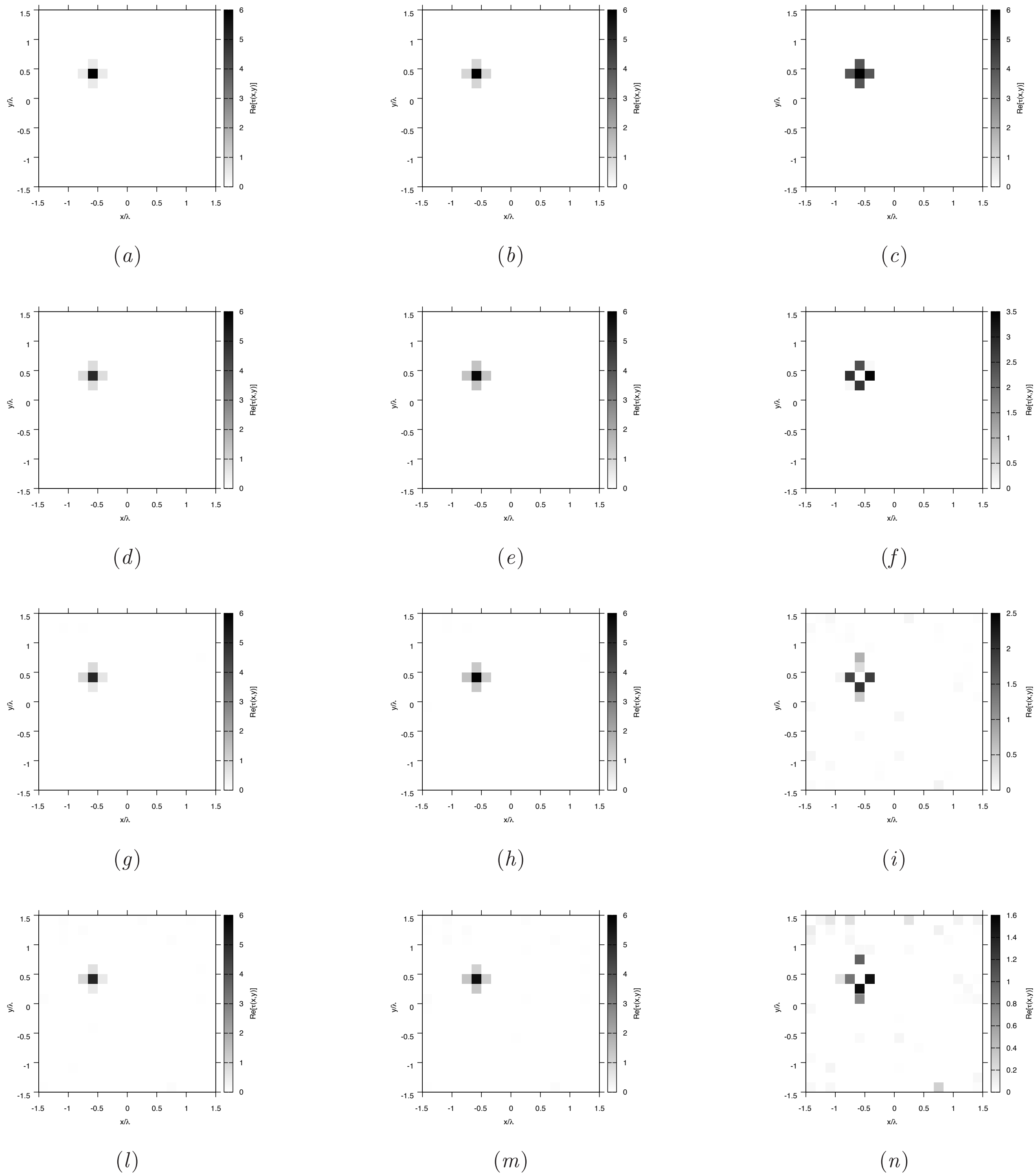

Figure 40. Actual object $(a)(b)(c)$ and MV-MT-BCS-Jmn reconstructed object with $\varepsilon_r = 1.5$ $(d)(g)(l)$, $\varepsilon_r = 2.0$ $(e)(h)(m)$, and $\varepsilon_r = 5.0$ $(f)(i)(n)$, for Noiseless case $(d)(e)(f)$, $SNR = 10$ [dB] $(g)(h)(i)$ and $SNR = 5$ [dB] $(l)(m)(n)$.

RESULTS: Cross-Shaped Cylinder - Reconstructions - Comparison ST-BCS/MT-BCS - $\varepsilon_r = 2.0$

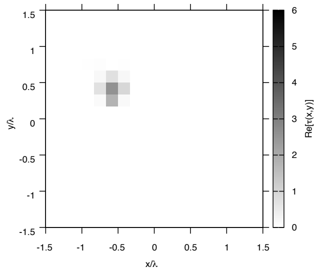

(a)

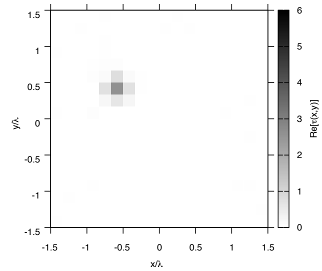

(b)

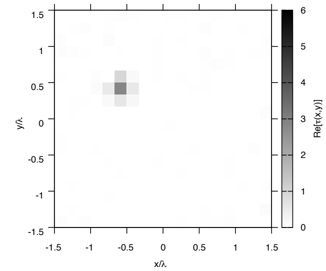

(c)

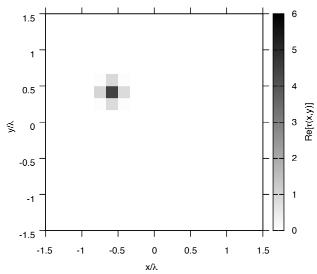

(d)

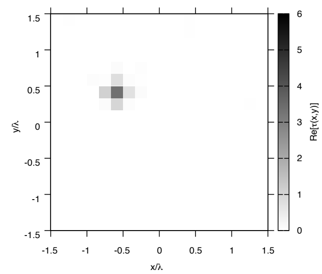

(e)

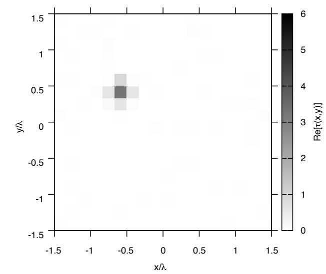

(f)

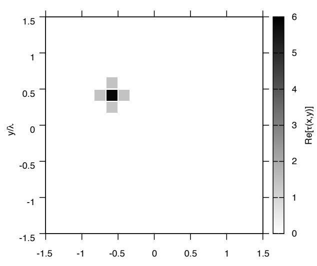

(g)

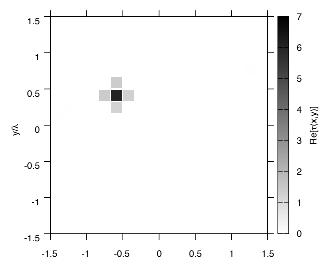

(h)

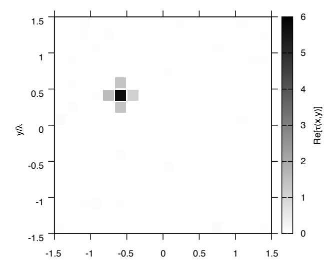

(i)

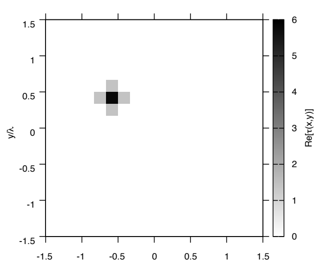

(l)

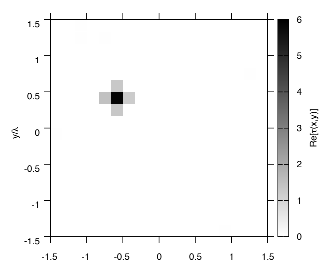

(m)

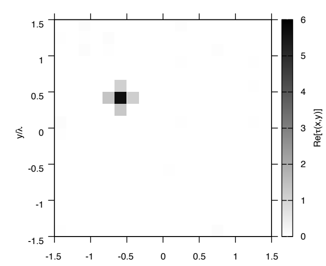

(n)

Figure 41. ST-BCS reconstructed object $(a)(b)(c)$, MT-BCS-Jmn reconstructed $(d)(e)(f)$ object, MV-MT-BCS reconstructed $(g)(h)(i)$ and MV-MT-BCS-Jmn reconstructed $(l)(m)(n)$ for Noiseless case $(a)(d)(g)(l)$, $SNR = 10$ [dB] $(b)(e)(h)(m)$ and $SNR = 5$ [dB] $(c)(f)(i)(n)$.

RESULTS: Cross-Shaped Cylinder - Error Figures - Comparison ST-BCS/MT-BCS

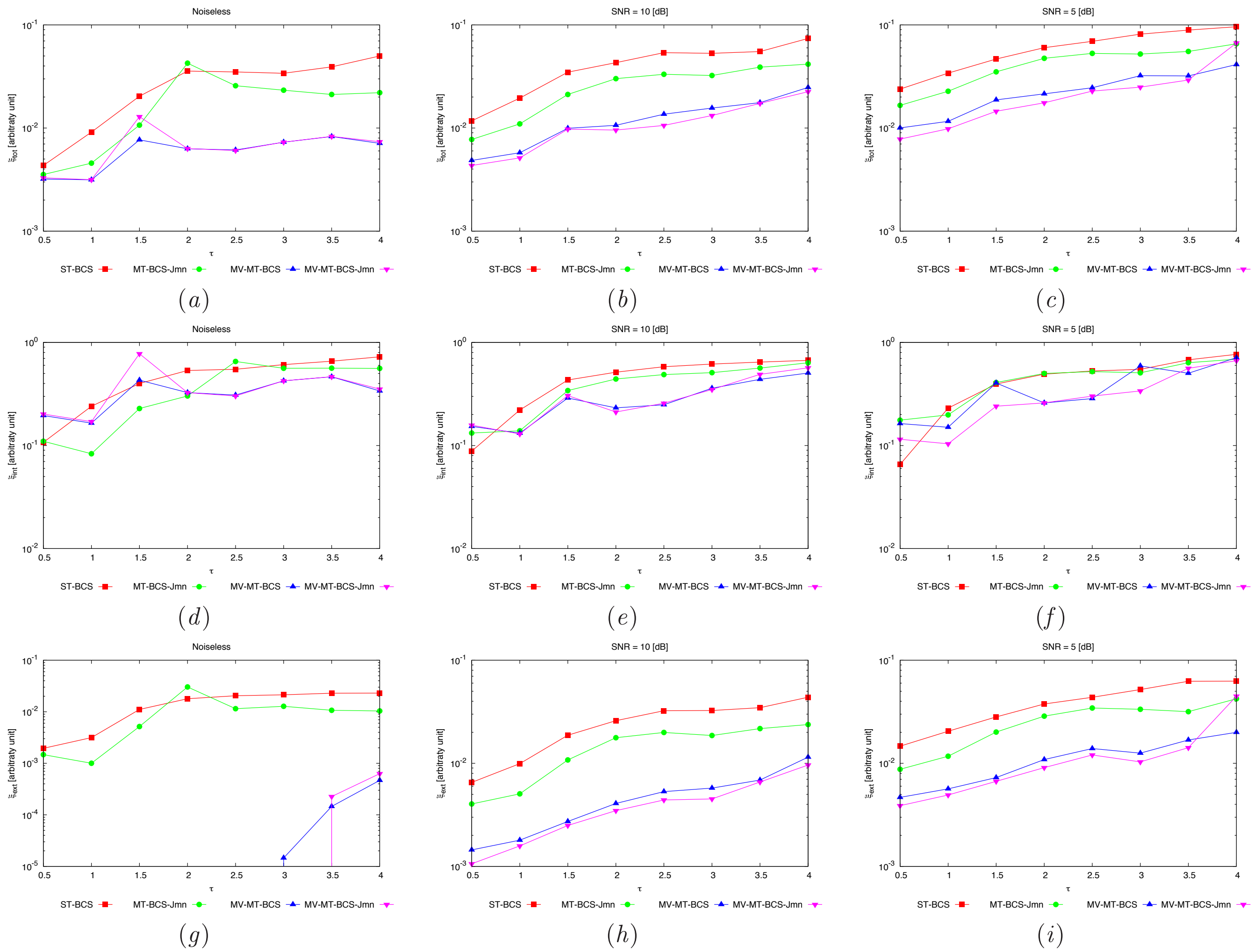

Figure 42. Behaviour of total error ξ_{tot} $(a)(b)(c)$, internal error ξ_{int} $(d)(e)(f)$ and external error ξ_{ext} $(g)(h)(i)$ for Noiseless case $(a)(d)(g)$, $SNR = 10$ [dB] $(b)(e)(h)$ and $SNR = 5$ [dB] $(c)(f)(i)$.

3.5 TEST CASE: L-Shaped Cylinder

Goal: show the performances of BCS when dealing with a sparse scatterer

- Number of Views: V
- Number of Measurements: M
- Number of Cells for the Inversion: N
- Number of Cells for the Direct solver: D
- Side of the investigation domain: L

Test Case Description

Direct solver:

- Square domain divided in $\sqrt{D} \times \sqrt{D}$ cells
- Domain side: $L = 3\lambda$
- $D = 1296$ (discretization for the direct solver: $< \lambda/10$)

Investigation domain:

- Square domain divided in $\sqrt{N} \times \sqrt{N}$ cells
- $L = 3\lambda$
- $2ka = 2 \times \frac{2\pi}{\lambda} \times \frac{L\sqrt{2}}{2} = 6\pi\sqrt{2} = 26.65$
- $\#DOF = \frac{(2ka)^2}{2} = \frac{(2\times\frac{2\pi}{\lambda}\times\frac{L\sqrt{2}}{2})^2}{2} = 4\pi^2\left(\frac{L}{\lambda}\right)^2 = 4\pi^2 \times 9 \approx 355.3$
- N scelto in modo da essere vicino a $\#DOF$: $N = 324$ (18×18)

Measurement domain:

- Measurement points taken on a circle of radius $\rho = 3\lambda$
- Full-aspect measurements
- $M \approx 2ka \rightarrow M = 27$

Sources:

- Plane waves
- $V \approx 2ka \rightarrow V = 27$
- Amplitude $A = 1$
- Frequency: 300 MHz ($\lambda = 1$)

Object:

- L-shaped cylinder
- $\varepsilon_r \in \{1.5, 2.0, 2.5, 3.0, 3.5, 4.0, 4.5, 5.0\}$
- $\sigma = 0$ [S/m]

MV-MT-BCS-Jmn parameters:

- Gamma prior on noise variance parameter: $a = 5 \times 10^0$
- Gamma prior on noise variance parameter: $b = 2 \times 10^{-2}$
- Convergenze parameter: $\tau = 1.0 \times 10^{-8}$

RESULTS: L-Shaped Cylinder

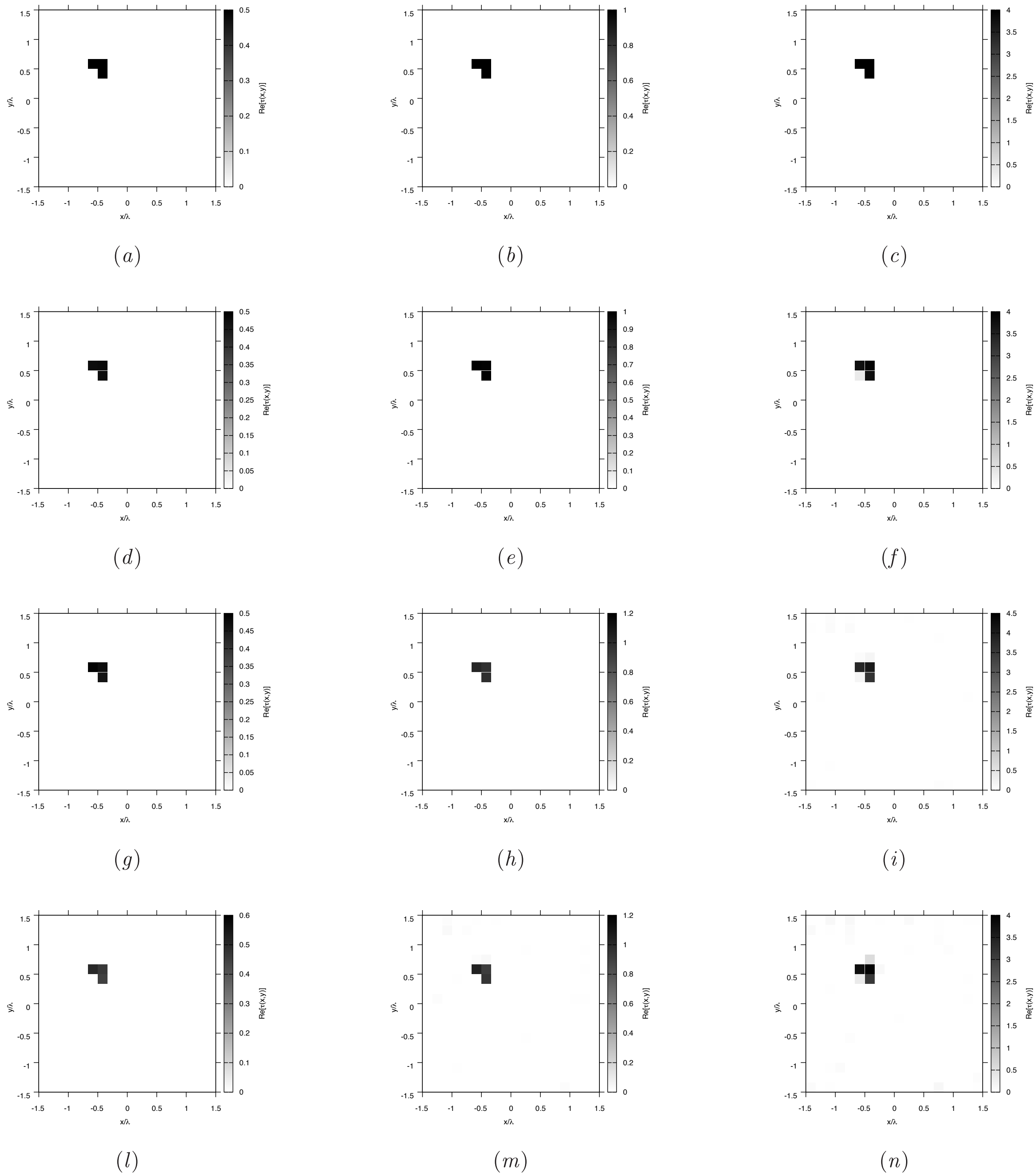

Figure 43. Actual object $(a)(b)(c)$ and MV-MT-BCS-Jmn reconstructed object with $\varepsilon_r = 1.5$ $(d)(g)(l)$, $\varepsilon_r = 2.0$ $(e)(h)(m)$, and $\varepsilon_r = 5.0$ $(f)(i)(n)$, for Noiseless case $(d)(e)(f)$, $SNR = 10$ [dB] $(g)(h)(i)$ and $SNR = 5$ [dB] $(l)(m)(n)$.

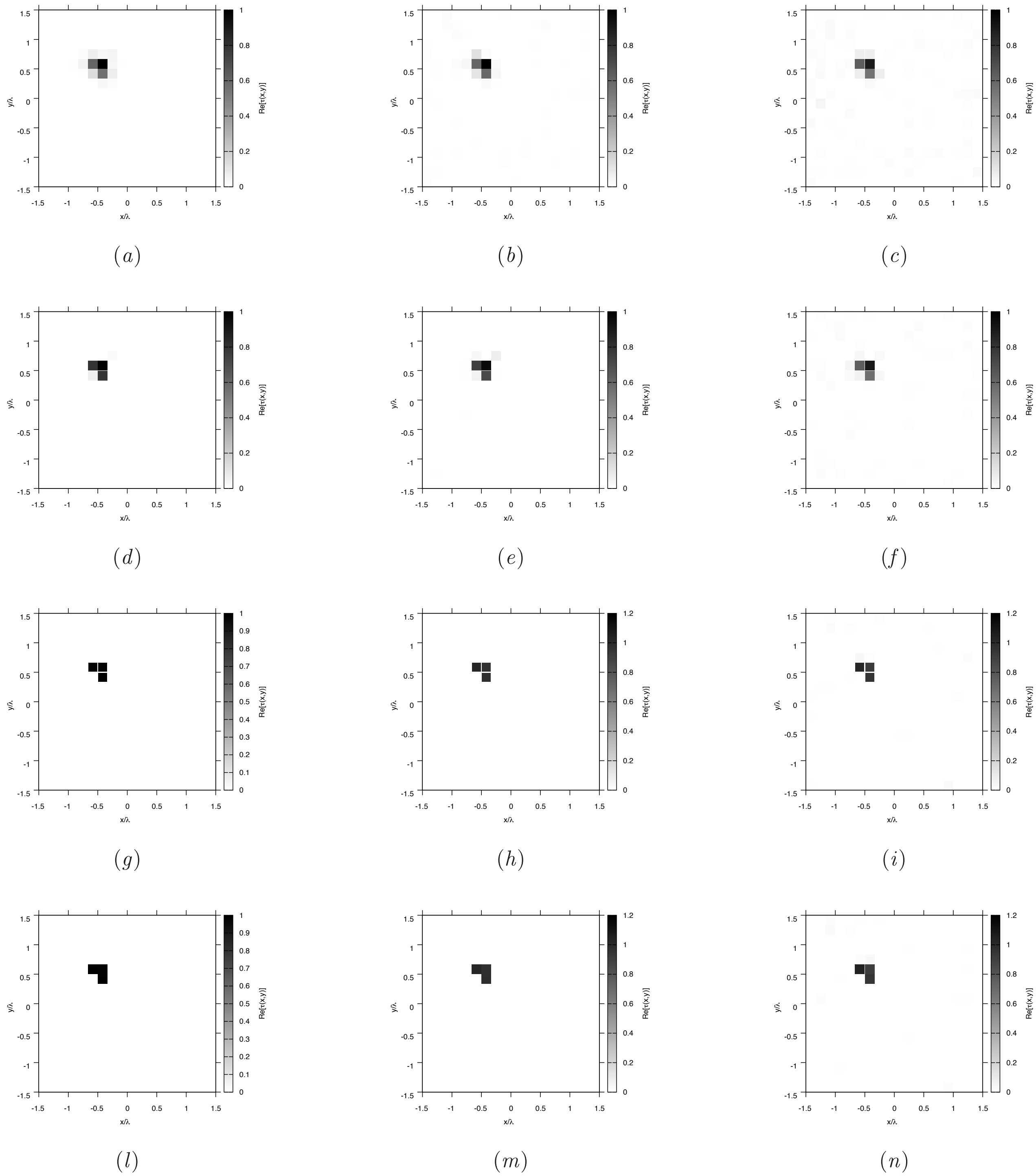

Figure 44. ST-BCS reconstructed object $(a)(b)(c)$, MT-BCS-Jmn reconstructed $(d)(e)(f)$ object, MV-MT-BCS reconstructed $(g)(h)(i)$ and MV-MT-BCS-Jmn reconstructed $(l)(m)(n)$ for Noiseless case $(a)(d)(g)(l)$, $SNR = 10$ [dB] $(b)(e)(h)(m)$ and $SNR = 5$ [dB] $(c)(f)(i)(n)$.

RESULTS: L-Shaped Cylinder - Error Figures - Comparison ST-BCS/MT-BCS

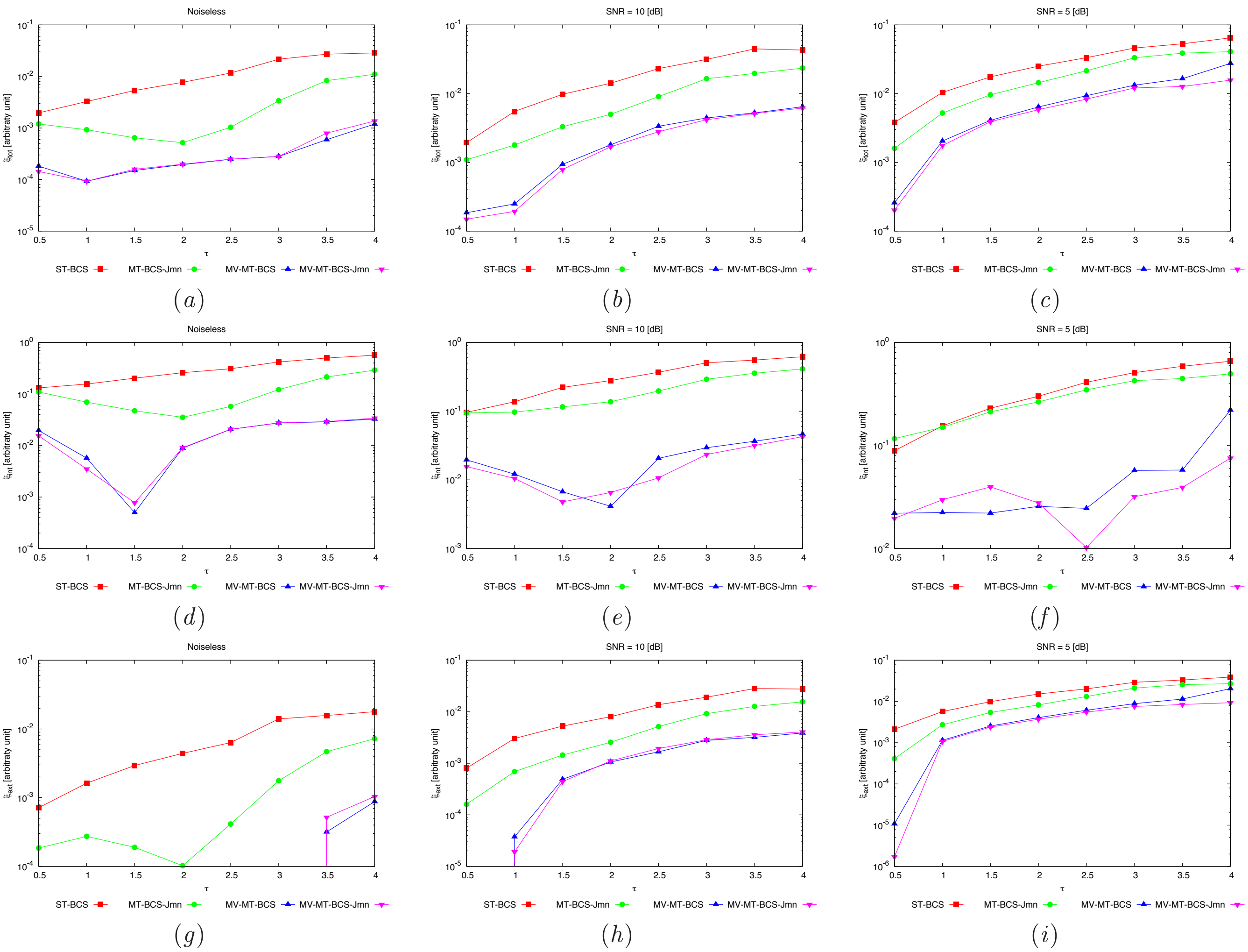

Figure 45. Behaviour of total error ξ_{tot} $(a)(b)(c)$, internal error ξ_{int} $(d)(e)(f)$ and external error ξ_{ext} $(g)(h)(i)$ for Noiseless case $(a)(d)(g)$, $SNR = 10$ [dB] $(b)(e)(h)$ and $SNR = 5$ [dB] $(c)(f)(i)$.

3.6 TEST CASE: Inhomogeneous L-Shaped Cylinder

Goal: show the performances of BCS when dealing with a sparse scatterer

- Number of Views: V
- Number of Measurements: M
- Number of Cells for the Inversion: N
- Number of Cells for the Direct solver: D
- Side of the investigation domain: L

Test Case Description

Direct solver:

- Square domain divided in $\sqrt{D} \times \sqrt{D}$ cells
- Domain side: $L = 3\lambda$
- $D = 1296$ (discretization for the direct solver: $< \lambda/10$)

Investigation domain:

- Square domain divided in $\sqrt{N} \times \sqrt{N}$ cells
- $L = 3\lambda$
- $2ka = 2 \times \frac{2\pi}{\lambda} \times \frac{L\sqrt{2}}{2} = 6\pi\sqrt{2} = 26.65$
- $\#DOF = \frac{(2ka)^2}{2} = \frac{(2\times\frac{2\pi}{\lambda}\times\frac{L\sqrt{2}}{2})^2}{2} = 4\pi^2\left(\frac{L}{\lambda}\right)^2 = 4\pi^2 \times 9 \approx 355.3$
- N scelto in modo da essere vicino a $\#DOF$: $N = 324$ (18×18)

Measurement domain:

- Measurement points taken on a circle of radius $\rho = 3\lambda$
- Full-aspect measurements
- $M \approx 2ka \rightarrow M = 27$

Sources:

- Plane waves
- $V \approx 2ka \rightarrow V = 27$
- Amplitude $A = 1$
- Frequency: 300 MHz ($\lambda = 1$)

Object:

- Inhomogeneous L-shaped cylinder
- $\varepsilon_r \in \{1.5, 2.0, 2.5, 3.0, 3.5, 4.0, 4.5, 5.0\}$
- $\sigma = 0$ [S/m]

MV-MT-BCS-Jmn parameters:

- Gamma prior on noise variance parameter: $a = 5 \times 10^0$
- Gamma prior on noise variance parameter: $b = 2 \times 10^{-2}$
- Convergenze parameter: $\tau = 1.0 \times 10^{-8}$

RESULTS: Inhomogeneous L-Shaped Cylinder

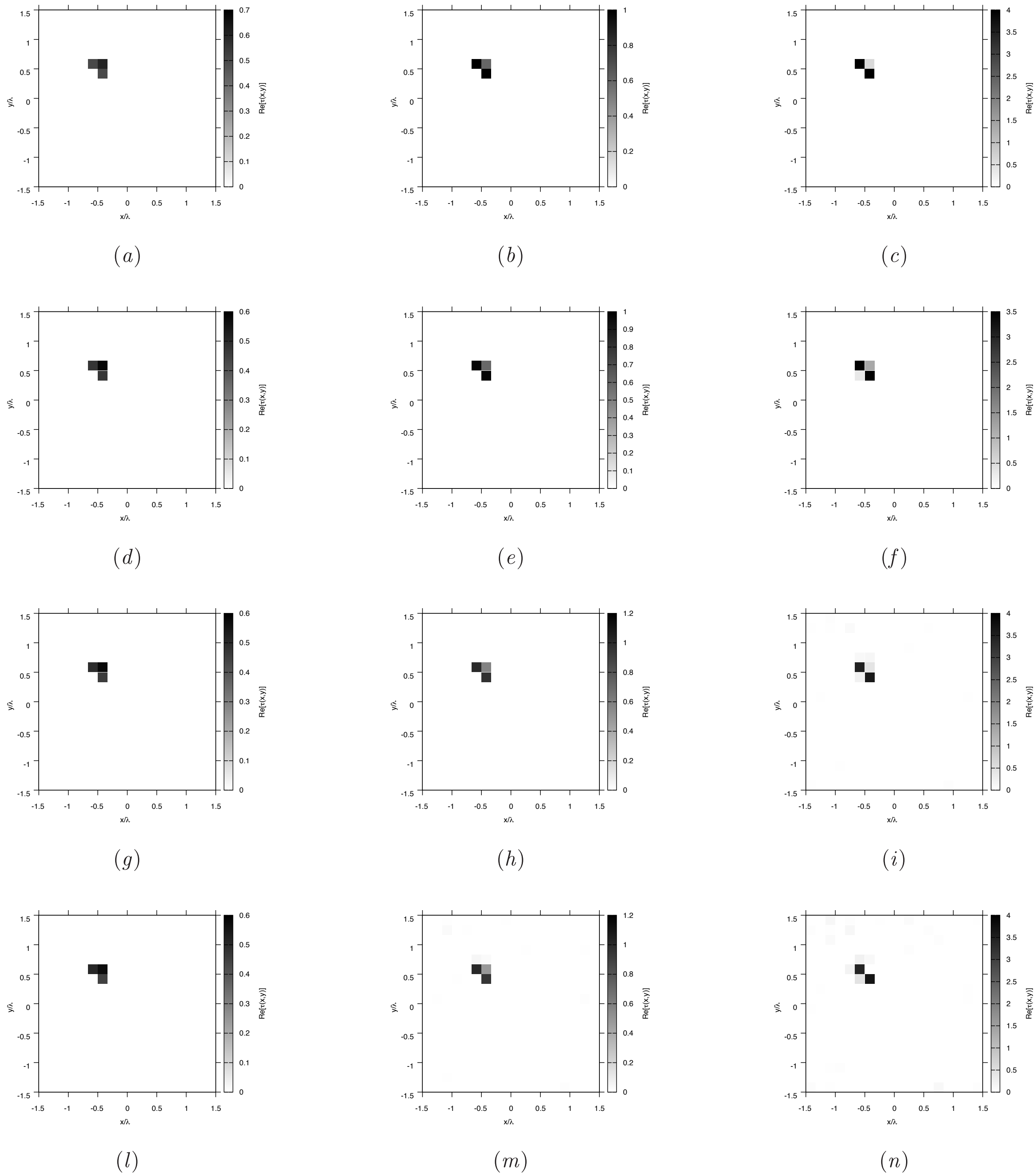

Figure 46. Actual object $(a)(b)(c)$ and MV-MT-BCS-Jmn reconstructed object with $\varepsilon_r = 1.5$ $(d)(g)(l)$, $\varepsilon_r = 2.0$ $(e)(h)(m)$, and $\varepsilon_r = 5.0$ $(f)(i)(n)$, for Noiseless case $(d)(e)(f)$, $SNR = 10$ [dB] $(g)(h)(i)$ and $SNR = 5$ [dB] $(l)(m)(n)$.

RESULTS: Inhomogeneous L-Shaped Cylinder - Reconstructions - Comparison ST-BCS/MT-BCS - $\varepsilon_r = 2.0$

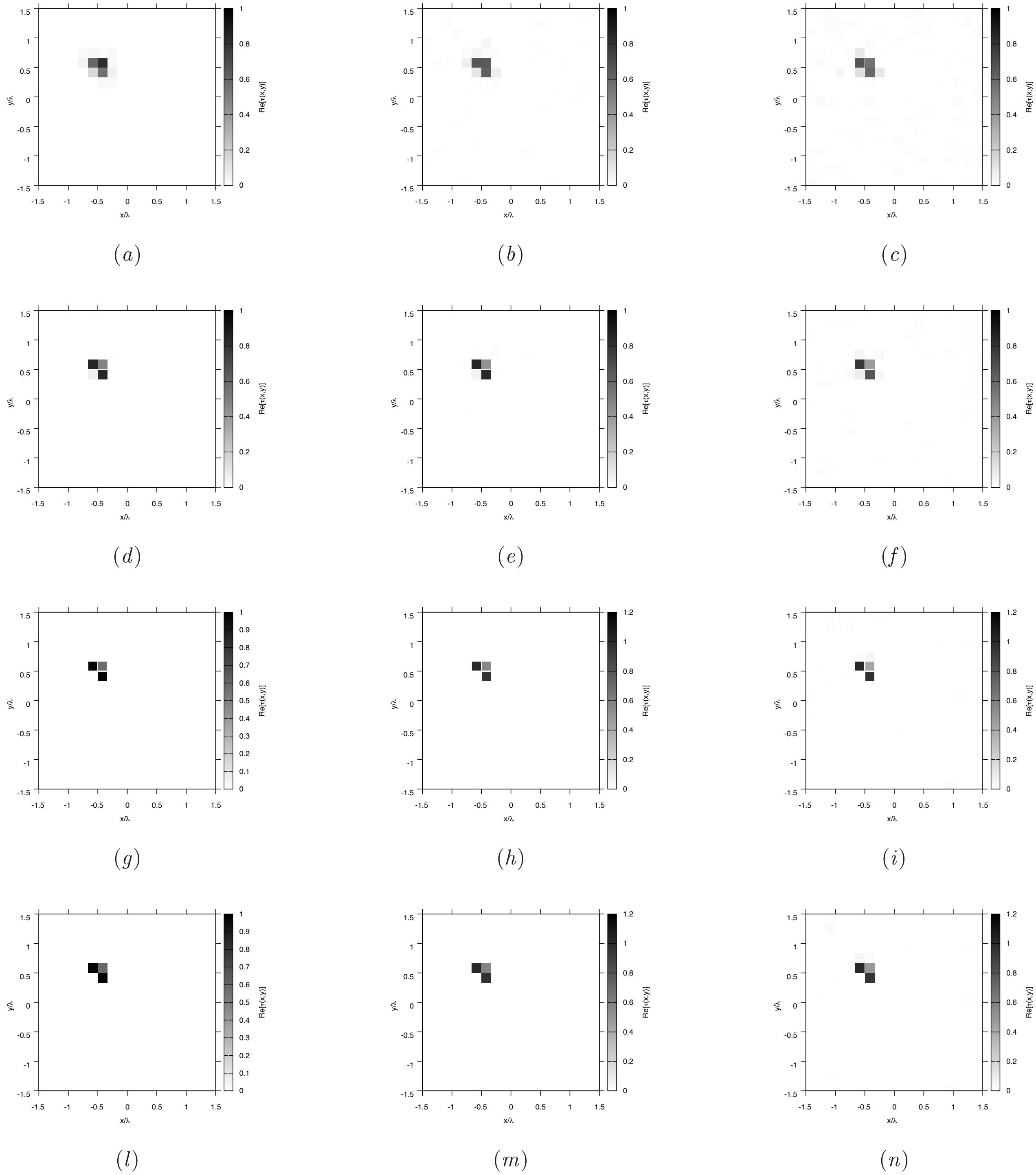

Figure 47. ST-BCS reconstructed object $(a)(b)(c)$, MT-BCS-Jmn reconstructed $(d)(e)(f)$ object, MV-MT-BCS reconstructed $(g)(h)(i)$ and MV-MT-BCS-Jmn reconstructed $(l)(m)(n)$ for Noiseless case $(a)(d)(g)(l)$, $SNR = 10$ [dB] $(b)(e)(h)(m)$ and $SNR = 5$ [dB] $(c)(f)(i)(n)$.

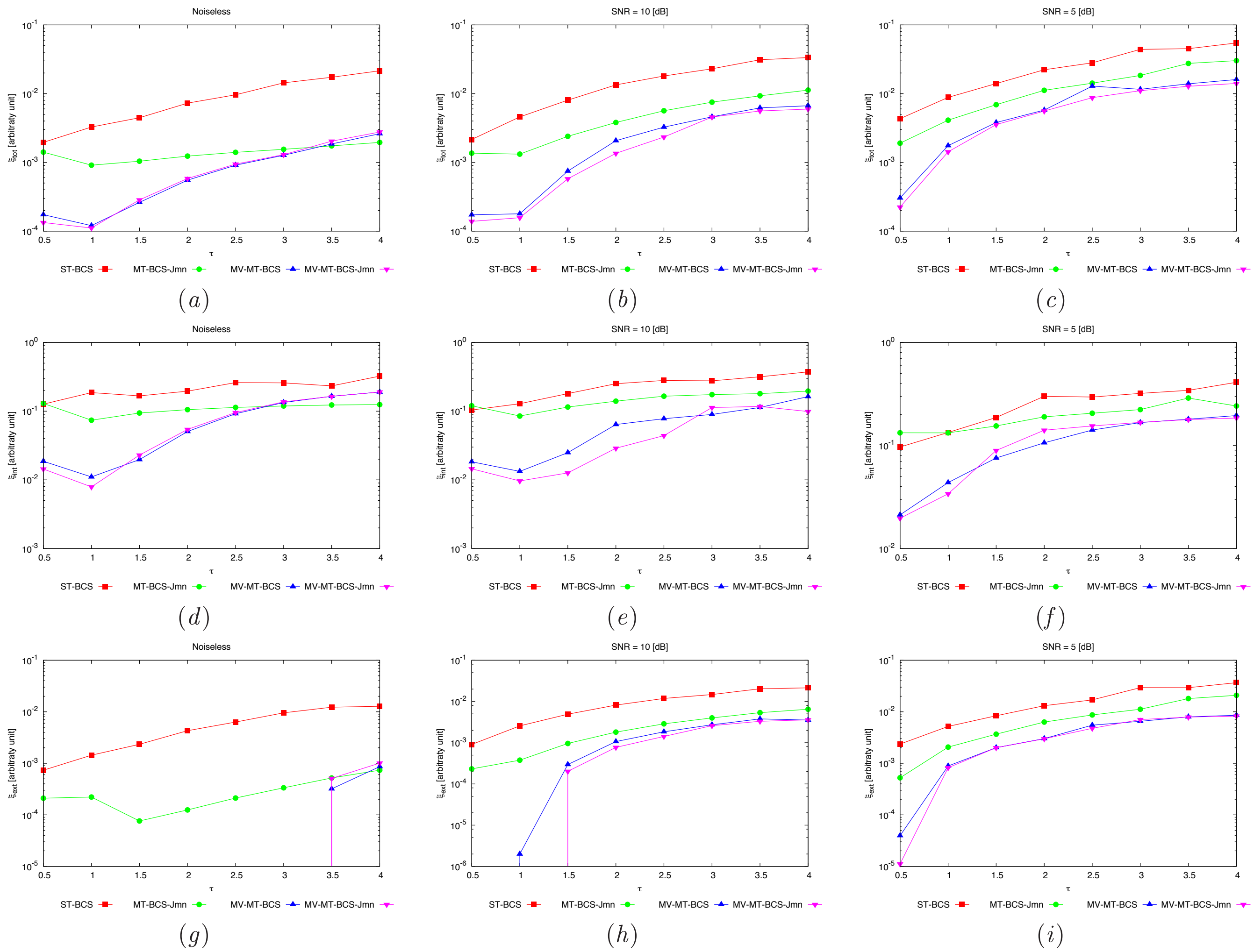

Figure 48. Behaviour of total error ξ_{tot} $(a)(b)(c)$, internal error ξ_{int} $(d)(e)(f)$ and external error ξ_{ext} $(g)(h)(i)$ for Noiseless case $(a)(d)(g)$, $SNR = 10$ [dB] $(b)(e)(h)$ and $SNR = 5$ [dB] $(c)(f)(i)$.

3.7 TEST CASE: Two Square Cylinders $L = 0.33\lambda$

Goal: show the performances of BCS when dealing with a sparse scatterer

- Number of Views: V
- Number of Measurements: M
- Number of Cells for the Inversion: N
- Number of Cells for the Direct solver: D
- Side of the investigation domain: L

Test Case Description

Direct solver:

- Square domain divided in $\sqrt{D} \times \sqrt{D}$ cells
- Domain side: $L = 3\lambda$
- $D = 1296$ (discretization for the direct solver: $< \lambda/10$)

Investigation domain:

- Square domain divided in $\sqrt{N} \times \sqrt{N}$ cells
- $L = 3\lambda$
- $2ka = 2 \times \frac{2\pi}{\lambda} \times \frac{L\sqrt{2}}{2} = 6\pi\sqrt{2} = 26.65$
- $\#DOF = \frac{(2ka)^2}{2} = \frac{(2\times\frac{2\pi}{\lambda}\times\frac{L\sqrt{2}}{2})^2}{2} = 4\pi^2\left(\frac{L}{\lambda}\right)^2 = 4\pi^2 \times 9 \approx 355.3$
- N scelto in modo da essere vicino a $\#DOF$: $N = 324$ (18×18)

Measurement domain:

- Measurement points taken on a circle of radius $\rho = 3\lambda$
- Full-aspect measurements
- $M \approx 2ka \rightarrow M = 27$

Sources:

- Plane waves
- $V \approx 2ka \rightarrow V = 27$
- Amplitude $A = 1$
- Frequency: 300 MHz ($\lambda = 1$)

Object:

- Two square cylinders of side $\frac{\lambda}{3} = 0.3333$
- $\varepsilon_r \in \{1.5, 2.0, 2.5, 3.0, 3.5, 4.0, 4.5, 5.0\}$
- $\sigma = 0$ [S/m]

MV-MT-BCS-Jmn parameters:

- Gamma prior on noise variance parameter: $a = 5 \times 10^0$
- Gamma prior on noise variance parameter: $b = 2 \times 10^{-2}$
- Convergenze parameter: $\tau = 1.0 \times 10^{-8}$

RESULTS: Two Square Cylinders $L = 0.33\lambda$

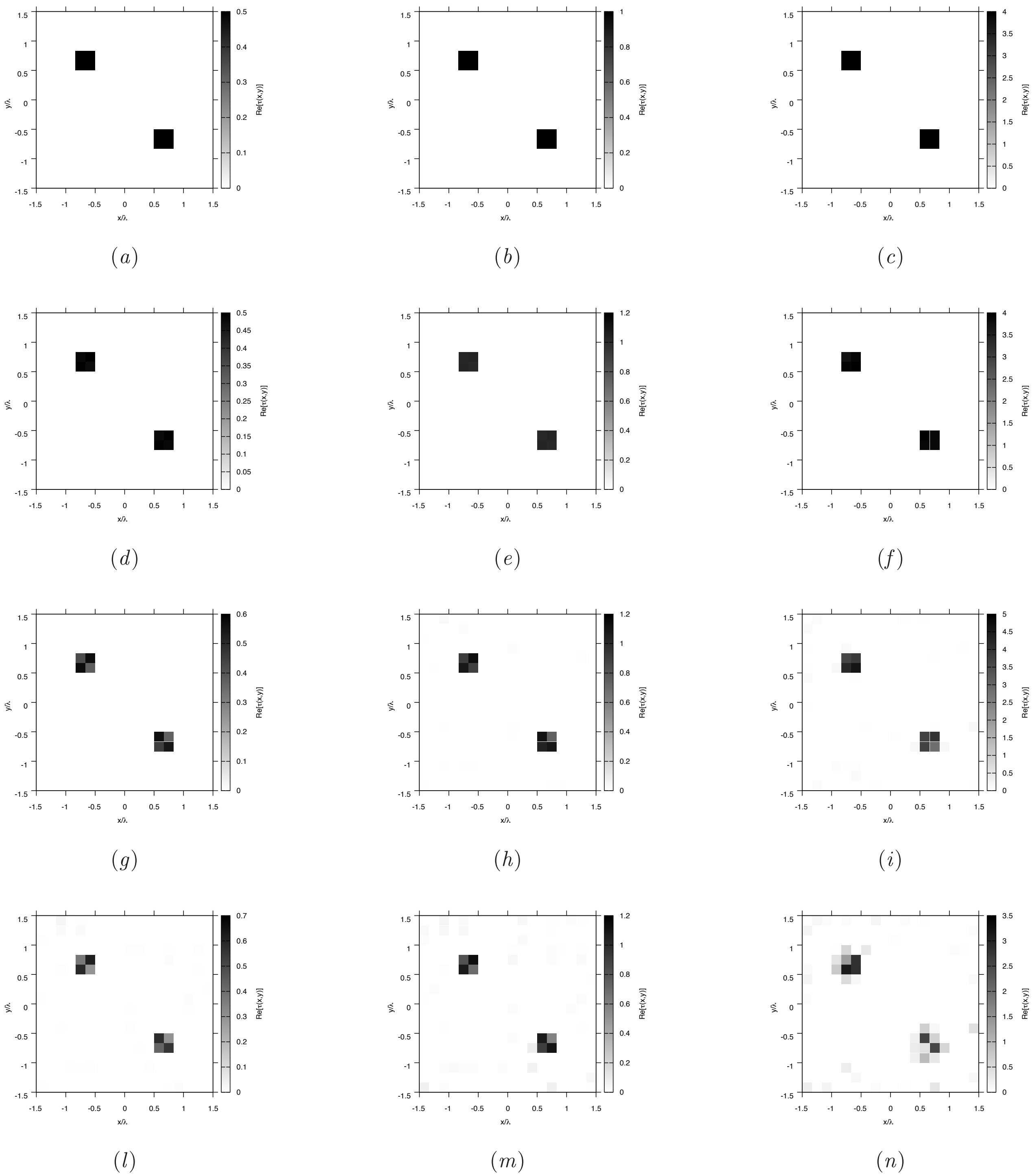

Figure 49. Actual object $(a)(b)(c)$ and MV-MT-BCS-Jmn reconstructed object with $\varepsilon_r = 1.5$ $(d)(g)(l)$, $\varepsilon_r = 2.0$ $(e)(h)(m)$, and $\varepsilon_r = 5.0$ $(f)(i)(n)$, for Noiseless case $(d)(e)(f)$, $SNR = 10$ [dB] $(g)(h)(i)$ and $SNR = 5$ [dB] $(l)(m)(n)$.

RESULTS: Two Square Cylinders $L = 0.33\lambda$ - Reconstructions - Comparison ST-BCS/MT-BCS - $\varepsilon_r = 2.0$

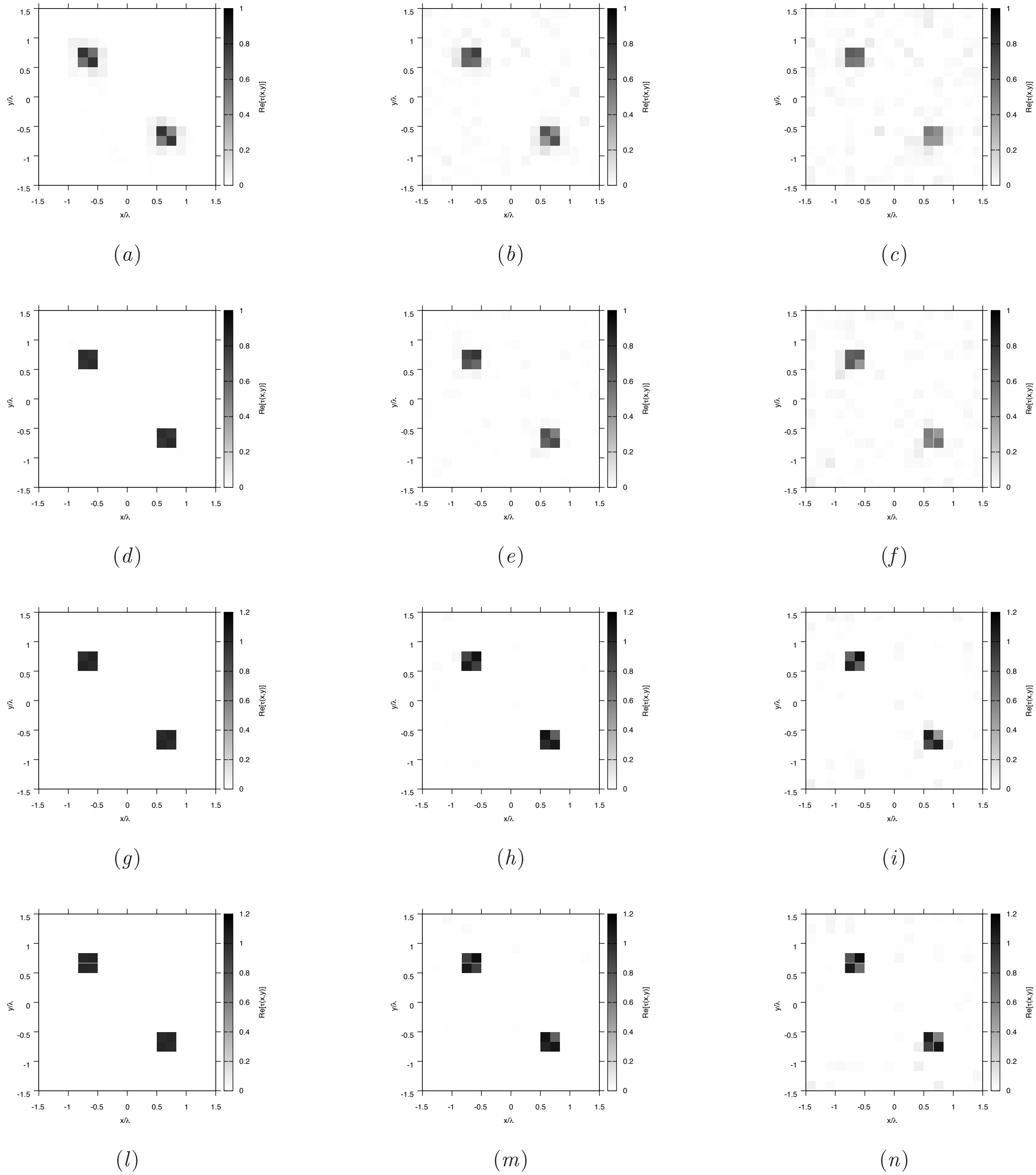

Figure 50. ST-BCS reconstructed object $(a)(b)(c)$, MT-BCS-Jmn reconstructed $(d)(e)(f)$ object, MV-MT-BCS reconstructed $(g)(h)(i)$ and MV-MT-BCS-Jmn reconstructed $(l)(m)(n)$ for Noiseless case $(a)(d)(g)(l)$, $SNR = 10$ [dB] $(b)(e)(h)(m)$ and $SNR = 5$ [dB] $(c)(f)(i)(n)$.

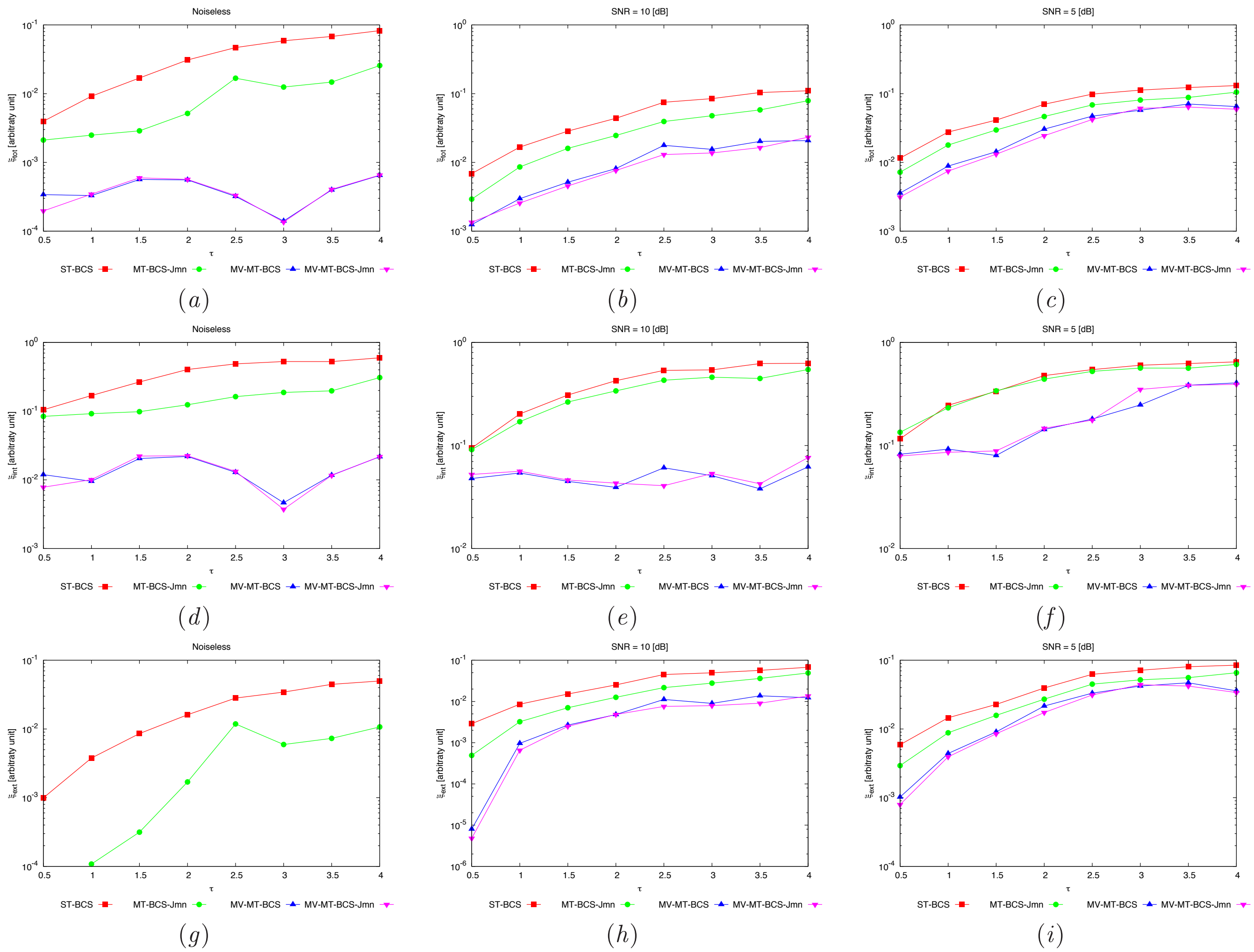

Figure 51. Behaviour of total error ξ_{tot} $(a)(b)(c)$, internal error ξ_{int} $(d)(e)(f)$ and external error ξ_{ext} $(g)(h)(i)$ for Noiseless case $(a)(d)(g)$, $SNR = 10$ [dB] $(b)(e)(h)$ and $SNR = 5$ [dB] $(c)(f)(i)$.

3.8 TEST CASE: Two L-shaped Cylinders

Goal: show the performances of BCS when dealing with a sparse scatterer

- Number of Views: V
- Number of Measurements: M
- Number of Cells for the Inversion: N
- Number of Cells for the Direct solver: D
- Side of the investigation domain: L

Test Case Description

Direct solver:

- Square domain divided in $\sqrt{D} \times \sqrt{D}$ cells
- Domain side: $L = 3\lambda$
- $D = 1296$ (discretization for the direct solver: $< \lambda/10$)

Investigation domain:

- Square domain divided in $\sqrt{N} \times \sqrt{N}$ cells
- $L = 3\lambda$
- $2ka = 2 \times \frac{2\pi}{\lambda} \times \frac{L\sqrt{2}}{2} = 6\pi\sqrt{2} = 26.65$
- $\#DOF = \frac{(2ka)^2}{2} = \frac{(2\times\frac{2\pi}{\lambda}\times\frac{L\sqrt{2}}{2})^2}{2} = 4\pi^2\left(\frac{L}{\lambda}\right)^2 = 4\pi^2 \times 9 \approx 355.3$
- N scelto in modo da essere vicino a $\#DOF$: $N = 324$ (18×18)

Measurement domain:

- Measurement points taken on a circle of radius $\rho = 3\lambda$
- Full-aspect measurements
- $M \approx 2ka \rightarrow M = 27$

Sources:

- Plane waves
- $V \approx 2ka \rightarrow V = 27$
- Amplitude $A = 1$
- Frequency: 300 MHz ($\lambda = 1$)

Object:

- Two L-shaped cylinders
- $\varepsilon_r \in \{1.5, 2.0, 2.5, 3.0, 3.5, 4.0, 4.5, 5.0\}$
- $\sigma = 0$ [S/m]

MV-MT-BCS-Jmn parameters:

- Gamma prior on noise variance parameter: $a = 5 \times 10^0$
- Gamma prior on noise variance parameter: $b = 2 \times 10^{-2}$
- Convergenze parameter: $\tau = 1.0 \times 10^{-8}$

RESULTS: Two L-Shaped Cylinders

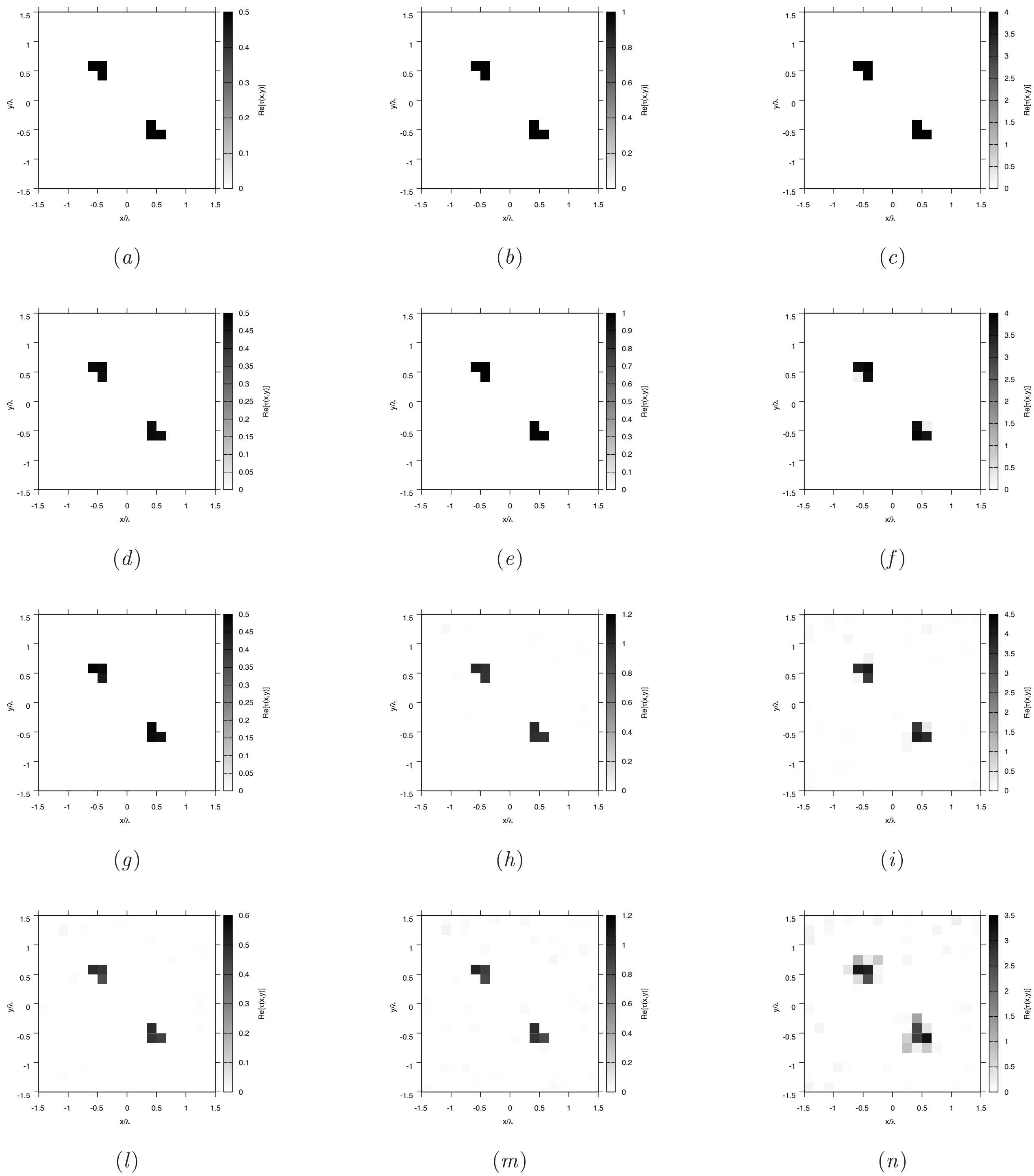

Figure 52. Actual object $(a)(b)(c)$ and MV-MT-BCS-Jmn reconstructed object with $\varepsilon_r = 1.5$ $(d)(g)(l)$, $\varepsilon_r = 2.0$ $(e)(h)(m)$, and $\varepsilon_r = 5.0$ $(f)(i)(n)$, for Noiseless case $(d)(e)(f)$, $SNR = 10$ [dB] $(g)(h)(i)$ and $SNR = 5$ [dB] $(l)(m)(n)$.

RESULTS: Two L-Shaped Cylinders - Reconstructions - Comparison ST-BCS/MT-BCS - $\varepsilon_r = 2.0$

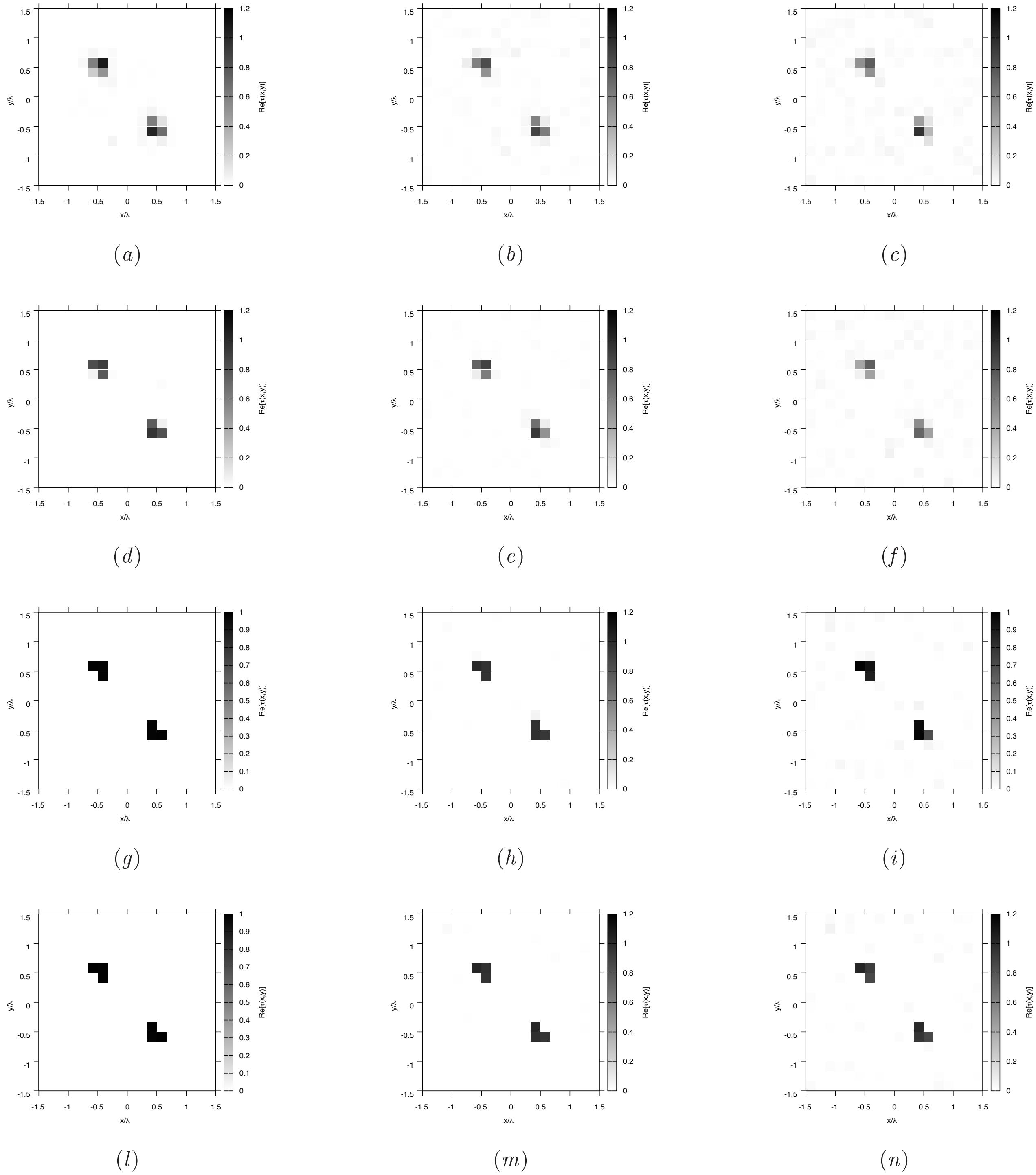

Figure 53. ST-BCS reconstructed object $(a)(b)(c)$, MT-BCS-Jmn reconstructed $(d)(e)(f)$ object, MV-MT-BCS reconstructed $(g)(h)(i)$ and MV-MT-BCS-Jmn reconstructed $(l)(m)(n)$ for Noiseless case $(a)(d)(g)(l)$, $SNR = 10$ [dB] $(b)(e)(h)(m)$ and $SNR = 5$ [dB] $(c)(f)(i)(n)$.

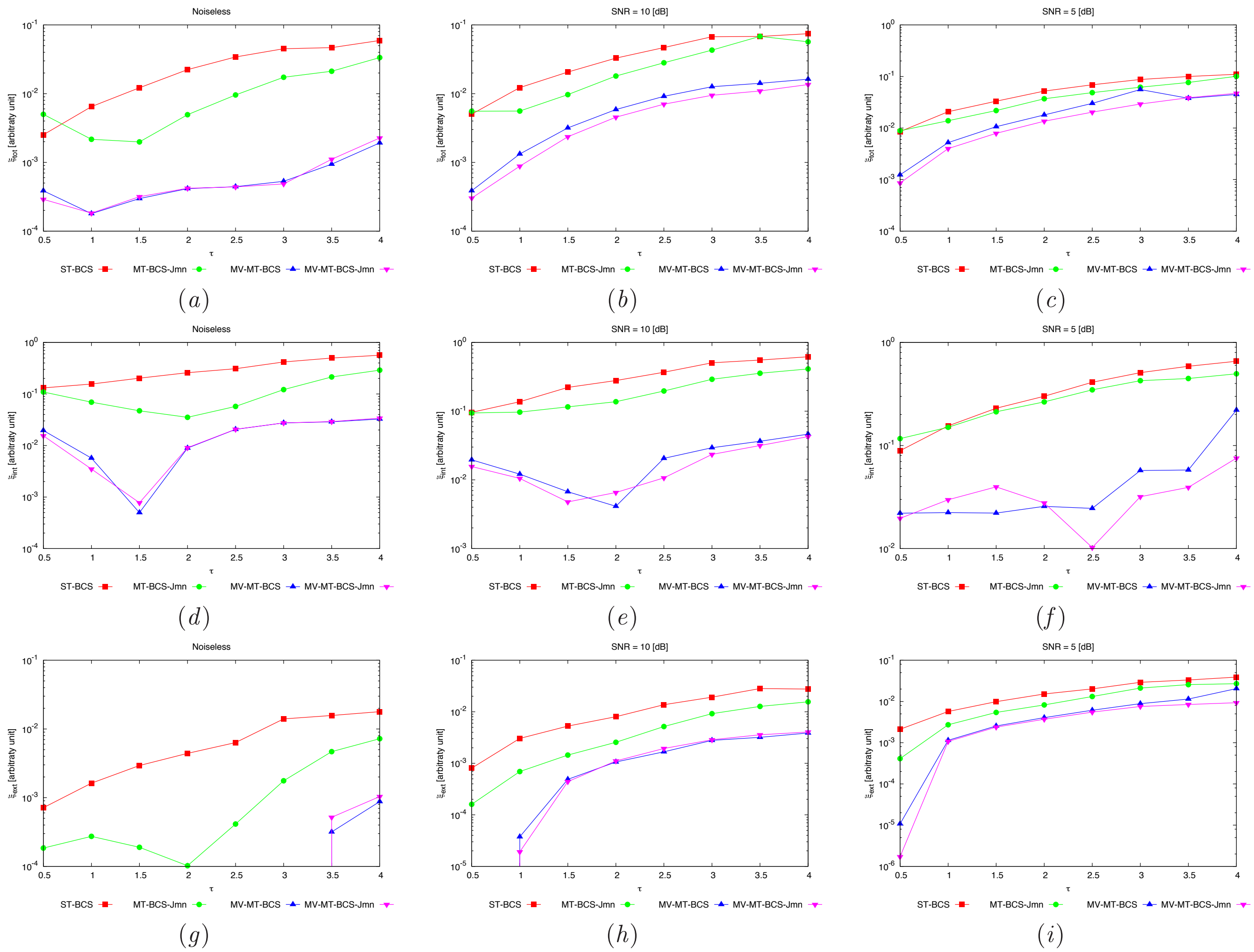

Figure 54. Behaviour of total error ξ_{tot} $(a)(b)(c)$, internal error ξ_{int} $(d)(e)(f)$ and external error ξ_{ext} $(g)(h)(i)$ for Noiseless case $(a)(d)(g)$, $SNR = 10$ [dB] $(b)(e)(h)$ and $SNR = 5$ [dB] $(c)(f)(i)$.

3.9 TEST CASE: Big L-shaped Cylinder

Goal: show the performances of BCS when dealing with a sparse scatterer

- Number of Views: V
- Number of Measurements: M
- Number of Cells for the Inversion: N
- Number of Cells for the Direct solver: D
- Side of the investigation domain: L

Test Case Description

Direct solver:

- Square domain divided in $\sqrt{D} \times \sqrt{D}$ cells
- Domain side: $L = 3\lambda$
- $D = 1296$ (discretization for the direct solver: $< \lambda/10$)

Investigation domain:

- Square domain divided in $\sqrt{N} \times \sqrt{N}$ cells
- $L = 3\lambda$
- $2ka = 2 \times \frac{2\pi}{\lambda} \times \frac{L\sqrt{2}}{2} = 6\pi\sqrt{2} = 26.65$
- $\#DOF = \frac{(2ka)^2}{2} = \frac{(2 \times \frac{2\pi}{\lambda} \times \frac{L\sqrt{2}}{2})^2}{2} = 4\pi^2 \left(\frac{L}{\lambda}\right)^2 = 4\pi^2 \times 9 \approx 355.3$
- N scelto in modo da essere vicino a $\#DOF$: $N = 324$ (18×18)

Measurement domain:

- Measurement points taken on a circle of radius $\rho = 3\lambda$
- Full-aspect measurements
- $M \approx 2ka \rightarrow M = 27$

Sources:

- Plane waves
- $V \approx 2ka \rightarrow V = 27$
- Amplitude $A = 1$
- Frequency: 300 MHz ($\lambda = 1$)

Object:

- Big L-shaped cylinder
- $\varepsilon_r \in \{1.5, 2.0, 2.5, 3.0, 3.5, 4.0, 4.5, 5.0\}$
- $\sigma = 0$ [S/m]

MV-MT-BCS-Jmn parameters:

- Gamma prior on noise variance parameter: $a = 5 \times 10^0$
- Gamma prior on noise variance parameter: $b = 2 \times 10^{-2}$
- Convergenze parameter: $\tau = 1.0 \times 10^{-8}$

RESULTS: Big L-Shaped Cylinder

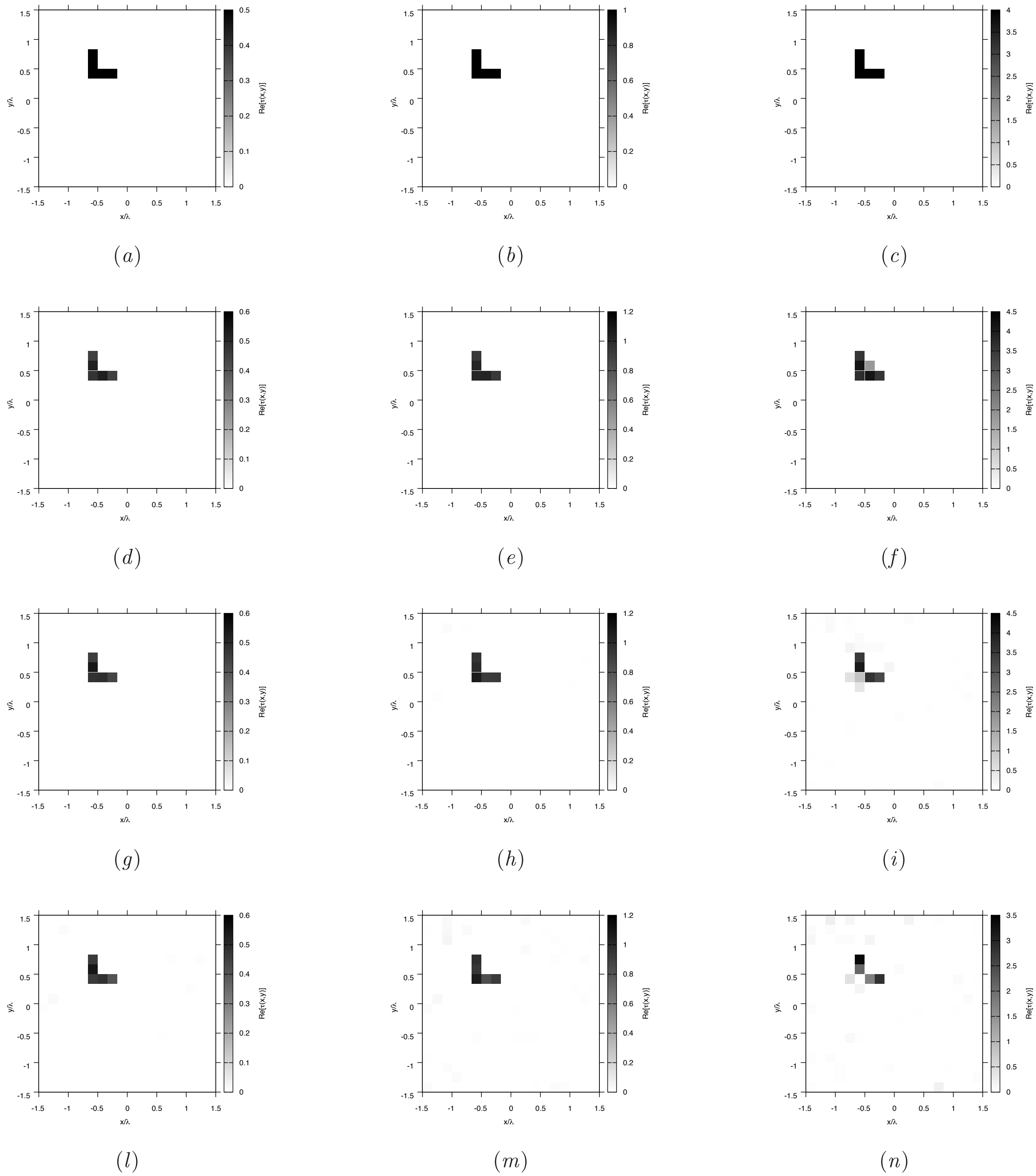

Figure 55. Actual object $(a)(b)(c)$ and MV-MT-BCS-Jmn reconstructed object with $\varepsilon_r = 1.5$ $(d)(g)(l)$, $\varepsilon_r = 2.0$ $(e)(h)(m)$, and $\varepsilon_r = 5.0$ $(f)(i)(n)$, for Noiseless case $(d)(e)(f)$, $SNR = 10$ [dB] $(g)(h)(i)$ and $SNR = 5$ [dB] $(l)(m)(n)$.

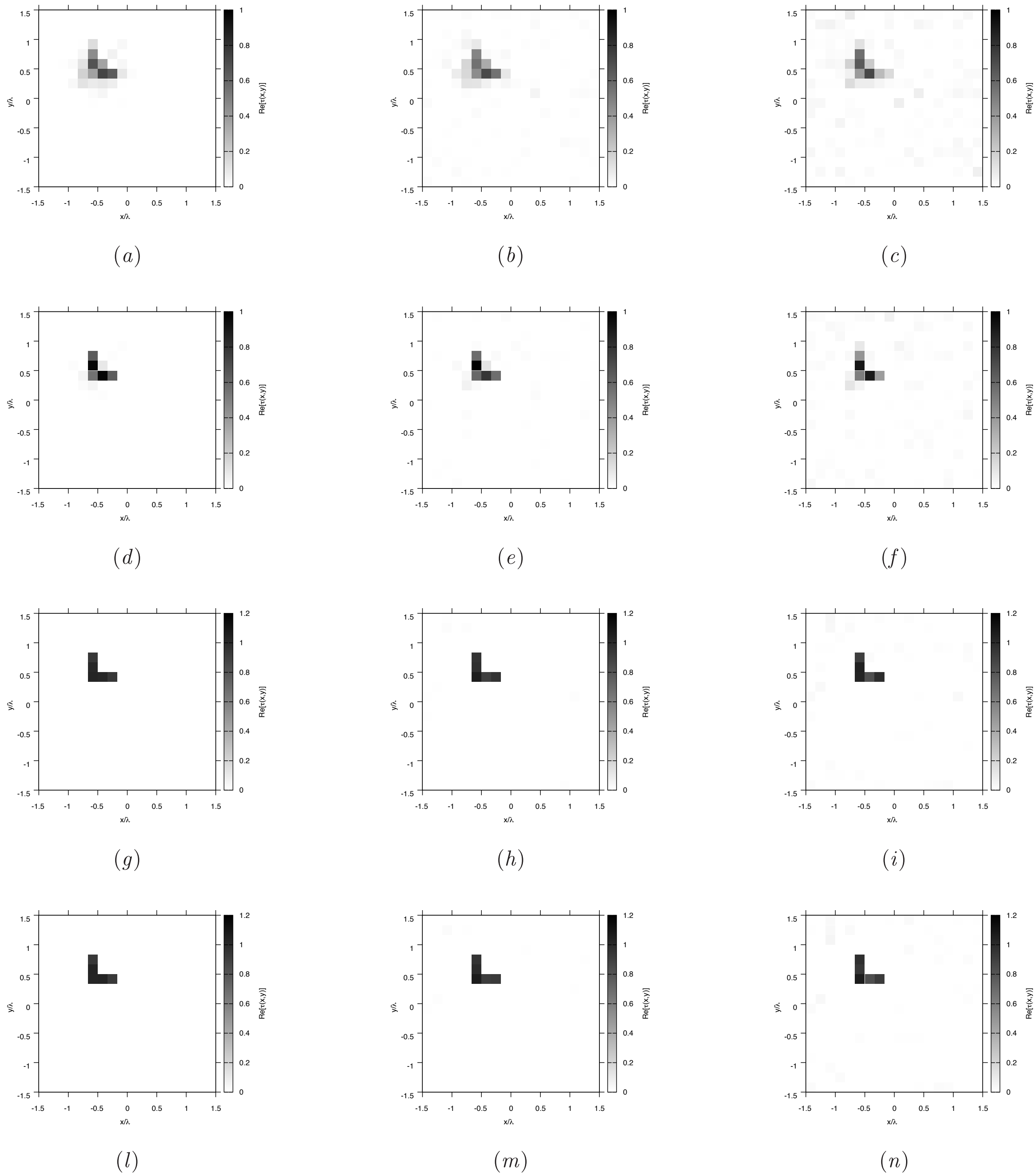

Figure 56. ST-BCS reconstructed object $(a)(b)(c)$, MT-BCS-Jmn reconstructed $(d)(e)(f)$ object, MV-MT-BCS reconstructed $(g)(h)(i)$ and MV-MT-BCS-Jmn reconstructed $(l)(m)(n)$ for Noiseless case $(a)(d)(g)(l)$, $SNR = 10$ [dB] $(b)(e)(h)(m)$ and $SNR = 5$ [dB] $(c)(f)(i)(n)$.

RESULTS: Big L-Shaped Cylinder - Error Figures - Comparison ST-BCS/MT-BCS

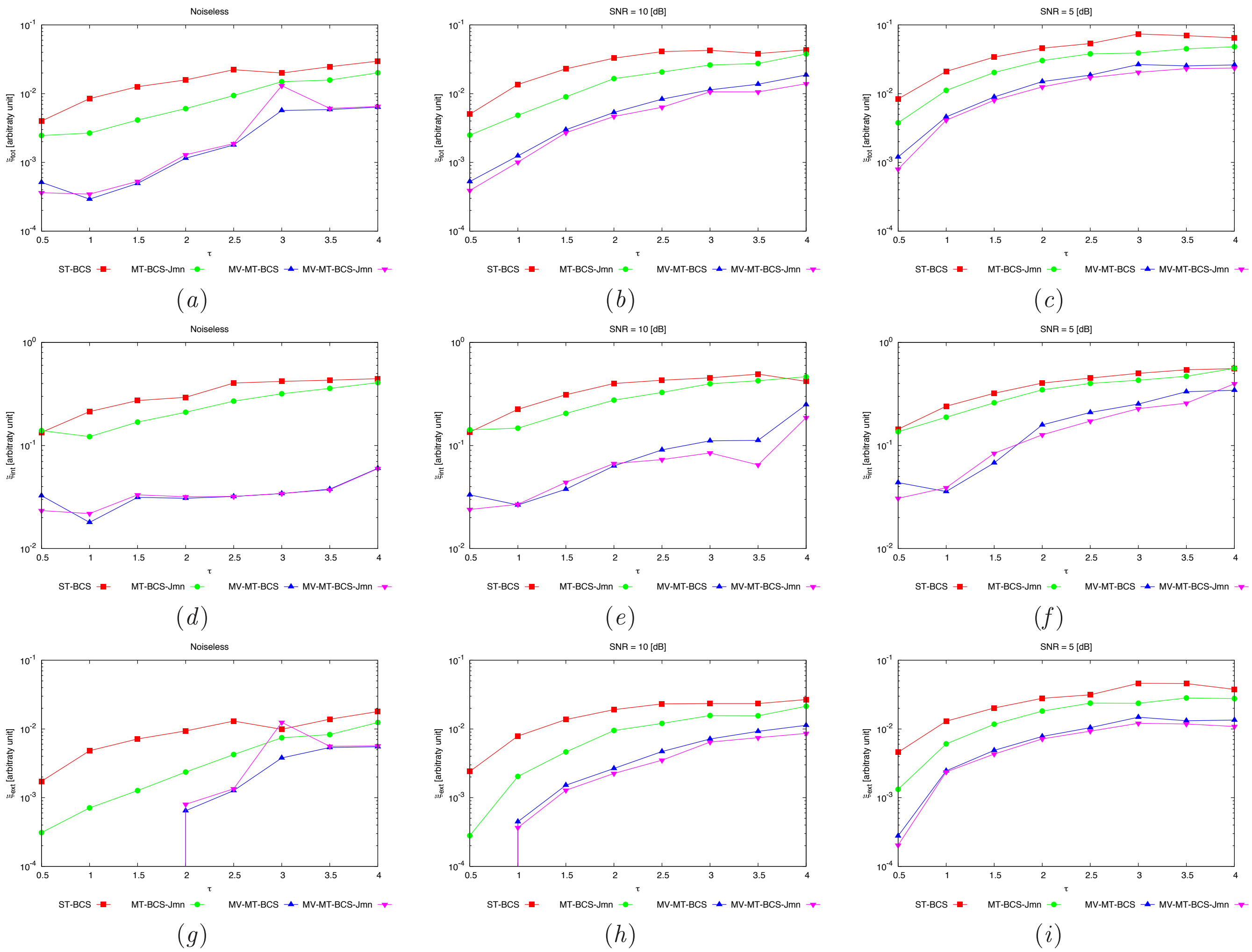

Figure 57. Behaviour of error figures as a function of ε_r, for different SNR values: (a) total error ξ_{tot}, (b) internal error ξ_{int}, (c) external error ξ_{ext}.

3.10 TEST CASE: Big T-shaped Cylinder

Goal: show the performances of BCS when dealing with a sparse scatterer

- Number of Views: V
- Number of Measurements: M
- Number of Cells for the Inversion: N
- Number of Cells for the Direct solver: D
- Side of the investigation domain: L

Test Case Description

Direct solver:

- Square domain divided in $\sqrt{D} \times \sqrt{D}$ cells
- Domain side: $L = 3\lambda$
- $D = 1296$ (discretization for the direct solver: $< \lambda/10$)

Investigation domain:

- Square domain divided in $\sqrt{N} \times \sqrt{N}$ cells
- $L = 3\lambda$
- $2ka = 2 \times \frac{2\pi}{\lambda} \times \frac{L\sqrt{2}}{2} = 6\pi\sqrt{2} = 26.65$
- $\#DOF = \frac{(2ka)^2}{2} = \frac{(2\times\frac{2\pi}{\lambda}\times\frac{L\sqrt{2}}{2})^2}{2} = 4\pi^2\left(\frac{L}{\lambda}\right)^2 = 4\pi^2 \times 9 \approx 355.3$
- N scelto in modo da essere vicino a $\#DOF$: $N = 324$ (18×18)

Measurement domain:

- Measurement points taken on a circle of radius $\rho = 3\lambda$
- Full-aspect measurements
- $M \approx 2ka \rightarrow M = 27$

Sources:

- Plane waves
- $V \approx 2ka \rightarrow V = 27$
- Amplitude $A = 1$
- Frequency: 300 MHz ($\lambda = 1$)

Object:

- Big T-shaped cylinder
- $\varepsilon_r \in \{1.5, 2.0, 2.5, 3.0, 3.5, 4.0, 4.5, 5.0\}$
- $\sigma = 0$ [S/m]

MV-MT-BCS-Jmn parameters:

- Gamma prior on noise variance parameter: $a = 5 \times 10^0$
- Gamma prior on noise variance parameter: $b = 2 \times 10^{-2}$
- Convergenze parameter: $\tau = 1.0 \times 10^{-8}$

RESULTS: Big T-Shaped Cylinder

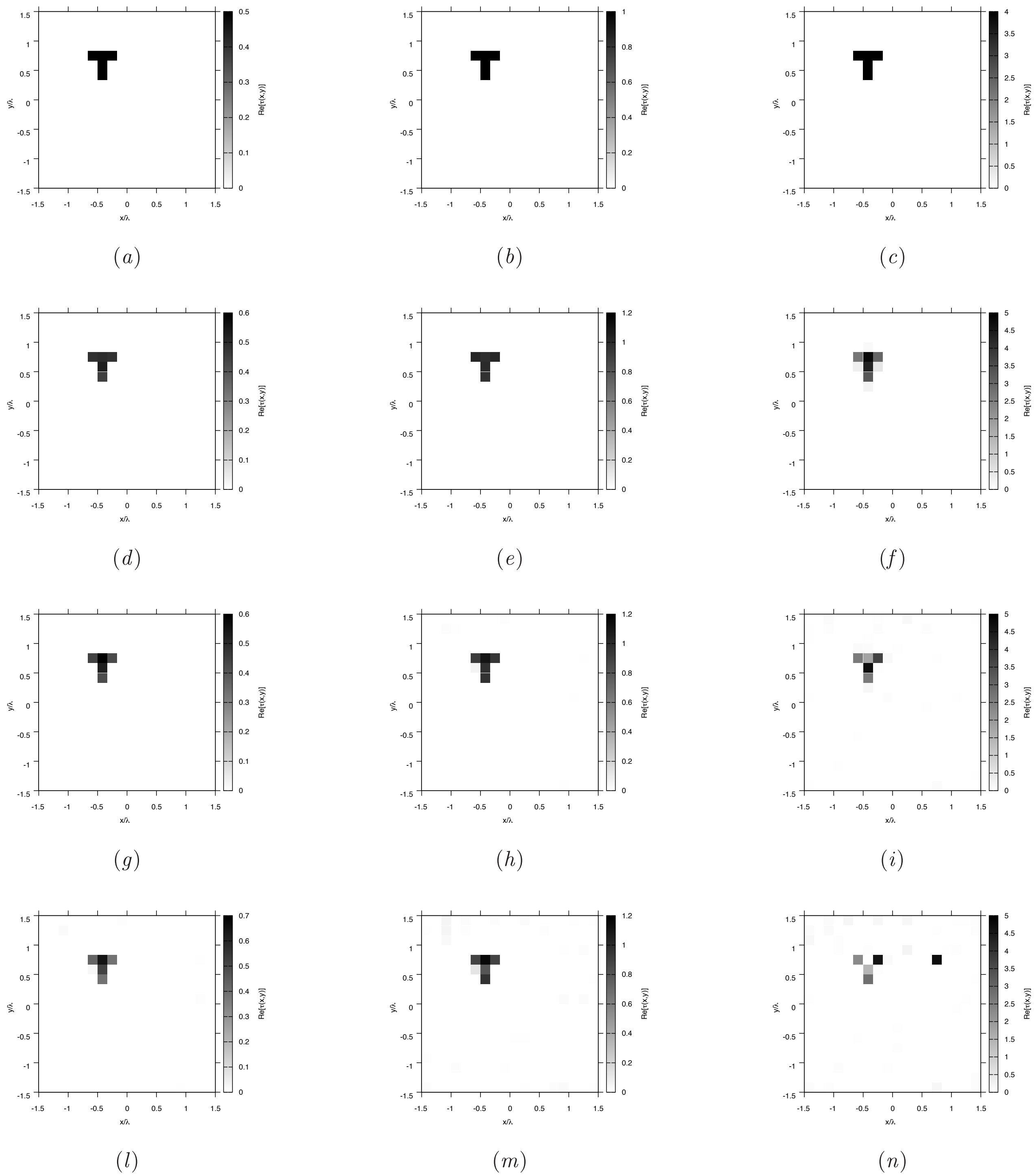

Figure 58. Actual object $(a)(b)(c)$ and MV-MT-BCS-Jmn reconstructed object with $\varepsilon_r = 1.5$ $(d)(g)(l)$, $\varepsilon_r = 2.0$ $(e)(h)(m)$, and $\varepsilon_r = 5.0$ $(f)(i)(n)$, for Noiseless case $(d)(e)(f)$, $SNR = 10$ [dB] $(g)(h)(i)$ and $SNR = 5$ [dB] $(l)(m)(n)$.

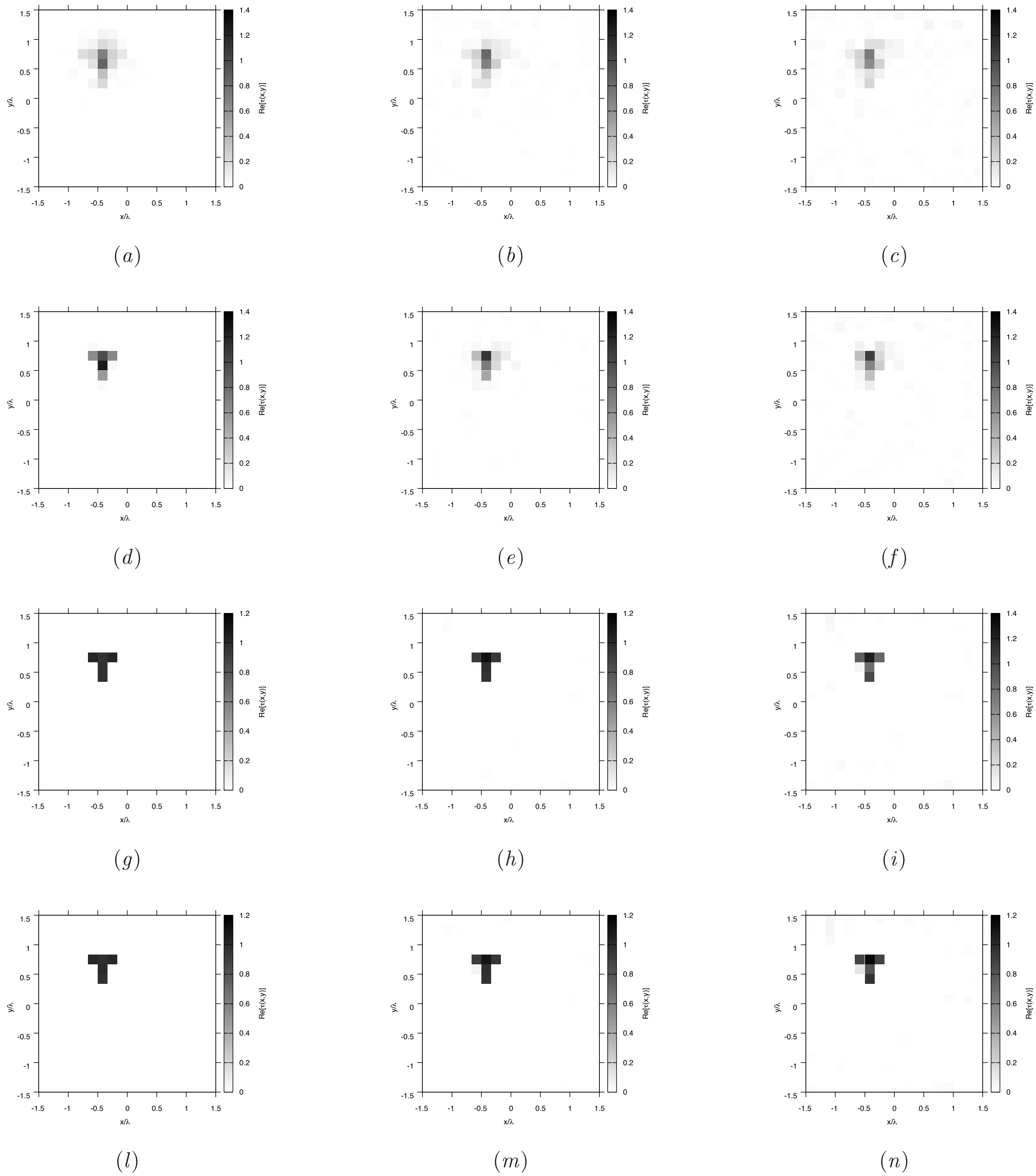

Figure 59. ST-BCS reconstructed object $(a)(b)(c)$, MT-BCS-Jmn reconstructed $(d)(e)(f)$ object, MV-MT-BCS reconstructed $(g)(h)(i)$ and MV-MT-BCS-Jmn reconstructed $(l)(m)(n)$ for Noiseless case $(a)(d)(g)(l)$, $SNR = 10$ [dB] $(b)(e)(h)(m)$ and $SNR = 5$ [dB] $(c)(f)(i)(n)$.

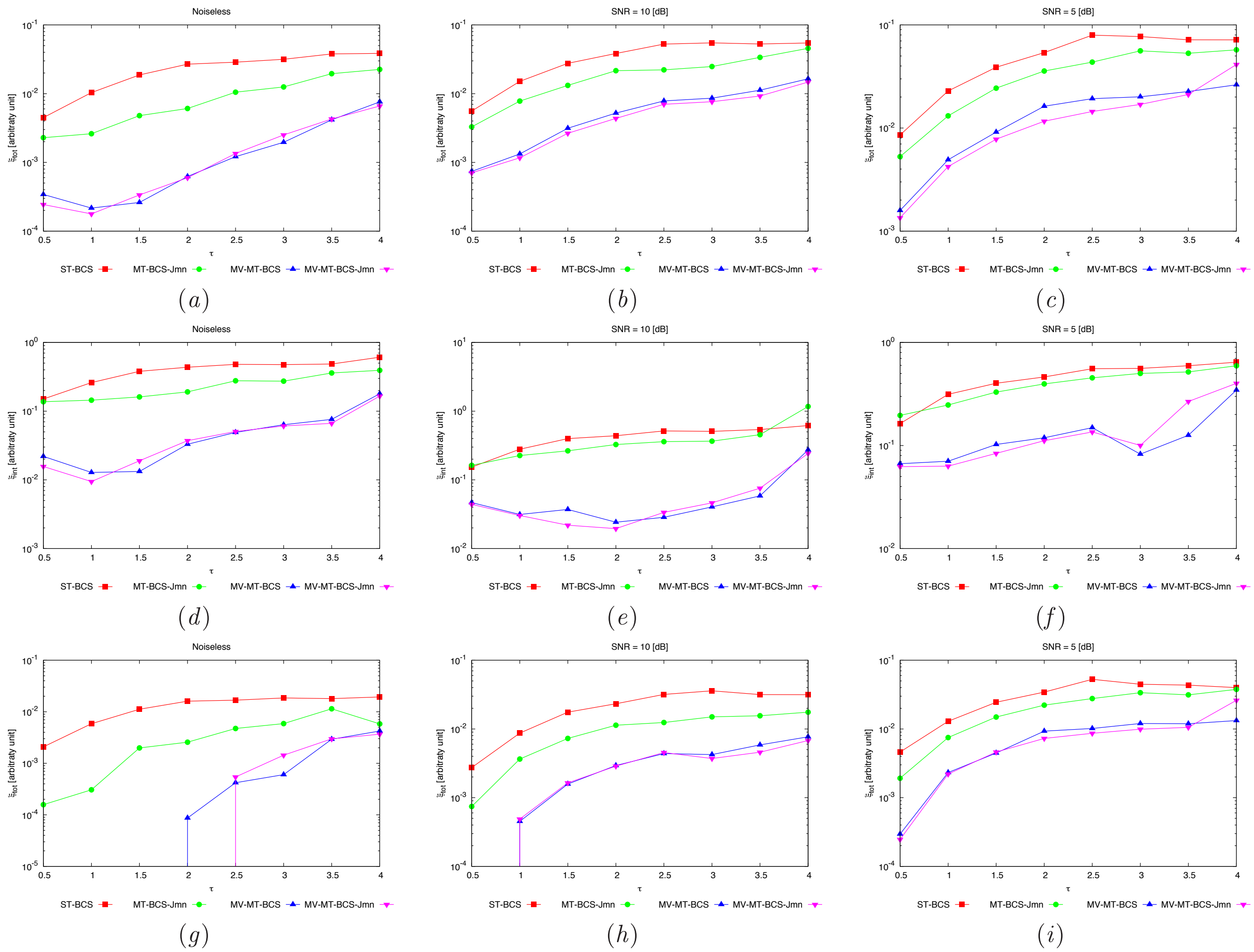

Figure 60. Behaviour of total error ξ_{tot} $(a)(b)(c)$, internal error ξ_{int} $(d)(e)(f)$ and external error ξ_{ext} $(g)(h)(i)$ for Noiseless case $(a)(d)(g)$, $SNR = 10$ [dB] $(b)(e)(h)$ and $SNR = 5$ [dB] $(c)(f)(i)$.

3.11 TEST CASE: Two Adjacent L-Shaped Cylinders

Goal: show the performances of BCS when dealing with a sparse scatterer

- Number of Views: V
- Number of Measurements: M
- Number of Cells for the Inversion: N
- Number of Cells for the Direct solver: D
- Side of the investigation domain: L

Test Case Description

Direct solver:

- Square domain divided in $\sqrt{D} \times \sqrt{D}$ cells
- Domain side: $L = 3\lambda$
- $D = 1296$ (discretization for the direct solver: $< \lambda/10$)

Investigation domain:

- Square domain divided in $\sqrt{N} \times \sqrt{N}$ cells
- $L = 3\lambda$
- $2ka = 2 \times \frac{2\pi}{\lambda} \times \frac{L\sqrt{2}}{2} = 6\pi\sqrt{2} = 26.65$
- $\#DOF = \frac{(2ka)^2}{2} = \frac{(2\times\frac{2\pi}{\lambda}\times\frac{L\sqrt{2}}{2})^2}{2} = 4\pi^2\left(\frac{L}{\lambda}\right)^2 = 4\pi^2 \times 9 \approx 355.3$
- N scelto in modo da essere vicino a $\#DOF$: $N = 324$ (18×18)

Measurement domain:

- Measurement points taken on a circle of radius $\rho = 3\lambda$
- Full-aspect measurements
- $M \approx 2ka \rightarrow M = 27$

Sources:

- Plane waves
- $V \approx 2ka \rightarrow V = 27$
- Amplitude $A = 1$
- Frequency: 300 MHz ($\lambda = 1$)

Object:

- Two adjacent L-shaped cylinder
- $\varepsilon_r \in \{1.5, 2.0, 2.5, 3.0, 3.5, 4.0, 4.5, 5.0\}$
- $\sigma = 0$ [S/m]

MV-MT-BCS-Jmn parameters:

- Gamma prior on noise variance parameter: $a = 5 \times 10^0$
- Gamma prior on noise variance parameter: $b = 2 \times 10^{-2}$
- Convergenze parameter: $\tau = 1.0 \times 10^{-8}$

RESULTS: Two Adjacent L-shaped Cylinders

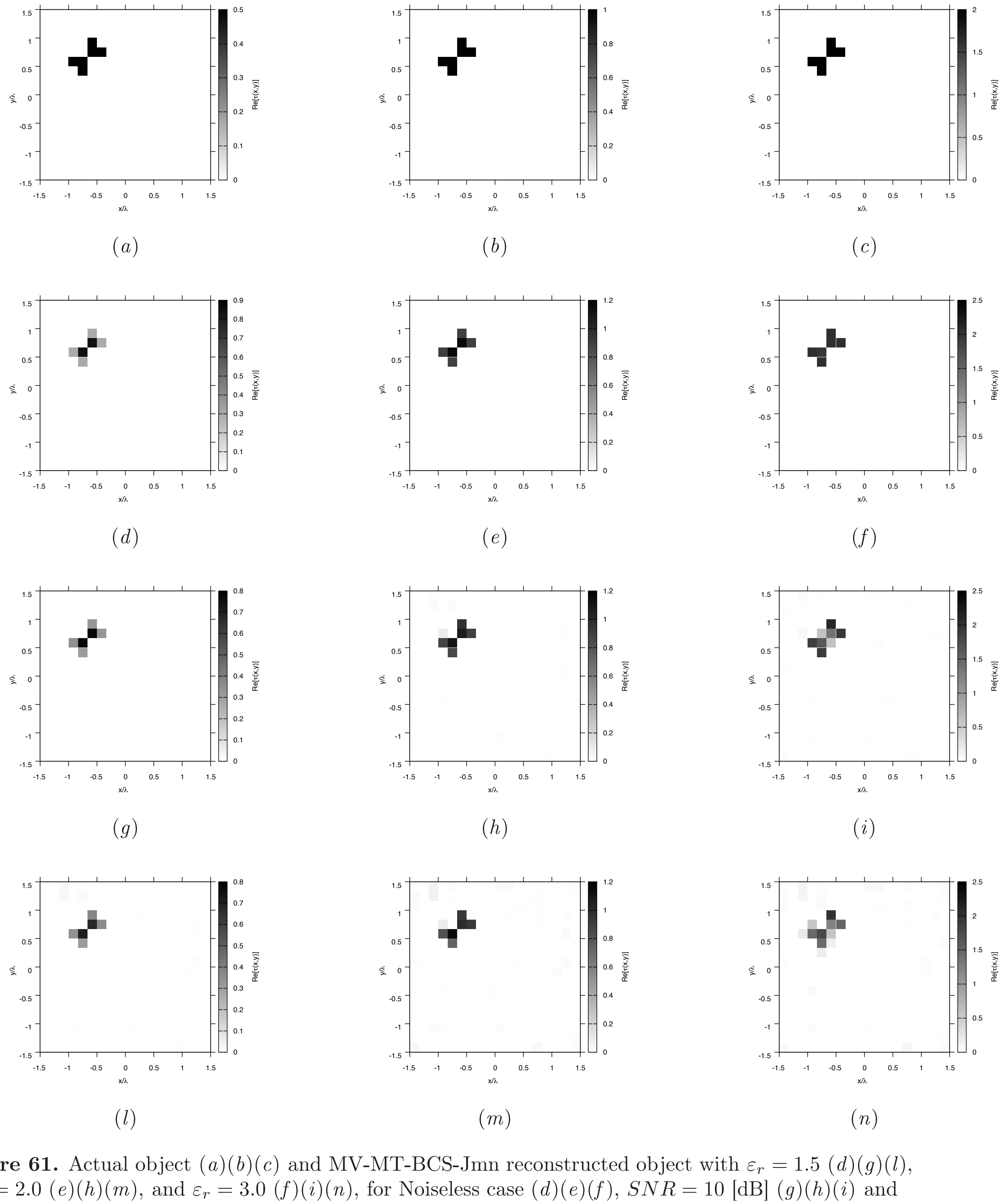

Figure 61. Actual object $(a)(b)(c)$ and MV-MT-BCS-Jmn reconstructed object with $\varepsilon_r = 1.5$ $(d)(g)(l)$, $\varepsilon_r = 2.0$ $(e)(h)(m)$, and $\varepsilon_r = 3.0$ $(f)(i)(n)$, for Noiseless case $(d)(e)(f)$, $SNR = 10$ [dB] $(g)(h)(i)$ and $SNR = 5$ [dB] $(l)(m)(n)$.

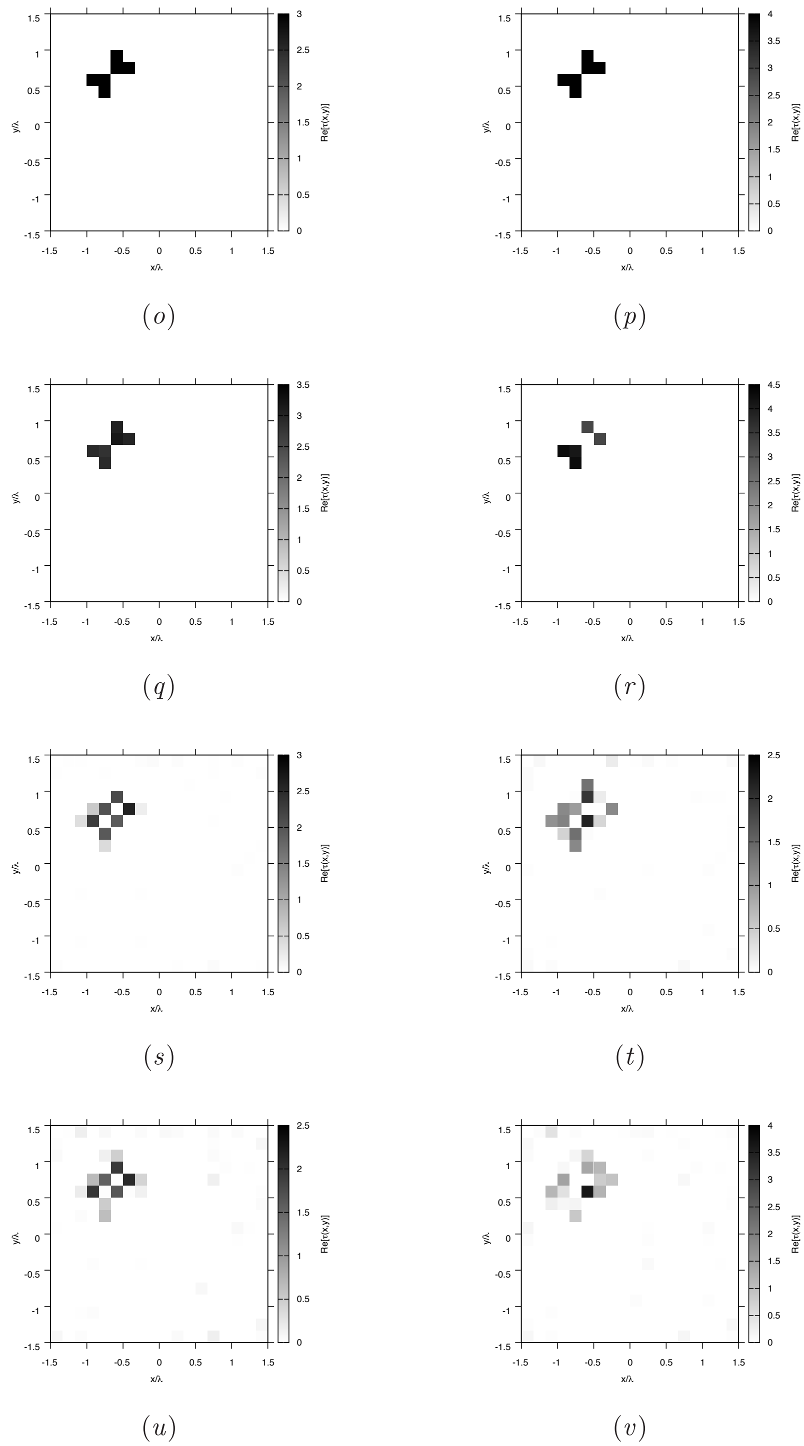

Figure 61. Actual object $(o)(p)$ and MV-MT-BCS-Jmn reconstructed object with $\varepsilon_r = 4.0$ $(q)(s)(u)$ and $\varepsilon_r = 5.0$ $(r)(t)(v)$ for Noiseless case $(q)(r)$, $SNR = 10$ [dB] $(s)(t)$ and $SNR = 5$ [dB] $(u)(v)$.

RESULTS: Two Adjacent L-shaped Cylinders - Reconstructions - Comparison ST-BCS/MT-BCS - $\varepsilon_r = 2.0$

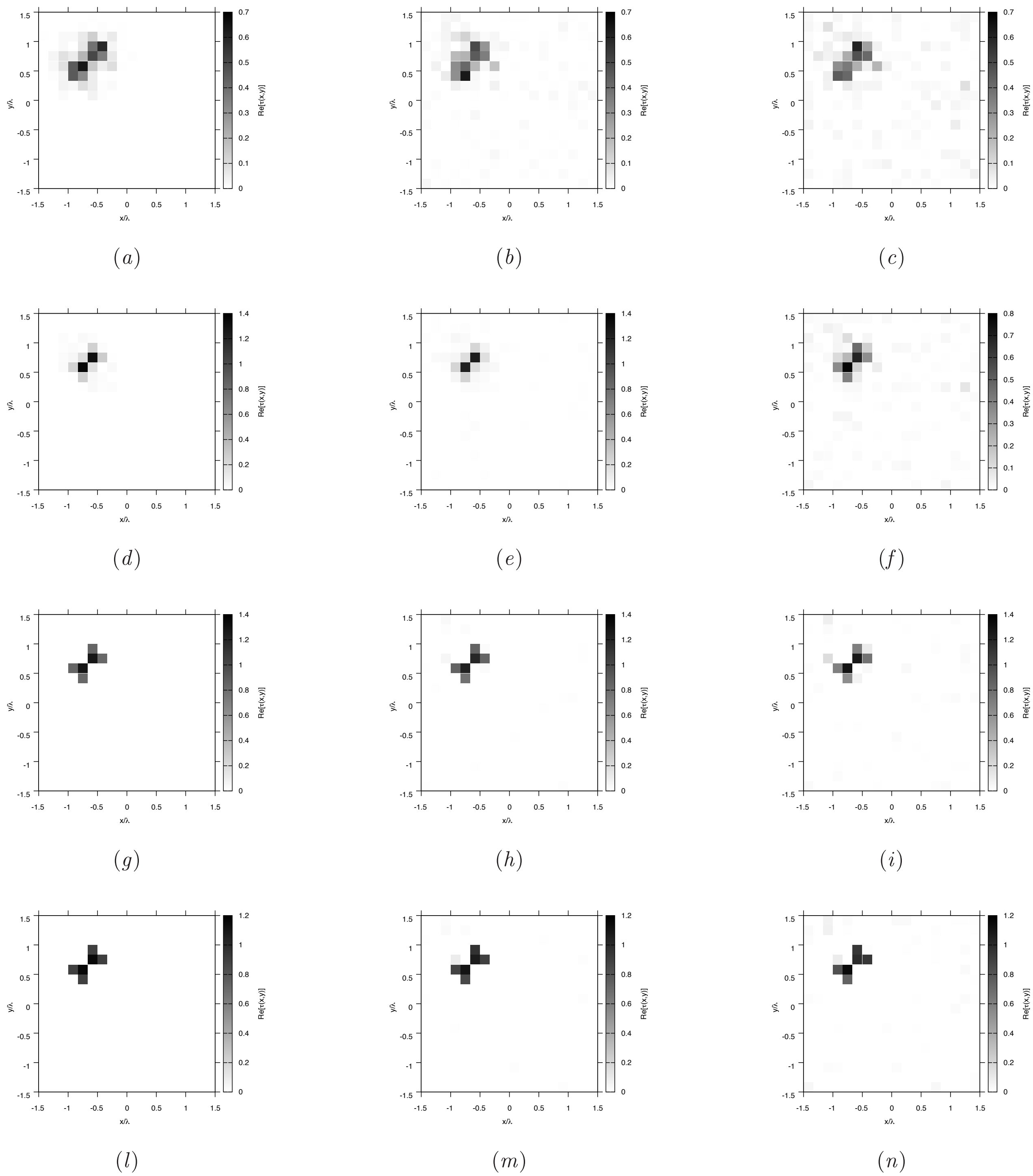

Figure 62. ST-BCS reconstructed object $(a)(b)(c)$, MT-BCS-Jmn reconstructed $(d)(e)(f)$ object, MV-MT-BCS reconstructed $(g)(h)(i)$ and MV-MT-BCS-Jmn reconstructed $(l)(m)(n)$ for Noiseless case $(a)(d)(g)(l)$, $SNR = 10$ [dB] $(b)(e)(h)(m)$ and $SNR = 5$ [dB] $(c)(f)(i)(n)$.

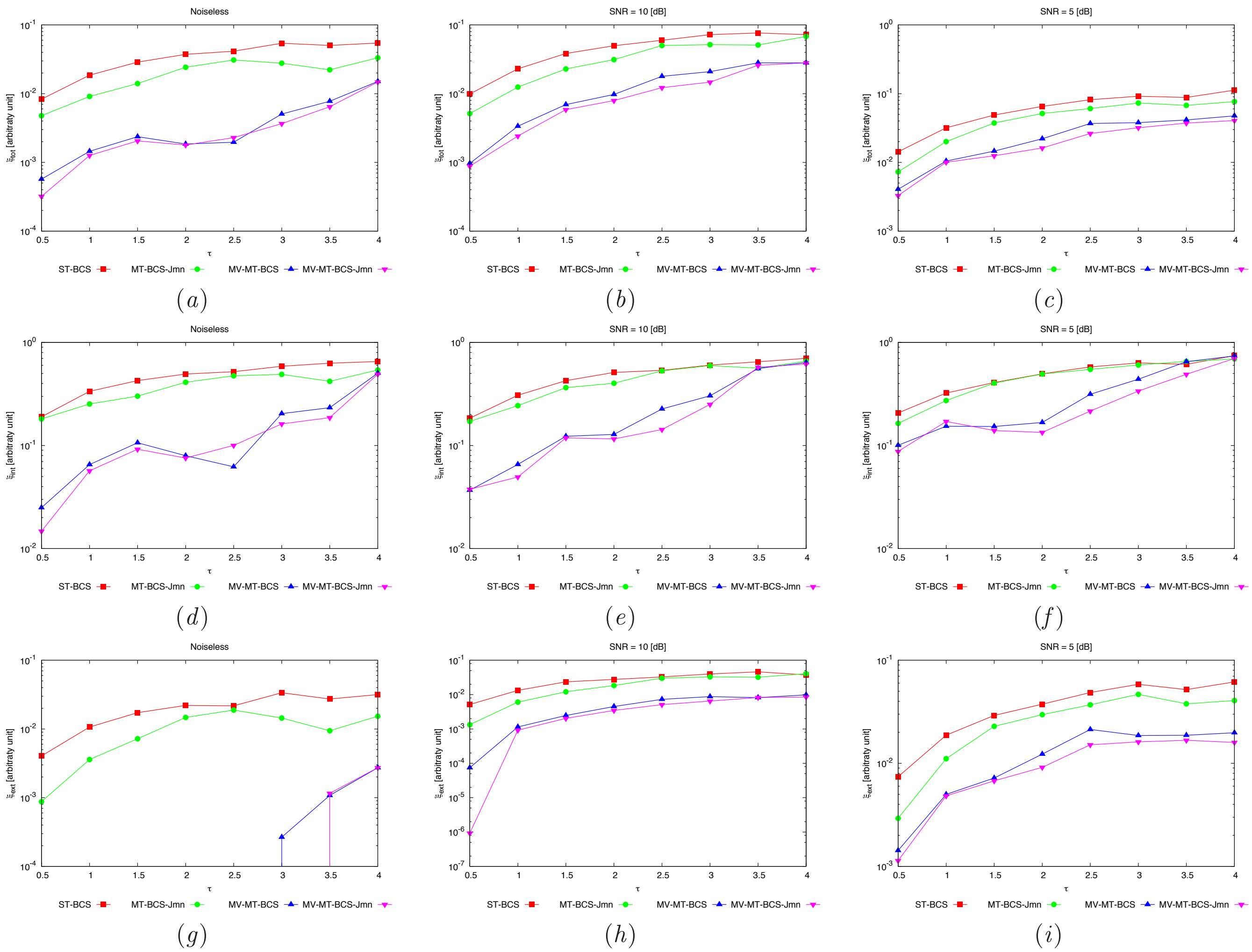

Figure 63. Behaviour of total error ξ_{tot} $(a)(b)(c)$, internal error ξ_{int} $(d)(e)(f)$ and external error ξ_{ext} $(g)(h)(i)$ for Noiseless case $(a)(d)(g)$, $SNR = 10$ [dB] $(b)(e)(h)$ and $SNR = 5$ [dB] $(c)(f)(i)$.

3.12 TEST CASE: H-shaped Cylinder

Goal: show the performances of BCS when dealing with a sparse scatterer

- Number of Views: V
- Number of Measurements: M
- Number of Cells for the Inversion: N
- Number of Cells for the Direct solver: D
- Side of the investigation domain: L

Test Case Description

Direct solver:

- Square domain divided in $\sqrt{D} \times \sqrt{D}$ cells
- Domain side: $L = 3\lambda$
- $D = 1296$ (discretization for the direct solver: $< \lambda/10$)

Investigation domain:

- Square domain divided in $\sqrt{N} \times \sqrt{N}$ cells
- $L = 3\lambda$
- $2ka = 2 \times \frac{2\pi}{\lambda} \times \frac{L\sqrt{2}}{2} = 6\pi\sqrt{2} = 26.65$
- $\#DOF = \frac{(2ka)^2}{2} = \frac{(2\times\frac{2\pi}{\lambda}\times\frac{L\sqrt{2}}{2})^2}{2} = 4\pi^2\left(\frac{L}{\lambda}\right)^2 = 4\pi^2 \times 9 \approx 355.3$
- N scelto in modo da essere vicino a $\#DOF$: $N = 324$ (18×18)

Measurement domain:

- Measurement points taken on a circle of radius $\rho = 3\lambda$
- Full-aspect measurements
- $M \approx 2ka \rightarrow M = 27$

Sources:

- Plane waves
- $V \approx 2ka \rightarrow V = 27$
- Amplitude $A = 1$
- Frequency: 300 MHz ($\lambda = 1$)

Object:

- H-shaped cylinder
- $\varepsilon_r \in \{1.5, 2.0, 2.5, 3.0, 3.5, 4.0, 4.5, 5.0\}$
- $\sigma = 0$ [S/m]

MV-MT-BCS-Jmn parameters:

- Gamma prior on noise variance parameter: $a = 5 \times 10^0$
- Gamma prior on noise variance parameter: $b = 2 \times 10^{-2}$
- Convergenze parameter: $\tau = 1.0 \times 10^{-8}$

RESULTS: H-Shaped Cylinder

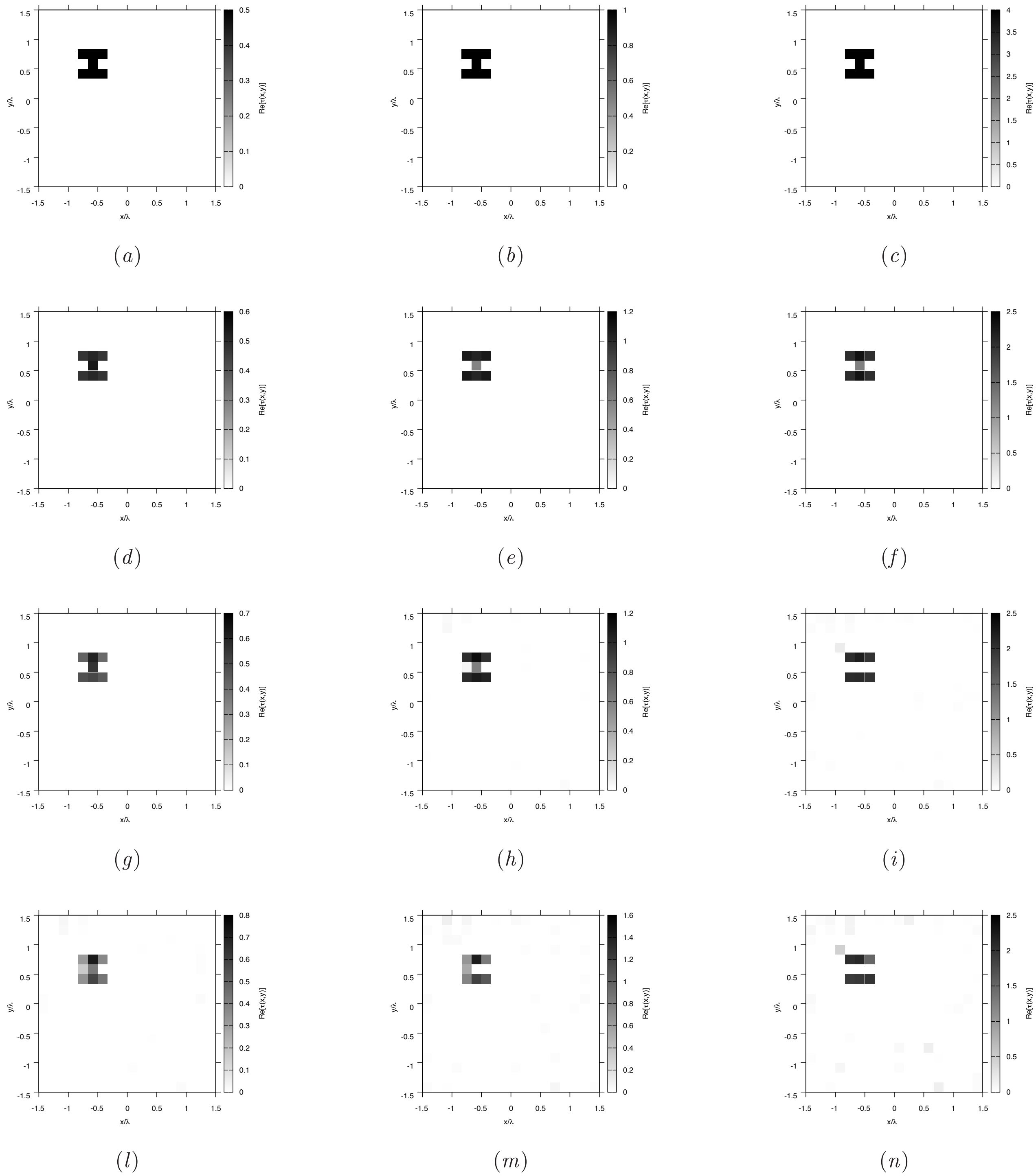

Figure 64. Actual object $(a)(b)(c)$ and MV-MT-BCS-Jmn reconstructed object with $\varepsilon_r = 1.5$ $(d)(g)(l)$, $\varepsilon_r = 2.0$ $(e)(h)(m)$, and $\varepsilon_r = 3.0$ $(f)(i)(n)$, for Noiseless case $(d)(e)(f)$, $SNR = 10$ [dB] $(g)(h)(i)$ and $SNR = 5$ [dB] $(l)(m)(n)$.

RESULTS: H-Shaped Cylinder

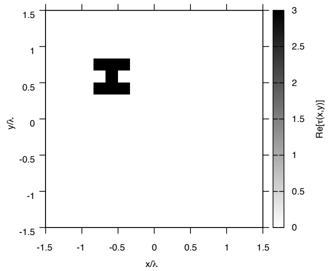

(o)

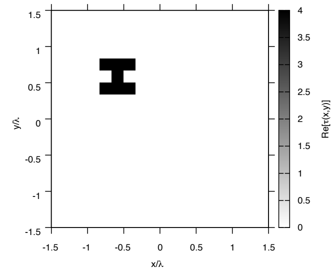

(p)

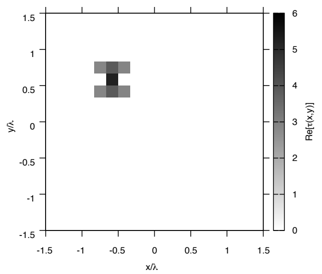

(q)

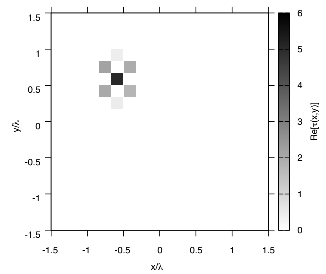

(r)

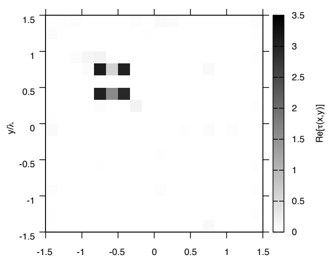

(s)

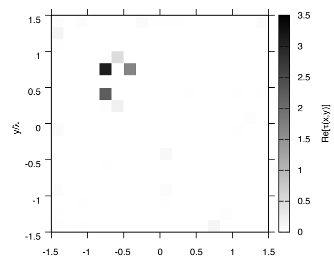

(t)

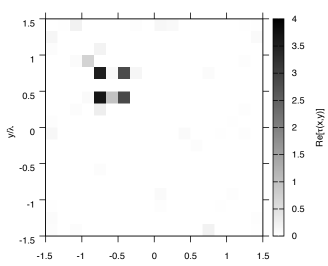

(u)

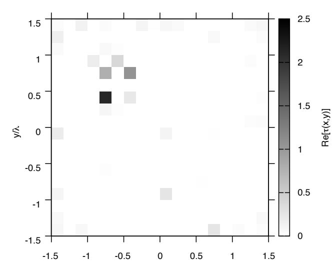

(v)

Figure 64. Actual object $(o)(p)$ and MV-MT-BCS-Jmn reconstructed object with $\varepsilon_r = 4.0$ $(q)(s)(u)$ and $\varepsilon_r = 5.0$ $(r)(t)(v)$ for Noiseless case $(q)(r)$, $SNR = 10$ [dB] $(s)(t)$ and $SNR = 5$ [dB] $(u)(v)$.

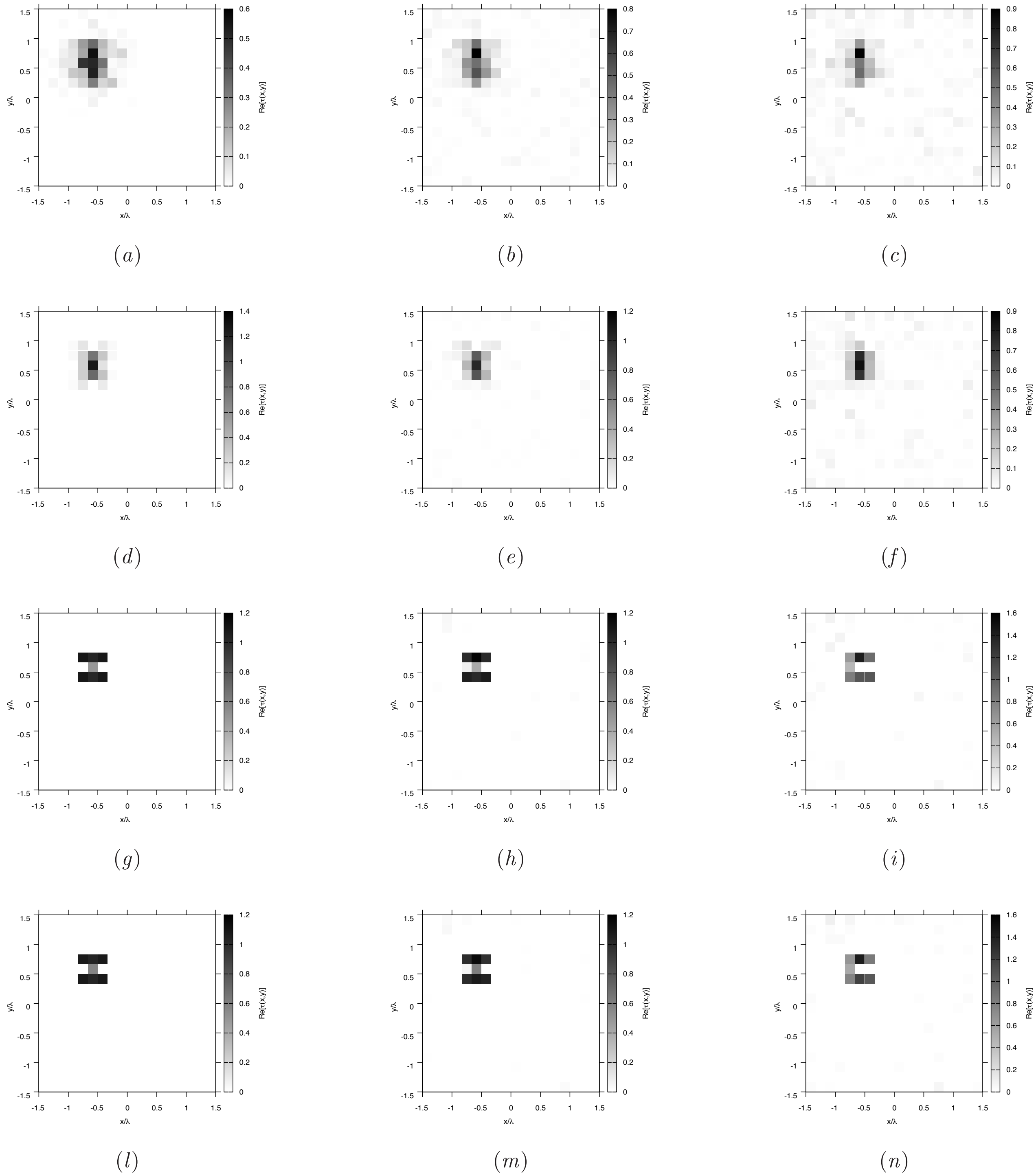

Figure 65. ST-BCS reconstructed object $(a)(b)(c)$, MT-BCS-Jmn reconstructed $(d)(e)(f)$ object, MV-MT-BCS reconstructed $(g)(h)(i)$ and MV-MT-BCS-Jmn reconstructed $(l)(m)(n)$ for Noiseless case $(a)(d)(g)(l)$, $SNR = 10$ [dB] $(b)(e)(h)(m)$ and $SNR = 5$ [dB] $(c)(f)(i)(n)$.

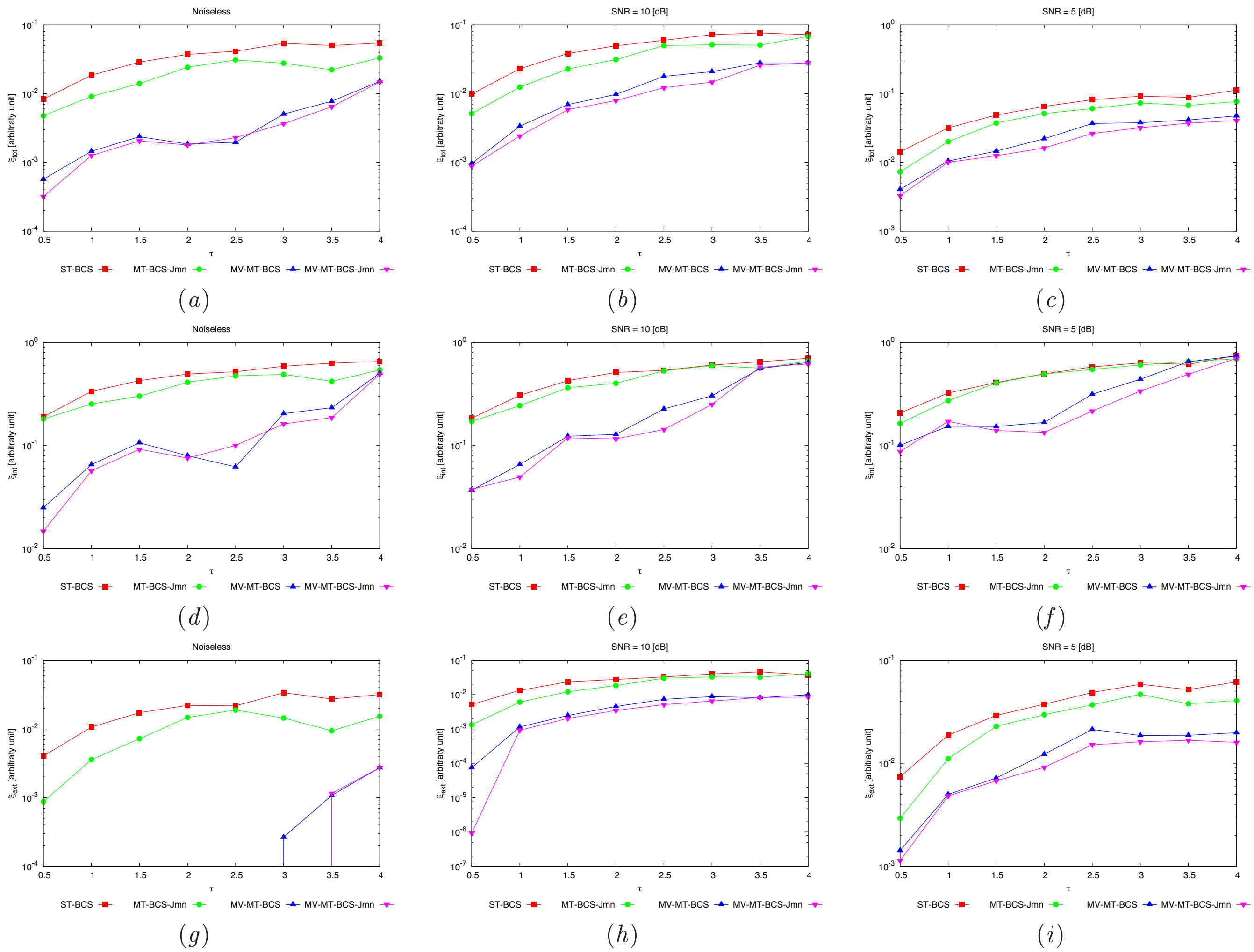

Figure 66. Behaviour of total error ξ_{tot} $(a)(b)(c)$, internal error ξ_{int} $(d)(e)(f)$ and external error ξ_{ext} $(g)(h)(i)$ for Noiseless case $(a)(d)(g)$, $SNR = 10$ [dB] $(b)(e)(h)$ and $SNR = 5$ [dB] $(c)(f)(i)$.

3.13 TEST CASE: Hollow Square Cylinder

Goal: show the performances of BCS when dealing with a sparse scatterer

- Number of Views: V
- Number of Measurements: M
- Number of Cells for the Inversion: N
- Number of Cells for the Direct solver: D
- Side of the investigation domain: L

Test Case Description

Direct solver:

- Square domain divided in $\sqrt{D} \times \sqrt{D}$ cells
- Domain side: $L = 3\lambda$
- $D = 1296$ (discretization for the direct solver: $< \lambda/10$)

Investigation domain:

- Square domain divided in $\sqrt{N} \times \sqrt{N}$ cells
- $L = 3\lambda$
- $2ka = 2 \times \frac{2\pi}{\lambda} \times \frac{L\sqrt{2}}{2} = 6\pi\sqrt{2} = 26.65$
- $\#DOF = \frac{(2ka)^2}{2} = \frac{(2\times\frac{2\pi}{\lambda}\times\frac{L\sqrt{2}}{2})^2}{2} = 4\pi^2\left(\frac{L}{\lambda}\right)^2 = 4\pi^2 \times 9 \approx 355.3$
- N scelto in modo da essere vicino a $\#DOF$: $N = 324$ (18×18)

Measurement domain:

- Measurement points taken on a circle of radius $\rho = 3\lambda$
- Full-aspect measurements
- $M \approx 2ka \rightarrow M = 27$

Sources:

- Plane waves
- $V \approx 2ka \rightarrow V = 27$
- Amplitude $A = 1$
- Frequency: 300 MHz ($\lambda = 1$)

Object:

- Hollow square cylinder
- $\varepsilon_r \in \{1.5, 2.0, 2.5, 3.0, 3.5, 4.0, 4.5, 5.0\}$
- $\sigma = 0$ [S/m]

MV-MT-BCS-Jmn parameters:

- Gamma prior on noise variance parameter: $a = 5 \times 10^0$
- Gamma prior on noise variance parameter: $b = 2 \times 10^{-2}$
- Convergenze parameter: $\tau = 1.0 \times 10^{-8}$

RESULTS: Hollow Square Cylinder

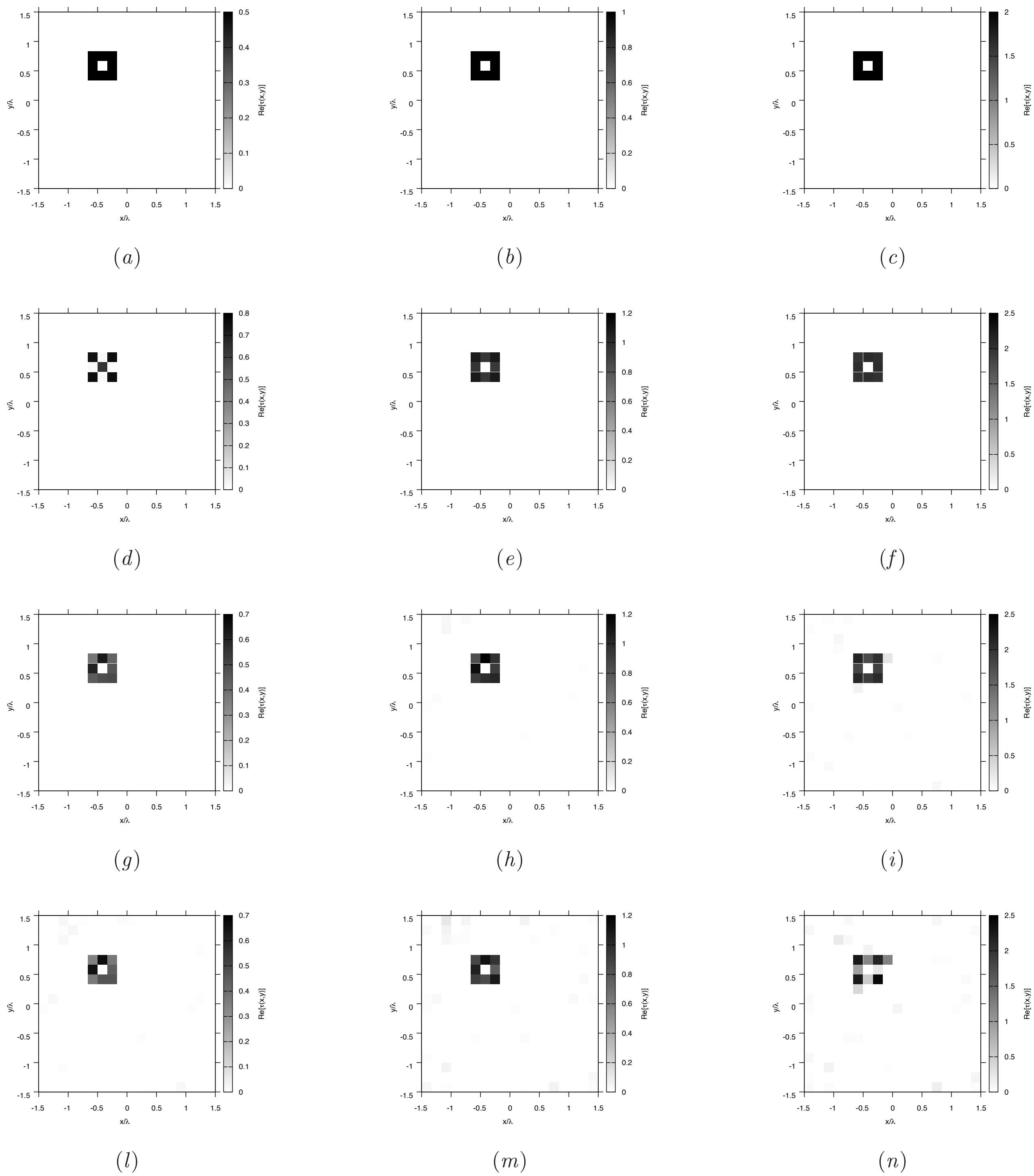

Figure 67. Actual object $(a)(b)(c)$ and MV-MT-BCS-Jmn reconstructed object with $\varepsilon_r = 1.5$ $(d)(g)(l)$, $\varepsilon_r = 2.0$ $(e)(h)(m)$, and $\varepsilon_r = 3.0$ $(f)(i)(n)$, for Noiseless case $(d)(e)(f)$, $SNR = 10$ [dB] $(g)(h)(i)$ and $SNR = 5$ [dB] $(l)(m)(n)$.

RESULTS: Hollow Square Cylinder

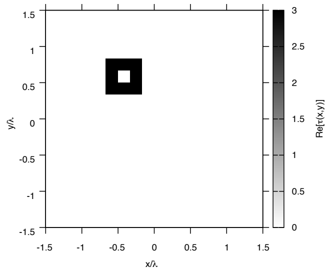

(o)

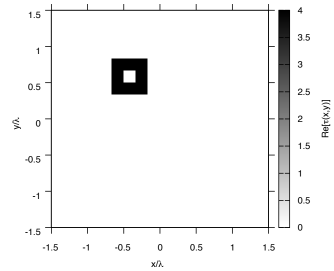

(p)

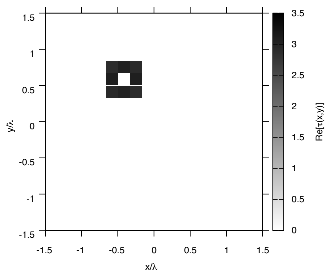

(q)

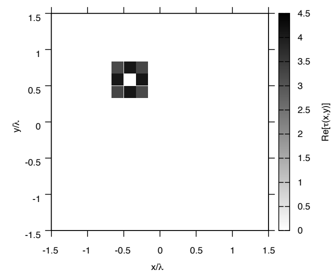

(r)

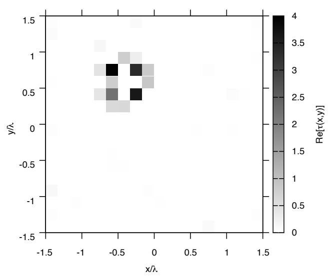

(s)

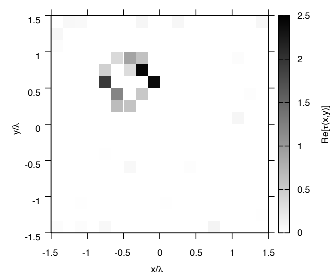

(t)

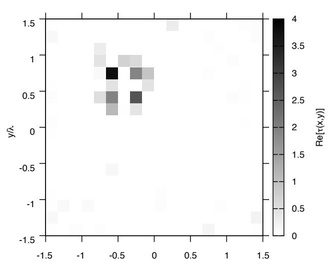

(u)

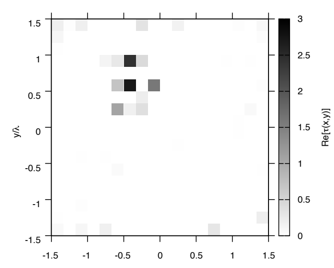

(v)

Figure 67. Actual object $(o)(p)$ and MV-MT-BCS-Jmn reconstructed object with $\varepsilon_r = 4.0$ $(q)(s)(u)$ and $\varepsilon_r = 5.0$ $(r)(t)(v)$ for Noiseless case $(q)(r)$, $SNR = 10$ [dB] $(s)(t)$ and $SNR = 5$ [dB] $(u)(v)$.

RESULTS: Hollow Square Cylinder - Reconstructions - Comparison ST-BCS/MT-BCS - $\varepsilon_r = 2.0$

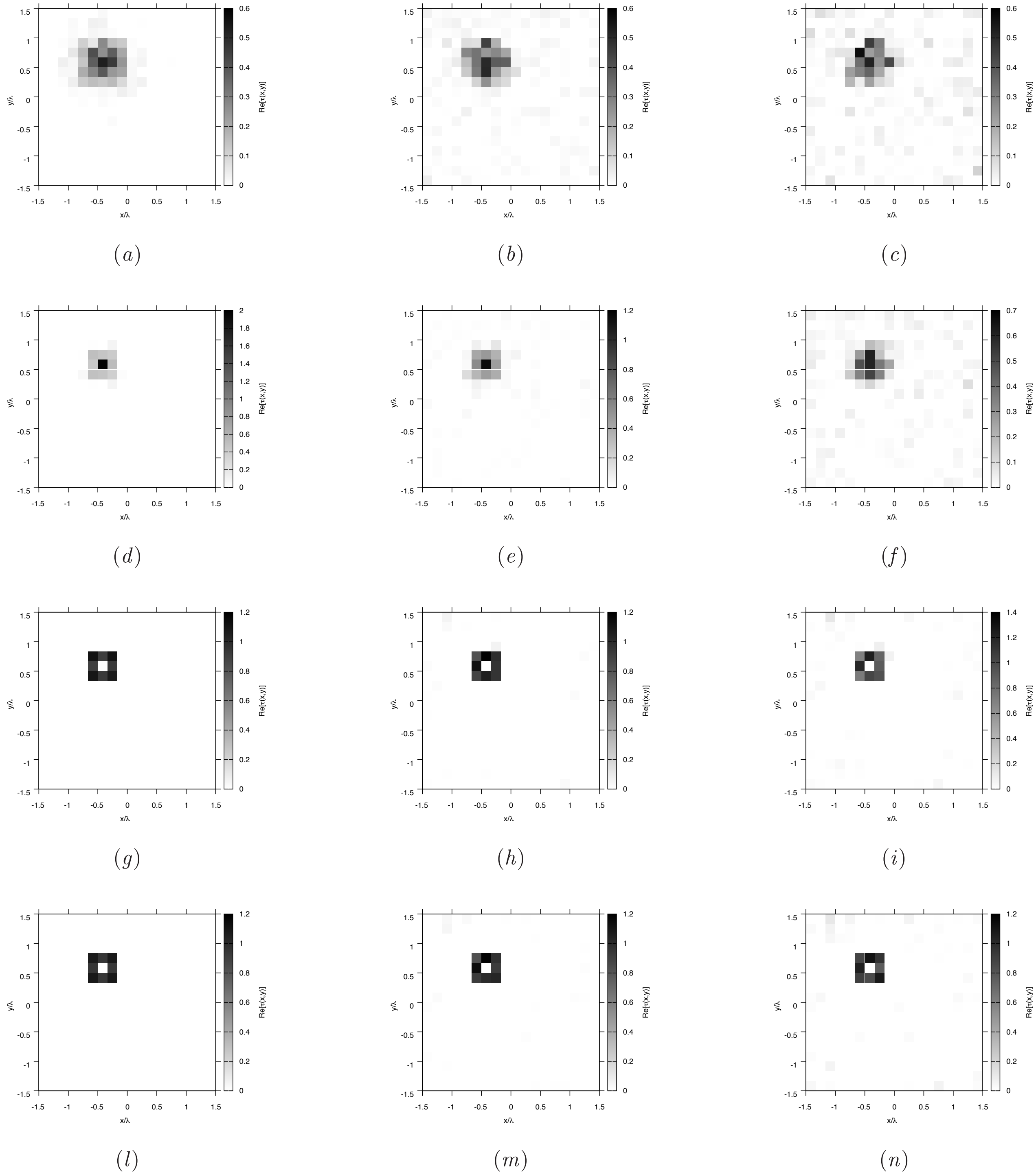

Figure 68. ST-BCS reconstructed object $(a)(b)(c)$, MT-BCS-Jmn reconstructed $(d)(e)(f)$ object, MV-MT-BCS reconstructed $(g)(h)(i)$ and MV-MT-BCS-Jmn reconstructed $(l)(m)(n)$ for Noiseless case $(a)(d)(g)(l)$, $SNR = 10$ [dB] $(b)(e)(h)(m)$ and $SNR = 5$ [dB] $(c)(f)(i)(n)$.

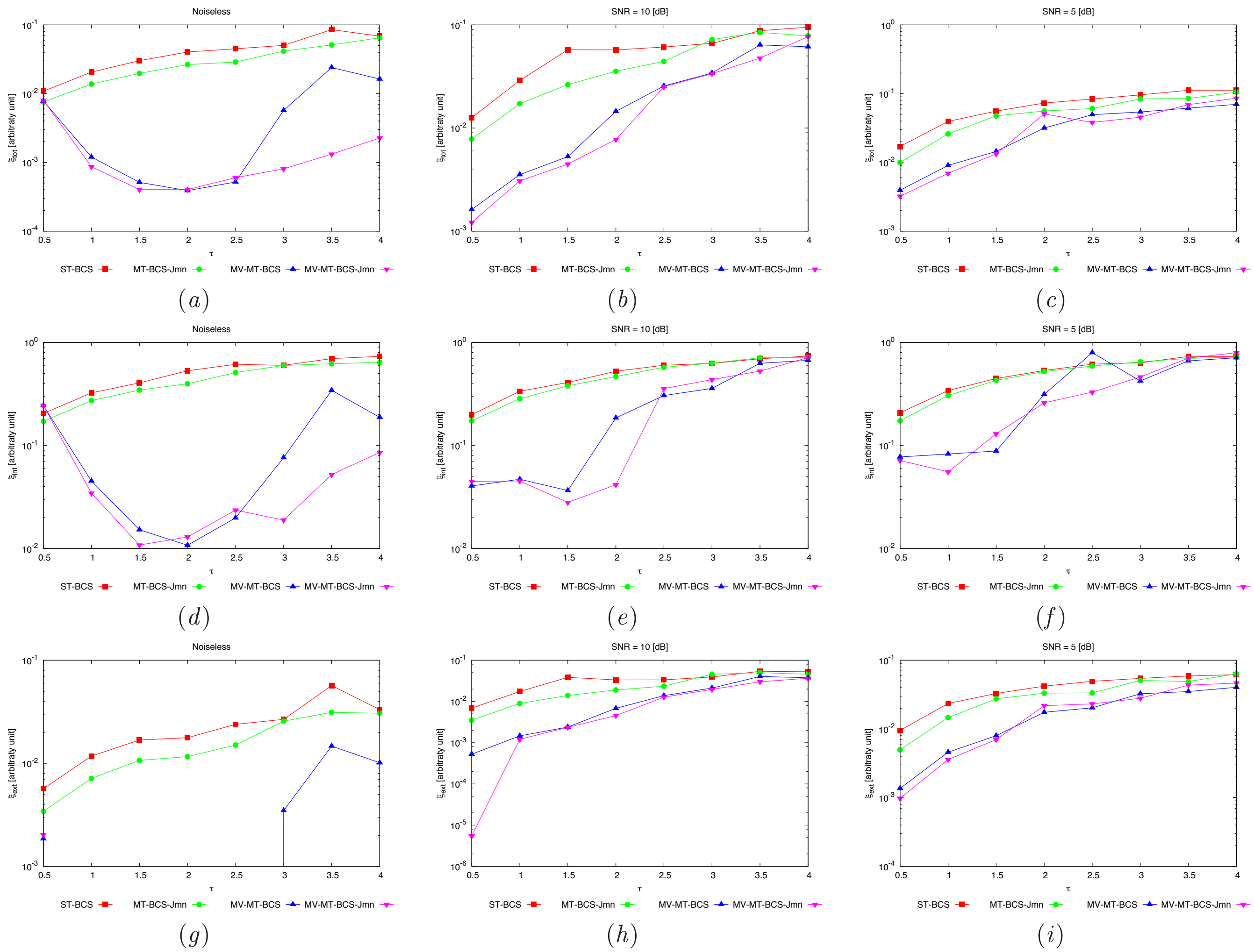

Figure 69. Behaviour of total error ξ_{tot} $(a)(b)(c)$, internal error ξ_{int} $(d)(e)(f)$ and external error ξ_{ext} $(g)(h)(i)$ for Noiseless case $(a)(d)(g)$, $SNR = 10$ [dB] $(b)(e)(h)$ and $SNR = 5$ [dB] $(c)(f)(i)$.

3.14 TEST CASE: Two Hollow Square Cylinders

Goal: show the performances of BCS when dealing with a sparse scatterer

- Number of Views: V
- Number of Measurements: M
- Number of Cells for the Inversion: N
- Number of Cells for the Direct solver: D
- Side of the investigation domain: L

Test Case Description

Direct solver:

- Square domain divided in $\sqrt{D} \times \sqrt{D}$ cells
- Domain side: $L = 3\lambda$
- $D = 1296$ (discretization for the direct solver: $< \lambda/10$)

Investigation domain:

- Square domain divided in $\sqrt{N} \times \sqrt{N}$ cells
- $L = 3\lambda$
- $2ka = 2 \times \frac{2\pi}{\lambda} \times \frac{L\sqrt{2}}{2} = 6\pi\sqrt{2} = 26.65$
- $\#DOF = \frac{(2ka)^2}{2} = \frac{(2\times\frac{2\pi}{\lambda}\times\frac{L\sqrt{2}}{2})^2}{2} = 4\pi^2\left(\frac{L}{\lambda}\right)^2 = 4\pi^2 \times 9 \approx 355.3$
- N scelto in modo da essere vicino a $\#DOF$: $N = 324$ (18×18)

Measurement domain:

- Measurement points taken on a circle of radius $\rho = 3\lambda$
- Full-aspect measurements
- $M \approx 2ka \rightarrow M = 27$

Sources:

- Plane waves
- $V \approx 2ka \rightarrow V = 27$
- Amplitude $A = 1$
- Frequency: 300 MHz ($\lambda = 1$)

Object:

- Two hollow square cylinder
- $\varepsilon_r \in \{1.5, 2.0, 2.5, 3.0, 3.5, 4.0, 4.5, 5.0\}$
- $\sigma = 0$ [S/m]

MV-MT-BCS-Jmn parameters:

- Gamma prior on noise variance parameter: $a = 5 \times 10^0$
- Gamma prior on noise variance parameter: $b = 2 \times 10^{-2}$
- Convergenze parameter: $\tau = 1.0 \times 10^{-8}$

RESULTS: Two Hollow Square Cylinders

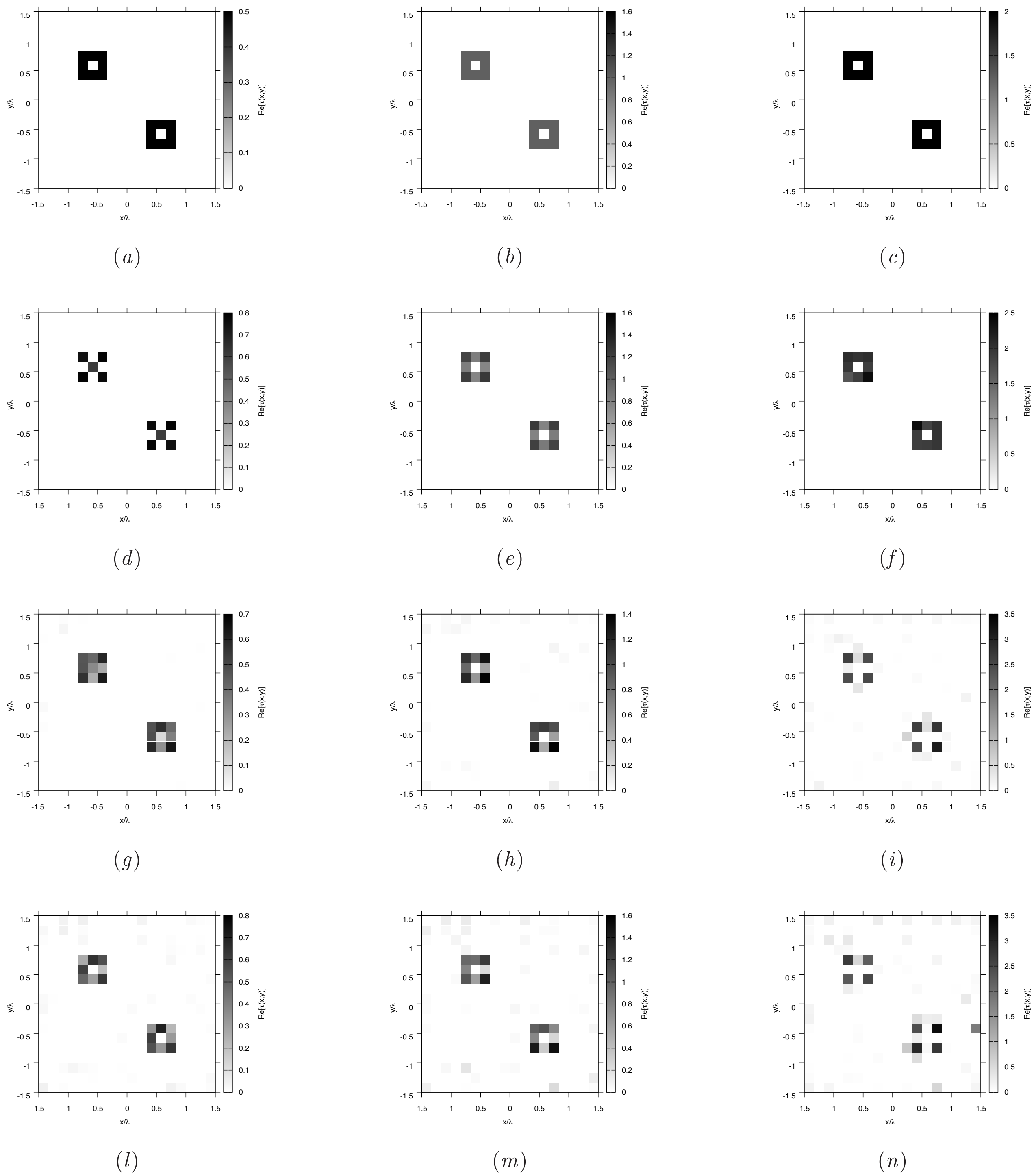

Figure 70. Actual object $(a)(b)(c)$ and MV-MT-BCS-Jmn reconstructed object with $\varepsilon_r = 1.5$ $(d)(g)(l)$, $\varepsilon_r = 2.0$ $(e)(h)(m)$, and $\varepsilon_r = 3.0$ $(f)(i)(n)$, for Noiseless case $(d)(e)(f)$, $SNR = 10$ [dB] $(g)(h)(i)$ and $SNR = 5$ [dB] $(l)(m)(n)$.

RESULTS: Two Hollow Square Cylinders

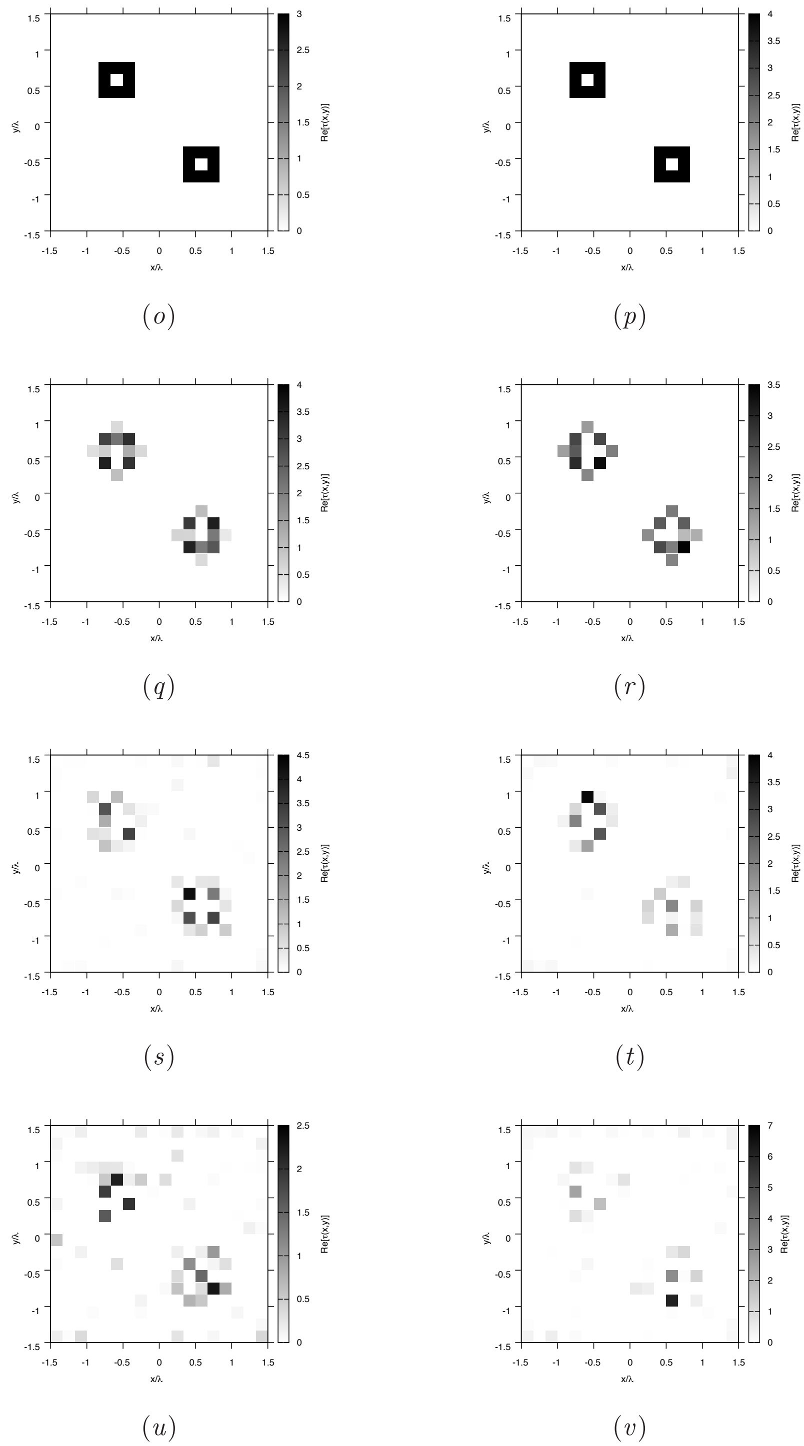

Figure 70. Actual object $(o)(p)$ and MV-MT-BCS-Jmn reconstructed object with $\varepsilon_r = 4.0$ $(q)(s)(u)$ and $\varepsilon_r = 5.0$ $(r)(t)(v)$ for Noiseless case $(q)(r)$, $SNR = 10$ [dB] $(s)(t)$ and $SNR = 5$ [dB] $(u)(v)$.

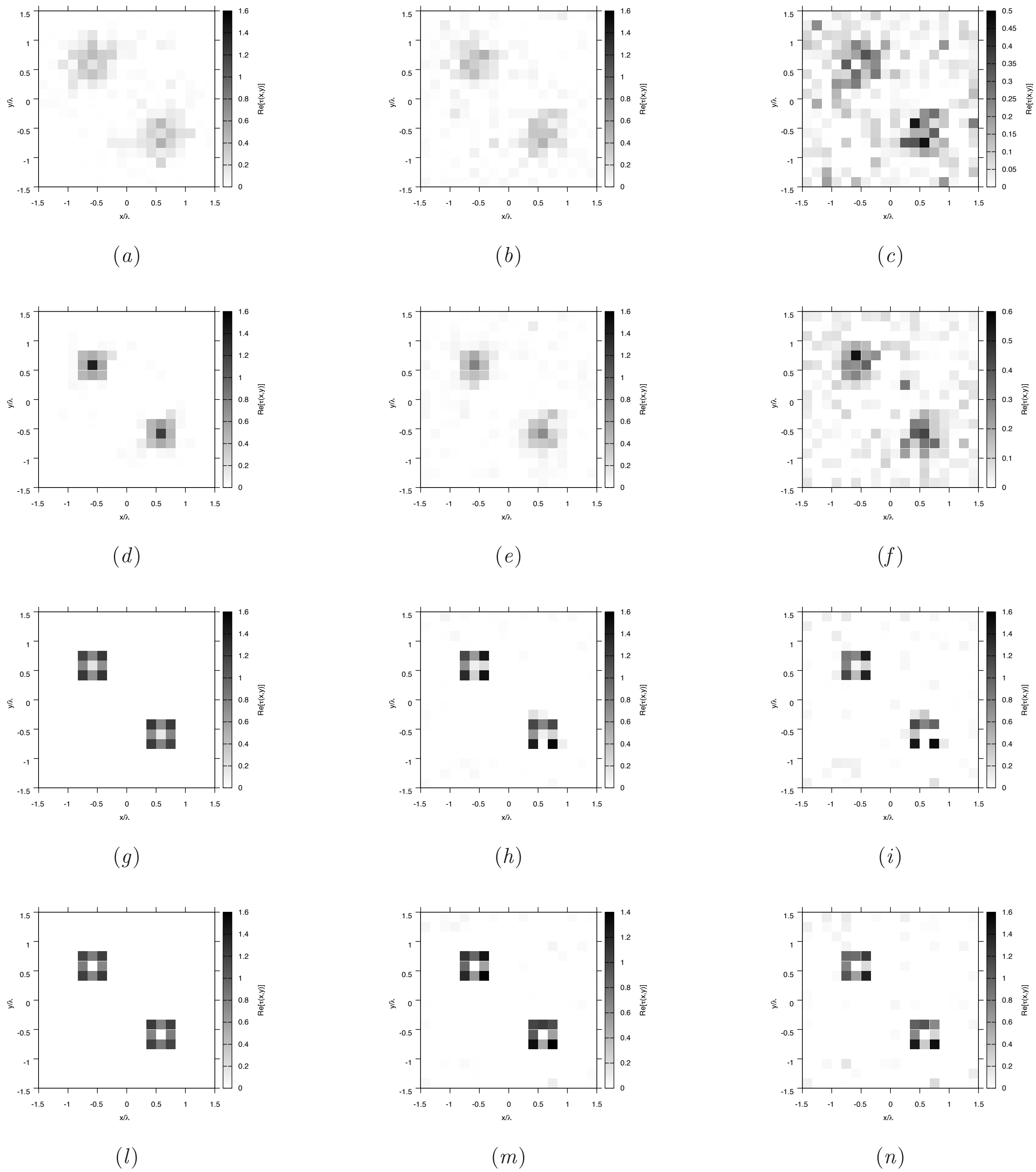

Figure 71. ST-BCS reconstructed object $(a)(b)(c)$, MT-BCS-Jmn reconstructed $(d)(e)(f)$ object, MV-MT-BCS reconstructed $(g)(h)(i)$ and MV-MT-BCS-Jmn reconstructed $(l)(m)(n)$ for Noiseless case $(a)(d)(g)(l)$, $SNR = 10$ [dB] $(b)(e)(h)(m)$ and $SNR = 5$ [dB] $(c)(f)(i)(n)$.

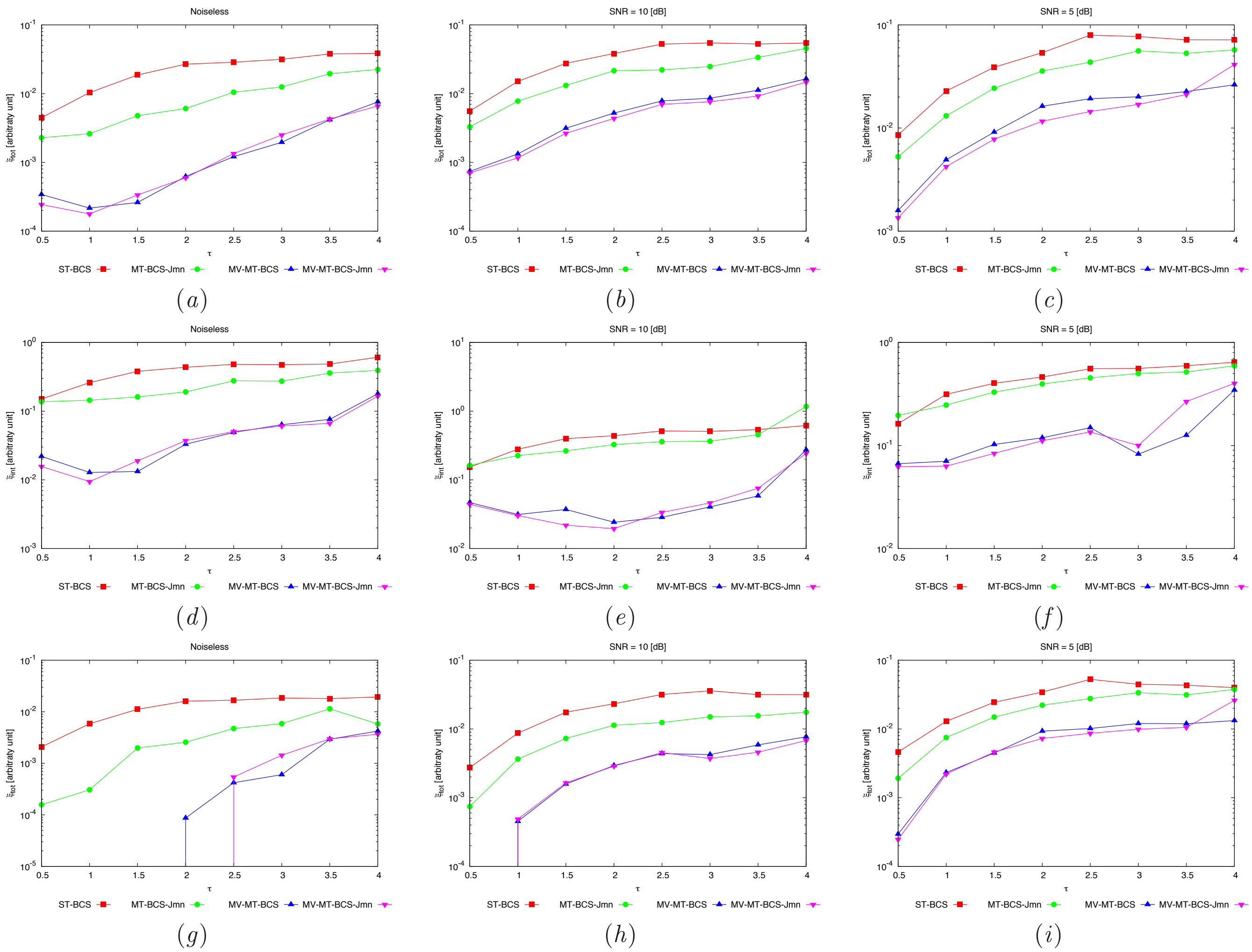

Figure 72. Behaviour of total error ξ_{tot} $(a)(b)(c)$, internal error ξ_{int} $(d)(e)(f)$ and external error ξ_{ext} $(g)(h)(i)$ for Noiseless case $(a)(d)(g)$, $SNR = 10$ [dB] $(b)(e)(h)$ and $SNR = 5$ [dB] $(c)(f)(i)$.

3.15 TEST CASE: Three Square Cylinders $L = 0.33\lambda$

Goal: show the performances of BCS when dealing with a sparse scatterer

- Number of Views: V
- Number of Measurements: M
- Number of Cells for the Inversion: N
- Number of Cells for the Direct solver: D
- Side of the investigation domain: L

Test Case Description

Direct solver:

- Square domain divided in $\sqrt{D} \times \sqrt{D}$ cells
- Domain side: $L = 3\lambda$
- $D = 1296$ (discretization for the direct solver: $< \lambda/10$)

Investigation domain:

- Square domain divided in $\sqrt{N} \times \sqrt{N}$ cells
- $L = 3\lambda$
- $2ka = 2 \times \frac{2\pi}{\lambda} \times \frac{L\sqrt{2}}{2} = 6\pi\sqrt{2} = 26.65$
- $\#DOF = \frac{(2ka)^2}{2} = \frac{(2\times\frac{2\pi}{\lambda}\times\frac{L\sqrt{2}}{2})^2}{2} = 4\pi^2\left(\frac{L}{\lambda}\right)^2 = 4\pi^2 \times 9 \approx 355.3$
- N scelto in modo da essere vicino a $\#DOF$: $N = 324$ (18×18)

Measurement domain:

- Measurement points taken on a circle of radius $\rho = 3\lambda$
- Full-aspect measurements
- $M \approx 2ka \rightarrow M = 27$

Sources:

- Plane waves
- $V \approx 2ka \rightarrow V = 27$
- Amplitude $A = 1$
- Frequency: 300 MHz ($\lambda = 1$)

Object:

- Three Square Cylinders $L = 0.33\lambda$
- $\varepsilon_r \in \{1.5, 2.0, 2.5, 3.0, 3.5, 4.0, 4.5, 5.0\}$,
- $\sigma = 0$ [S/m]

MV-MT-BCS-Jmn parameters:

- Gamma prior on noise variance parameter: $a = 5 \times 10^0$
- Gamma prior on noise variance parameter: $b = 2 \times 10^{-2}$
- Convergenze parameter: $\tau = 1.0 \times 10^{-8}$

RESULTS: Three Square Cylinders $L = 0.33\lambda$

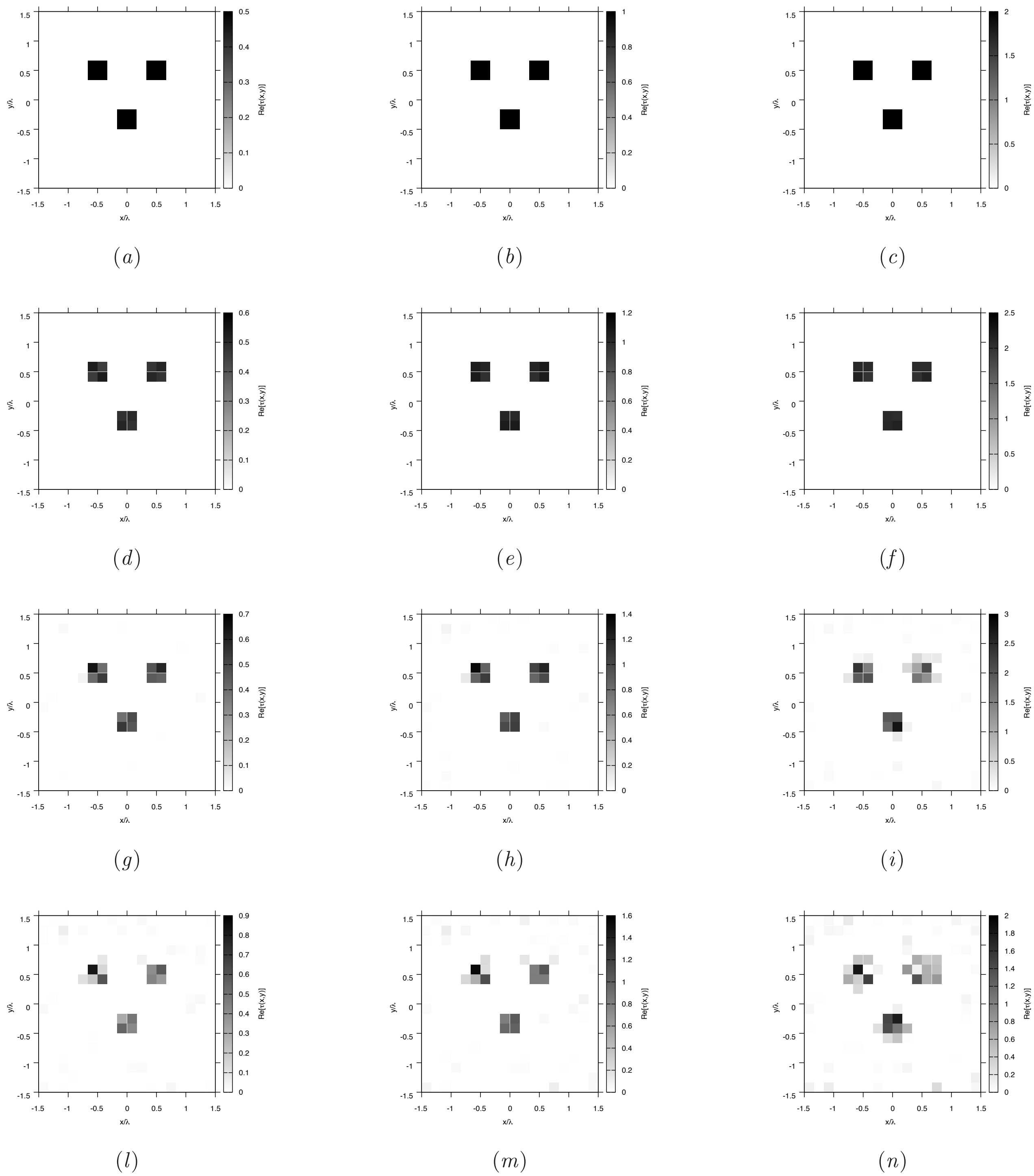

Figure 73. Actual object $(a)(b)(c)$ and MV-MT-BCS-Jmn reconstructed object with $\varepsilon_r = 1.5$ $(d)(g)(l)$, $\varepsilon_r = 2.0$ $(e)(h)(m)$, and $\varepsilon_r = 3.0$ $(f)(i)(n)$, for Noiseless case $(d)(e)(f)$, $SNR = 10$ [dB] $(g)(h)(i)$ and $SNR = 5$ [dB] $(l)(m)(n)$.

RESULTS: Three Square Cylinders $L = 0.33\lambda$

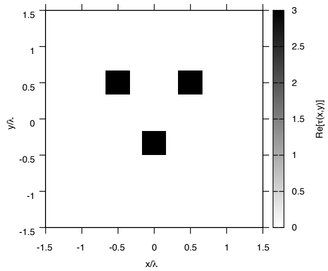

(o)

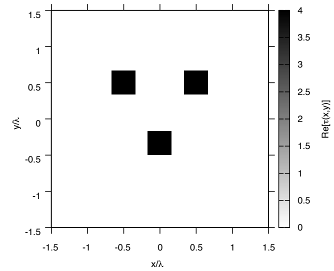

(p)

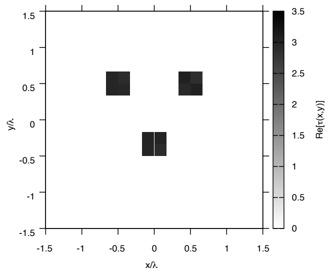

(q)

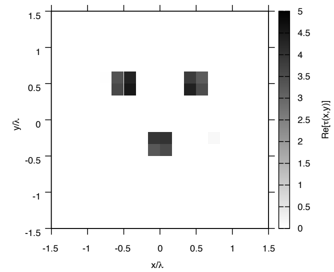

(r)

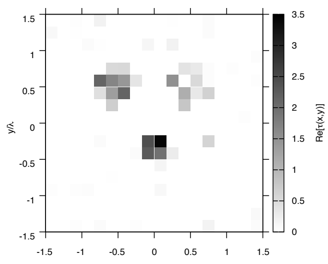

(s)

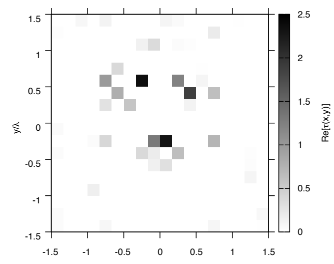

(t)

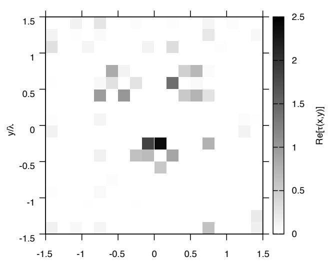

(u)

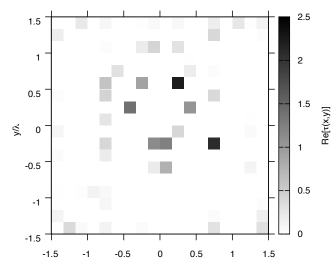

(v)

Figure 73. Actual object $(o)(p)$ and MV-MT-BCS-Jmn reconstructed object with $\varepsilon_r = 4.0$ $(q)(s)(u)$ and $\varepsilon_r = 5.0$ $(r)(t)(v)$ for Noiseless case $(q)(r)$, $SNR = 10$ [dB] $(s)(t)$ and $SNR = 5$ [dB] $(u)(v)$.

RESULTS: Three Square Cylinders $L = 0.33\lambda$ - Reconstructions - Comparison ST-BCS/MT-BCS - $\varepsilon_r = 2.0$

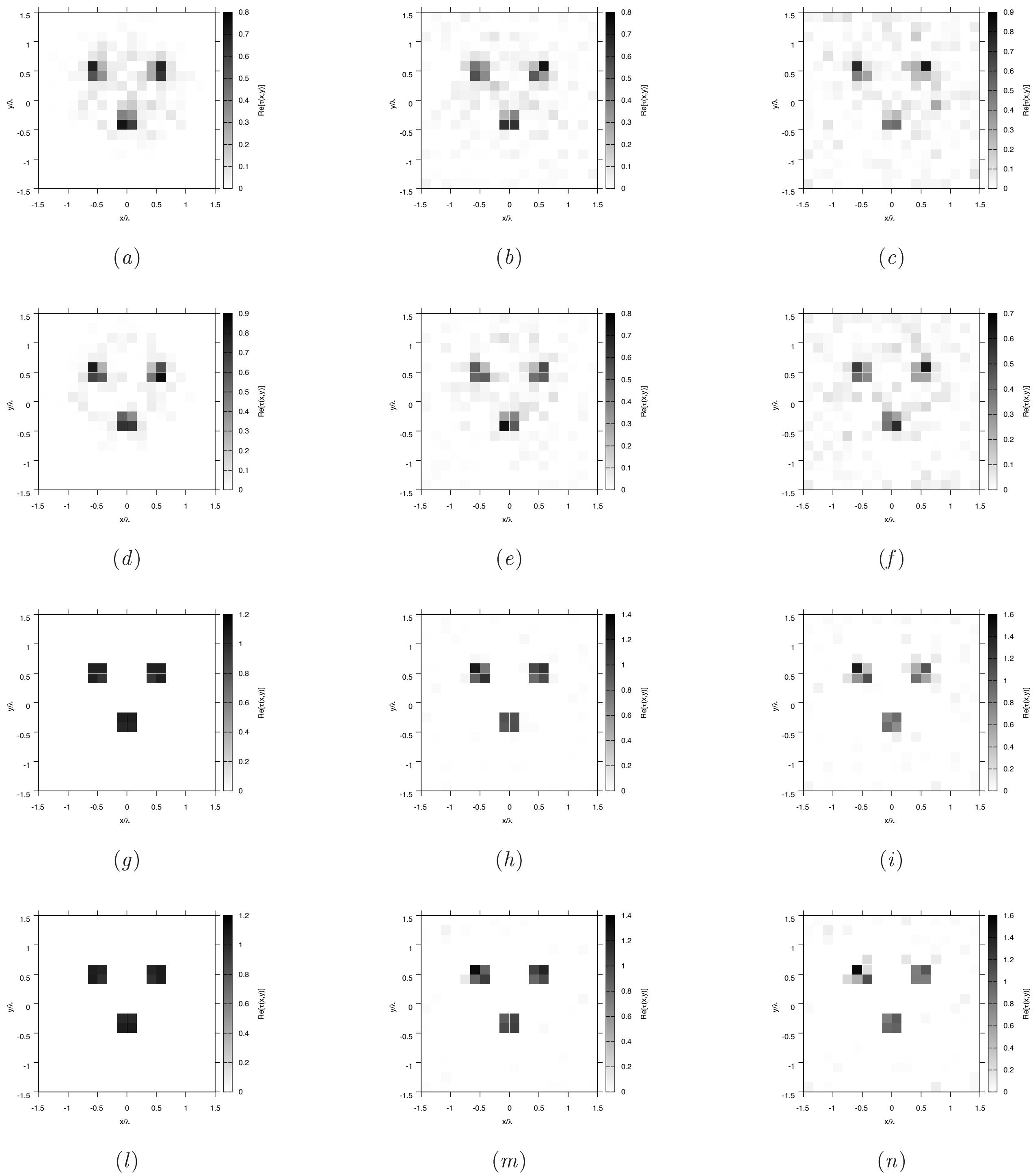

Figure 74. ST-BCS reconstructed object $(a)(b)(c)$, MT-BCS-Jmn reconstructed $(d)(e)(f)$ object, MV-MT-BCS reconstructed $(g)(h)(i)$ and MV-MT-BCS-Jmn reconstructed $(l)(m)(n)$ for Noiseless case $(a)(d)(g)(l)$, $SNR = 10$ [dB] $(b)(e)(h)(m)$ and $SNR = 5$ [dB] $(c)(f)(i)(n)$.

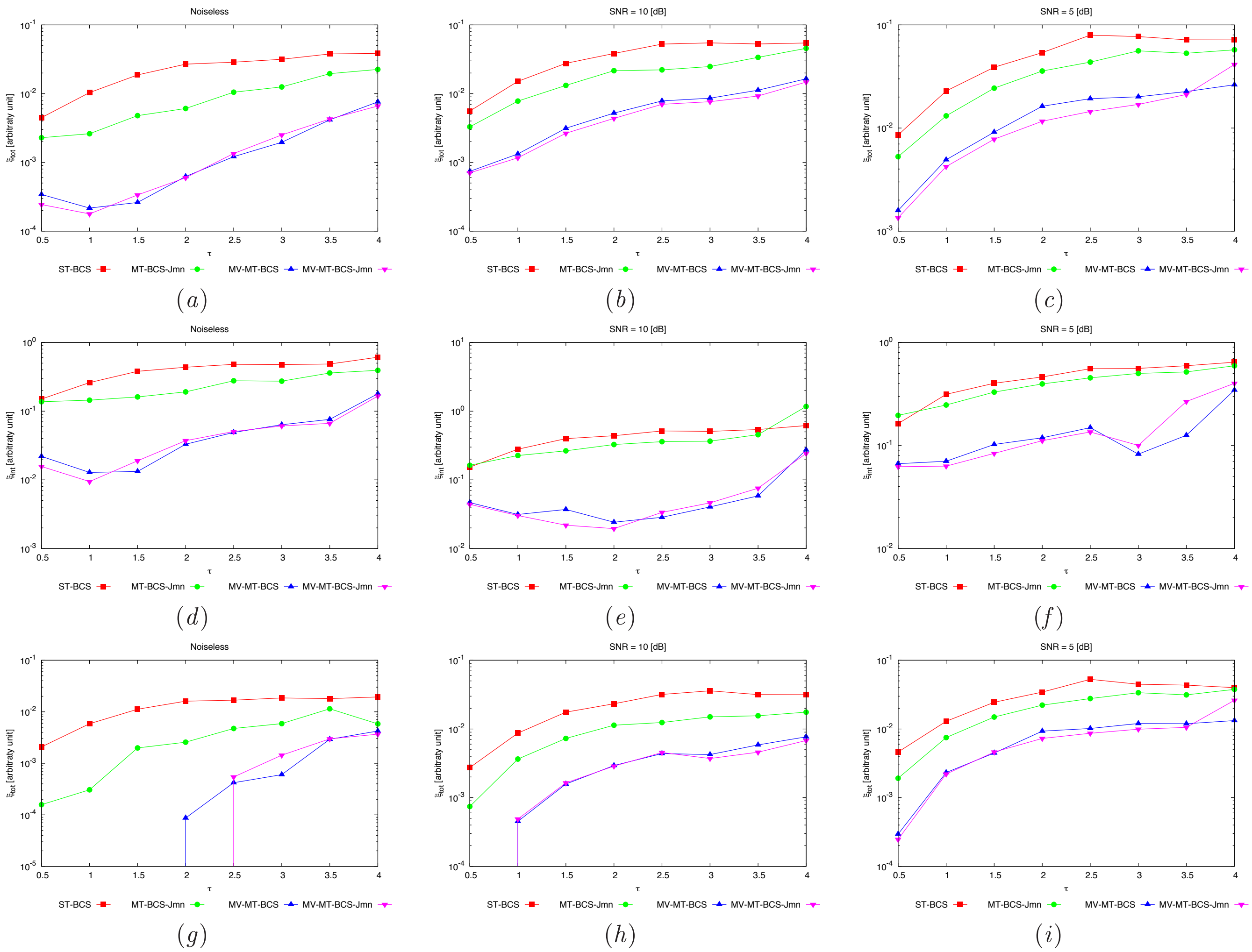

Figure 75. Behaviour of total error ξ_{tot} $(a)(b)(c)$, internal error ξ_{int} $(d)(e)(f)$ and external error ξ_{ext} $(g)(h)(i)$ for Noiseless case $(a)(d)(g)$, $SNR = 10$ [dB] $(b)(e)(h)$ and $SNR = 5$ [dB] $(c)(f)(i)$.

3.16 TEST CASE: Three Square Cylinders Different Sisez

Goal: show the performances of BCS when dealing with a sparse scatterer

- Number of Views: V
- Number of Measurements: M
- Number of Cells for the Inversion: N
- Number of Cells for the Direct solver: D
- Side of the investigation domain: L

Test Case Description

Direct solver:

- Square domain divided in $\sqrt{D} \times \sqrt{D}$ cells
- Domain side: $L = 3\lambda$
- $D = 1296$ (discretization for the direct solver: $< \lambda/10$)

Investigation domain:

- Square domain divided in $\sqrt{N} \times \sqrt{N}$ cells
- $L = 3\lambda$
- $2ka = 2 \times \frac{2\pi}{\lambda} \times \frac{L\sqrt{2}}{2} = 6\pi\sqrt{2} = 26.65$
- $\#DOF = \frac{(2ka)^2}{2} = \frac{(2\times\frac{2\pi}{\lambda}\times\frac{L\sqrt{2}}{2})^2}{2} = 4\pi^2\left(\frac{L}{\lambda}\right)^2 = 4\pi^2 \times 9 \approx 355.3$
- N scelto in modo da essere vicino a $\#DOF$: $N = 324$ (18×18)

Measurement domain:

- Measurement points taken on a circle of radius $\rho = 3\lambda$
- Full-aspect measurements
- $M \approx 2ka \rightarrow M = 27$

Sources:

- Plane waves
- $V \approx 2ka \rightarrow V = 27$
- Amplitude $A = 1$
- Frequency: 300 MHz ($\lambda = 1$)

Object:

- Three Square Cylinders Different Sisez
- $L = 0.16\lambda$ square: $\varepsilon_r \in= 1.9$, $L = 0.33\lambda$ square: $\varepsilon_r \in \{1.5, 2.0, 2.5, 3.0, 3.5, 4.0, 4.5, 5.0\}$, $L = 0.50\lambda$ square: $\varepsilon_r = 1.6$
- $\sigma = 0$ [S/m]

MV-MT-BCS-Jmn parameters:

- Gamma prior on noise variance parameter: $a = 5 \times 10^0$
- Gamma prior on noise variance parameter: $b = 2 \times 10^{-2}$
- Convergenze parameter: $\tau = 1.0 \times 10^{-8}$

RESULTS: Three Square Cylinders Different Sizes

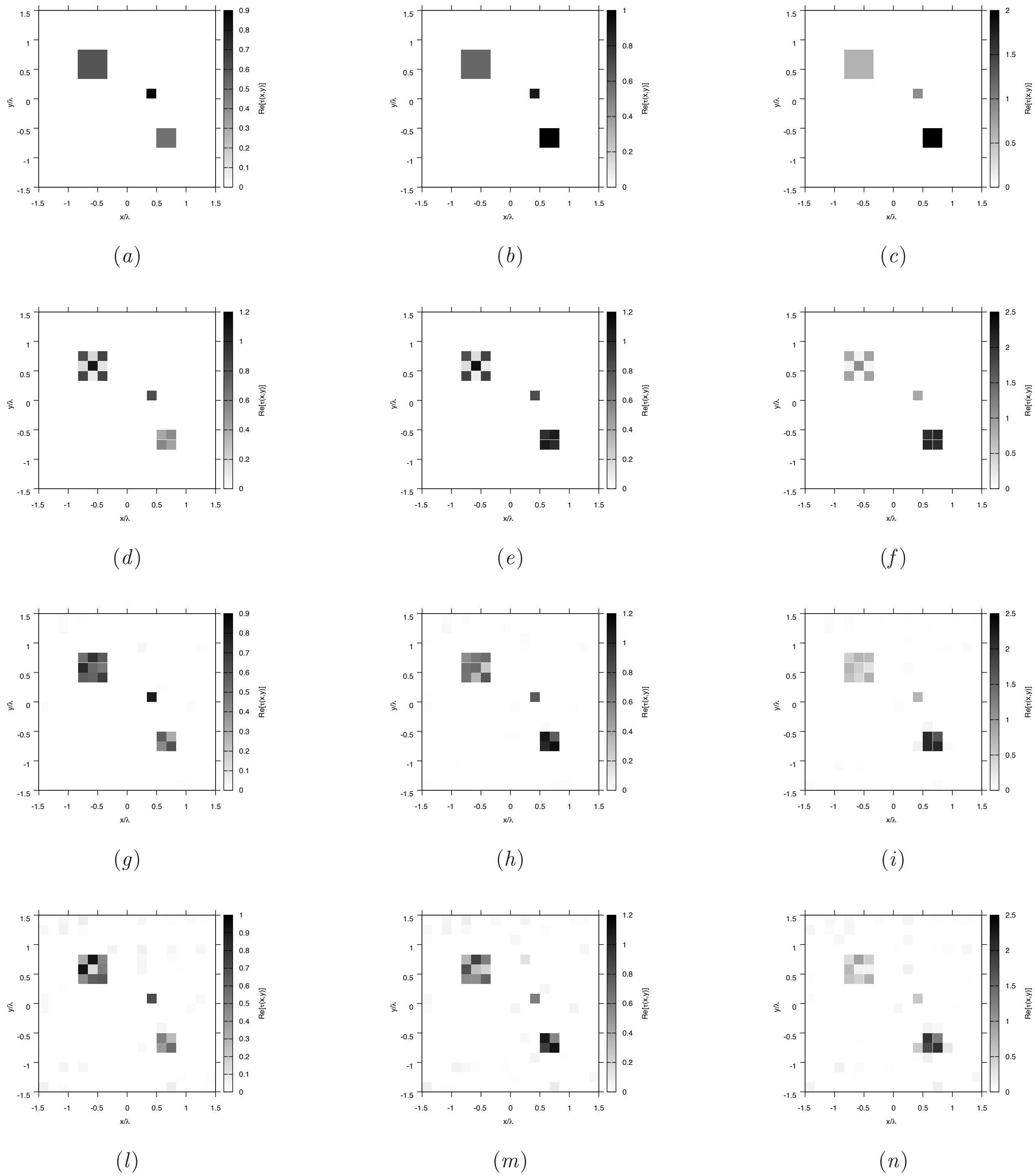

Figure 76. Actual object $(a)(b)(c)$ and MV-MT-BCS-Jmn reconstructed object with $\varepsilon_r = 1.5$ $(d)(g)(l)$, $\varepsilon_r = 2.0$ $(e)(h)(m)$, and $\varepsilon_r = 3.0$ $(f)(i)(n)$, for Noiseless case $(d)(e)(f)$, $SNR = 10$ [dB] $(g)(h)(i)$ and $SNR = 5$ [dB] $(l)(m)(n)$.

RESULTS: Three Square Cylinders Different Sizes

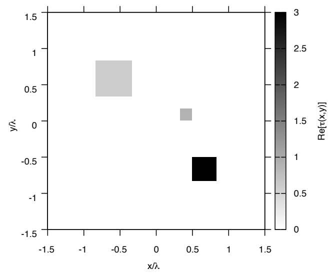

(o)

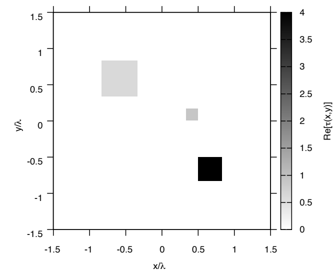

(p)

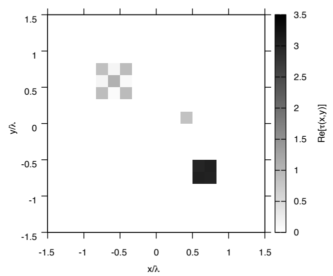

(q)

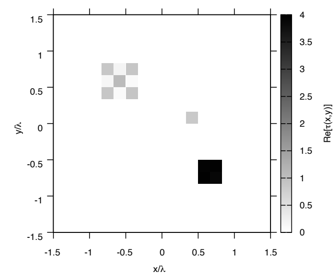

(r)

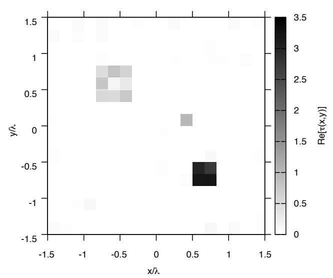

(s)

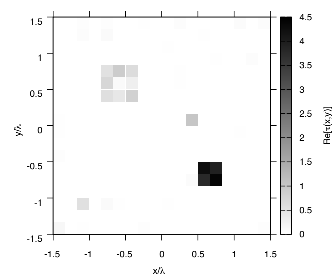

(t)

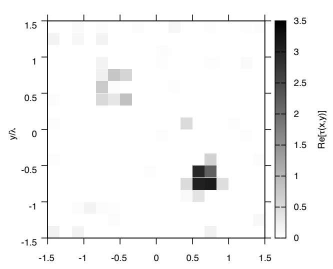

(u)

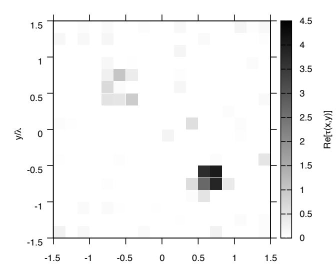

(v)

Figure 76. Actual object $(o)(p)$ and MV-MT-BCS-Jmn reconstructed object with $\varepsilon_r = 4.0$ $(q)(s)(u)$ and $\varepsilon_r = 5.0$ $(r)(t)(v)$ for Noiseless case $(q)(r)$, $SNR = 10$ [dB] $(s)(t)$ and $SNR = 5$ [dB] $(u)(v)$.

RESULTS: Three Square Cylinders $L = 0.33\lambda$ - Reconstructions - Comparison ST-BCS/MT-BCS - $\varepsilon_r = 2.0$

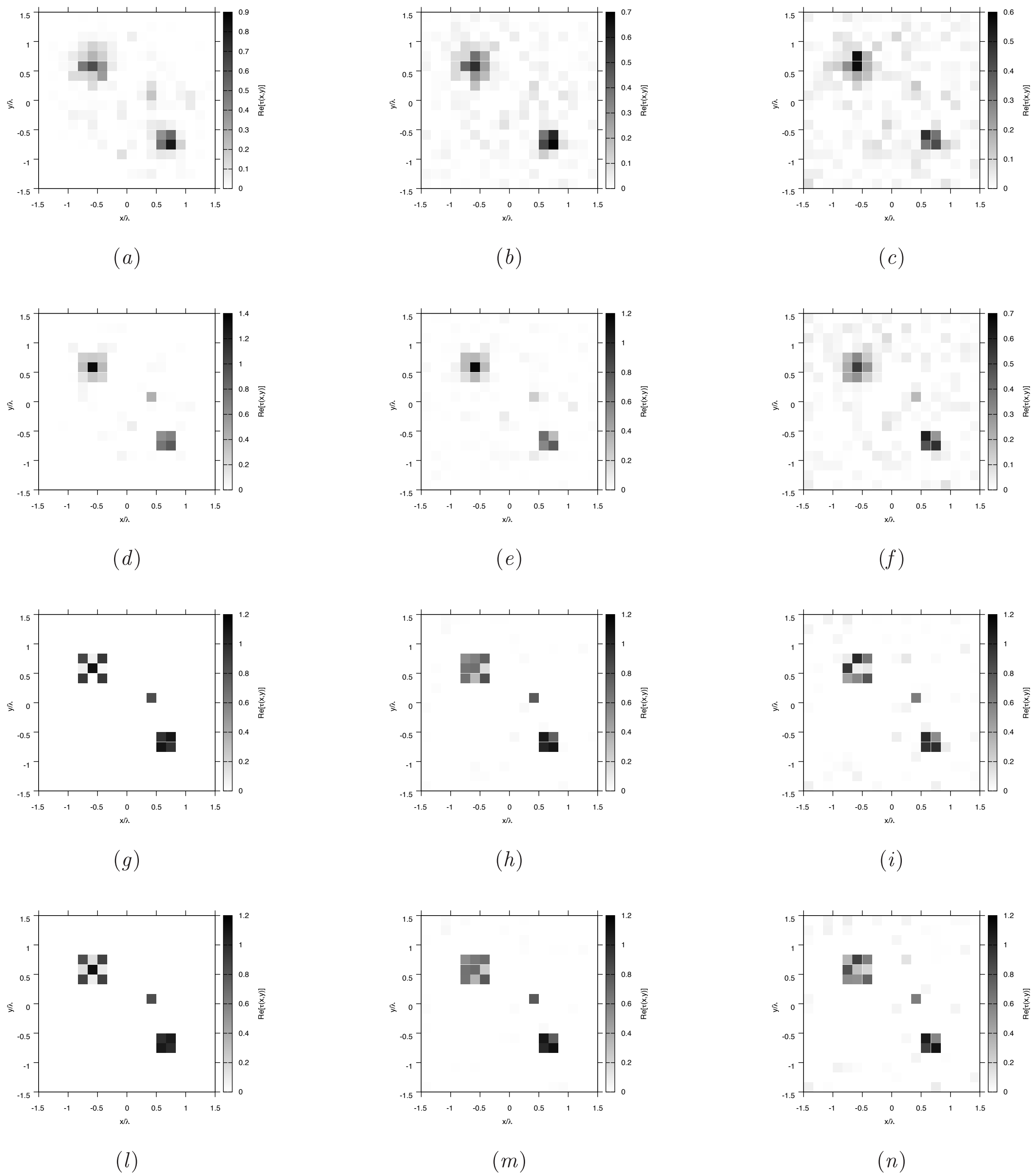

Figure 77. ST-BCS reconstructed object $(a)(b)(c)$, MT-BCS-Jmn reconstructed $(d)(e)(f)$ object, MV-MT-BCS reconstructed $(g)(h)(i)$ and MV-MT-BCS-Jmn reconstructed $(l)(m)(n)$ for Noiseless case $(a)(d)(g)(l)$, $SNR = 10$ [dB] $(b)(e)(h)(m)$ and $SNR = 5$ [dB] $(c)(f)(i)(n)$.

RESULTS: Three Square Cylinders Different Sizes - Error Figures - Comparison ST-BCS/MT-BCS

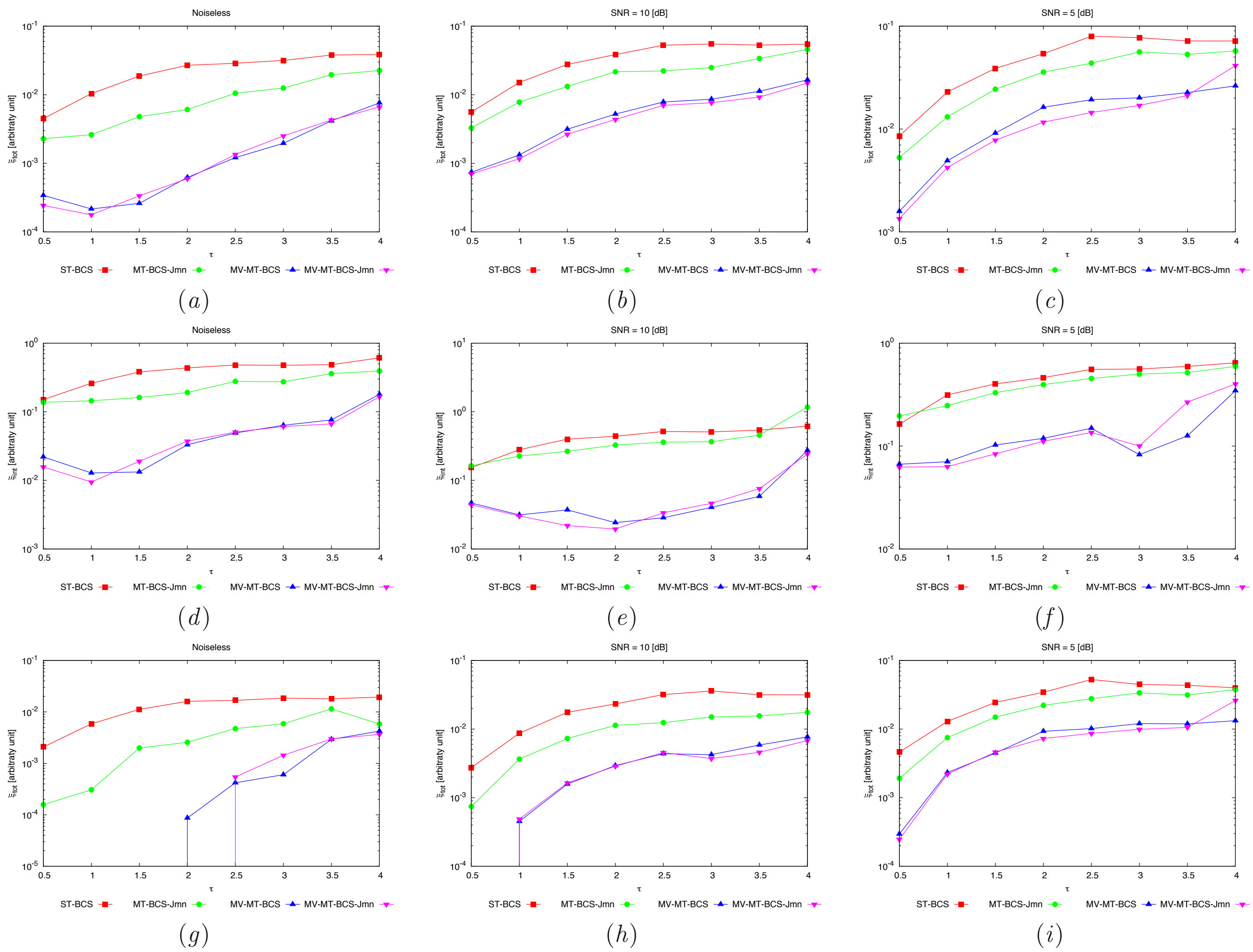

Figure 78. Behaviour of total error ξ_{tot} $(a)(b)(c)$, internal error ξ_{int} $(d)(e)(f)$ and external error ξ_{ext} $(g)(h)(i)$ for Noiseless case $(a)(d)(g)$, $SNR = 10$ [dB] $(b)(e)(h)$ and $SNR = 5$ [dB] $(c)(f)(i)$.

3.17 TEST CASE: Lossy Cylinder $L = 0.33\lambda$

Goal: show the performances of BCS when dealing with a sparse scatterer

- Number of Views: V
- Number of Measurements: M
- Number of Cells for the Inversion: N
- Number of Cells for the Direct solver: D
- Side of the investigation domain: L

Test Case Description

Direct solver:

- Square domain divided in $\sqrt{D} \times \sqrt{D}$ cells
- Domain side: $L = 3\lambda$
- $D = 1296$ (discretization for the direct solver: $< \lambda/10$)

Investigation domain:

- Square domain divided in $\sqrt{N} \times \sqrt{N}$ cells
- $L = 3\lambda$
- $2ka = 2 \times \frac{2\pi}{\lambda} \times \frac{L\sqrt{2}}{2} = 6\pi\sqrt{2} = 26.65$
- $\#DOF = \frac{(2ka)^2}{2} = \frac{(2\times\frac{2\pi}{\lambda}\times\frac{L\sqrt{2}}{2})^2}{2} = 4\pi^2\left(\frac{L}{\lambda}\right)^2 = 4\pi^2 \times 9 \approx 355.3$
- N scelto in modo da essere vicino a $\#DOF$: $N = 324$ (18×18)

Measurement domain:

- Measurement points taken on a circle of radius $\rho = 3\lambda$
- Full-aspect measurements
- $M \approx 2ka \rightarrow M = 27$

Sources:

- Plane waves
- $V \approx 2ka \rightarrow V = 27$
- Amplitude $A = 1$
- Frequency: 300 MHz ($\lambda = 1$)

Object:

- Lossy cylinder $L = 0.33\lambda$
- $\varepsilon_r \in \{1.5, 2.0, 3.0, 4.0, 5.0\}$
- $\sigma = \in \{0.01, 0.02, 0.03, 0.04, 0.05, 0.06, 0.07, 0.08, 0.09, 0.1\}$ [S/m]

MV-MT-BCS-Jmn parameters:

- Gamma prior on noise variance parameter: $a = 5 \times 10^0$
- Gamma prior on noise variance parameter: $b = 2 \times 10^{-2}$
- Convergenze parameter: $\tau = 1.0 \times 10^{-8}$

RESULTS: Lossy Cylinder $L = 0.33\lambda$ - $\sigma = 0.01$ - Reconstruction of $Real[\tau]$

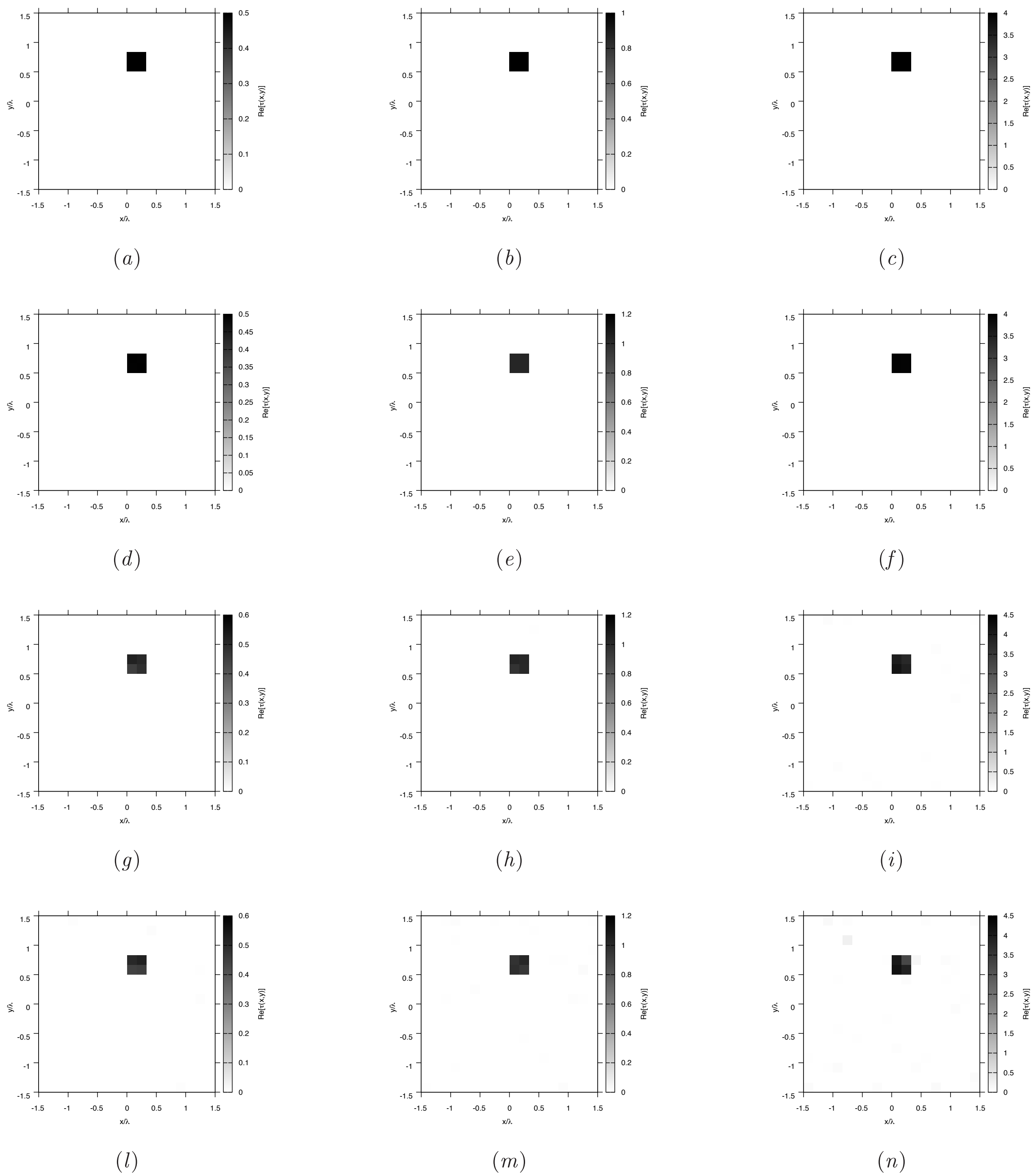

Figure 79. Actual object $(a)(b)(c)$ and MV-MT-BCS-Jmn reconstructed object with $\varepsilon_r = 1.5$ $(d)(g)(l)$, $\varepsilon_r = 2.0$ $(e)(h)(m)$, and $\varepsilon_r = 5.0$ $(f)(i)(n)$, for Noiseless case $(d)(e)(f)$, $SNR = 10$ [dB] $(g)(h)(i)$ and $SNR = 5$ [dB] $(l)(m)(n)$.

RESULTS: Lossy Cylinder $L = 0.33\lambda$ - $\sigma = 0.01$ - Reconstruction of $Imag[\tau]$

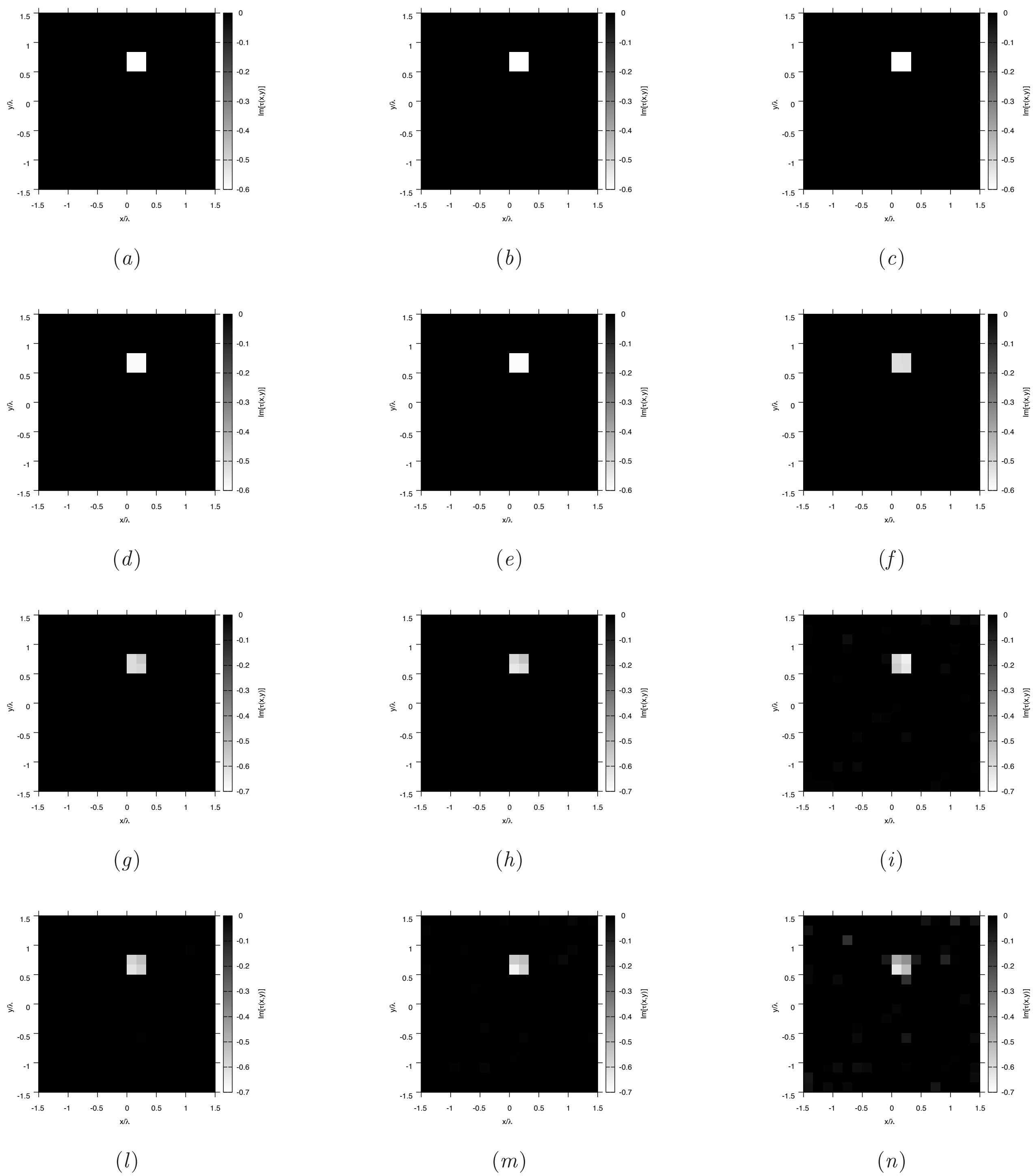

Figure 80. Actual object $(a)(b)(c)$ and MV-MT-BCS-Jmn reconstructed object with $\varepsilon_r = 1.5$ $(d)(g)(l)$, $\varepsilon_r = 2.0$ $(e)(h)(m)$, and $\varepsilon_r = 5.0$ $(f)(i)(n)$, for Noiseless case $(d)(e)(f)$, $SNR = 10$ [dB] $(g)(h)(i)$ and $SNR = 5$ [dB] $(l)(m)(n)$.

RESULTS: Lossy Cylinder $L = 0.33\lambda$ - $\sigma = 0.1$ - Reconstruction of $Real[\tau]$

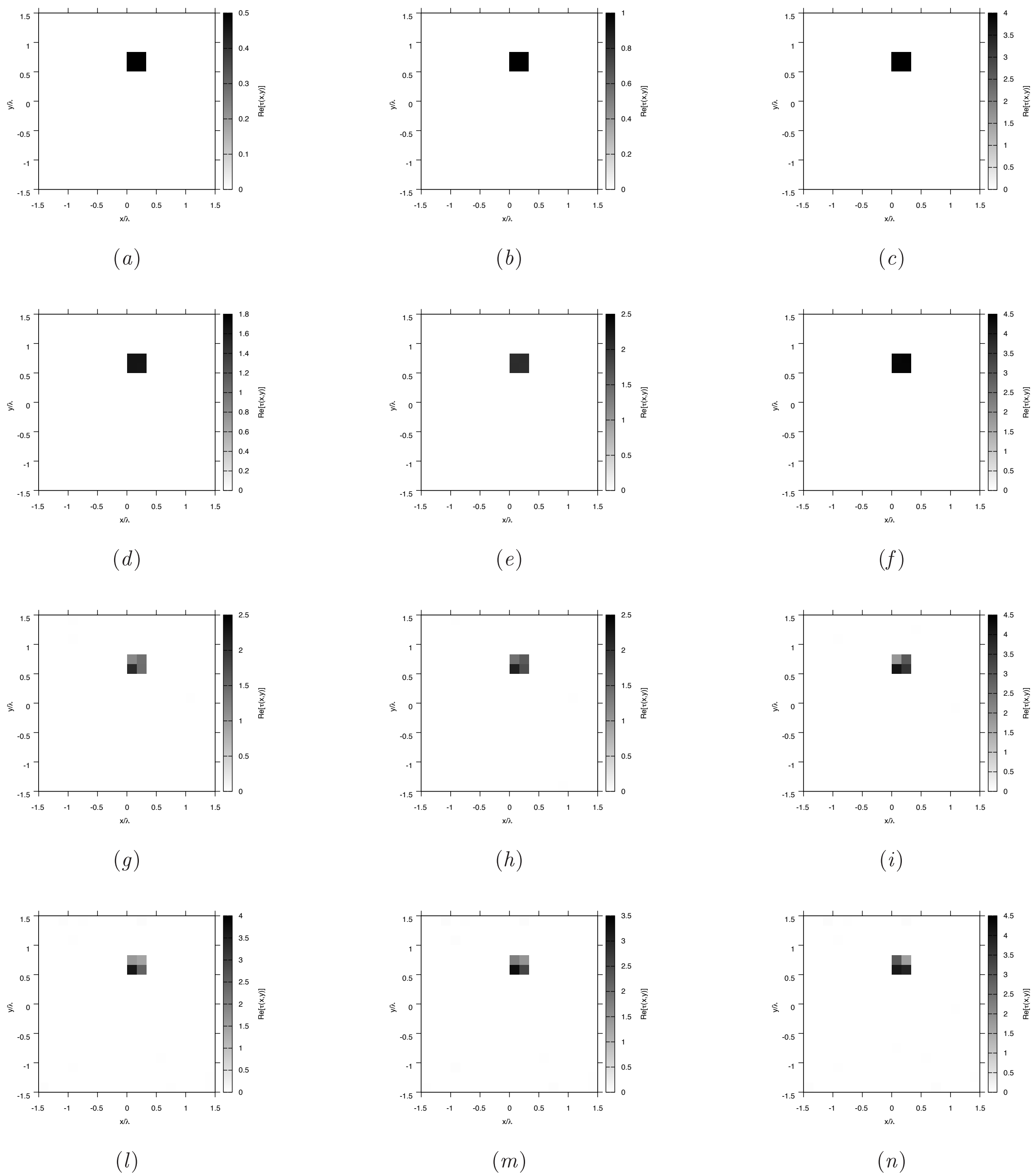

Figure 81. Actual object $(a)(b)(c)$ and MV-MT-BCS-Jmn reconstructed object with $\varepsilon_r = 1.5$ $(d)(g)(l)$, $\varepsilon_r = 2.0$ $(e)(h)(m)$, and $\varepsilon_r = 5.0$ $(f)(i)(n)$, for Noiseless case $(d)(e)(f)$, $SNR = 10$ [dB] $(g)(h)(i)$ and $SNR = 5$ [dB] $(l)(m)(n)$.

RESULTS: Lossy Cylinder $L = 0.33\lambda$ - $\sigma = 0.1$ - Reconstruction of $Imag[\tau]$

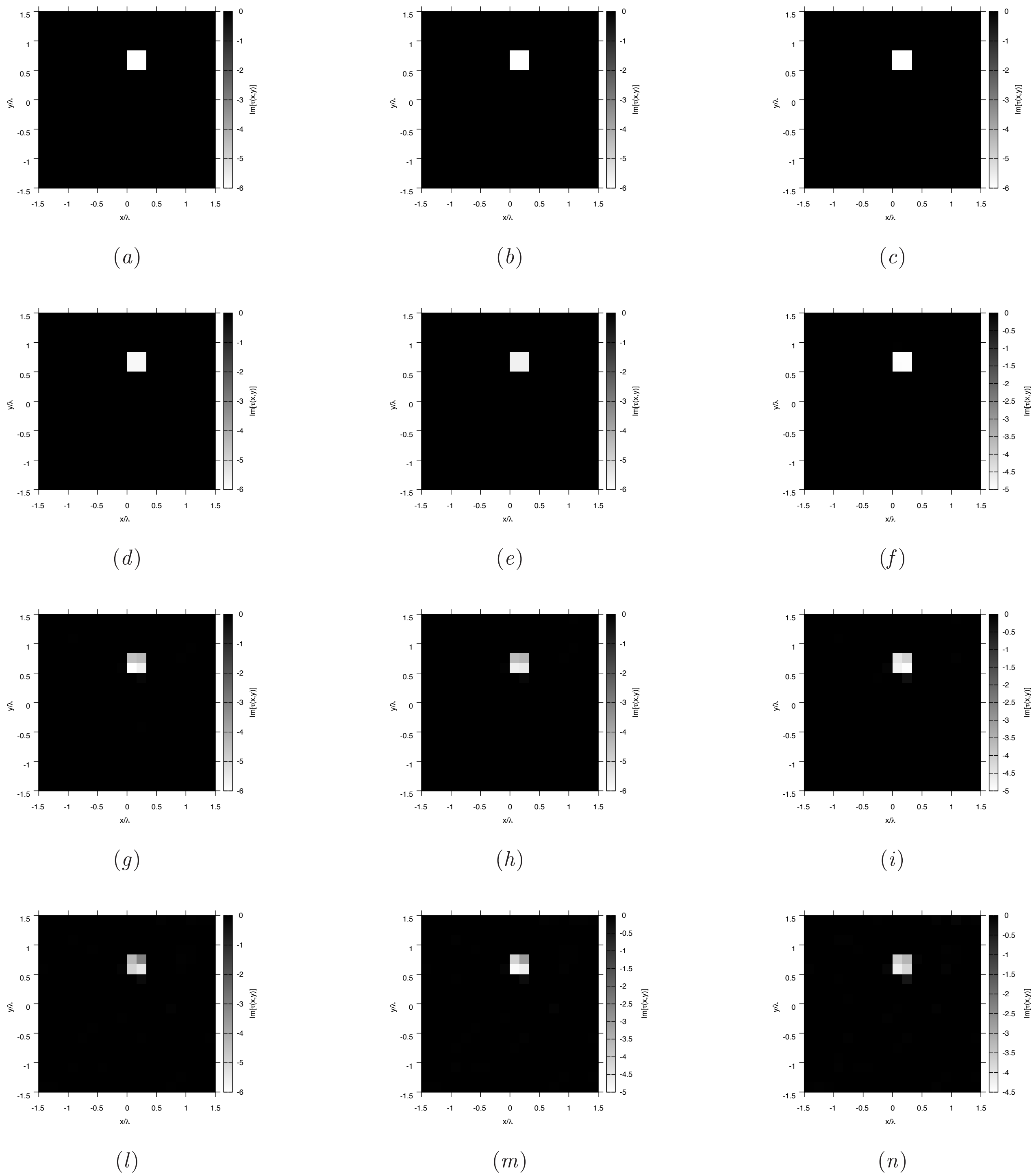

Figure 82. Actual object $(a)(b)(c)$ and MV-MT-BCS-Jmn reconstructed object with $\varepsilon_r = 1.5$ $(d)(g)(l)$, $\varepsilon_r = 2.0$ $(e)(h)(m)$, and $\varepsilon_r = 5.0$ $(f)(i)(n)$, for Noiseless case $(d)(e)(f)$, $SNR = 10$ [dB] $(g)(h)(i)$ and $SNR = 5$ [dB] $(l)(m)(n)$.

RESULTS: Lossy Cylinder $L = 0.33\lambda$ - Reconstructions - Comparison ST-BCS/MT-BCS - $\varepsilon_r = 2.0$, $\sigma = 0.1$

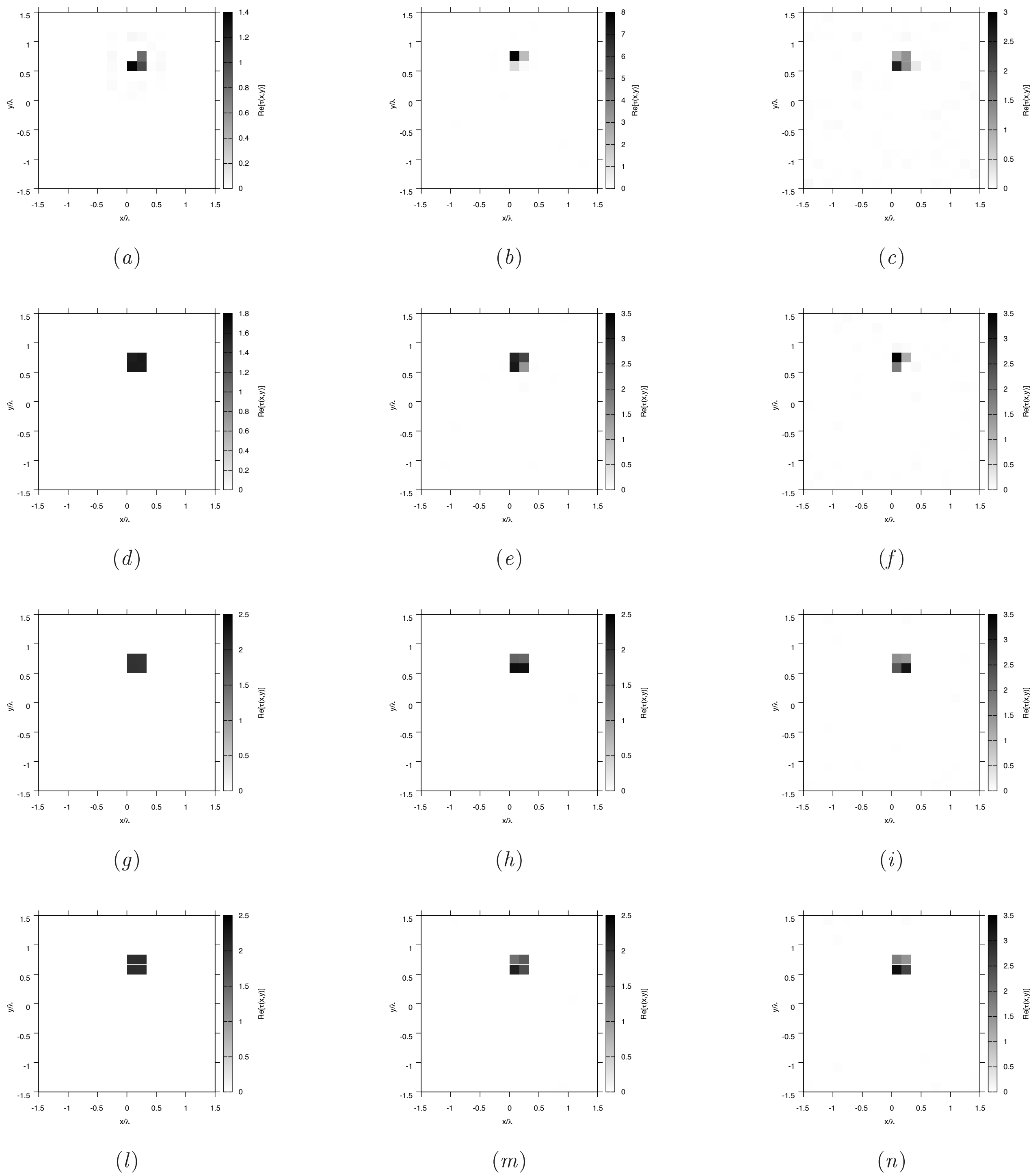

Figure 83. ST-BCS reconstructed object $(a)(b)(c)$, MT-BCS-Jmn reconstructed $(d)(e)(f)$ object, MV-MT-BCS reconstructed $(g)(h)(i)$ and MV-MT-BCS-Jmn reconstructed $(l)(m)(n)$ for Noiseless case $(a)(d)(g)(l)$, $SNR = 10$ [dB] $(b)(e)(h)(m)$ and $SNR = 5$ [dB] $(c)(f)(i)(n)$.

RESULTS: Lossy Cylinder $L = 0.33\lambda$ - Reconstructions - Comparison ST-BCS/MT-BCS - $\varepsilon_r = 2.0$, $\sigma = 0.1$

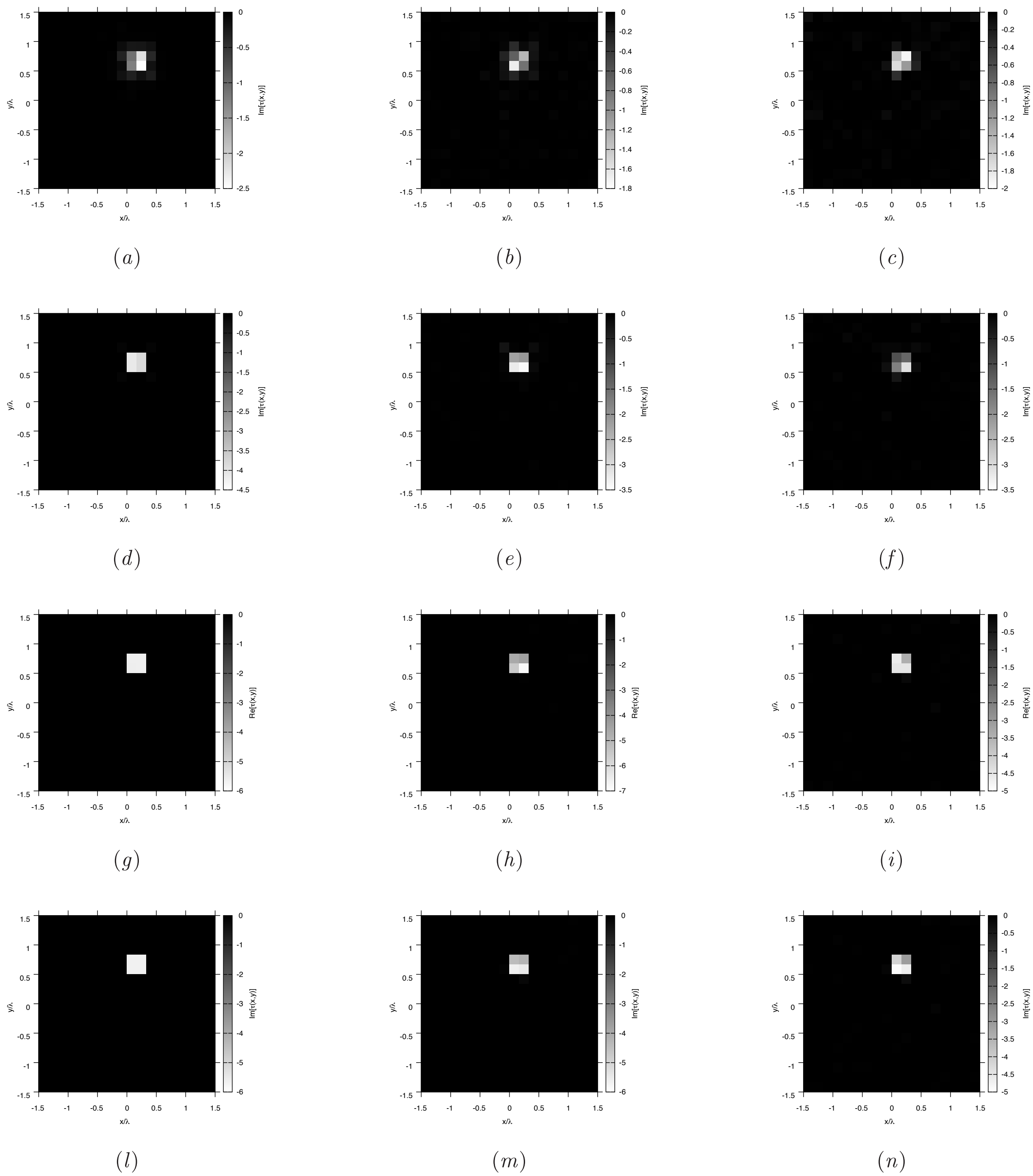

Figure 84. ST-BCS reconstructed object $(a)(b)(c)$, MT-BCS-Jmn reconstructed $(d)(e)(f)$ object, MV-MT-BCS reconstructed $(g)(h)(i)$ and MV-MT-BCS-Jmn reconstructed $(l)(m)(n)$ for Noiseless case $(a)(d)(g)(l)$, $SNR = 10$ [dB] $(b)(e)(h)(m)$ and $SNR = 5$ [dB] $(c)(f)(i)(n)$.

RESULTS: Lossy Cylinder $L = 0.33\lambda$ - Reconstruction Errors for $Real[\tau]$ - Comparison ST-BCS/MT-BCS - $\varepsilon_r = 1.5$ varying σ

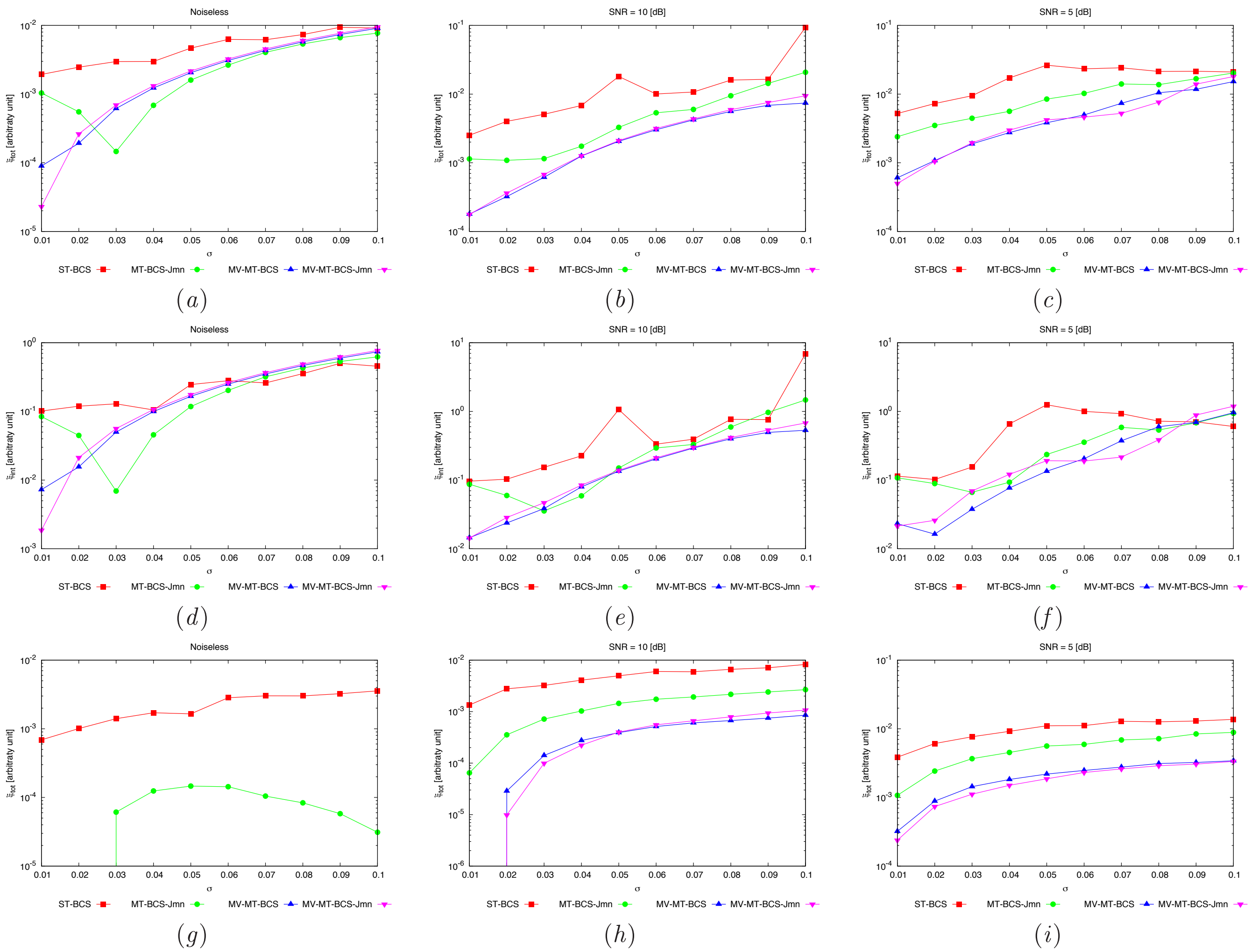

Figure 85. Behaviour of total error ξ_{tot} $(a)(b)(c)$, internal error ξ_{int} $(d)(e)(f)$ and external error ξ_{ext} $(g)(h)(i)$ for Noiseless case $(a)(d)(g)$, $SNR = 10$ [dB] $(b)(e)(h)$ and $SNR = 5$ [dB] $(c)(f)(i)$.

RESULTS: Lossy Cylinder $L = 0.33\lambda$ - Reconstruction Errors for $Imag[\tau]$ - Comparison ST-BCS/MT-BCS - $\varepsilon_r = 1.5$ varying σ

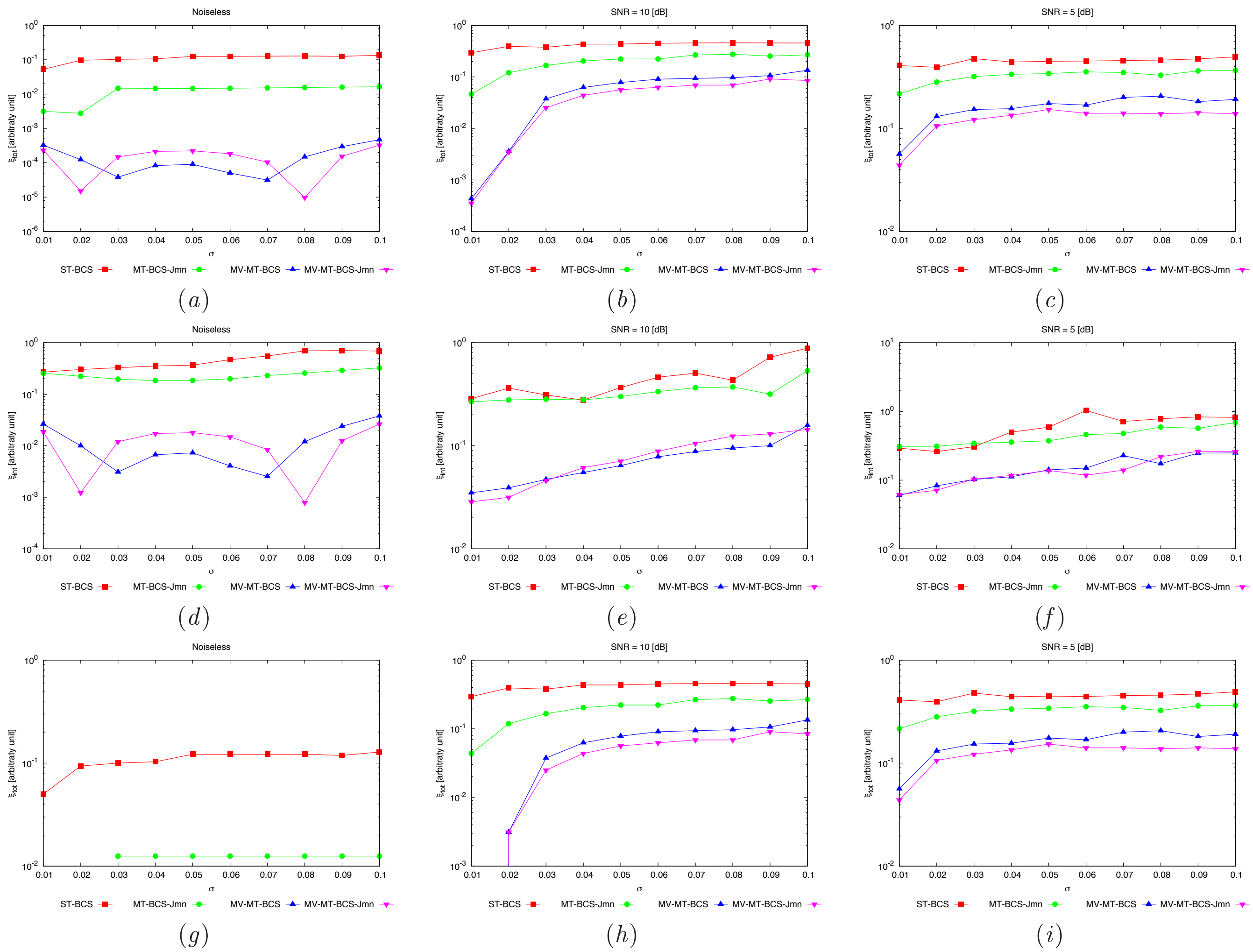

Figure 86. Behaviour of total error ξ_{tot} $(a)(b)(c)$, internal error ξ_{int} $(d)(e)(f)$ and external error ξ_{ext} $(g)(h)(i)$ for Noiseless case $(a)(d)(g)$, $SNR = 10$ [dB] $(b)(e)(h)$ and $SNR = 5$ [dB] $(c)(f)(i)$.

RESULTS: Lossy Cylinder $L = 0.33\lambda$ - Reconstruction Errors for $Real[\tau]$ - Comparison ST-BCS/MT-BCS - $\varepsilon_r = 2.0$ varying σ

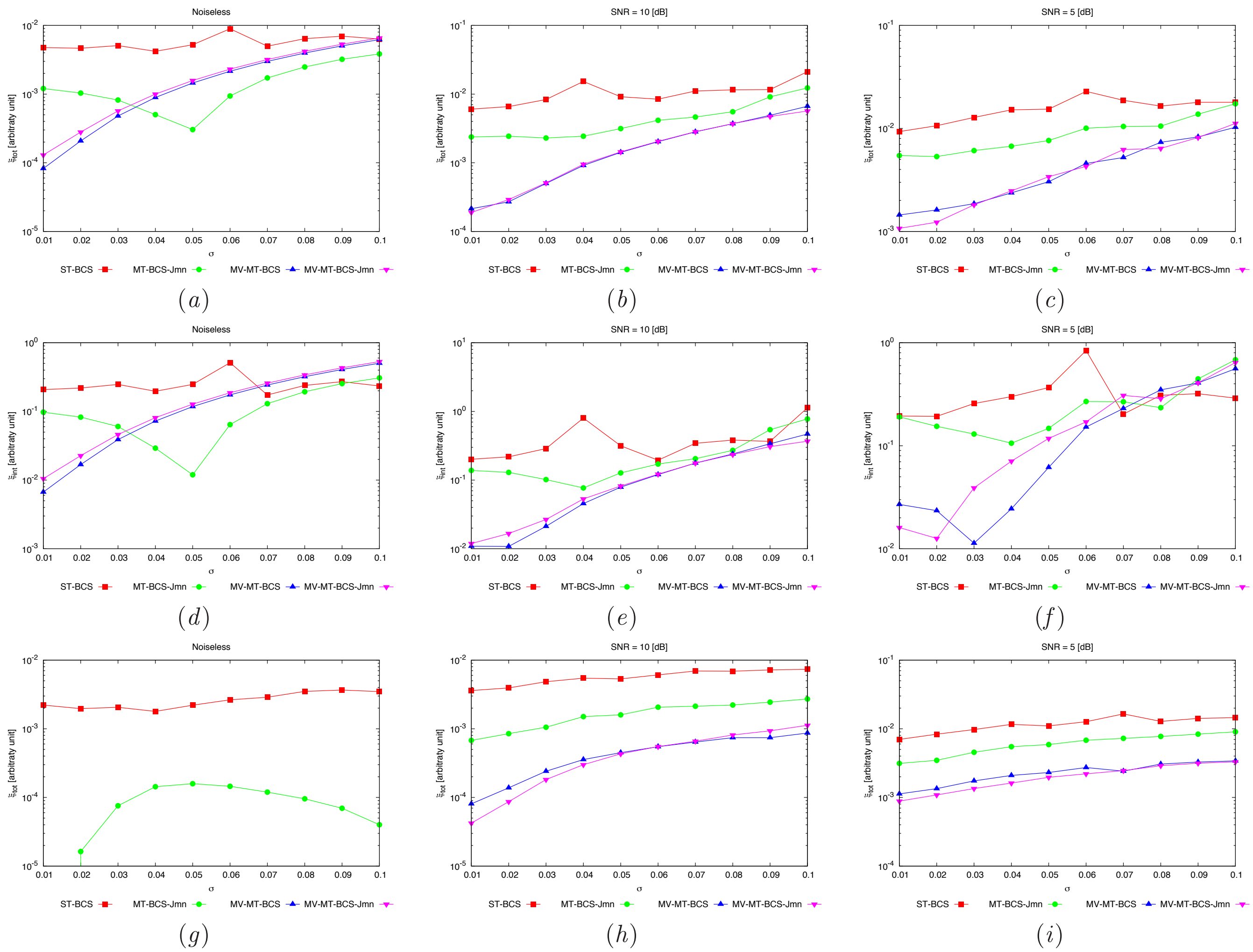

Figure 87. Behaviour of total error ξ_{tot} $(a)(b)(c)$, internal error ξ_{int} $(d)(e)(f)$ and external error ξ_{ext} $(g)(h)(i)$ for Noiseless case $(a)(d)(g)$, $SNR = 10$ [dB] $(b)(e)(h)$ and $SNR = 5$ [dB] $(c)(f)(i)$.

RESULTS: Lossy Cylinder $L = 0.33\lambda$ - Reconstruction Errors for $Imag[\tau]$ - Comparison ST-BCS/MT-BCS - $\varepsilon_r = 2.0$ varying σ

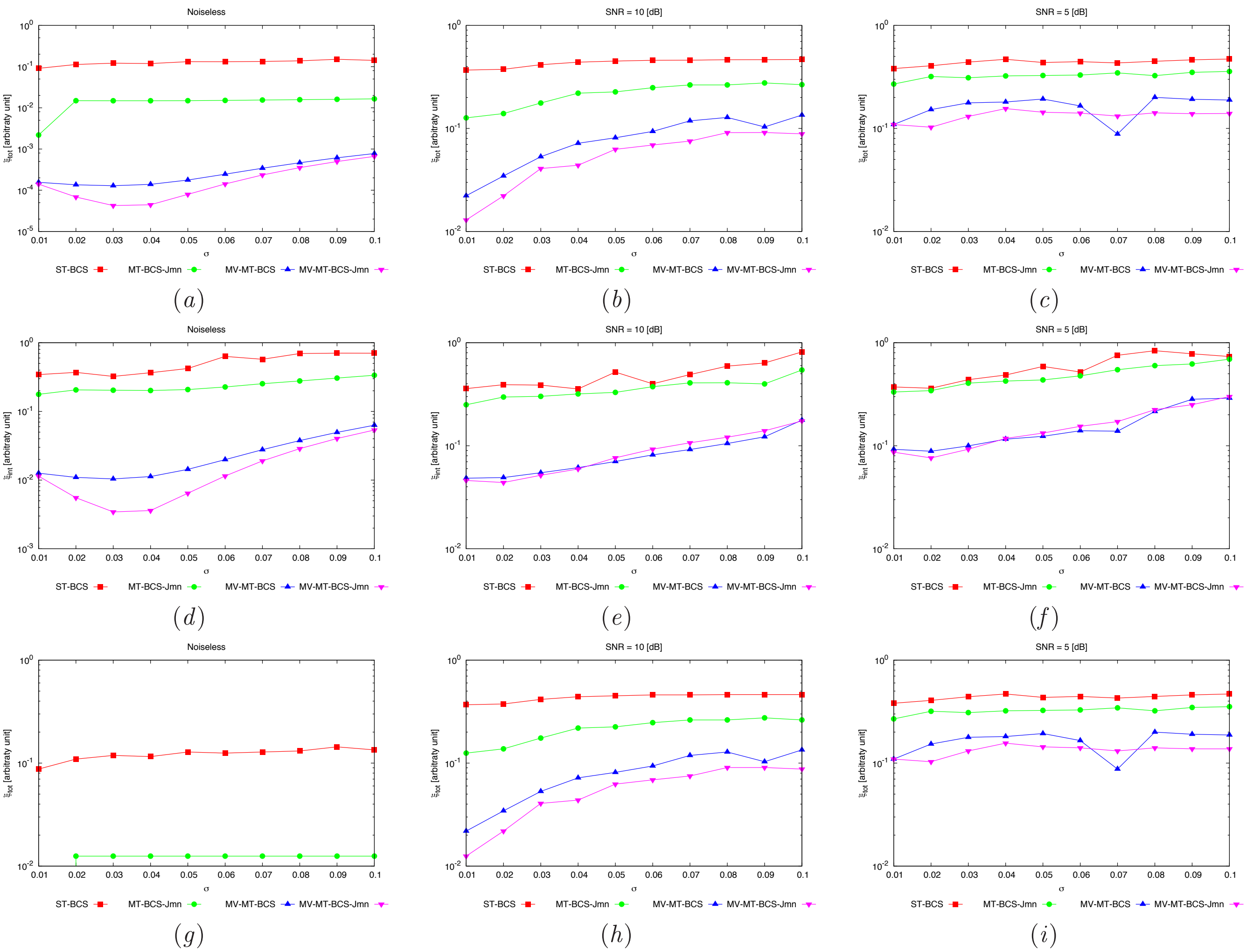

Figure 88. Behaviour of total error ξ_{tot} $(a)(b)(c)$, internal error ξ_{int} $(d)(e)(f)$ and external error ξ_{ext} $(g)(h)(i)$ for Noiseless case $(a)(d)(g)$, $SNR = 10$ [dB] $(b)(e)(h)$ and $SNR = 5$ [dB] $(c)(f)(i)$.

RESULTS: Lossy Cylinder $L = 0.33\lambda$ - Reconstruction Errors for $Real[\tau]$ - Comparison ST-BCS/MT-BCS - $\varepsilon_r = 5.0$ varying σ

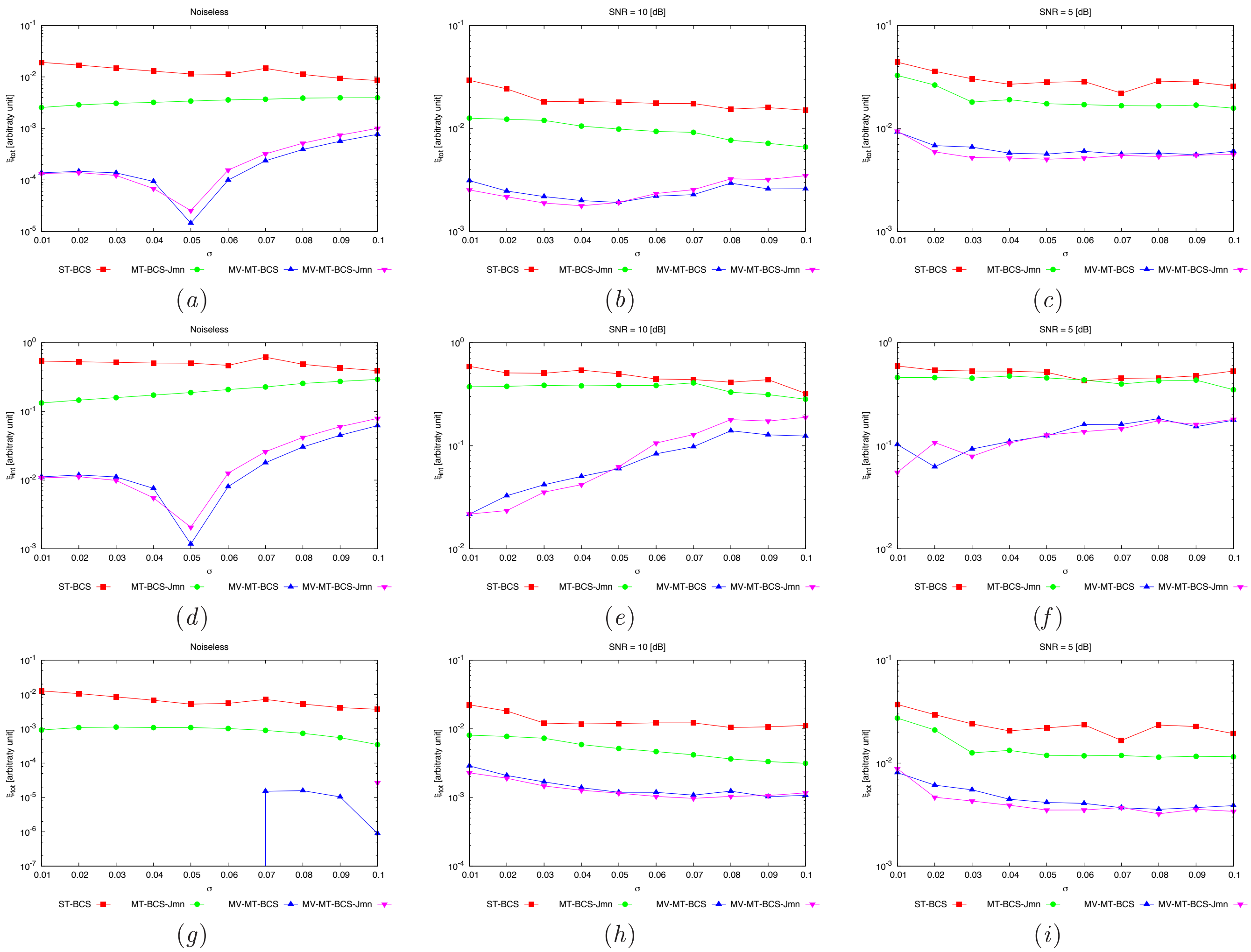

Figure 89. Behaviour of total error ξ_{tot} $(a)(b)(c)$, internal error ξ_{int} $(d)(e)(f)$ and external error ξ_{ext} $(g)(h)(i)$ for Noiseless case $(a)(d)(g)$, $SNR = 10$ [dB] $(b)(e)(h)$ and $SNR = 5$ [dB] $(c)(f)(i)$.

RESULTS: Lossy Cylinder $L = 0.33\lambda$ - Reconstruction Errors for $Imag[\tau]$ - Comparison ST-BCS/MT-BCS - $\varepsilon_r = 5.0$ varying σ

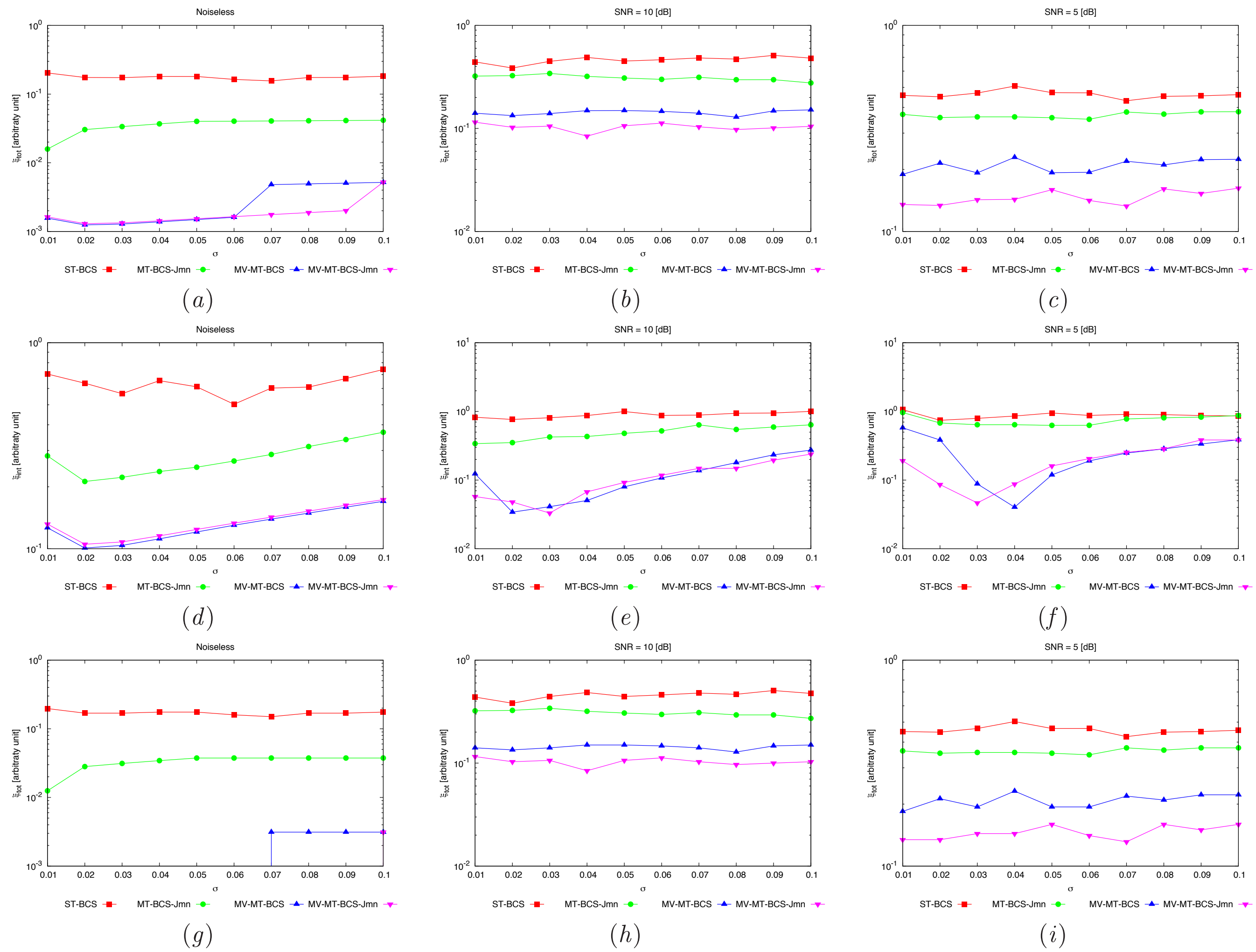

Figure 90. Behaviour of total error ξ_{tot} $(a)(b)(c)$, internal error ξ_{int} $(d)(e)(f)$ and external error ξ_{ext} $(g)(h)(i)$ for Noiseless case $(a)(d)(g)$, $SNR = 10$ [dB] $(b)(e)(h)$ and $SNR = 5$ [dB] $(c)(f)(i)$.

3.18 TEST CASE: Statistical Analysis - Square Cylinders $L = 0.16\lambda$

Goal: evaluate the performances of BCS

- Number of Views: V
- Number of Measurements: M
- Number of Cells for the Inversion: N
- Number of Cells for the Direct solver: D
- Side of the investigation domain: L

Test Case Description

Direct solver:

- Square domain divided in $\sqrt{D} \times \sqrt{D}$ cells
- Domain side: $L = 3\lambda$
- $D = 1296$ (discretization for the direct solver: $< \lambda/10$)

Investigation domain:

- Square domain divided in $\sqrt{N} \times \sqrt{N}$ cells
- $L = 3\lambda$
- $N = 324$

Measurement domain:

- Measurement points taken on a circle of radius $\rho = 3\lambda$
- Full-aspect measurements
- $M \approx 2ka \rightarrow M = 27$

Sources:

- Plane waves
- $V \approx 2ka \rightarrow V = 27$
- Amplitude $A = 1$
- Frequency: 300 MHz ($\lambda = 1$)

Object:

- $S \in \{1, 2, 3, 4, 5, 6\}$ Square cylinders of side $\frac{\lambda}{6} = 0.16667$
- $\varepsilon_r \in \{1.5, 2.0, 3.0, 4.0, 5.0\}$
- $\sigma = 0$ [S/m]

MV-MT-BCS-Jmn parameters:

- Gamma prior on noise variance parameter: $a = 5 \times 10^0$
- Gamma prior on noise variance parameter: $b = 2 \times 10^{-2}$
- Convergenze parameter: $\tau = 1.0 \times 10^{-8}$

Statistical Analysis:

- $K = 10$ random seeds used for each case

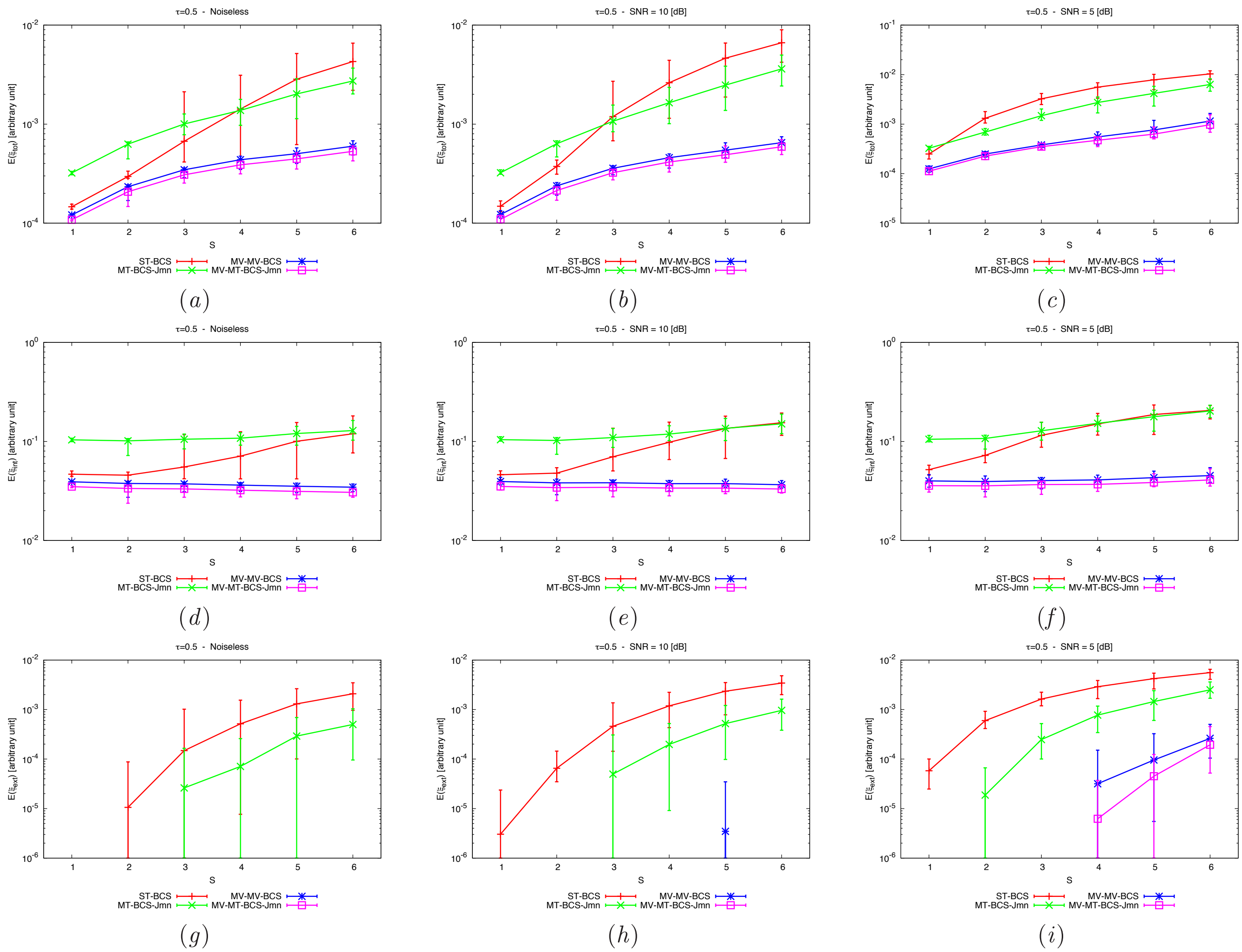

Figure 91. *Statistical analysis* $[K = 10,\ \varepsilon_r = 1.5]$ - Behaviour of mean, maximum and minimum of the error figures as a function of S (sparsity factor) of the total error ξ_{tot} $(a)(b)(c)$, internal error ξ_{int} $(d)(e)(f)$ and external error ξ_{ext} $(g)(h)(i)$ for Noiseless case $(a)(d)(g)$, $SNR = 10$ [dB] $(b)(e)(h)$ and $SNR = 5$ [dB] $(c)(f)(i)$.

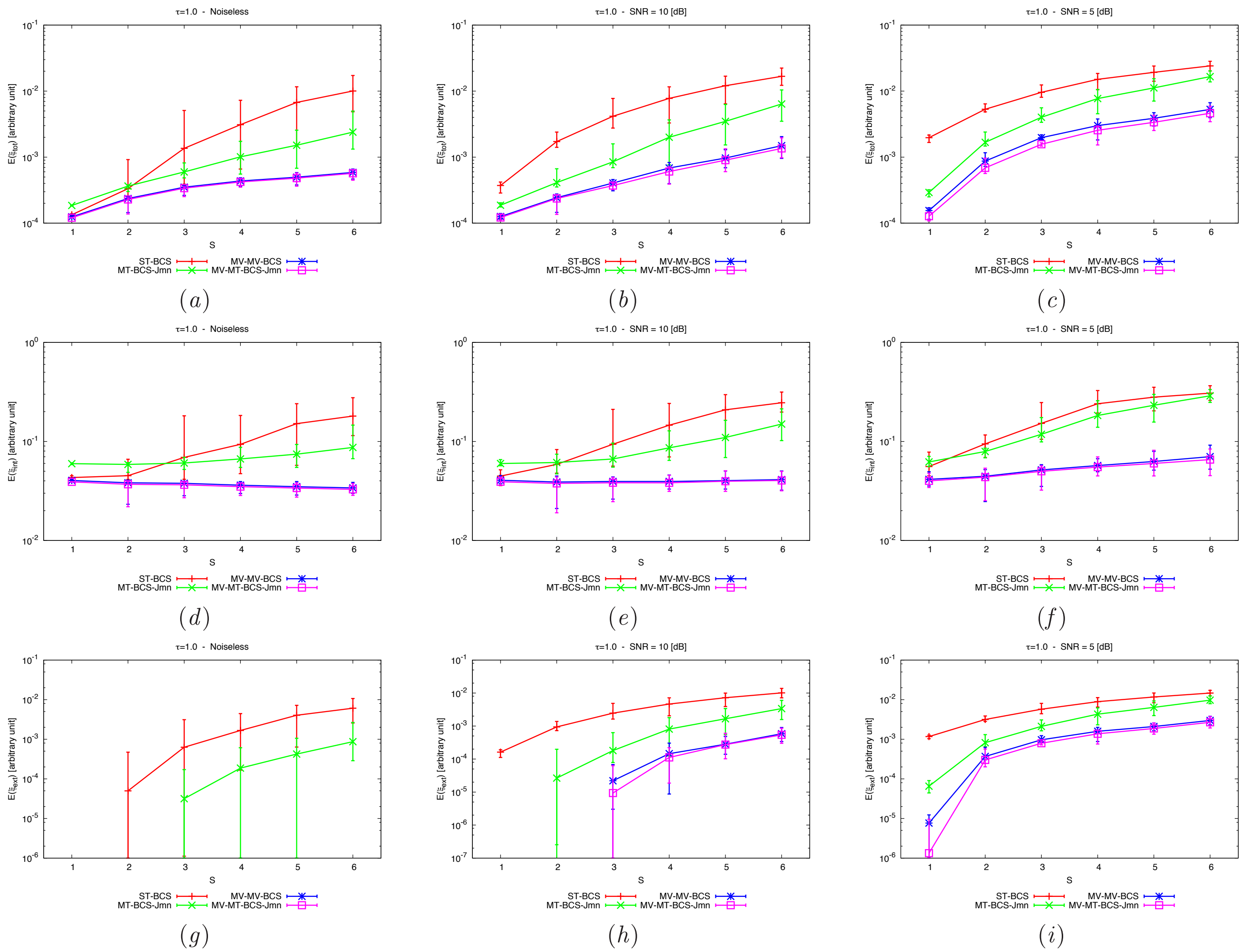

Figure 92. *Statistical analysis* $[K = 10,\ \varepsilon_r = 2.0]$ - Behaviour of mean, maximum and minimum of the error figures as a function of S (sparsity factor) of the total error ξ_{tot} $(a)(b)(c)$, internal error ξ_{int} $(d)(e)(f)$ and external error ξ_{ext} $(g)(h)(i)$ for Noiseless case $(a)(d)(g)$, $SNR = 10$ [dB] $(b)(e)(h)$ and $SNR = 5$ [dB] $(c)(f)(i)$.

RESULTS: Statistical Analysis - Error Figures - Comparison ST-BCS/MT-BCS - $\varepsilon_r = 3.0$

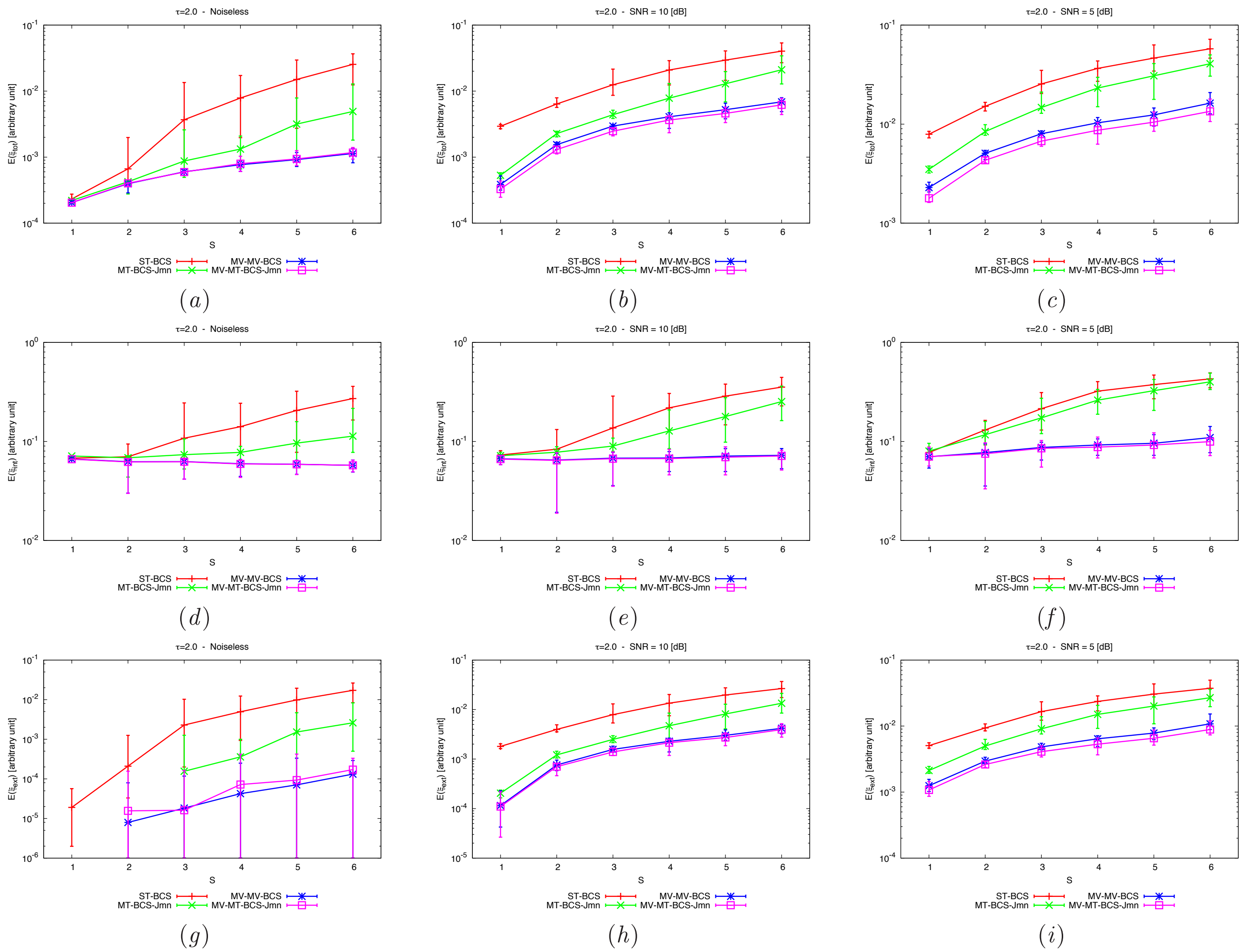

Figure 93. *Statistical analysis* $[K = 10,\ \varepsilon_r = 3.0]$ - Behaviour of mean, maximum and minimum of the error figures as a function of S (sparsity factor) of the total error ξ_{tot} $(a)(b)(c)$, internal error ξ_{int} $(d)(e)(f)$ and external error ξ_{ext} $(g)(h)(i)$ for Noiseless case $(a)(d)(g)$, $SNR = 10$ [dB] $(b)(e)(h)$ and $SNR = 5$ [dB] $(c)(f)(i)$.

RESULTS: Statistical Analysis - Error Figures - Comparison ST-BCS/MT-BCS - $\varepsilon_r = 4.0$

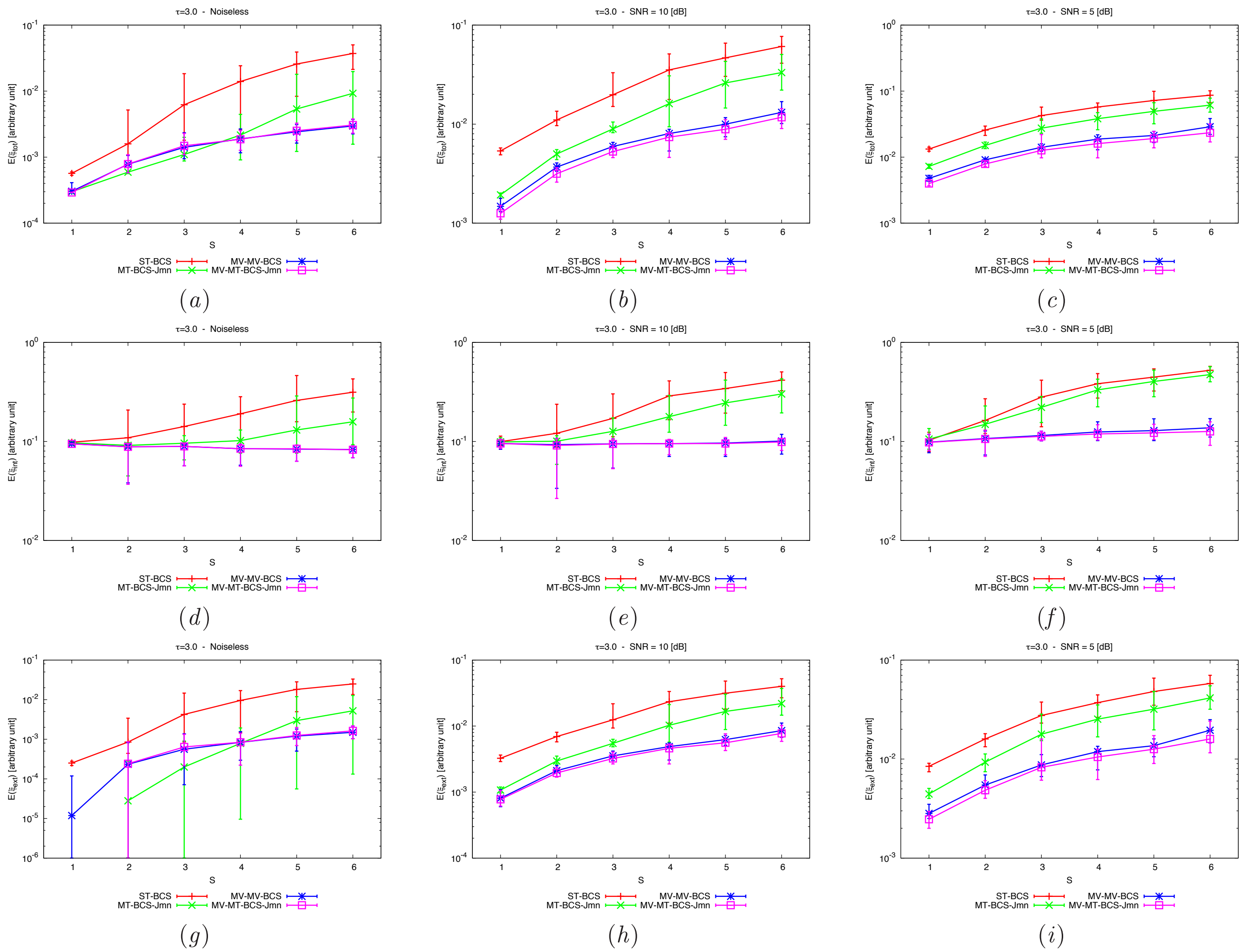

Figure 94. *Statistical analysis* $[K = 10, \varepsilon_r = 4.0]$ - Behaviour of mean, maximum and minimum of the error figures as a function of S (sparsity factor) of the total error ξ_{tot} $(a)(b)(c)$, internal error ξ_{int} $(d)(e)(f)$ and external error ξ_{ext} $(g)(h)(i)$ for Noiseless case $(a)(d)(g)$, $SNR = 10$ [dB] $(b)(e)(h)$ and $SNR = 5$ [dB] $(c)(f)(i)$.

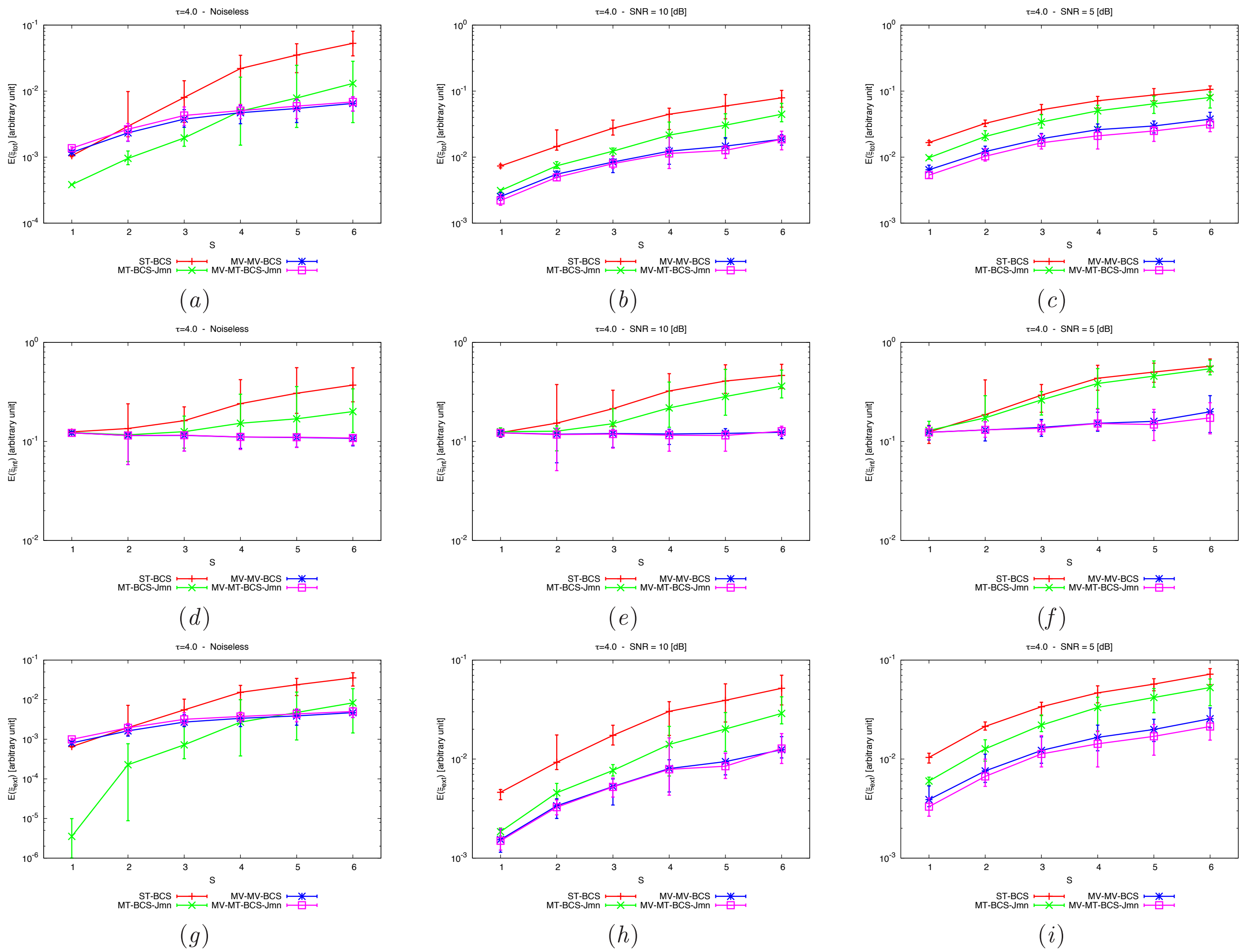

Figure 95. *Statistical analysis* $[K = 10,\, \varepsilon_r = 5.0]$ - Behaviour of mean, maximum and minimum of the error figures as a function of S (sparsity factor) of the total error ξ_{tot} $(a)(b)(c)$, internal error ξ_{int} $(d)(e)(f)$ and external error ξ_{ext} $(g)(h)(i)$ for Noiseless case $(a)(d)(g)$, $SNR = 10$ [dB] $(b)(e)(h)$ and $SNR = 5$ [dB] $(c)(f)(i)$.

TEST CASE: Statistical Analysis - Square Cylinders $L = 0.33\lambda$

Goal: evaluate the performances of *BCS*

- Number of Views: V
- Number of Measurements: M
- Number of Cells for the Inversion: N
- Number of Cells for the Direct solver: D
- Side of the investigation domain: L

Test Case Description

Direct solver:

- Square domain divided in $\sqrt{D} \times \sqrt{D}$ cells
- Domain side: $L = 3\lambda$
- $D = 1296$ (discretization for the direct solver: $< \lambda/10$)

Investigation domain:

- Square domain divided in $\sqrt{N} \times \sqrt{N}$ cells
- $L = 3\lambda$
- $N = 324$

Measurement domain:

- Measurement points taken on a circle of radius $\rho = 3\lambda$
- Full-aspect measurements
- $M \approx 2ka \rightarrow M = 27$

Sources:

- Plane waves
- $V \approx 2ka \rightarrow V = 27$
- Amplitude $A = 1$
- Frequency: 300 MHz ($\lambda = 1$)

Object:

- $S \in \{1, 2, 3, 4, 5, 6\}$ Square cylinders of side $\frac{\lambda}{3} = 0.3333$
- $\varepsilon_r = 2.0$
- $\sigma = 0$ [S/m]

MV-MT-BCS-Jmn parameters:

- Gamma prior on noise variance parameter: $a = 5 \times 10^0$
- Gamma prior on noise variance parameter: $b = 2 \times 10^{-2}$
- Convergenze parameter: $\tau = 1.0 \times 10^{-8}$

Statistical Analysis:

- $K = 10$ random seeds used for each case

RESULTS: Statistical Analysis - Error Figures - Comparison ST-BCS/MT-BCS - $\varepsilon_r = 2.0$

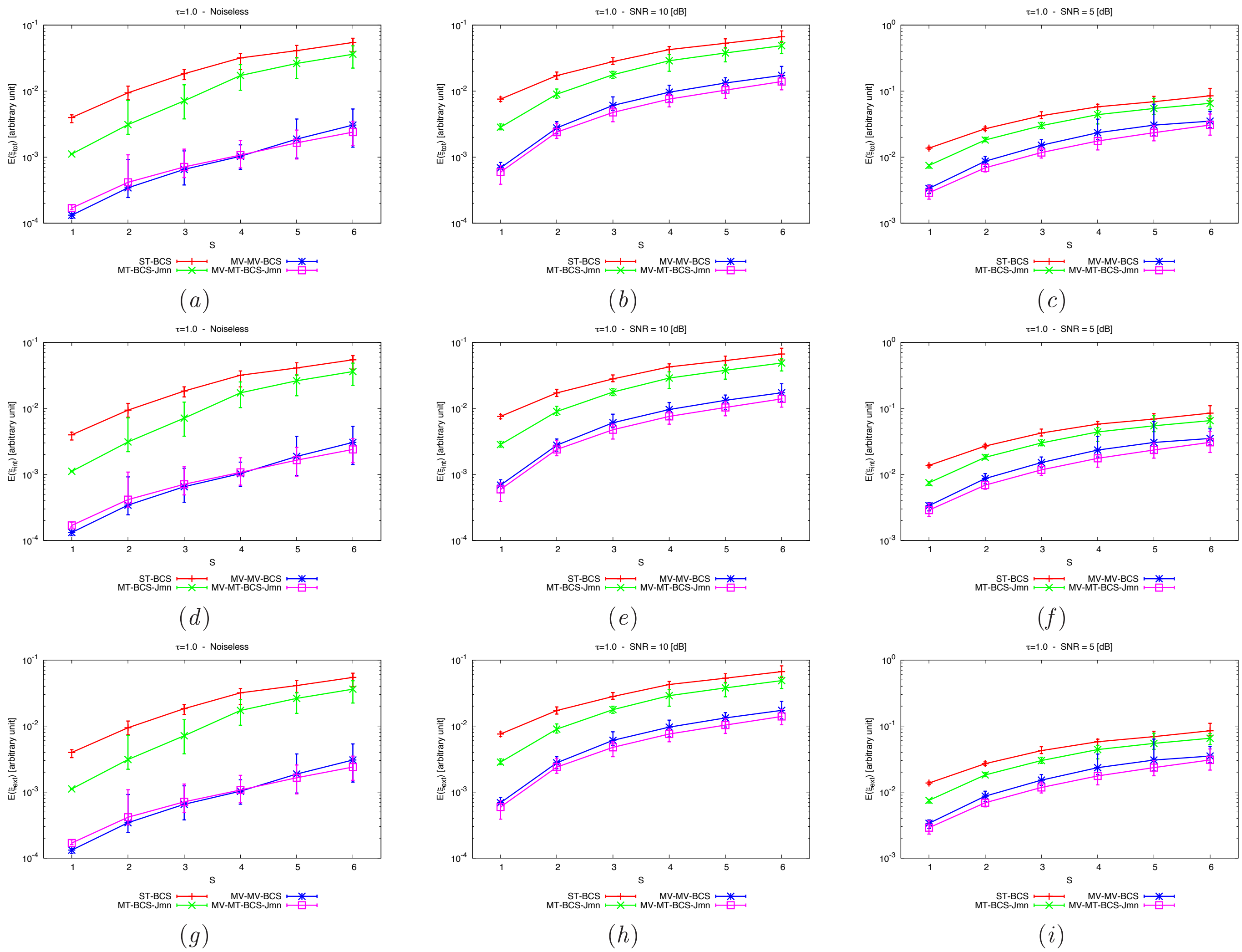

Figure 96. *Statistical analysis* $[K = 10,\ \varepsilon_r = 2.0]$ - Behaviour of mean, maximum and minimum of the error figures as a function of S (sparsity factor) of the total error ξ_{tot} $(a)(b)(c)$, internal error ξ_{int} $(d)(e)(f)$ and external error ξ_{ext} $(g)(h)(i)$ for Noiseless case $(a)(d)(g)$, $SNR = 10$ [dB] $(b)(e)(h)$ and $SNR = 5$ [dB] $(c)(f)(i)$.

RESULTS: Statistical Analysis (Random case 2) $L = 0.33\lambda$ - Reconstructions - Comparison ST-BCS/MT-BCS - $\varepsilon_r = 2.0$

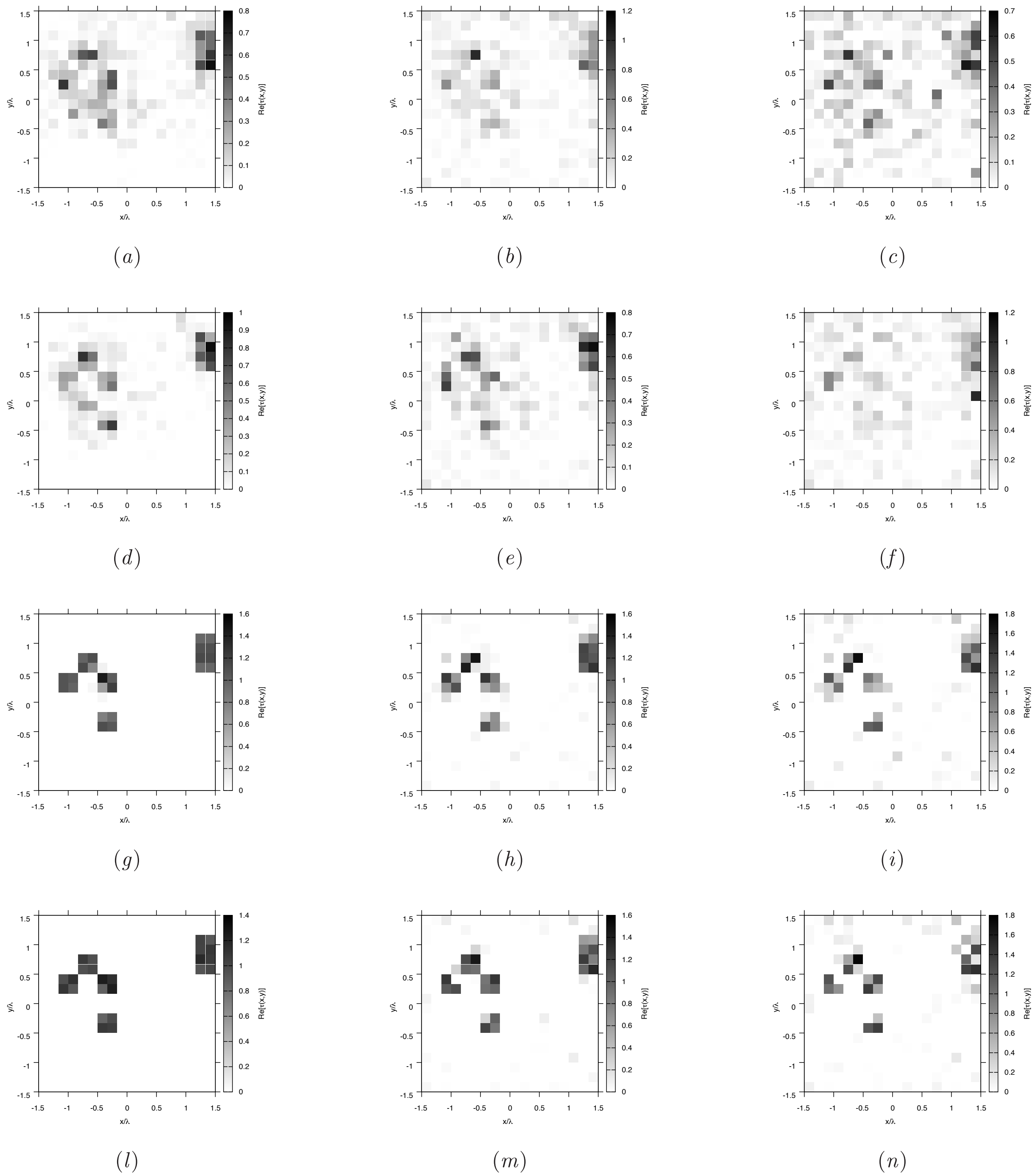

Figure 97. ST-BCS reconstructed object $(a)(b)(c)$, MT-BCS-Jmn reconstructed $(d)(e)(f)$ object, MV-MT-BCS reconstructed $(g)(h)(i)$ and MV-MT-BCS-Jmn reconstructed $(l)(m)(n)$ for Noiseless case $(a)(d)(g)(l)$, $SNR = 10$ [dB] $(b)(e)(h)(m)$ and $SNR = 5$ [dB] $(c)(f)(i)(n)$.

RESULTS: Statistical Analysis (Random case 10) $L = 0.33\lambda$ - Reconstructions - Comparison ST-BCS/MT-BCS - $\varepsilon_r = 2.0$

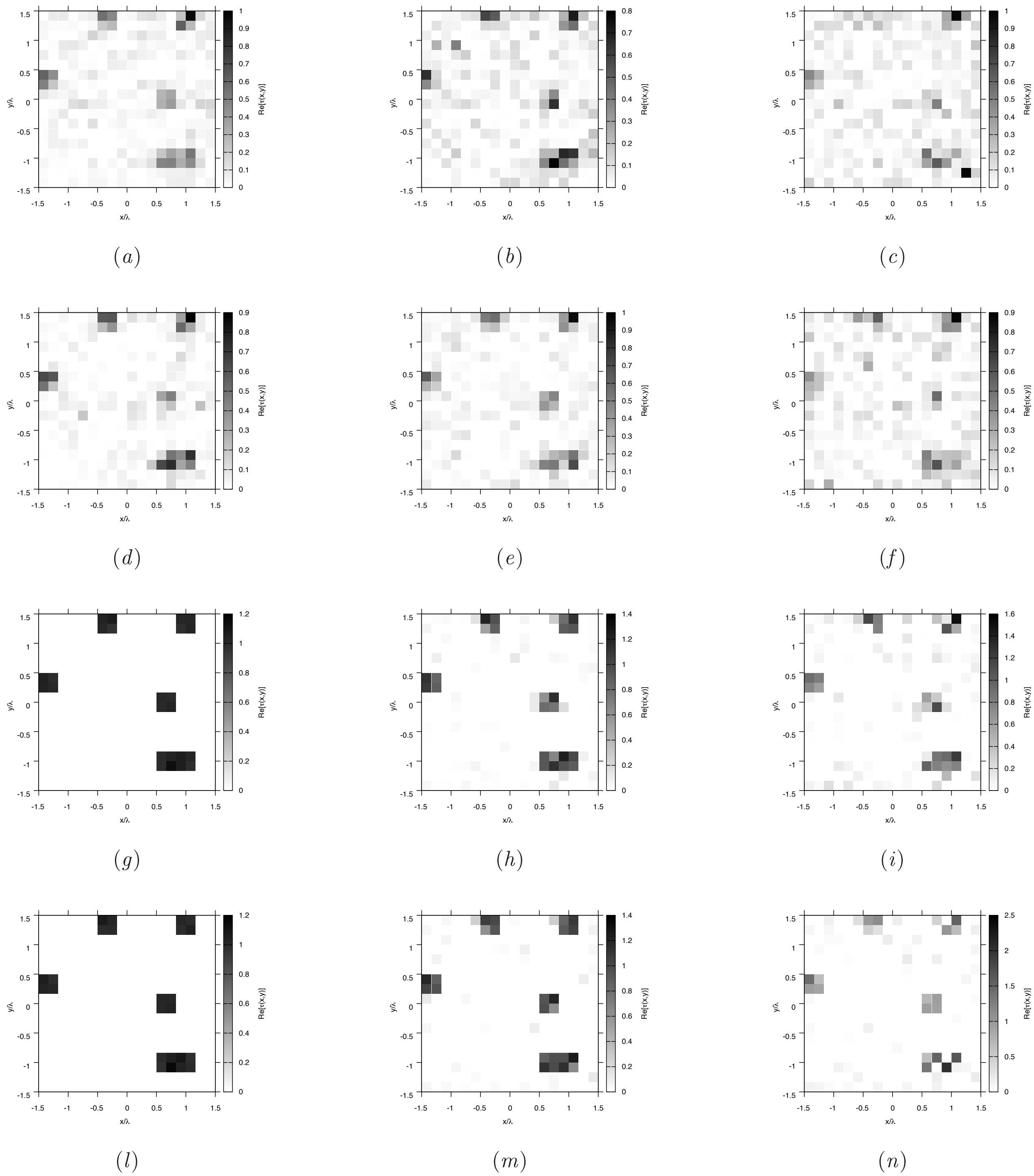

Figure 98. ST-BCS reconstructed object $(a)(b)(c)$, MT-BCS-Jmn reconstructed $(d)(e)(f)$ object, MV-MT-BCS reconstructed $(g)(h)(i)$ and MV-MT-BCS-Jmn reconstructed $(l)(m)(n)$ for Noiseless case $(a)(d)(g)(l)$, $SNR = 10$ [dB] $(b)(e)(h)(m)$ and $SNR = 5$ [dB] $(c)(f)(i)(n)$.

3.19 TEST CASE: Two Square Cylinders on the Diagonal

Goal: evaluate the the performances of BCS

- Number of Views: V
- Number of Measurements: M
- Number of Cells for the Inversion: N
- Number of Cells for the Direct solver: D
- Side of the investigation domain: L

Test Case Description

Direct solver:

- Square domain divided in $\sqrt{D} \times \sqrt{D}$ cells
- Domain side: $L = 3\lambda$
- $D = 1296$ (discretization for the direct solver: $< \lambda/10$)

Investigation domain:

- Square domain divided in $\sqrt{N} \times \sqrt{N}$ cells
- $L = 3\lambda$
- $N = 324$

Measurement domain:

- Measurement points taken on a circle of radius $\rho = 3\lambda$
- Full-aspect measurements
- $M \approx 2ka \rightarrow M = 27$

Sources:

- Plane waves
- $V \approx 2ka \rightarrow V = 27$
- Amplitude $A = 1$
- Frequency: 300 MHz ($\lambda = 1$)

Object:

- Two square cylinders of side $\frac{\lambda}{6} = 0.16667$ at a distance Δx, Δy from each other
- $\varepsilon_r \in \{1.5, 2.0, 3.0, 4.0, 5.0\}$
- $\sigma = 0$ [S/m]

MV-MT-BCS-Jmn parameters:

- Gamma prior on noise variance parameter: $a = 5 \times 10^0$
- Gamma prior on noise variance parameter: $b = 2 \times 10^{-2}$
- Convergenze parameter: $\tau = 1.0 \times 10^{-8}$

Resolution Analysis:

- $\Delta x = \Delta y = \{k\lambda/10,\ k = 0, ..., 8\}$

RESULTS: Resolution Analysis - Error Figures - Comparison ST-BCS/MT-BCS - $\varepsilon_r = 1.5$

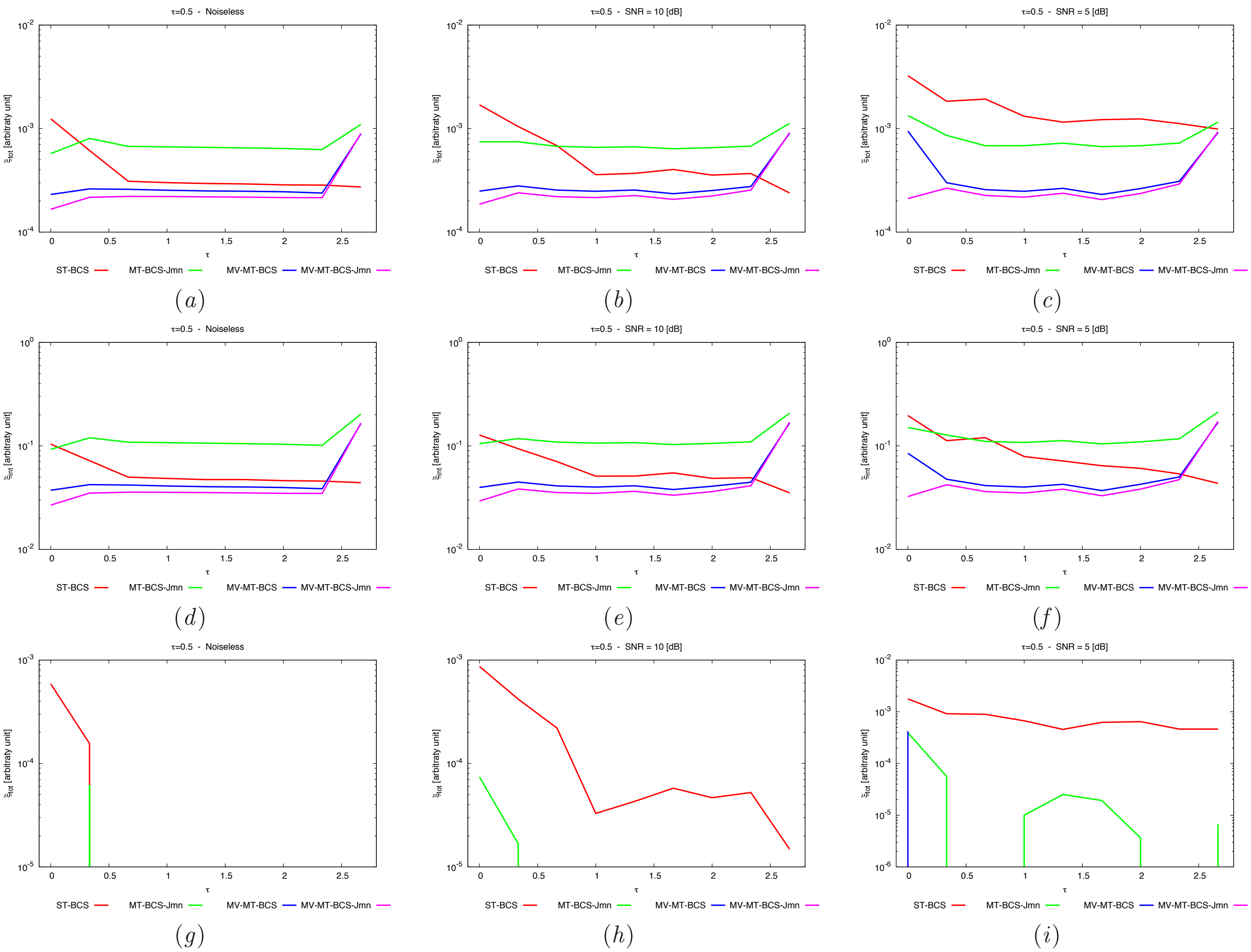

Figure 99. *Resolution analysis* $[\varepsilon_r = 1.5]$ - Behaviour of mean, maximum and minimum of the error figures as a function of the distance $\Delta x = \Delta y$ of two pixels on the diagonal from each other, of the total error ξ_{tot} $(a)(b)(c)$, internal error ξ_{int} $(d)(e)(f)$ and external error ξ_{ext} $(g)(h)(i)$ for Noiseless case $(a)(d)(g)$, $SNR = 10$ [dB] $(b)(e)(h)$ and $SNR = 5$ [dB] $(c)(f)(i)$.

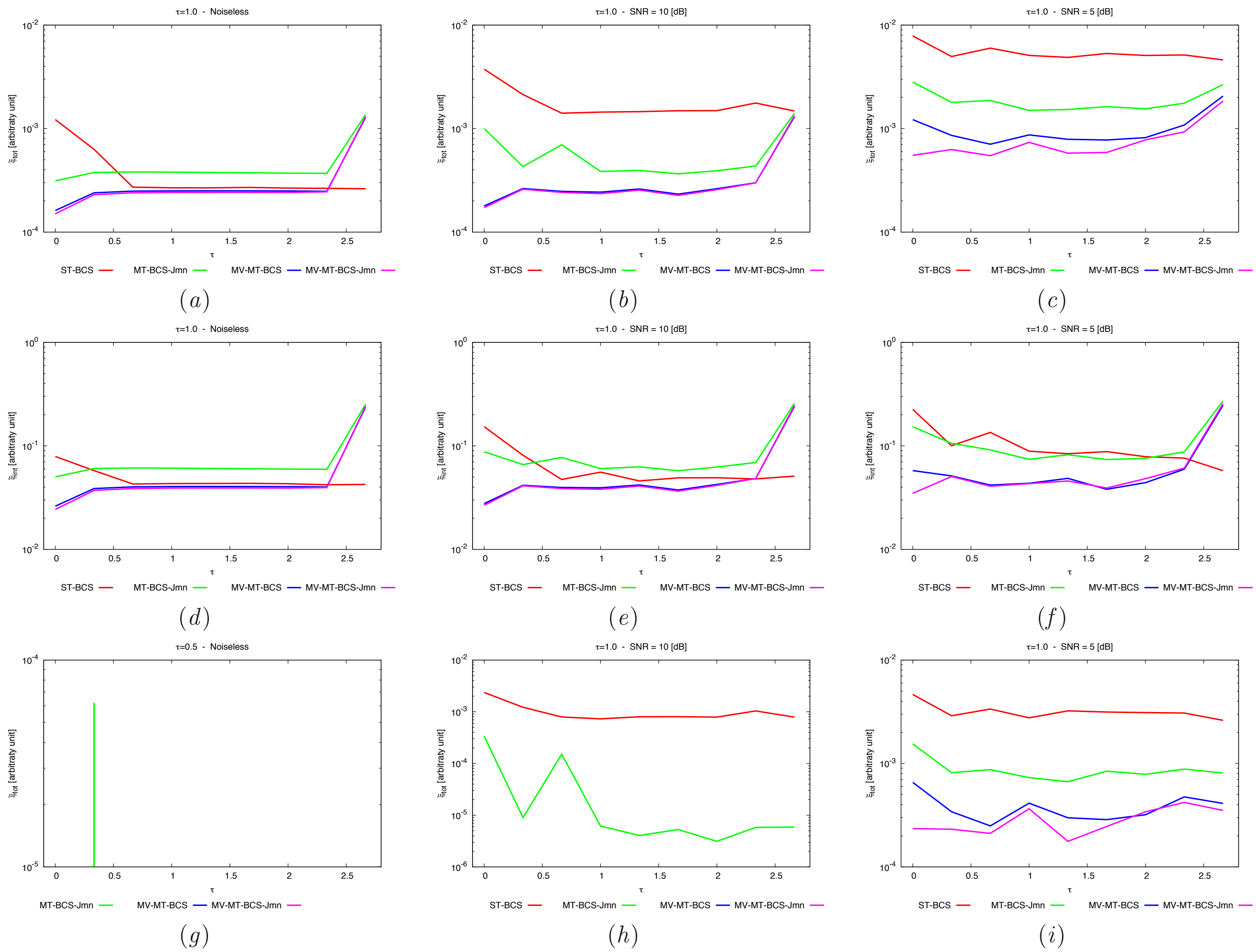

Figure 100. *Resolution analysis* $[\varepsilon_r = 2.0]$ - Behaviour of mean, maximum and minimum of the error figures as a function of the distance $\Delta x = \Delta y$ of two pixels on the diagonal from each other, of the total error ξ_{tot} $(a)(b)(c)$, internal error ξ_{int} $(d)(e)(f)$ and external error ξ_{ext} $(g)(h)(i)$ for Noiseless case $(a)(d)(g)$, $SNR = 10$ [dB] $(b)(e)(h)$ and $SNR = 5$ [dB] $(c)(f)(i)$.

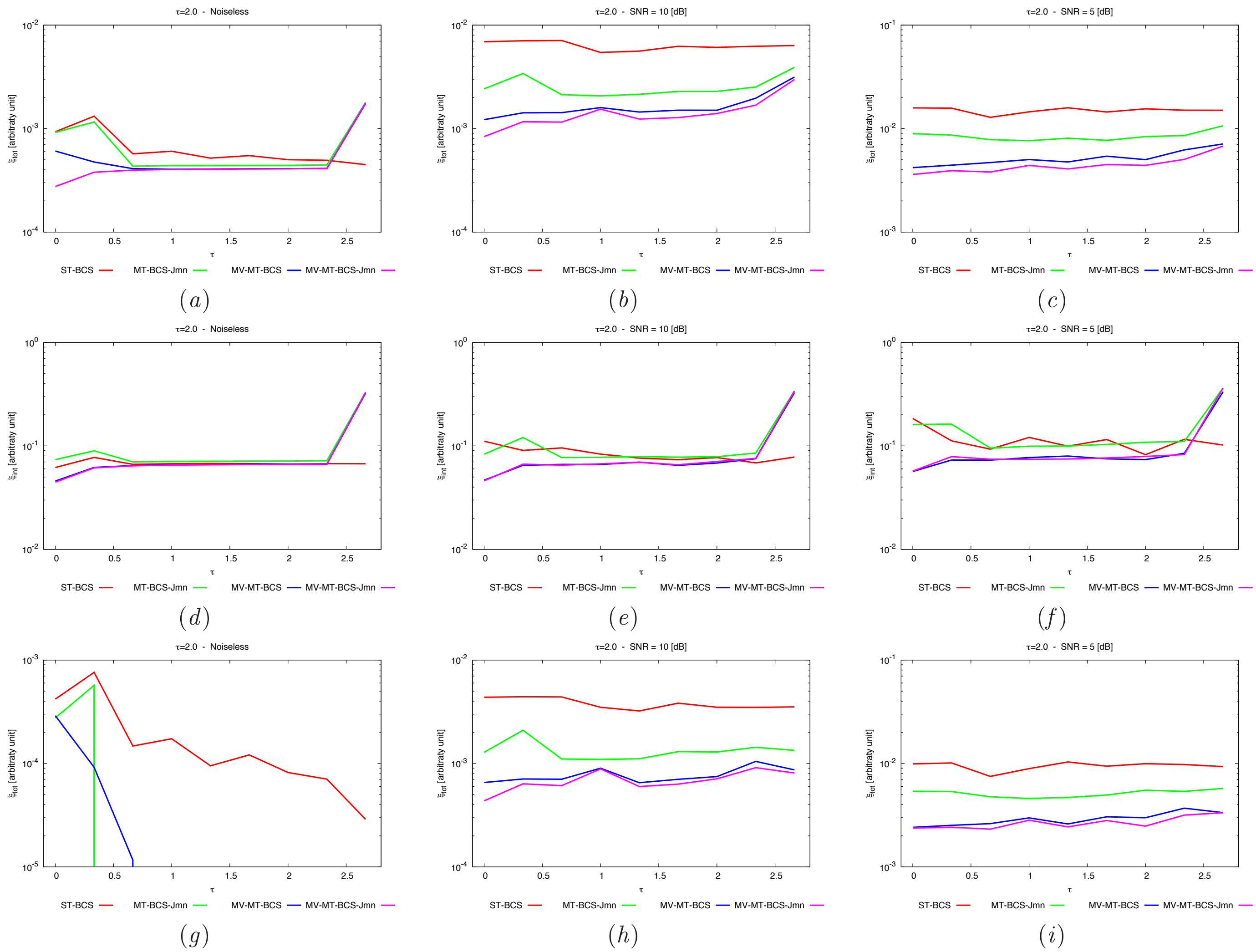

Figure 101. *Resolution analysis* [$\varepsilon_r = 3.0$] - Behaviour of mean, maximum and minimum of the error figures as a function of the distance $\Delta x = \Delta y$ of two pixels on the diagonal from each other, of the total error ξ_{tot} $(a)(b)(c)$, internal error ξ_{int} $(d)(e)(f)$ and external error ξ_{ext} $(g)(h)(i)$ for Noiseless case $(a)(d)(g)$, $SNR = 10$ [dB] $(b)(e)(h)$ and $SNR = 5$ [dB] $(c)(f)(i)$.

RESULTS: Resolution Analysis - Error Figures - Comparison ST-BCS/MT-BCS - $\varepsilon_r = 4.0$

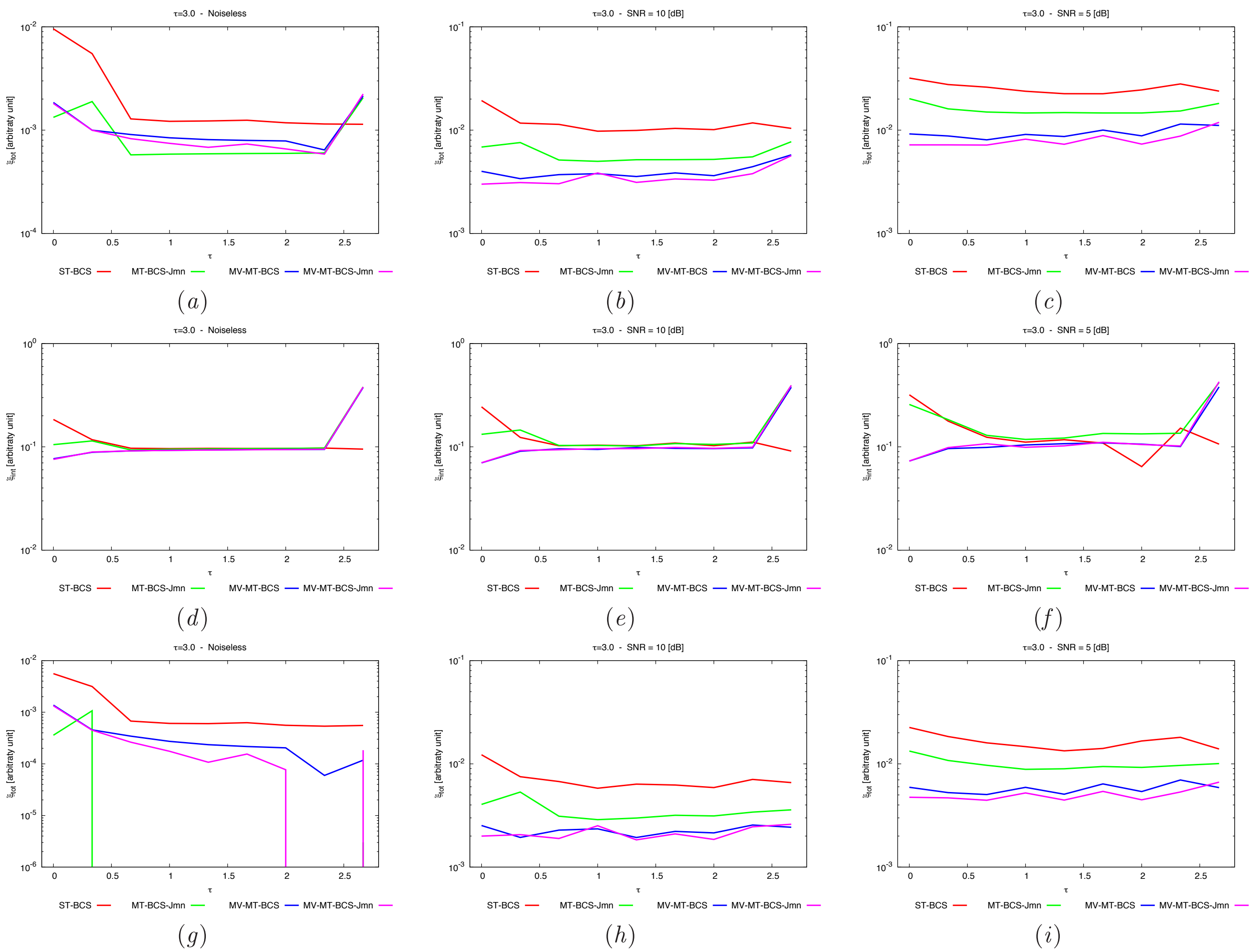

Figure 102. *Resolution analysis* [$\varepsilon_r = 4.0$] - Behaviour of mean, maximum and minimum of the error figures as a function of the distance $\Delta x = \Delta y$ of two pixels on the diagonal from each other, of the total error ξ_{tot} $(a)(b)(c)$, internal error ξ_{int} $(d)(e)(f)$ and external error ξ_{ext} $(g)(h)(i)$ for Noiseless case $(a)(d)(g)$, $SNR = 10$ [dB] $(b)(e)(h)$ and $SNR = 5$ [dB] $(c)(f)(i)$.

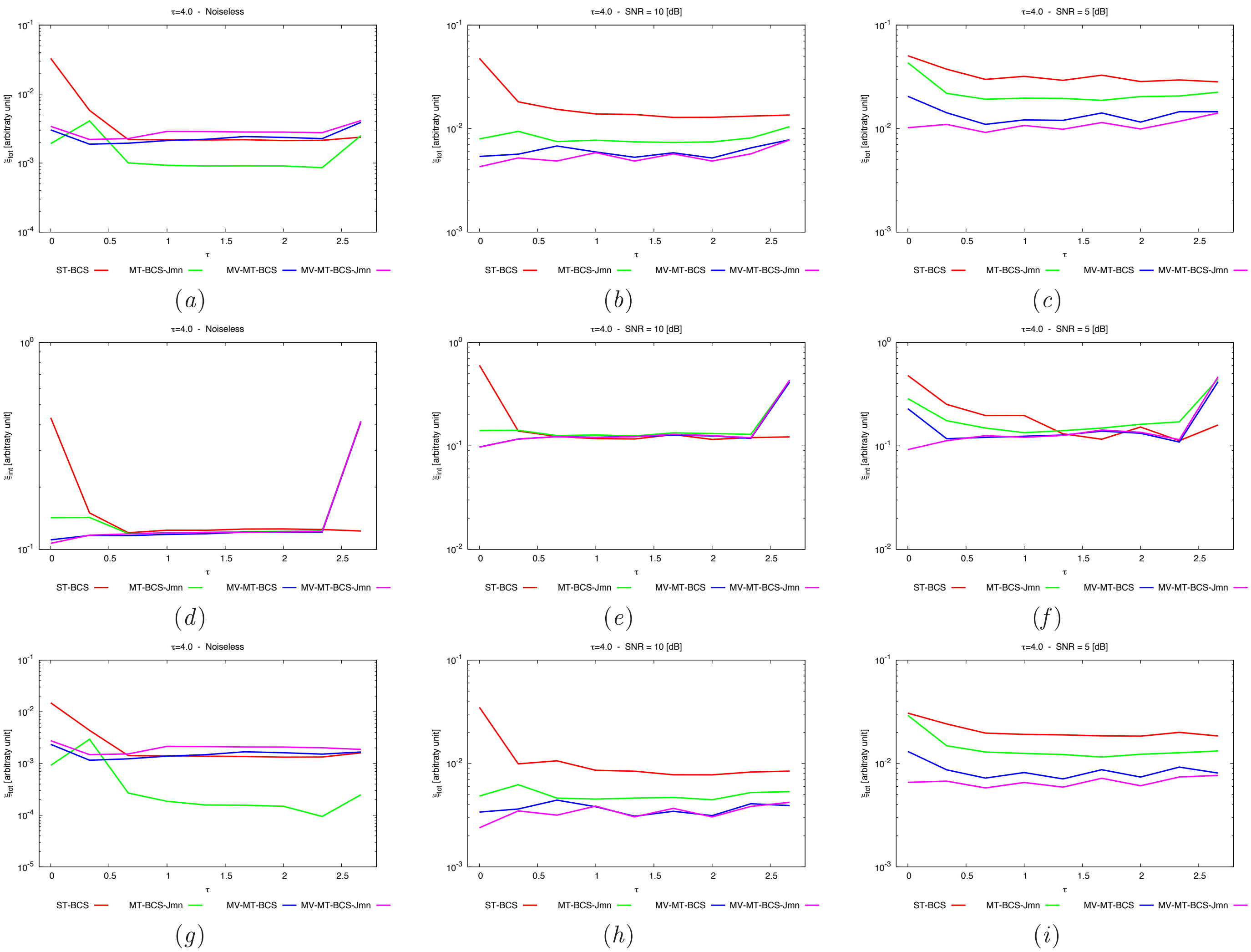

Figure 103. *Resolution analysis* $[\varepsilon_r = 5.0]$ - Behaviour of mean, maximum and minimum of the error figures as a function of the distance $\Delta x = \Delta y$ of two pixels on the diagonal from each other, of the total error ξ_{tot} $(a)(b)(c)$, internal error ξ_{int} $(d)(e)(f)$ and external error ξ_{ext} $(g)(h)(i)$ for Noiseless case $(a)(d)(g)$, $SNR = 10$ [dB] $(b)(e)(h)$ and $SNR = 5$ [dB] $(c)(f)(i)$.

4 Tests Dominio $L = 6.00\lambda$

4.1 TEST CASE: Two L-shaped Cylinders

Goal: show the performances of BCS when dealing with a sparse scatterer

- Number of Views: V
- Number of Measurements: M
- Number of Cells for the Inversion: N
- Number of Cells for the Direct solver: D
- Side of the investigation domain: L

Test Case Description

Direct solver:

- Square domain divided in $\sqrt{D} \times \sqrt{D}$ cells
- Domain side: $L = 6\lambda$
- $D = 6400$ (discretization for the direct solver: $< \lambda/10$)

Investigation domain:

- Square domain divided in $\sqrt{N} \times \sqrt{N}$ cells
- $L = 6\lambda$
- N scelto in modo da essere vicino a $\#DOF$: $N = 1600$ (40×40)

Measurement domain:

- Measurement points taken on a circle of radius $\rho = 4.5\lambda$
- Full-aspect measurements
- $M \approx 2ka \rightarrow M = 60$

Sources:

- Plane waves
- $V \approx 2ka \rightarrow V = 60$
- Amplitude $A = 1$
- Frequency: 300 MHz ($\lambda = 1$)

Object:

- Two L-shaped cylinders
- $\varepsilon_r \in \{1.5, 2.0, 2.5, 3.0, 3.5, 4.0, 4.5, 5.0\}$
- $\sigma = 0$ [S/m]

MT-BCS-Jmn parameters:

- Gamma prior on noise variance parameter: $a = 5 \times 10^0$

- Gamma prior on noise variance parameter: $b = 1 \times 10^{-1}$
- Convergenze parameter: $\tau = 1.0 \times 10^{-8}$

MV-MT-BCS-Jmn parameters:

- Gamma prior on noise variance parameter: $a = 5 \times 10^{0}$
- Gamma prior on noise variance parameter: $b = 2 \times 10^{-2}$
- Convergenze parameter: $\tau = 1.0 \times 10^{-8}$

RESULTS: Two L-shaped Cylinders

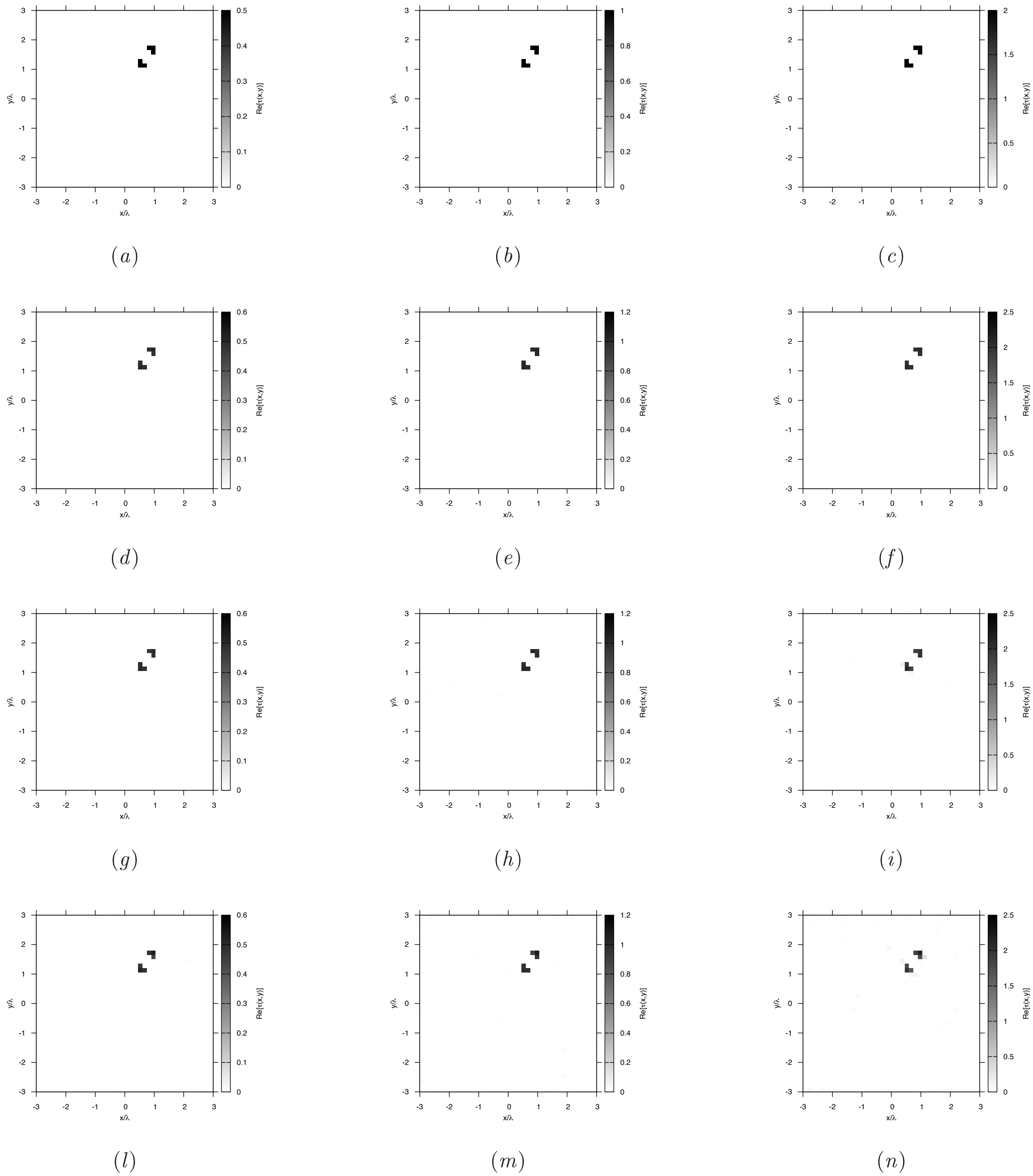

Figure 109. Actual object $(a)(b)(c)$ and BCS reconstructed object with $\varepsilon_r = 1.5$ $(d)(g)(l)$, $\varepsilon_r = 2.0$ $(e)(h)(m)$, and $\varepsilon_r = 3.0$ $(f)(i)(n)$, for Noiseless case $(d)(e)(f)$, $SNR = 10$ [dB] $(g)(h)(i)$ and $SNR = 5$ [dB] $(l)(m)(n)$.

RESULTS: Two L-shaped Cylinders - Reconstructions - Comparison MT-BCS-Jmn/MV-MT-BCS-Jmn - $\varepsilon_r = 2.0$

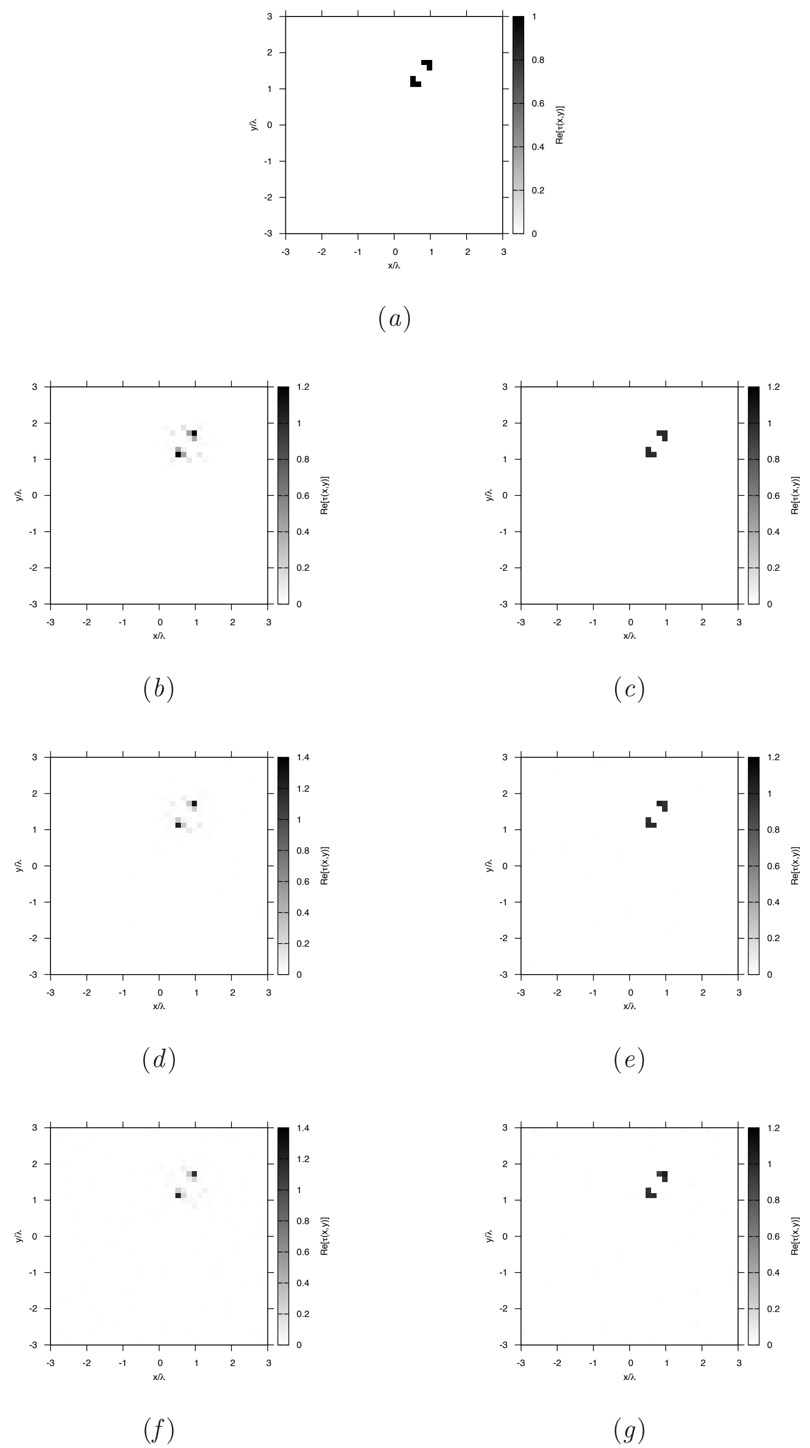

Figure 110. Actual object (a), MT-BCS-Jmn reconstructed object $(b)(d)(f)$ and MV-MT-BCS-Jmn reconstructed object $(c)(e)(g)$ for Noiseless case $(b)(c)$, $SNR = 10$ [dB] $(d)(e)$ and $SNR = 5$ [dB] $(f)(g)$.

RESULTS: Two L-shaped Cylinders - Error Figures - Comparison MT-BCS-Jmn/MV-MT-BCS-Jmn

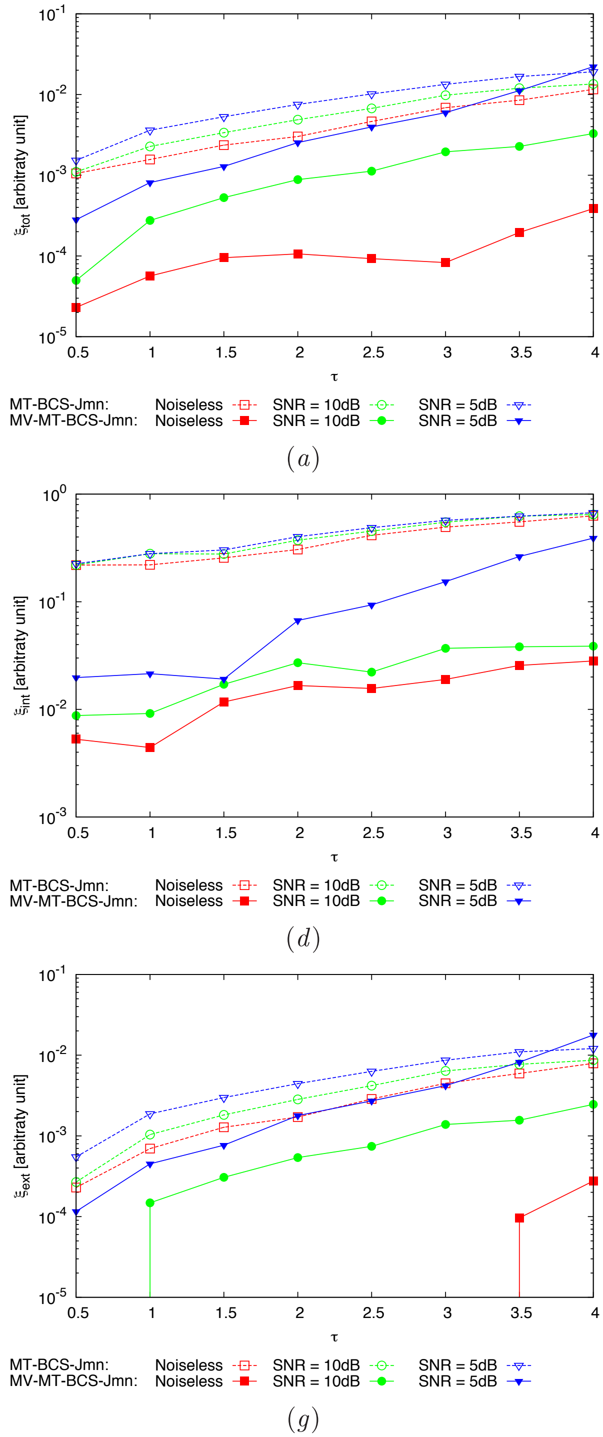

Figure 111. Behaviour of error figures as a function of ε_r, for different SNR values: (a) total error ξ_{tot}, (b) internal error ξ_{int}, (c) external error ξ_{ext}.

4.2 TEST CASE: Five L-shaped Cylinders

Goal: show the performances of BCS when dealing with a sparse scatterer

- Number of Views: V
- Number of Measurements: M
- Number of Cells for the Inversion: N
- Number of Cells for the Direct solver: D
- Side of the investigation domain: L

Test Case Description

Direct solver:

- Square domain divided in $\sqrt{D} \times \sqrt{D}$ cells
- Domain side: $L = 6\lambda$
- $D = 6400$ (discretization for the direct solver: $< \lambda/10$)

Investigation domain:

- Square domain divided in $\sqrt{N} \times \sqrt{N}$ cells
- $L = 6\lambda$
- N scelto in modo da essere vicino a $\#DOF$: $N = 1600$ (40×40)

Measurement domain:

- Measurement points taken on a circle of radius $\rho = 4.5\lambda$
- Full-aspect measurements
- $M \approx 2ka \rightarrow M = 60$

Sources:

- Plane waves
- $V \approx 2ka \rightarrow V = 60$
- Amplitude $A = 1$
- Frequency: 300 MHz $(\lambda = 1)$

Object:

- Five L-shaped cylinders
- $\varepsilon_r \in \{1.5, 2.0, 2.5, 3.0, 3.5, 4.0, 4.5, 5.0\}$
- $\sigma = 0$ [S/m]

MT-BCS-Jmn parameters:

- Gamma prior on noise variance parameter: $a = 5 \times 10^0$
- Gamma prior on noise variance parameter: $b = 1 \times 10^{-1}$
- Convergenze parameter: $\tau = 1.0 \times 10^{-8}$

MV-MT-BCS-Jmn parameters:

- Gamma prior on noise variance parameter: $a = 5 \times 10^0$
- Gamma prior on noise variance parameter: $b = 2 \times 10^{-2}$
- Convergenze parameter: $\tau = 1.0 \times 10^{-8}$

RESULTS: Five L-shaped Cylinders

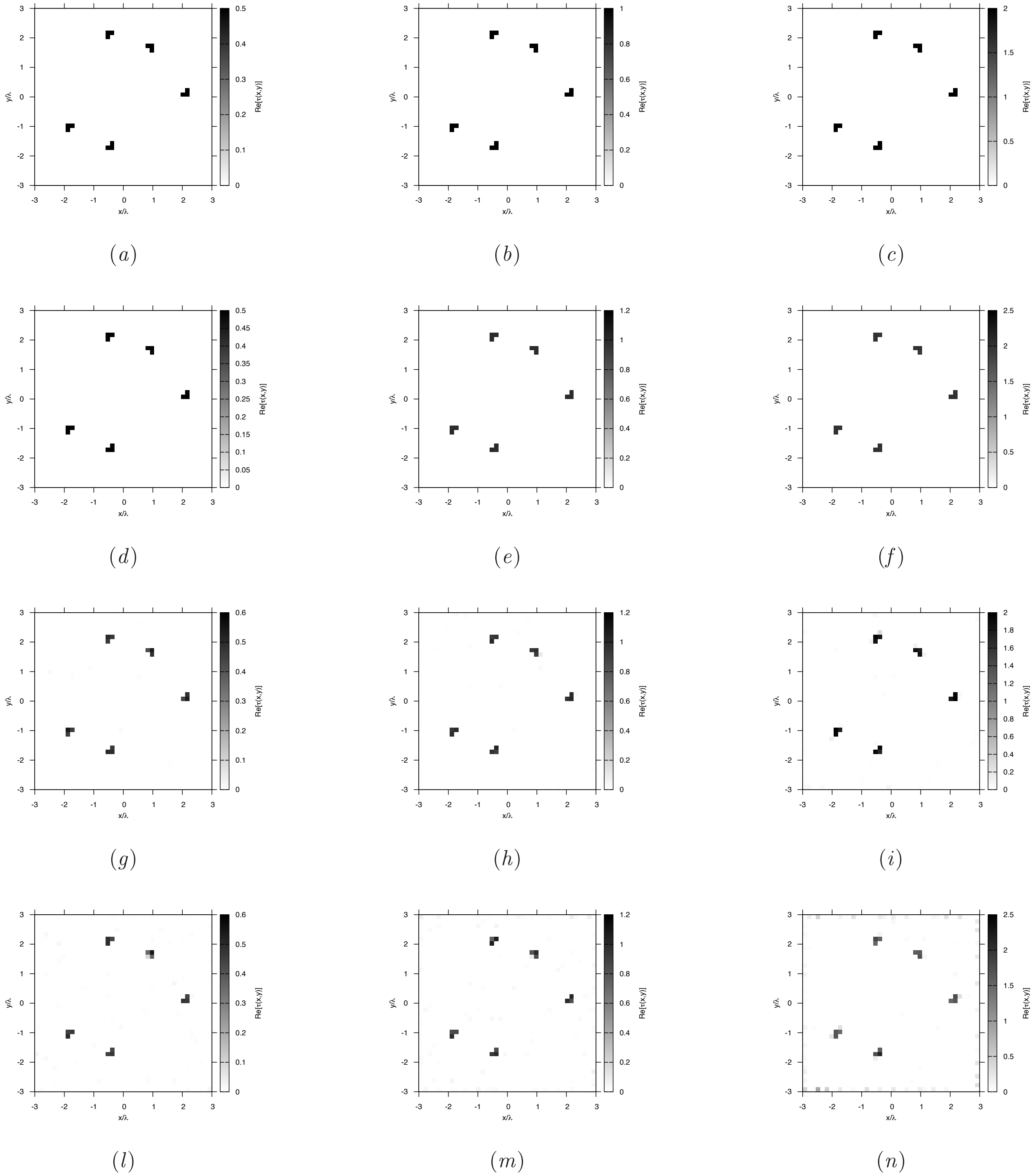

Figure 112. Actual object $(a)(b)(c)$ and BCS reconstructed object with $\varepsilon_r = 1.5$ $(d)(g)(l)$, $\varepsilon_r = 2.0$ $(e)(h)(m)$, and $\varepsilon_r = 3.0$ $(f)(i)(n)$, for Noiseless case $(d)(e)(f)$, $SNR = 10$ [dB] $(g)(h)(i)$ and $SNR = 5$ [dB] $(l)(m)(n)$.

RESULTS: Five L-shaped Cylinders - Reconstructions - Comparison MT-BCS-Jmn/MV-MT-BCS-Jmn - $\varepsilon_r = 2.0$

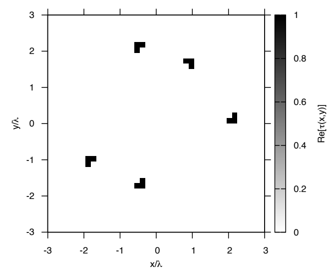

(a)

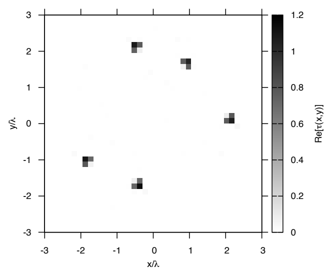

(b)

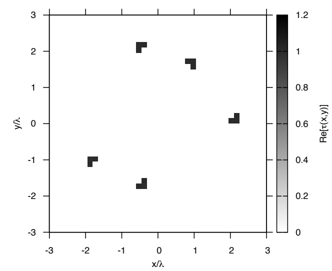

(c)

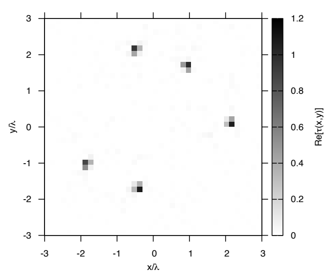

(d)

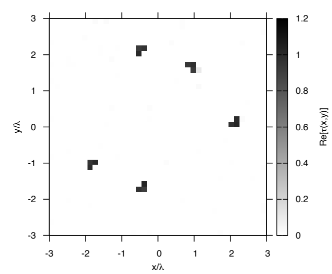

(e)

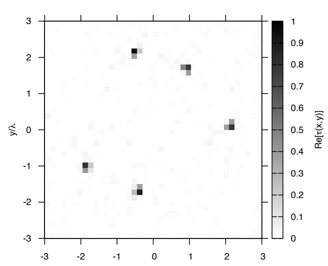

(f)

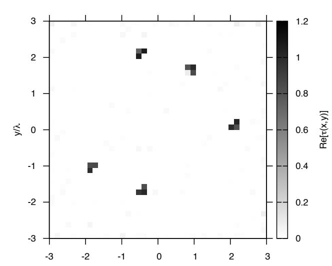

(g)

Figure 113. Actual object (a), MT-BCS-Jmn reconstructed object $(b)(d)(f)$ and MV-MT-BCS-Jmn reconstructed object $(c)(e)(g)$ for Noiseless case $(b)(c)$, $SNR = 10$ [dB] $(d)(e)$ and $SNR = 5$ [dB] $(f)(g)$.

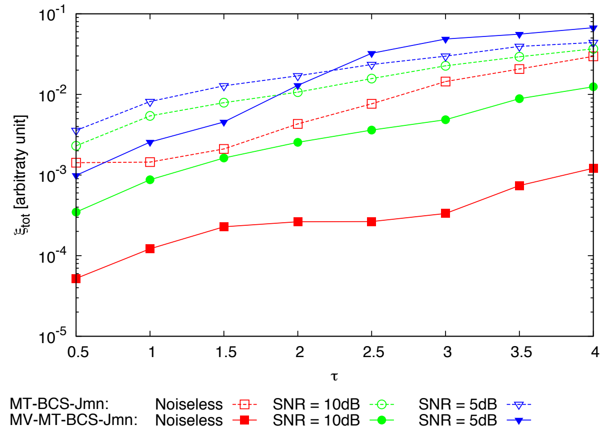

(a)

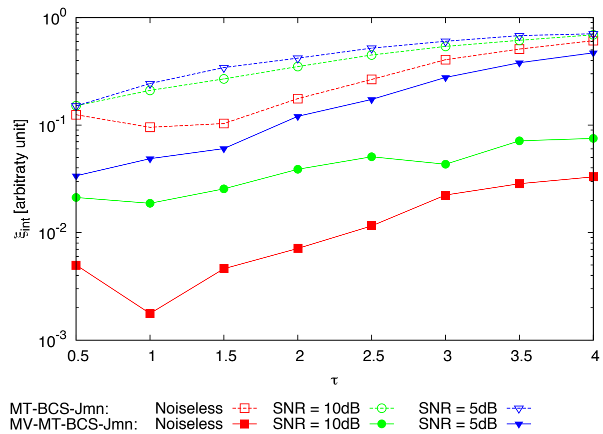

(d)

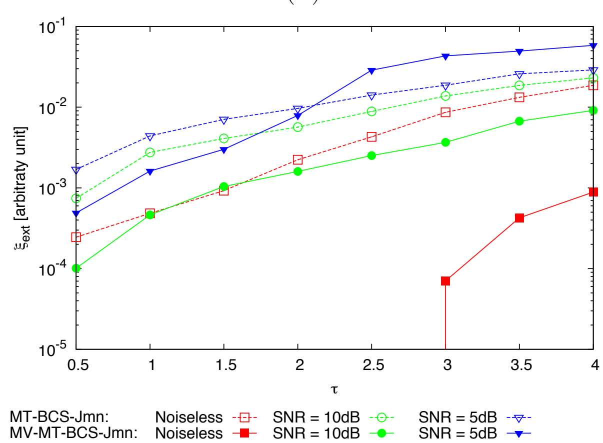

(g)

Figure 114. Behaviour of error figures as a function of ε_r, for different SNR values: (a) total error ξ_{tot}, (b) internal error ξ_{int}, (c) external error ξ_{ext}.

4.3 TEST CASE: Hollow Square Cylinder $L = 0.45\lambda$

Goal: show the performances of BCS when dealing with a sparse scatterer

- Number of Views: V
- Number of Measurements: M
- Number of Cells for the Inversion: N
- Number of Cells for the Direct solver: D
- Side of the investigation domain: L

Test Case Description

Direct solver:

- Square domain divided in $\sqrt{D} \times \sqrt{D}$ cells
- Domain side: $L = 6\lambda$
- $D = 6400$ (discretization for the direct solver: $< \lambda/10$)

Investigation domain:

- Square domain divided in $\sqrt{N} \times \sqrt{N}$ cells
- $L = 6\lambda$
- N scelto in modo da essere vicino a $\#DOF$: $N = 1600$ (40×40)

Measurement domain:

- Measurement points taken on a circle of radius $\rho = 4.5\lambda$
- Full-aspect measurements
- $M \approx 2ka \rightarrow M = 60$

Sources:

- Plane waves
- $V \approx 2ka \rightarrow V = 60$
- Amplitude $A = 1$
- Frequency: 300 MHz ($\lambda = 1$)

Object:

- Hollow square cylinder $L = 0.45\lambda$
- $\varepsilon_r \in \{1.5, 2.0, 2.5, 3.0, 3.5, 4.0, 4.5, 5.0\}$
- $\sigma = 0$ [S/m]

MT-BCS-Jmn parameters:

- Gamma prior on noise variance parameter: $a = 5 \times 10^0$
- Gamma prior on noise variance parameter: $b = 1 \times 10^{-1}$
- Convergenze parameter: $\tau = 1.0 \times 10^{-8}$

MV-MT-BCS-Jmn parameters:

- Gamma prior on noise variance parameter: $a = 5 \times 10^0$
- Gamma prior on noise variance parameter: $b = 2 \times 10^{-2}$
- Convergenze parameter: $\tau = 1.0 \times 10^{-8}$

RESULTS: Hollow Square Cylinder $L = 0.45\lambda$

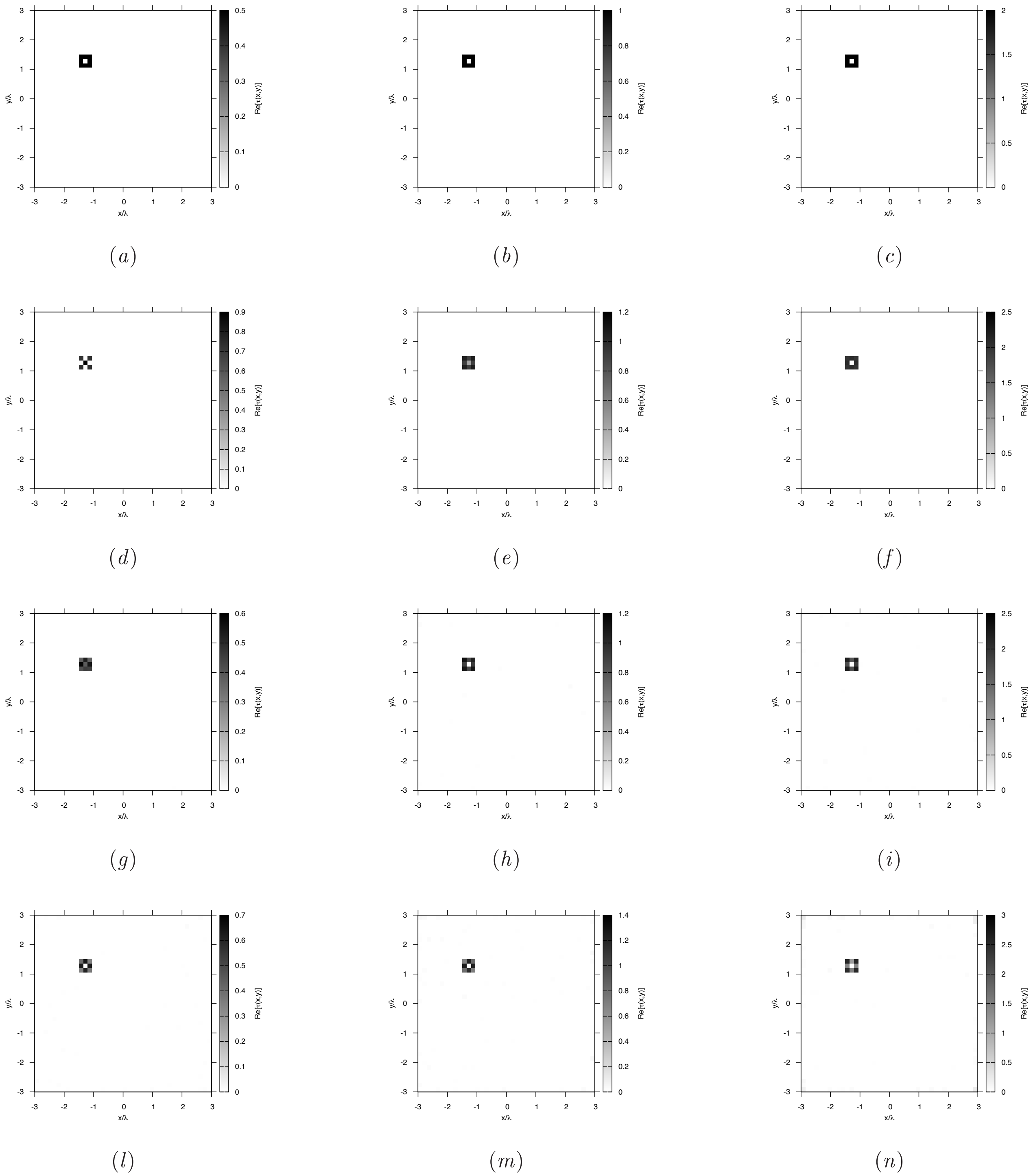

Figure 115. Actual object $(a)(b)(c)$ and BCS reconstructed object with $\varepsilon_r = 1.5$ $(d)(g)(l)$, $\varepsilon_r = 2.0$ $(e)(h)(m)$, and $\varepsilon_r = 3.0$ $(f)(i)(n)$, for Noiseless case $(d)(e)(f)$, $SNR = 10$ [dB] $(g)(h)(i)$ and $SNR = 5$ [dB] $(l)(m)(n)$.

RESULTS: Hollow Square Cylinder $L = 0.45\lambda$ - Reconstructions - Comparison MT-BCS-Jmn/MV-MT-BCS-Jmn - $\varepsilon_r = 2.0$

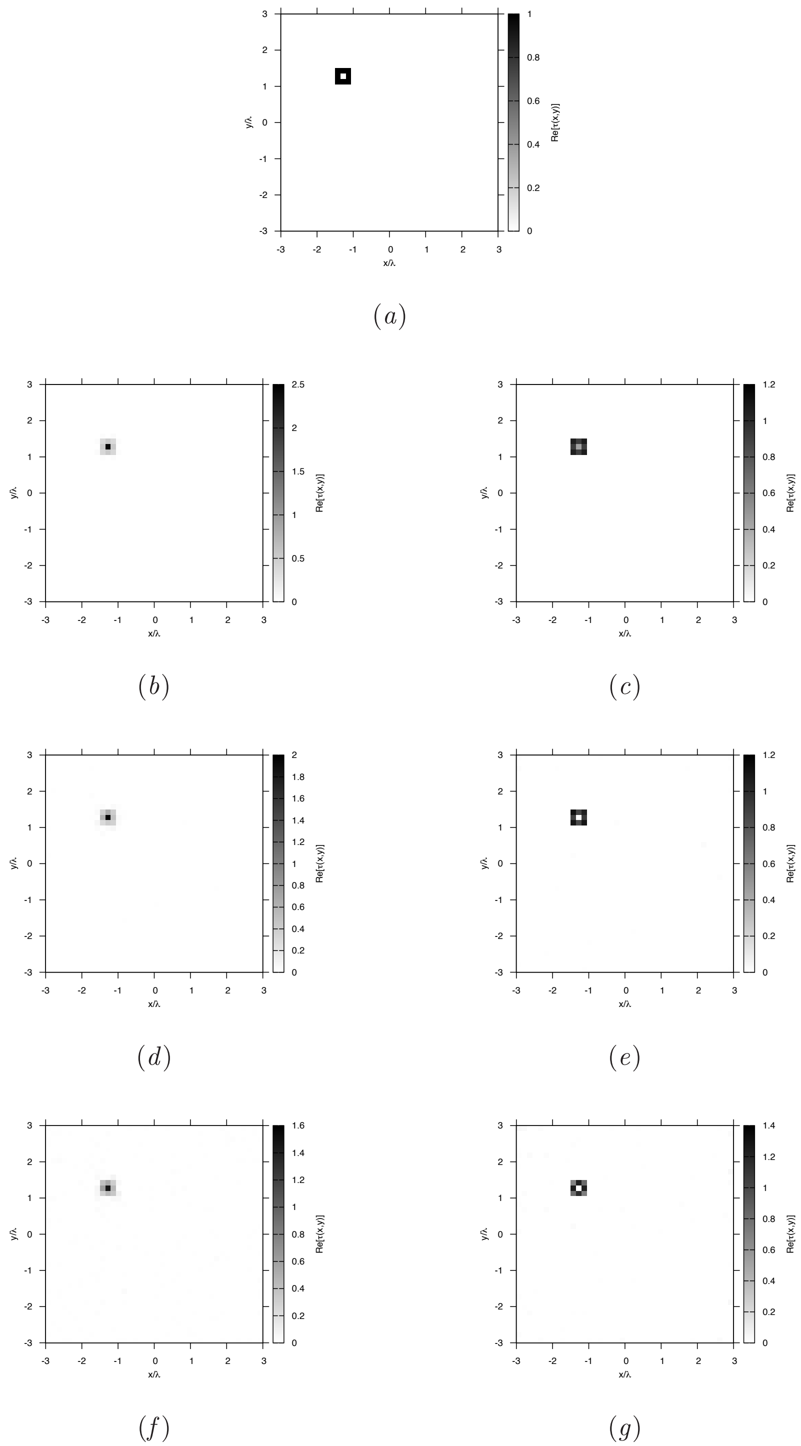

Figure 116. Actual object (a), MT-BCS-Jmn reconstructed object $(b)(d)(f)$ and MV-MT-BCS-Jmn reconstructed object $(c)(e)(g)$ for Noiseless case $(b)(c)$, $SNR = 10$ [dB] $(d)(e)$ and $SNR = 5$ [dB] $(f)(g)$.

RESULTS: Hollow Square Cylinder $L = 0.45\lambda$ - Error Figures - Comparison MT-BCS-Jmn/MV-MT-BCS-Jmn

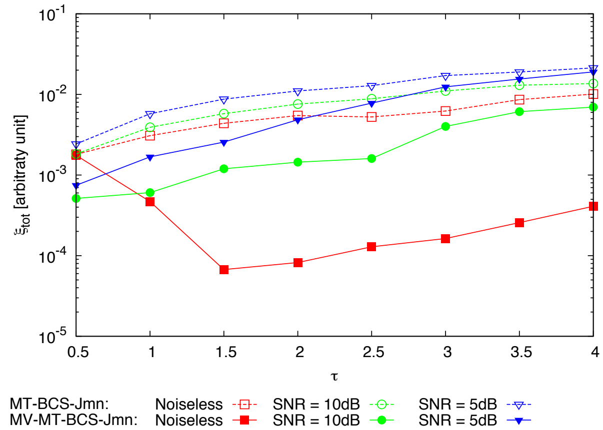

(a)

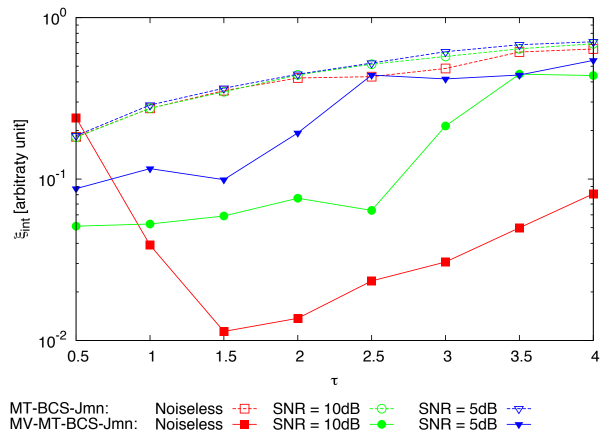

(b)

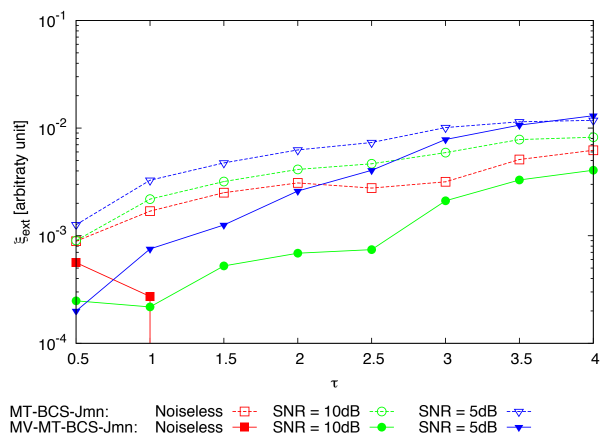

(c)

Figure 117. Behaviour of error figures as a function of ε_r, for different SNR values: (a) total error ξ_{tot}, (b) internal error ξ_{int}, (c) external error ξ_{ext}.

4.4 TEST CASE: Two Hollow Square Cylinders $L = 0.45\lambda$

Goal: show the performances of BCS when dealing with a sparse scatterer

- Number of Views: V
- Number of Measurements: M
- Number of Cells for the Inversion: N
- Number of Cells for the Direct solver: D
- Side of the investigation domain: L

Test Case Description

Direct solver:

- Square domain divided in $\sqrt{D} \times \sqrt{D}$ cells
- Domain side: $L = 6\lambda$
- $D = 6400$ (discretization for the direct solver: $< \lambda/10$)

Investigation domain:

- Square domain divided in $\sqrt{N} \times \sqrt{N}$ cells
- $L = 6\lambda$
- N scelto in modo da essere vicino a $\#DOF$: $N = 1600$ (40×40)

Measurement domain:

- Measurement points taken on a circle of radius $\rho = 4.5\lambda$
- Full-aspect measurements
- $M \approx 2ka \rightarrow M = 60$

Sources:

- Plane waves
- $V \approx 2ka \rightarrow V = 60$
- Amplitude $A = 1$
- Frequency: 300 MHz ($\lambda = 1$)

Object:

- Two hollow square cylinders $L = 0.45\lambda$
- $\varepsilon_r \in \{1.5, 2.0, 2.5, 3.0, 3.5, 4.0, 4.5, 5.0\}$
- $\sigma = 0$ [S/m]

MT-BCS-Jmn parameters:

- Gamma prior on noise variance parameter: $a = 5 \times 10^0$
- Gamma prior on noise variance parameter: $b = 1 \times 10^{-1}$
- Convergenze parameter: $\tau = 1.0 \times 10^{-8}$

MV-MT-BCS-Jmn parameters:

- Gamma prior on noise variance parameter: $a = 5 \times 10^0$
- Gamma prior on noise variance parameter: $b = 2 \times 10^{-2}$
- Convergenze parameter: $\tau = 1.0 \times 10^{-8}$

RESULTS: Two Hollow Square Cylinders $L = 0.45\lambda$

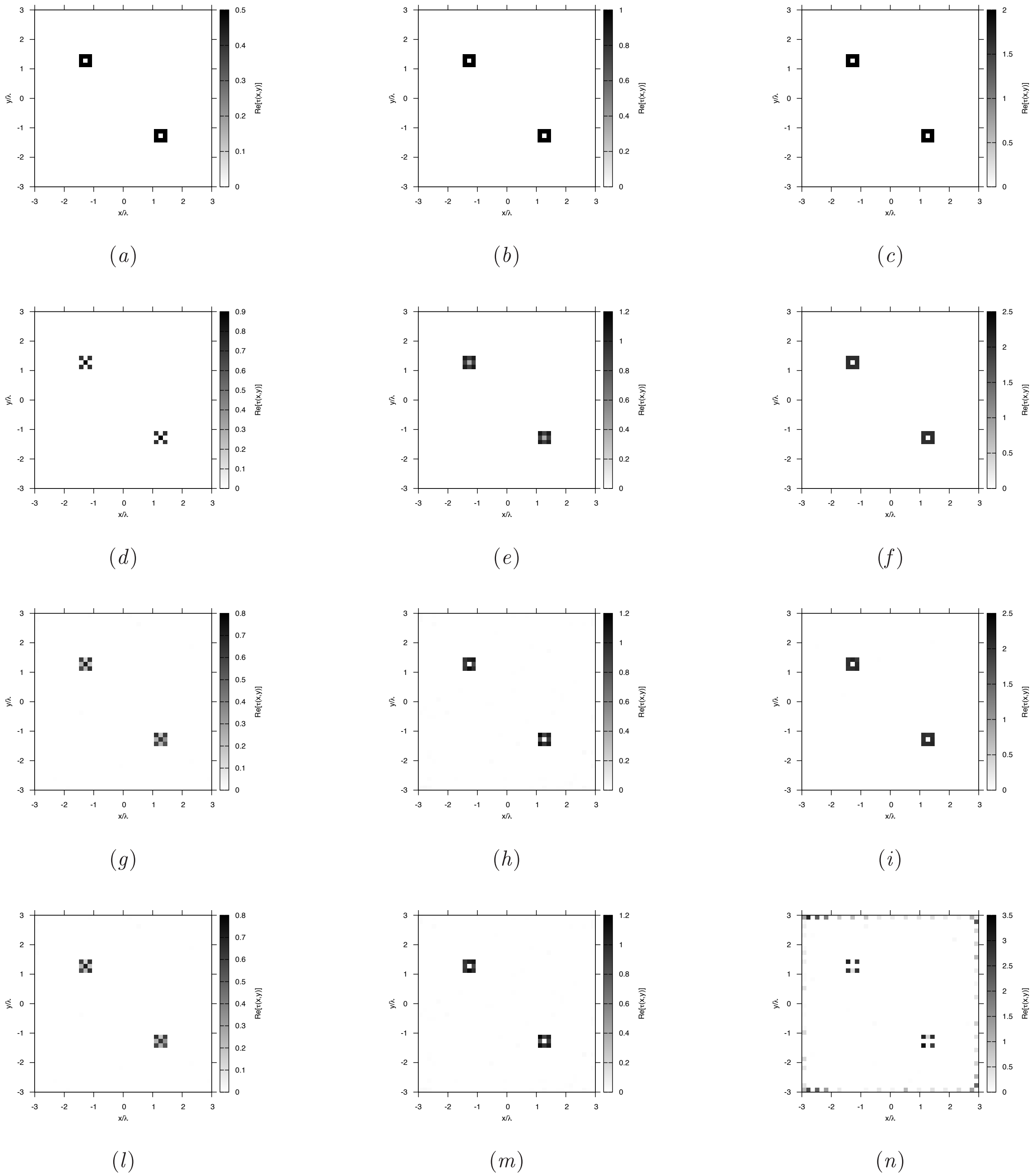

Figure 118. Actual object $(a)(b)(c)$ and BCS reconstructed object with $\varepsilon_r = 1.5$ $(d)(g)(l)$, $\varepsilon_r = 2.0$ $(e)(h)(m)$, and $\varepsilon_r = 3.0$ $(f)(i)(n)$, for Noiseless case $(d)(e)(f)$, $SNR = 10$ [dB] $(g)(h)(i)$ and $SNR = 5$ [dB] $(l)(m)(n)$.

RESULTS: Two Hollow Square Cylinders $L = 0.45\lambda$ - Reconstructions - Comparison MT-BCS-Jmn/MV-MT-BCS-Jmn - $\varepsilon_r = 2.0$

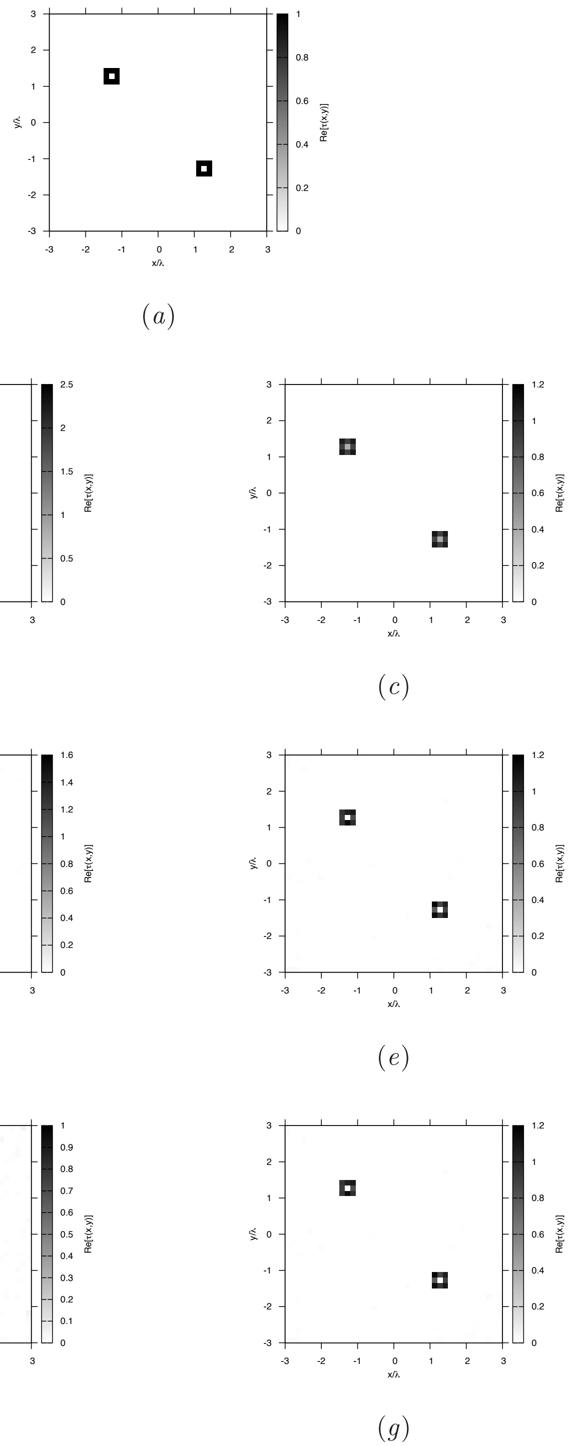

Figure 119. Actual object (a), MT-BCS-Jmn reconstructed object $(b)(d)(f)$ and MV-MT-BCS-Jmn reconstructed object $(c)(e)(g)$ for Noiseless case $(b)(c)$, $SNR = 10$ [dB] $(d)(e)$ and $SNR = 5$ [dB] $(f)(g)$.

RESULTS: Two Hollow Square Cylinders $L = 0.45\lambda$ - Error Figures - Comparison MT-BCS-Jmn/MV-MT-BCS-Jmn

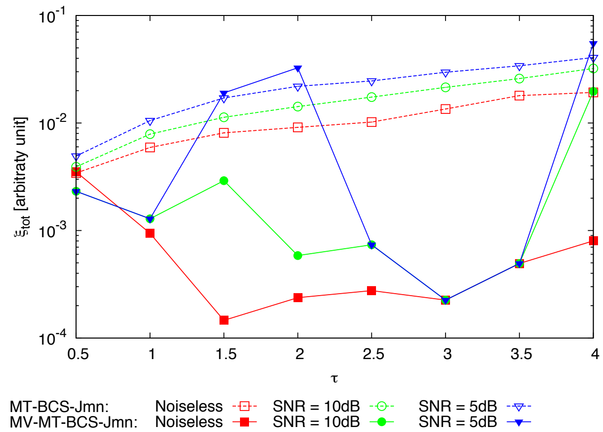

(a)

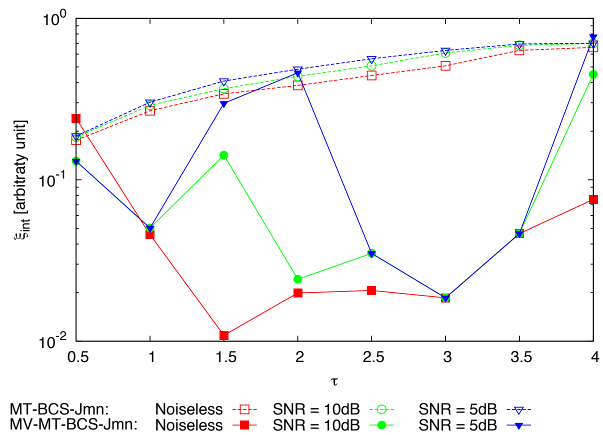

(b)

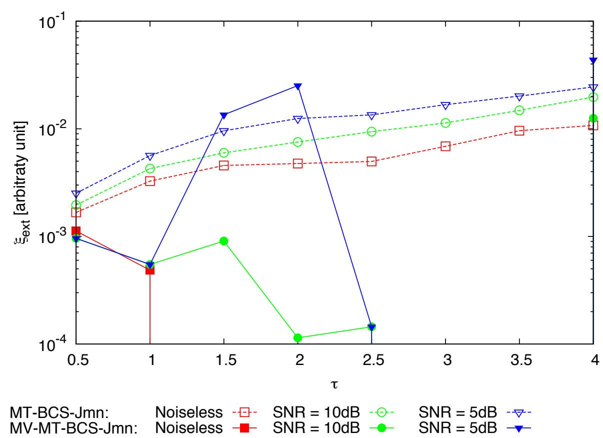

(c)

Figure 120. Behaviour of error figures as a function of ε_r, for different SNR values: (a) total error ξ_{tot}, (b) internal error ξ_{int}, (c) external error ξ_{ext}.

4.5 TEST CASE: Hollow Rectangular Cylinder

Goal: show the performances of BCS when dealing with a sparse scatterer

- Number of Views: V
- Number of Measurements: M
- Number of Cells for the Inversion: N
- Number of Cells for the Direct solver: D
- Side of the investigation domain: L

Test Case Description

Direct solver:

- Square domain divided in $\sqrt{D} \times \sqrt{D}$ cells
- Domain side: $L = 6\lambda$
- $D = 6400$ (discretization for the direct solver: $< \lambda/10$)

Investigation domain:

- Square domain divided in $\sqrt{N} \times \sqrt{N}$ cells
- $L = 6\lambda$
- N scelto in modo da essere vicino a $\#DOF$: $N = 1600$ (40×40)

Measurement domain:

- Measurement points taken on a circle of radius $\rho = 4.5\lambda$
- Full-aspect measurements
- $M \approx 2ka \rightarrow M = 60$

Sources:

- Plane waves
- $V \approx 2ka \rightarrow V = 60$
- Amplitude $A = 1$
- Frequency: 300 MHz ($\lambda = 1$)

Object:

- Hollow rectangular cylinder
- $\varepsilon_r \in \{1.5, 2.0, 2.5, 3.0, 3.5, 4.0, 4.5, 5.0\}$
- $\sigma = 0$ [S/m]

MT-BCS-Jmn parameters:

- Gamma prior on noise variance parameter: $a = 5 \times 10^0$
- Gamma prior on noise variance parameter: $b = 1 \times 10^{-1}$
- Convergenze parameter: $\tau = 1.0 \times 10^{-8}$

MV-MT-BCS-Jmn parameters:

- Gamma prior on noise variance parameter: $a = 5 \times 10^0$
- Gamma prior on noise variance parameter: $b = 2 \times 10^{-2}$
- Convergenze parameter: $\tau = 1.0 \times 10^{-8}$

RESULTS: Hollow Rectangular Cylinder

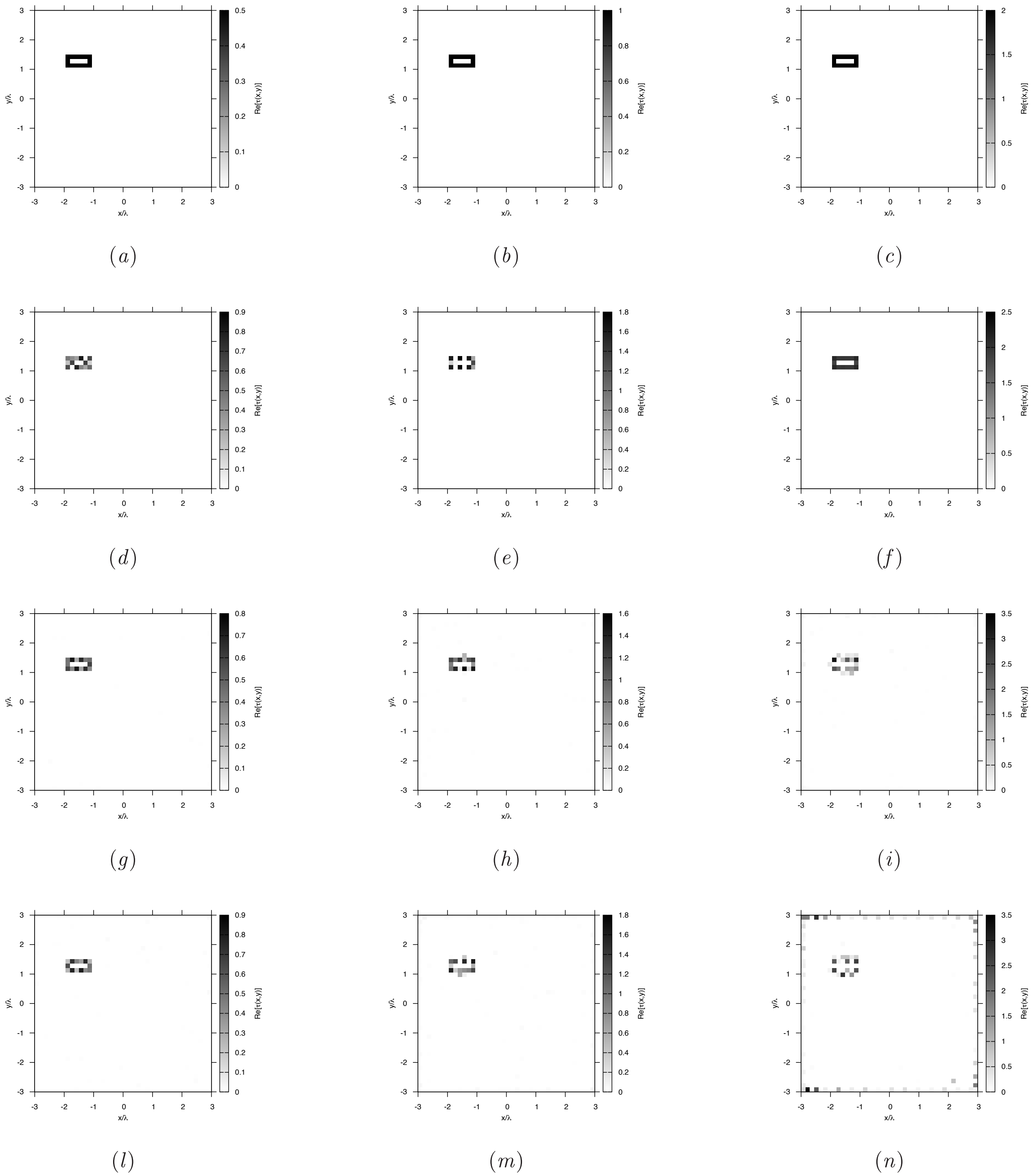

Figure 121. Actual object $(a)(b)(c)$ and BCS reconstructed object with $\varepsilon_r = 1.5$ $(d)(g)(l)$, $\varepsilon_r = 2.0$ $(e)(h)(m)$, and $\varepsilon_r = 3.0$ $(f)(i)(n)$, for Noiseless case $(d)(e)(f)$, $SNR = 10$ [dB] $(g)(h)(i)$ and $SNR = 5$ [dB] $(l)(m)(n)$.

RESULTS: Hollow Rectangular Cylinder - Reconstructions - Comparison MT-BCS-Jmn/MV-MT-BCS-Jmn - $\varepsilon_r = 2.0$

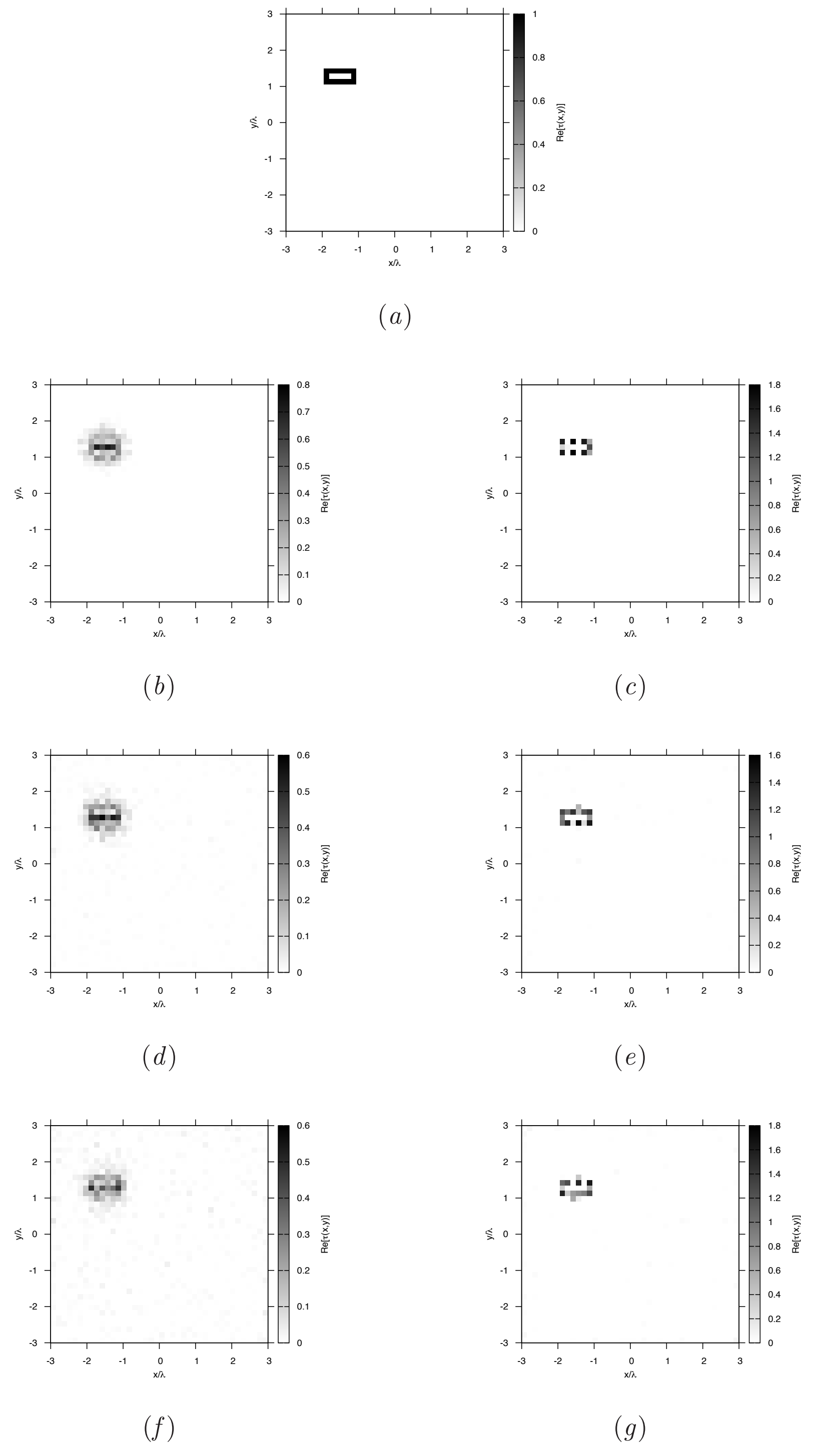

Figure 122. Actual object (a), MT-BCS-Jmn reconstructed object $(b)(d)(f)$ and MV-MT-BCS-Jmn reconstructed object $(c)(e)(g)$ for Noiseless case $(b)(c)$, $SNR = 10$ [dB] $(d)(e)$ and $SNR = 5$ [dB] $(f)(g)$.

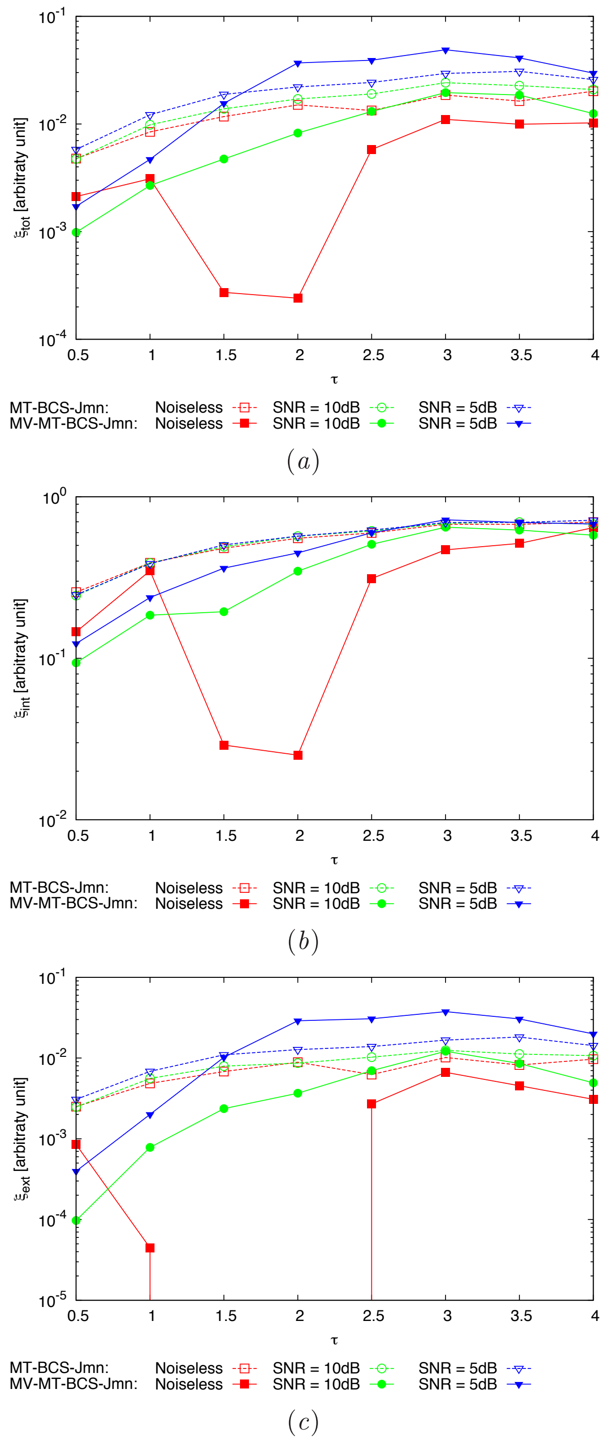

Figure 123. Behaviour of error figures as a function of ε_r, for different SNR values: (a) total error ξ_{tot}, (b) internal error ξ_{int}, (c) external error ξ_{ext}.

4.6 TEST CASE: Test Multiple Objects

Goal: show the performances of BCS when dealing with a sparse scatterer

- Number of Views: V
- Number of Measurements: M
- Number of Cells for the Inversion: N
- Number of Cells for the Direct solver: D
- Side of the investigation domain: L

Test Case Description

Direct solver:

- Square domain divided in $\sqrt{D} \times \sqrt{D}$ cells
- Domain side: $L = 6\lambda$
- $D = 6400$ (discretization for the direct solver: $< \lambda/10$)

Investigation domain:

- Square domain divided in $\sqrt{N} \times \sqrt{N}$ cells
- $L = 6\lambda$
- N scelto in modo da essere vicino a $\#DOF$: $N = 1600$ (40×40)

Measurement domain:

- Measurement points taken on a circle of radius $\rho = 4.5\lambda$
- Full-aspect measurements
- $M \approx 2ka \rightarrow M = 60$

Sources:

- Plane waves
- $V \approx 2ka \rightarrow V = 60$
- Amplitude $A = 1$
- Frequency: 300 MHz $(\lambda = 1)$

Object:

- Multiple Objects (various forms)
- $\varepsilon_r \in \{1.5, 2.0, 2.5, 3.0, 3.5, 4.0, 4.5, 5.0\}$
- $\sigma = 0$ [S/m]

MT-BCS-Jmn parameters:

- Gamma prior on noise variance parameter: $a = 5 \times 10^0$
- Gamma prior on noise variance parameter: $b = 1 \times 10^{-1}$
- Convergenze parameter: $\tau = 1.0 \times 10^{-8}$

MV-MT-BCS-Jmn parameters:

- Gamma prior on noise variance parameter: $a = 5 \times 10^0$
- Gamma prior on noise variance parameter: $b = 2 \times 10^{-2}$
- Convergenze parameter: $\tau = 1.0 \times 10^{-8}$

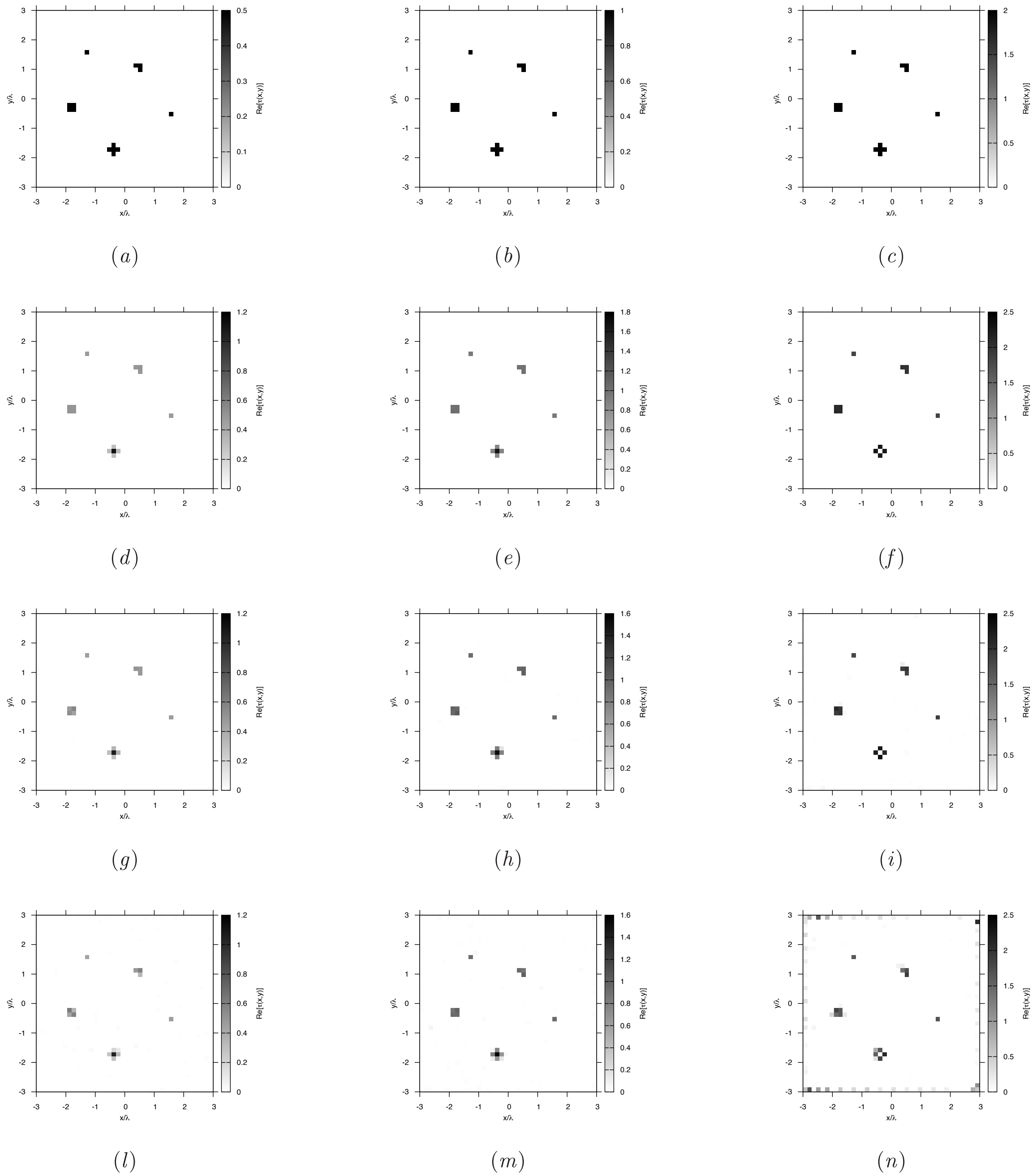

Figure 124. Actual object $(a)(b)(c)$ and BCS reconstructed object with $\varepsilon_r = 1.5$ $(d)(g)(l)$, $\varepsilon_r = 2.0$ $(e)(h)(m)$, and $\varepsilon_r = 3.0$ $(f)(i)(n)$, for Noiseless case $(d)(e)(f)$, $SNR = 10$ [dB] $(g)(h)(i)$ and $SNR = 5$ [dB] $(l)(m)(n)$.

RESULTS: Multiple Objects - Reconstructions - Comparison MT-BCS-Jmn/MV-MT-BCS-Jmn - $\varepsilon_r = 2.0$

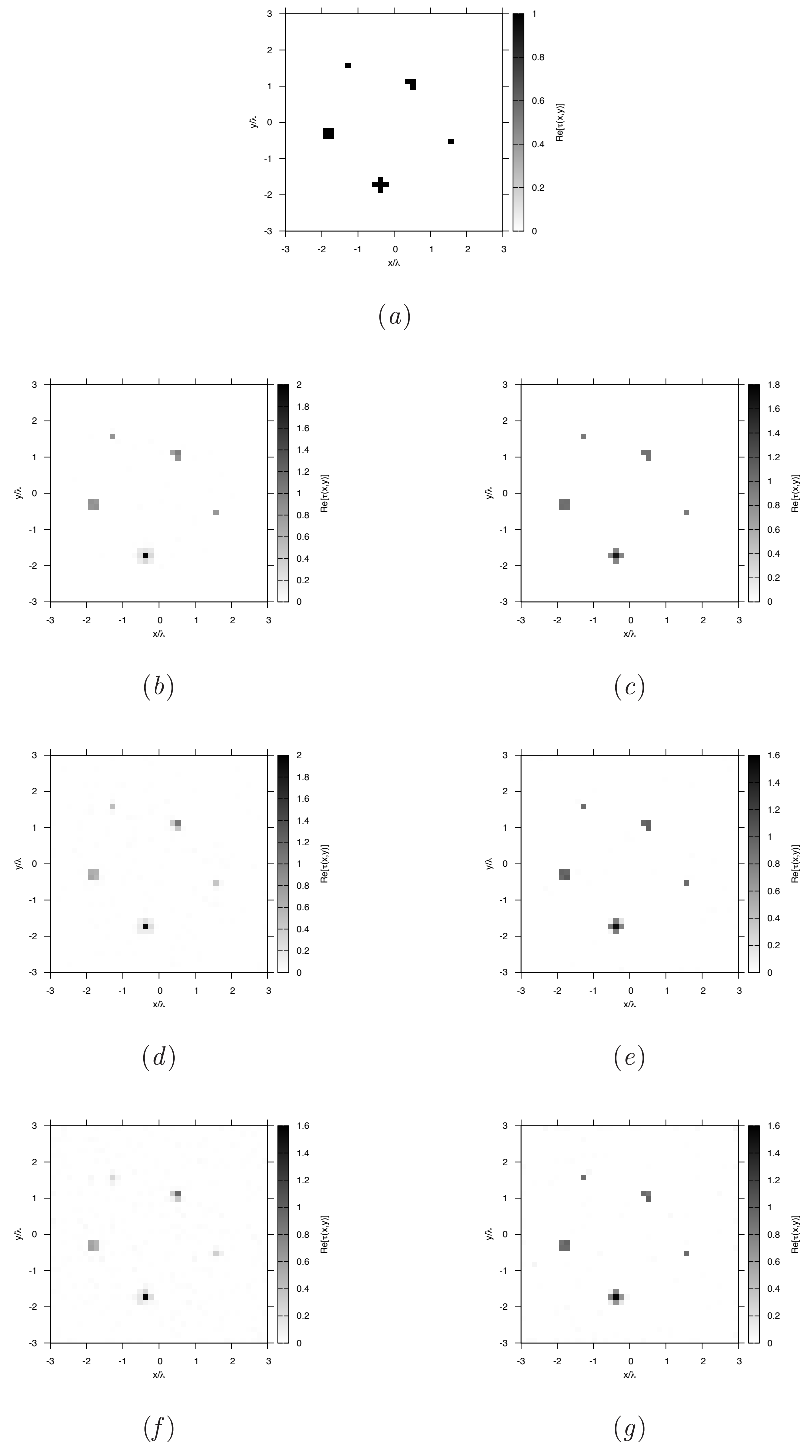

Figure 125. Actual object (a), MT-BCS-Jmn reconstructed object $(b)(d)(f)$ and MV-MT-BCS-Jmn reconstructed object $(c)(e)(g)$ for Noiseless case $(b)(c)$, $SNR = 10$ [dB] $(d)(e)$ and $SNR = 5$ [dB] $(f)(g)$.

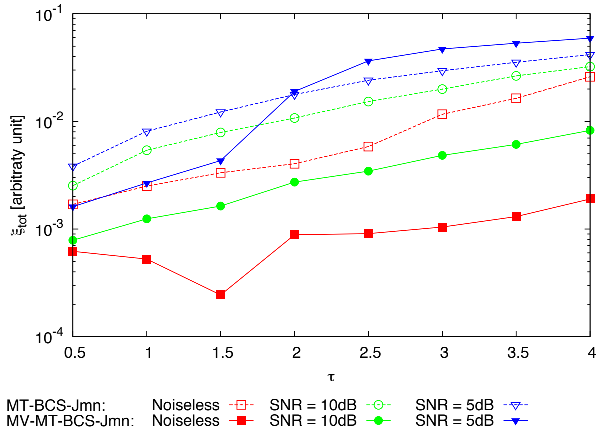

(a)

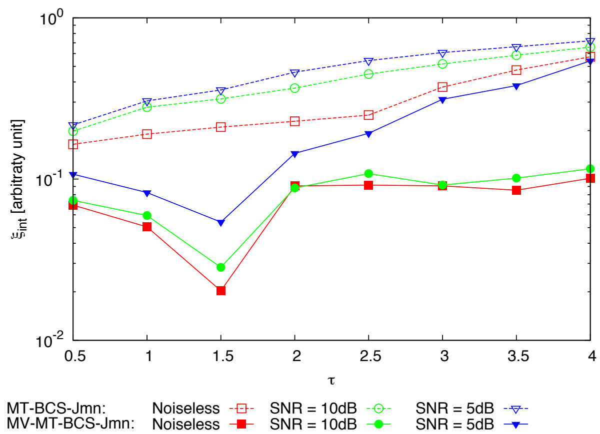

(b)

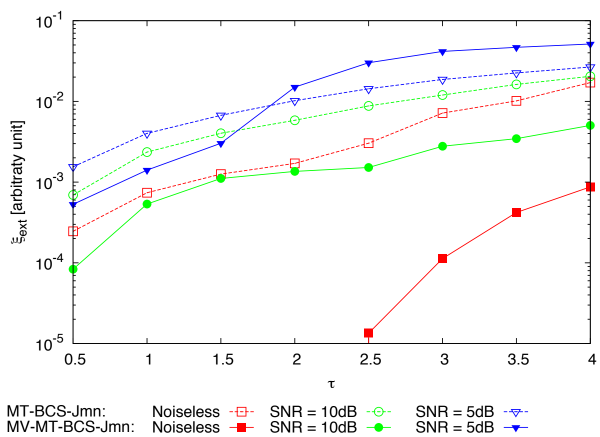

(c)

Figure 126. Behaviour of error figures as a function of ε_r, for different SNR values: (a) total error ξ_{tot}, (b) internal error ξ_{int}, (c) external error ξ_{ext}.

References

[1] G. Oliveri, N. Anselmi, and A. Massa, "Compressive sensing imaging of non-sparse 2D scatterers by a total-variation approach within the Born approximation," IEEE Trans. Antennas Propag., vol. 62, no. 10, pp. 5157-5170, Oct. 2014.

[2] L. Poli, G. Oliveri, and A. Massa, "Imaging sparse metallic cylinders through a Local Shape Function Bayesian Compressive Sensing approach," Journal of Optical Society of America A, vol. 30, no. 6, pp. 1261-1272, 2013.

[3] F. Viani, L. Poli, G. Oliveri, F. Robol, and A. Massa, "Sparse scatterers imaging through approximated multitask compressive sensing strategies," Microwave Opt. Technol. Lett., vol. 55, no. 7, pp. 1553-1558, Jul. 2013.

[4] L. Poli, G. Oliveri, P. Rocca, and A. Massa, "Bayesian compressive sensing approaches for the reconstruction of two-dimensional sparse scatterers under TE illumination," IEEE Trans. Geosci. Remote Sensing, vol. 51, no. 5, pp. 2920-2936, May. 2013.

[5] L. Poli, G. Oliveri, and A. Massa, "Microwave imaging within the first-order Born approximation by means of the contrast-field Bayesian compressive sensing," IEEE Trans. Antennas Propag., vol. 60, no. 6, pp. 2865-2879, Jun. 2012.

[6] G. Oliveri, P. Rocca, and A. Massa, "A bayesian compressive sampling-based inversion for imaging sparse scatterers," IEEE Trans. Geosci. Remote Sensing, vol. 49, no. 10, pp. 3993-4006, Oct. 2011.

[7] G. Oliveri, L. Poli, P. Rocca, and A. Massa, "Bayesian compressive optical imaging within the Rytov approximation," Optics Letters, vol. 37, no. 10, pp. 1760-1762, 2012.

[8] L. Poli, G. Oliveri, F. Viani, and A. Massa, "MT-BCS-based microwave imaging approach through minimum-norm current expansion," IEEE Trans. Antennas Propag., vol. 61, no. 9, pp. 4722-4732, Sept. 2013.

[9] P. Rocca, M. Carlin, L. Manica, and A. Massa, "Microwave imaging within the interval analysis framework," Progress in Electromagnetic Research, vol. 143, pp. 675-708, 2013.

[10] P. Rocca, M. Carlin, G. Oliveri, and A. Massa, "Interval analysis as applied to inverse scattering," IEEE International Symposium on Antennas Propag. (APS/URSI 2013), Chicago, Illinois, USA, Jul. 8-14, 2012.

[11] L. Manica, P. Rocca, M. Salucci, M. Carlin, and A. Massa, "Scattering data inversion through interval analysis under Rytov approximation," 7th European Conference on Antennas Propag. (EuCAP 2013), Gothenburg, Sweden, Apr. 8-12, 2013.

[12] P. Rocca, M. Carlin, and A. Massa, "Imaging weak scatterers by means of an innovative inverse scattering technique based on the interval analysis," 6th European Conference on Antennas Propag. (EuCAP 2012), Prague, Czech Republic, Mar. 26-30, 2012.